Trinity College Dublin
Coláiste na Tríonóide, Baile Átha Cliath
The University of Dublin

# The manufacture of fixed dose combination products using advanced pharmaceutical techniques for the treatment of cardiovascular disease and type II diabetes

A thesis submitted for the degree of

**Doctor of Philosophy**

at the

**School of Pharmacy and Pharmaceutical Sciences,**

**Trinity College Dublin, The University of Dublin**

by

**Jeremiah Kelleher**

**B.Pharm., M.Pharm., P.Grad.Cert. (Statistics), M.P.S.I.**

Under the direction and supervision of

**Professor Anne Marie Healy**

**B.Sc. (Pharm), Ph.D., M.P.S.I., F.T.C.D.**

**April 2020**

## Declaration

I declare that this thesis has not been submitted as an exercise for a degree at this or any other university. A small proportion of the work presented in this thesis was carried out by others and is duly acknowledged where relevant. I declare that all other work is entirely my own.

I agree to deposit this thesis in the University's open access institutional repository or allow the Library to do so on my behalf, subject to Irish Copyright Legislation and Trinity College Library conditions of use and acknowledgement.

_____

Jeremiah Kelleher

*“It ain’t what you don’t know that gets you into trouble. It’s what you know for sure that just ain’t so.”*

*-Anonymous*

# Contents

## Summary

The thesis has focused on the use of continuous manufacturing techniques to produce fixed dose combination (FDC) products for the treatment of type II diabetes mellitus and cardiovascular diseases (CVDs). FDC products with monophasic and biphasic release profiles of the active pharmaceutical ingredients (APIs) were successfully manufactured via spray drying (SD), hot melt extrusion (HME), melt granulation (MG) and spray coating (SC). The impact of manufacturing technique on the products was studied, as well as the role excipients and their molecular makeup have on the final product characteristics.

Monolithic FDC products of hydrochlorothiazide (HCTZ) and ramipril (RAM), with an immediate release (IR) profile, were manufactured via HME and SD and the resulting physicochemical characteristics were analysed and compared with one another. The same formulations were used for both HME and SD. One of the challenges associated with RAM is that it is a thermolabile API and starts to degrade upon melting at its relatively low melting point of around 115°C. The addition of appropriate plasticiser (PEG 3350) successfully overcame the degradation of RAM seen during HME with the IR polymers chosen for the study (Kollidon® VA 64 and Soluplus®). No degradation of RAM was observed during the SD process due to the lower temperatures the formulations were subjected to because of the suitable solvents available to dissolve the formulation contents. While all SD formulations were fully amorphous post processing, HME formulations were partially crystalline. In general, amorphous materials display higher solubility and higher dissolution rates when compared to crystalline materials. When the corresponding SD and HME formulations were compressed in the Wood's apparatus and dissolution rates for both APIs studied, it was found the partially crystalline HME formulations displayed higher dissolution rates than the corresponding amorphous SD formulations in the relevant formulations. No release of API was observed from formulations containing Soluplus® due to the extensive swelling of the polymer. Surface topography studies of the compressed Wood's apparatus discs revealed HME formulations to have significantly rougher surfaces than SD discs. It is hypothesized the differences in surface texture give rise to varying turbulence levels at the hydrodynamic boundary layer and as a result, the dissolution rates differ from what might be expected when predicting release profiles based on the solid state of the formulations. While both manufacturing techniques were successful in producing IR monolithic FDC products, the comparative study highlights the importance of choosing an appropriate manufacturing

technique to produce the final desirable product characteristics as well as avoiding degradation of the API.

Monolithic FDC products of metformin hydrochloride (MET) and sitagliptin phosphate (SIT), with a desired IR profile, were manufactured via MG and SD. The influence manufacturing technique as well as hydroxypropyl cellulose (HPC) polymer composition were analysed and studied for their influence on the final product characteristics. The same formulations were used for both MG and SD. Due to the large dosage size of MET, the quantities of excipients used for processing had to be kept to a minimum. Two HPC polymers were chosen for the formulations which varied in molecular weight and degree of hydroxypropoxy substitution. These different polymer characteristics led to differences in caplet characteristics irrespective of manufacturing technique, highlighting the role polymer composition has in producing final products for patient consumption. While final products were manufactured via both techniques and using both polymers, only one product, produced by MG and compressed at 8000 N, passed all the common compendial tests for IR oral tablets. The work highlights that MG is a suitable technique for producing high dose combination products and it may be more suitable than SD for a number of reasons. Firstly, it is seen as more environmentally friendly due to no solvents being required. Secondly, granules produced by the MG process have better flowability characteristics than powders produced via SD. Thirdly, while both MG and SD can be considered continuous manufacturing techniques due to constant input resulting in a constant output, SD powders have to be collected in a collecting vessel and removed before further processing whereas MG products can directly feed into the next phase of processing. The work also highlights that sufficient compression has to be applied to powers/granules to produce final products suitable for delivery to patients.

A delayed release formulation of simvastatin (SIM) was successfully manufactured via HME followed by coating via a fluid bed dryer (FBD) of an IR formulation of HCTZ and RAM to create a unique FDC product for the treatment of cardiovascular diseases (CVDs). Manipulation of formulation components such as plasticiser concentration, drug loading, and polymer ratio impacted the release profile of SIM to get it to the delayed desired release profile avoiding potential areas in the gut that can lead to degradation of the API. Once the core SIM formulation was manufactured, the extrudate was cut into pellets and spheronised into spherical pellets for coating. Various polymers and solvents as well as different processing parameters were trialled until successful application of the desired amount of HCTZ and RAM was achieved. The work carried out highlights the possibility of using HME to manufacture core material that can then be spheronised and

coated using a FBD. Due to the flexibility of the coating, different drug loadings of various concentrations can be easily achieved.

A sustained released formulation of the thermolabile API, gliclazide (GLZ), was successfully manufactured via HME that gave a similar release profile to the marketed products available that are produced via direct compression. By manipulating formulation components such as polymer ratio, plasticiser selection and pH modifiers, the desired release profile, while also ensuring thermal degradation of the API was kept to a minimum, was achieved. The work highlights while thermal degradation is a significant factor in API degradation of thermolabile products during the HME process, local undesirable pH levels can cause degradation of the API also. Once the desired core GLZ formulation was manufactured, the extrudate was cut into pellets and spheronised into spherical pellets for coating. Pharmacoat® 603 was chosen as the polymer to aid SIT coating of the core material due to its film forming characteristics. Various solvent compositions were trialled during the coating process. The quantity of core material to be coated was also varied, with larger amounts of core material providing a higher coating efficiency due to a higher surface area being available for coating. The work highlights the possibility of producing sustained release thermolabile APIs via HME. It also highlights the flexibility of producing unique FDC products by applying additional API via SC.

The work conducted and presented in this thesis highlights the many modern continuous methods of manufacturing that can be applicable for FDC product production. Solvent free methods such as MG and HME may be more favourable due to being seen as a “greener” technology that is better for the environment due to no harsh solvents being used. While thermolabile API manufacturing via MG and HME may be difficult, the work in this thesis has shown with the correct excipients and conditions chosen, product manufacture via these methods is possible. While solvent methods such as SD and SC may be seen as less favourable production techniques, they still have a vital role in developing formulations with desirable characteristics and release profiles.

## Acknowledgements

First and foremost, I wish to thank my supervisor, Professor Anne Marie Healy, for providing me with the wonderful opportunity of undergoing this PhD programme in Trinity College Dublin. Throughout the course of the PhD, she has been more than supportive and always has had time to discuss and find solutions to any issues that may have occurred, for which, I will be eternally grateful.

I would like to thank Science Foundation Ireland (SFI) for providing the funding which made this research possible in conjunction with the Department for the Economy of Northern Ireland. To my Queen's University Belfast colleagues on the project, Professor Gavin Andrews, Dr. Shu Li, Dr. Yiwei Tian, Dr. Ammar Almajaan, Dr. Zoe Senta-Loys, Dr. Bingyuan Lu and Gareth Gilvary, I wish to express my sincere gratitude for your input and insight into the project to make it the success it is today. I have to express a special word of thanks to my colleague on the project here in Trinity College Dublin, Dr. Atif Madi, for all his guidance and help throughout the course of our time here together. Atif was very generous with his time and was never too busy to help me in any way that he could.

To my fellow PhD students, whom I am fortunate enough now to call friends, my sincere thanks for all your support, encouragement and many a late night out and about around Dublin over the past four years. To Alan, Claire, Caoimhe, David, Emer, Erika, Fiona, Gloria, James, Johannes, Kate, Karl, Kieran, Michael, Ricardo and Svenja, I wish continued success and happiness for the future, wherever you may end up and whatever you may end up doing. Regarding my fellow PhD students, I could not write my acknowledgements without a special word of thanks to Emer for having to put up with me over the last four years in the confined space of our lab. I'm sure there were many days you were fit to kill me but always kept your cool. Wherever you end up in life, I'm sure the time spent there will be a walk in the park compared with the time spent having to put up with me! I would also like to thank all the postdocs in the lab who, whenever help was needed, were more than obliging to offer their time; Loli, Zelalem, May, Valerio, Dinesh and Stefano.

To all the technical staff in the School of Pharmacy, especially, Brian Talbot, Conan Murphy, Edelle Harris and Trevor Woods, thank you for all your help resolving technical, ordering and equipment issues over the past four years. A special word of thanks to Peter O'Connell for all your help regarding any HPLC queries and work in general. Even

though you’re a Tipperary man, you never held the fact that I’m from Cork against me when helping me out.

I have always considered myself lucky to have a great group of friends, many of whom have settled down in faraway places but always make the effort to support me in whatever I do. At times when I felt like quitting, they were the ones who provided me with encouragement and words of wisdom which kept me going. To Adrian, Brendan, Colm, Daniel, Declan, Paul, Tommy and Tony, I cannot thank each and every one of you enough.

I would like to thank my family for their unconditional support throughout the PhD, my brother, Sean, my sister, Siobhan, my father, John Joe, but especially my mother, Marion. My mother has always been my biggest supporter in every walk of life. She has always encouraged me to pursue my dreams and always emphasised the importance of education. Without you and your encouragement, I would not be where I am today. Words cannot adequately express my gratitude for all the sacrifices you have made for me throughout my life and from the bottom of my heart, thank you.

Finally, to my girlfriend, Evelyn, thank you for putting up with me and my mood swings over the last two years. I am forever grateful for the support you have provided me with through the good and the not so good times while completing this work. Hopefully I will be able to repay you somehow in the future.

## Publications and presentations

Publications Associated with the thesis:

- Kelleher, J. F., Gilvary, G.C., Madi, A.M., Jones, D.S., Li, S., Tian, Y., Almajaan, A., Senta-Loys, Z., Andrews, G.P., Healy, A.M. (2018) 'A comparative study between hot-melt extrusion and spray-drying for the manufacture of anti-hypertension compatible monolithic fixed-dose combination products', International Journal of Pharmaceutics. Elsevier, 545(1–2), pp. 183–196. https://doi.org/10.1016/j.ijpharm.2018.05.008
- Kelleher, J. F., Madi, A.M., Gilvary, G.C., Jones, D.S., Li, S., Tian, Y., Almajaan, A., Senta-Loys, Z., Andrews, G.P., Healy, A.M. (2020) 'Metformin Hydrochloride and Sitagliptin Phosphate Fixed-Dose Combination Product Prepared Using Melt Granulation Continuous Processing Technology' AAPS PharmSciTech. Springer https://doi.org/10.1208/s12249-019-1553-2

Other publications:

- Andrews, G. P., Jones, D.S., Senta-Loys, Z., Almajaan, A., Li, S., Chevallier, O., Elliot, C., Healy, A.M., Kelleher, J.F., Madi, A.M., Gilvary, G.C., Tian, Y. (2019) 'The development of an inline Raman spectroscopic analysis method as a quality control tool for hot melt extruded ramipril fixed-dose combination products', International Journal of Pharmaceutics. Elsevier, 566, pp. 476–487. https://doi.org/10.1016/j.ijpharm.2019.05.029
- Almajaan A., Healy A., Jones D., Gilvary G., Andrews G. P., Kelleher J. F., Li S., Tian Y., Senta-Loys Z. (2019) "Hot-melt co-extrusion technology as a manufacturing platform for anti-hypertensive fixed-dose combinations", British Journal of Pharmacy. 4(1). https://doi.org/10.5920/bjpharm.596

Oral presentations:

- "Fixed Dose Combination (FDC) products using advanced pharmaceutical processing techniques, a comparative study to assess the suitability of spray drying versus hot melt extrusion in the production of compatible monolithic FDC products." Oral presentation delivered at the United Kingdom and Ireland Controlled Release Society (UKICRS), University of Strathclyde, Scotland, May 2017. (J. F. Kelleher, G. C. Gilvary, Y. Tian, S. Li, G.P. Andrews, A.M. Madi, A.M. Healy)

- "The manufacture of Fixed Dose Combination (FDC) products using solvent and solvent-free methods of production" Oral presentation delivered at the Trinity College Dublin Seminar Series, TCD, Dublin, January 2018. (J. F. Kelleher, A.M. Madi, A.M. Healy)

Poster presentations:

- "Fixed Dose Combination (FDC) products using advanced pharmaceutical processing techniques", presented at the American Association of Pharmaceutical Scientists (AAPS) annual conference, Denver Convention Centre, USA, November 2016. (J. F. Kelleher, Y. Tian, S. Li, G.P. Andrews, A.M. Madi, Z.A. Worku, A.M. Healy)

- "A Comparative Study to Assess the Suitability of Spray Drying Versus Hot Melt Extrusion in the Production of Compatible Monolithic Fixed Dose Combination (FDC) products", presented at the All Ireland School of Pharmacy Conference, University College Cork, Ireland, April 2017. (J. F. Kelleher, G. C. Gilvary, Y. Tian, S. Li, G.P. Andrews, A.M. Madi, A.M. Healy)

- "A Comparative Study to Assess the Suitability of Spray Drying Versus Hot Melt Extrusion in the Production of Compatible Antihypertensive Monolithic Fixed Dose Combination (FDC) products", presented at the United Kingdom and Ireland Controlled Release Society (UKICRS), University of Strathclyde, Scotland, May 2017. (J. F. Kelleher, G. C. Gilvary, Y. Tian, S. Li, G.P. Andrews, A.M. Madi, A.M. Healy)

- "Manufacture of a Fixed Dose Combination Product for the Treatment of Type II Diabetes by Hot Melt Continuous Granulation" presented at the American Association of Pharmaceutical Scientists (AAPS) annual conference, Washington Convention Centre, USA, November 2018. (J. F. Kelleher, A.M. Madi, A.M. Healy)

## Abbreviations and symbols

| | |
|---|---|
| °(2θ) | Degree 2 theta |
| °C/min | Degree Celsius per minute |
| °C | Degrees Celsius |
| ANDA | Abbreviated new drug application |
| ACN | Acetonitrile |
| API | Active pharmaceutical ingredient |
| ASD | Amorphous solid dispersions |
| ANOVA | Analysis of variance |
| Ang | Angiotensin |
| ACE | Angiotensin converting enzyme |
| ARBs | Angiotensin receptor blockers |
| AIF | Angle of internal friction |
| AV | Atrioventricular |
| ATR - FTIR | Attenuated total reflectance Fourier transform infrared spectroscopy |
| BCS | Biopharmaceutical classification system |
| BP | Blood pressure |
| CCBs | Calcium channels blockers |
| CVDs | Cardiovascular diseases |
| cm/s | Centimeters per second |
| Ct | Concentration of the drug at time (t) |
| DSC | Differential scanning calorimetry |
| DPP-4i | Dipeptidyl peptidase-4 inhibitors |
| EMA | European Medicines Agency |
| EP | European Pharmacopoeia |
| ^Exo | Exothermic direction |
| FDC | Fixed dose combination |
| FF | Flow function |
| FBD | Fluidized bed dryer |
| FDA | Food and Drug Administration |
| $T_g$ | Glass transition temperature |
| $T_m$ | Melting temperature |
| GLZ | Gliclazide |
| GLP-1 | Glucagon like peptide-1 agonist |

| | |
|---|---|
| GLUT | Glucose transporter type |
| h | hours |
| HbA1c | Glycosylated haemoglobin |
| HDL | High Density Lipoprotein |
| HPLC | High performance liquid chromatography |
| HMCE | Hot Melt Co-Extrusion |
| HME | Hot melt extrusion |
| HMG-CoA | 3-hydroxy-3-methyl-glutaryl-CoA |
| HPC | Hydroxypropyl cellulose |
| HPMC | Hydroxypropyl methylcellulose |
| HPMC-AS | Hypromellose acetate succinate |
| IBAT | Ileal bile acid transport |
| IR | Immediate release |
| LC-MS | Liquid chromatography-mass spectroscopy |
| LDL | Low Density Lipoprotein |
| MPa | Megapascal |
| MG | Melt granulation |
| MET | Metformin hydrochloride |
| MCC | Microcrystalline cellulose |
| MR | Modified release |
| mDSC | Modulated differential scanning calorimetry |
| NDA | New drug application |
| PSA | Particle size analysis |
| PPARγ | Peroxisome proliferator-activated receptor |
| PEG | Polyethylene glycol |
| PTFE | Polytetrafluoroethylene |
| PXRD | Powder x-ray diffraction |
| PAT | Process analytical techniques |
| PCT | Proximal convoluted tubule |
| QbD | Quality by design |
| dc / dt | Rate of dissolution |
| RH | Relative humidity |
| RAAS | Renin–Angiotensin–Aldosterone System |
| rpm | Revolutions per minute |
| Cs | Saturation solubility of the drug |
| SEM | Scanning electron microscopy |

| | |
|---|---|
| SIM | Simvastatin |
| SA | Sinoatrial |
| SIT | Sitagliptin phosphate |
| SGLT | Sodium-glucose transporter |
| SD | Spray drying |
| SUs | Sulphonylureas |
| TGA | Thermogravimetric analysis |
| TZDs | Thiazolidinediones |
| TEC | Triethyl citrate |

## Origin and scope

Poor adherence to medication regimes contributes to the practice-outcome gap, in which clinical guidelines are implemented but expected benefits are not realised. For chronic conditions such as type II diabetes and cardiovascular diseases (CVDs), polypharmacy and complexity of treatment regimens are known to be two of the determinants of poor medication compliance (Yap et al. 2016). By simplifying regimens and reducing the pill burden, medication compliance increases, which translates to better clinical outcomes. Fixed dose combination (FDC) products provide us with a strong basis to reduce the pill burden by simply combining several active pharmaceutical ingredients (APIs) into one convenient dosage unit form. Statistically, the risk of non-compliance to medication regimens is reduced by 24 % - 26 % with FDC products (Bangalore et al. 2007).

Continuous manufacturing is relatively new in drug product manufacturing with increasing numbers of companies moving towards this method (instead of the traditional batch manufacturing method) as it promises to reduce manufacturing costs while also increasing the quality, agility and flexibility of products (Mascia et al. 2013). Built in process analytical techniques (PAT) and quality by design (QbD) allow continuous sampling of the product to be conducted during manufacturing. This allows any deviations from the process to be detected immediately and the manufacturing process halted, if required. Regulatory bodies have also started to implement new legislation regarding the continuous manufacturing process as its implementation becomes more widespread. For example, the Food and Drug Administration (FDA) states “a batch” in continuous manufacturing may be defined by a time stamp, amount of drug produced, or the amount of raw input material.

Hot melt extrusion (HME), melt granulation (MG) and spray drying (SD) are various techniques that may be used continuous manufacturing of solid dosage forms (Maniruzzaman and Nokhodchi 2016; Masters 2002), with spray coating (SC) also possibly being utilised to add additional APIs or specific characteristic polymers to form final products. In this thesis, the aim was to utilise these techniques in a continuous and semi-continuous manner in order to develop FDCs for the treatment of type II diabetes and CVDs. The overall aim of the thesis was to produce both established and novel combinations of APIs via the various manufacturing techniques outlined.

The scope of the thesis was to:

1. Produce solid oral dose FDC products with varying types of release profiles including; immediate release, delayed release and sustained release.
2. Investigate how different manufacturing techniques influence physicochemical properties of products as well as the manufacturability, product performance and physical stability of the FDC products prepared.
3. Identify the critical parameters of the various manufacturing techniques used and their influence on the final product characteristics.

# Chapter 1:

# Introduction

## 1.1 Diabetes Mellitus

Diabetes mellitus is a metabolic disorder associated with high blood glucose levels (hyperglycemia) as a result of defects in insulin secretion and/or insulin action (American Diabetes Association 2011). Glucose is vital in maintaining a person's health as it is the main energy source for cells that make up muscles and tissues. It is also the brain's main fuel source (Mayo Clinic 2018a). However, excess amounts of glucose in the bloodstream can result in severe medical complications. There are two main chronic forms of diabetes, type I and type II, which can generally be categorized by their respective pathogenesis, clinical presentation and treatment requirements (Figure 1.1). There are also two potentially reversible types of diabetes, prediabetes and gestational diabetes. Prediabetes is when an individual's blood glucose levels are higher than normal, but not high enough to be classified as diabetes. Gestational diabetes occurs during pregnancy when blood glucose levels reach levels high enough to be diagnosed with diabetes. Often once the pregnancy has been completed, blood levels return to normal (Mayo Clinic 2018a).

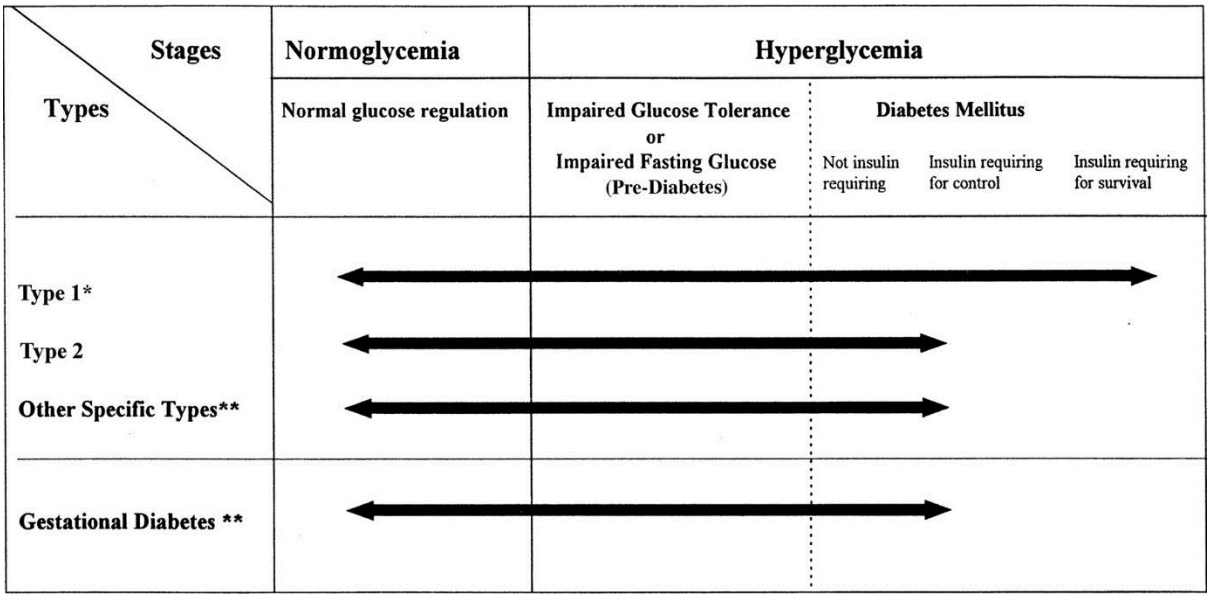


*Figure 1. 1: Disorders of glycemia: etiologic types and stages. *Even after presenting in ketoacidosis, these patients can briefly return to normoglycemia without requiring continuous therapy (i.e., "honeymoon" remission); **in rare instances, patients in these categories (e.g., Vacor toxicity (a type of rat poison), type I diabetes presenting in pregnancy) may require insulin for survival* (American Diabetes Association 2011).

### 1.1.1 Insulin and its role in diabetes

Insulin is a hormone excreted by the β-cells of the pancreas and is one of the hormones responsible for the control of blood glucose levels in the body. Insulin exerts its effects by signaling insulin-sensitive tissues to increase their glucose uptake by binding to specific receptors present on the cells of these tissues (Aronoff and Berkowitz 2004). Insulin binding to the specific insulin sensitive tissues, promotes glycogenesis in the liver and inhibits glucagon secretion from α-cells in the pancreas (Aronoff and Berkowitz 2004; Gerich et al. 1974). Glucose levels in the body are regulated by a feedback loop involving the β-cells in the pancreas and insulin sensitive tissues (Kahn et al. 1993). If insulin resistance is evident in insulin sensitive cells, the pancreatic β-cells maintain normal blood glucose levels by increasing insulin output. However, when the β-cells become unable to excrete sufficient quantities of insulin, blood glucose levels rise resulting in hyperglycemia (Kahn et al. 2014).

### 1.1.2 Type I Diabetes Mellitus

Type I diabetes mellitus is a disease that causes the insulin producing β-cells of the pancreas to be destroyed (Diabetes.co.uk 2018; Mayo Clinic 2018b). This results in the body being unable to produce sufficient quantities of insulin to regulate blood glucose levels. Type I diabetes, which was also previously known as juvenile or insulin dependent diabetes, usually appears during childhood or adolescence but can also develop in adults. It accounts for between 5 – 10 % of all diabetic cases.

Currently, there is no known cure for type I diabetes and due to the impairment of the pancreas to produce insulin, insulin treatment is necessary to treat the condition. Most people will get their insulin requirements via injection with insulin pens, but it may also be delivered via an insulin pump (Diabetes.co.uk 2018).

### 1.1.3 Type II Diabetes Mellitus

Type II diabetes mellitus is associated with diminished insulin secretion, impaired insulin action and increased hepatic glucose production (Stumvoll et al. 2005). It is seen as a complex condition, involving genetic and environmental factors and is often accompanied by other symptoms of metabolic syndrome, such as dyslipidemia and hypertension (Lin and Sun 2010). Type II diabetes mellitus accounts for about 90 % of all diabetes cases and is characterised by insulin resistance at target cells and a relative rather than absolute deficiency in insulin activity which is associated with type I diabetes mellitus (Zimmet et al. 2001). It was previously known as adult-onset diabetes or noninsulin dependent diabetes as it was primarily seen in middle aged adults over the age of 40. However, with the increased incidence and prevalence of obesity, type II diabetes has

become more common in younger populations (Barnett 2019). Figure 1.2 below, outlines several of the tissues and organs involved in the pathogenesis of type II diabetes.

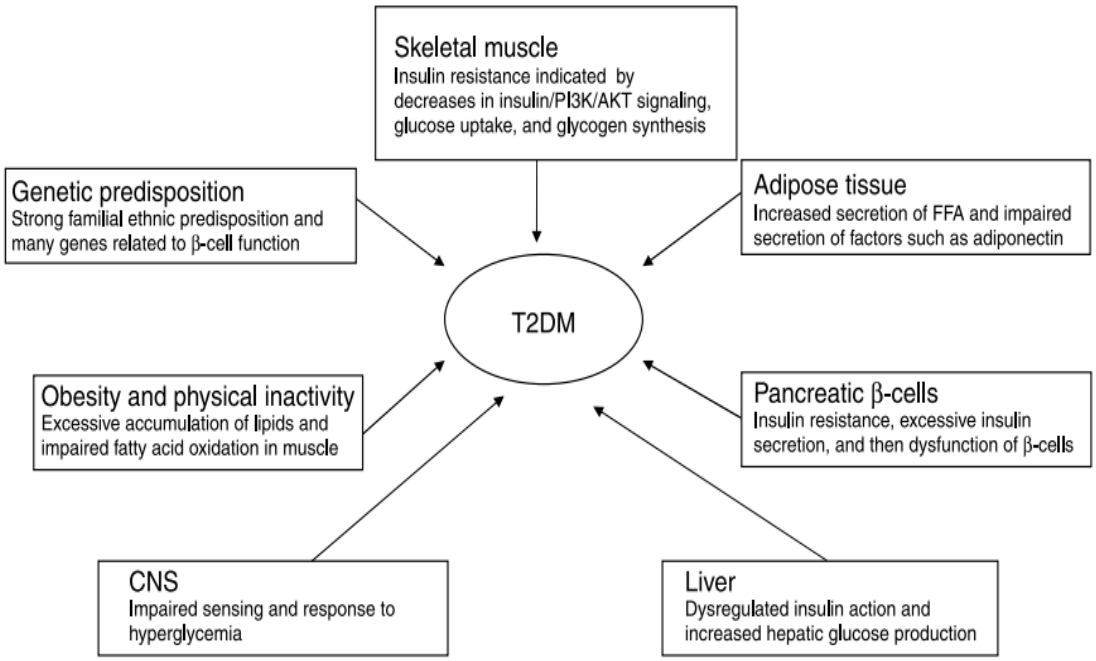


*Figure 1. 2:* Key factors involved in the pathogenesis of type II diabetes mellitus (Lin and Sun 2010). (T2DM = Type 2 diabetes mellitus, PI3K = Phosphoinositide 3-kinase, FFA = Free fatty acids).

### 1.1.4 Medical Management of blood glucose levels in type II diabetes

In the management of type II diabetes, the choice of therapeutic interventions should consider the long-term complications of the disease itself. As insulin resistance plays a substantial role in the pathogenesis of the disease, intervention should initially be aimed at improving tissue insulin sensitivity (Stumvoll et al. 2005). First steps often involve lifestyle intervention, with increased exercise and weight loss. These lifestyle interventions clearly reduce the risk of progression of impaired glucose tolerance to diabetes and can improve many of the cardiovascular risk parameters of the metabolic syndrome (Diabetes Prevention Program Research Group 2002). If lifestyle interventions are not satisfactory in reducing blood glucose levels, medical intervention is necessary. Figure 1.3 summarises the target mechanisms of the different classes of antidiabetic medications.

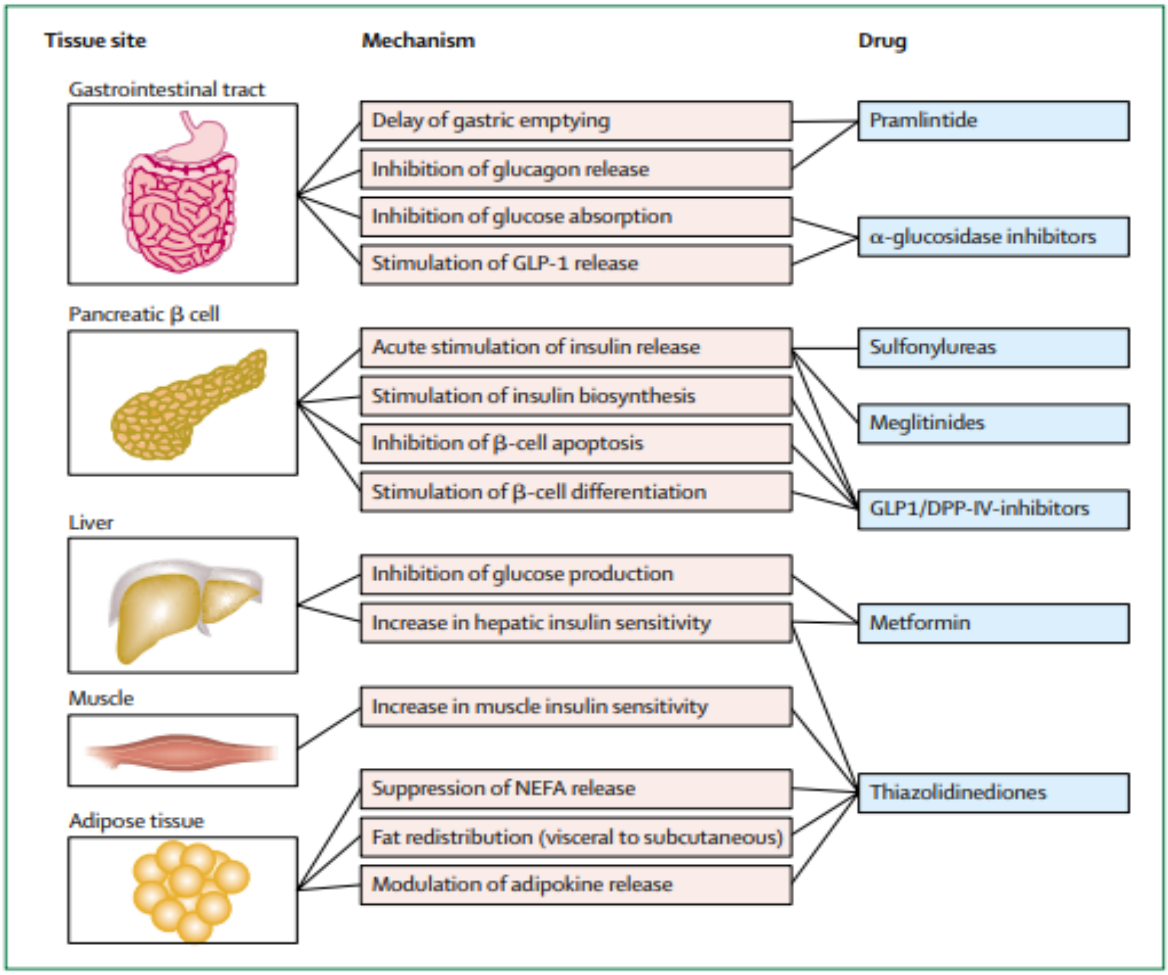


*Figure 1. 3:* Pharmacological treatment of hyperglycemia according to site of action (GLP1=glucagon-like peptide 1. DPP-IV=dipeptidyl peptidase IV) (Stumvoll et al. 2005).

#### 1.1.4.1 Biguanide (metformin)

Metformin (MET) is a biguanide with antihyperglycemic effects, lowering both basal and postprandial plasma glucose. It is the most widely used oral antidiabetic agent and has been marketed since 1957. The dose of MET may vary from 500 mg once daily up to 1000 mg three times daily depending on response. It does not stimulate insulin secretion and therefore does not induce hypoglycemia. MET may exert its effects via 3 mechanisms (Merck 2016):

- reduction of hepatic glucose production by inhibiting gluconeogenesis and glycogenolysis;
- in muscle, by increasing insulin sensitivity, improving peripheral glucose uptake and utilization;
- delaying intestinal glucose absorption.

MET is relatively cheap and has a very favorable cost benefit ratio associated with it (Inzucchi et al. 2012). MET is associated with initial gastrointestinal side effects; however, these may be overcome by advising the patient to take with or just after food.

#### 1.1.4.2 Sulphonylureas

Sulphonylureas (SUs) are the oldest oral antidiabetic agent and have been available since the early 1950s. The major adverse effect associated with SUs is hypoglycemia (Binder and Bendtson 1992; Marks and Teale 1999), which is due to the mechanism of action of the SUs. SUs reduce blood glucose levels by stimulating insulin secretion from the β-cells of the islets of Langerhans.

SUs are licensed as monotherapy in type II diabetes mellitus when diet, exercise and weight loss are not sufficient to control blood glucose levels (medicines.ie 2019d). However, most guidelines recommend them as monotherapy only when MET is contraindicated or not tolerated, and also as an add on agent to MET monotherapy when MET alone is unsatisfactory in reducing blood glucose levels (National Institute for Clinical Excellence 2018). Gliclazide (GLZ) is one of the most commonly prescribed SUs and is usually administered once a day.

#### 1.1.4.3 Thiazolidinediones

Thiazolidinediones (TZDs) or 'glitazones', as they are also commonly known, are a class of antidiabetic drugs that improve the glycemic control in patients with type II diabetes through the improvement of insulin sensitivity and reduction in hepatic glucose production (Hauner 2002; Yki-Järvinen 2004). TZDs exert their antidiabetic effects through a mechanism that involves activation of the gamma isoform of the peroxisome proliferator-activated receptor (PPARγ), a nuclear receptor.

#### 1.1.4.4 Meglitinides

Similar to the mechanism of the SUs, meglitinides analogs such as repaglinide, nateglinide, and mitiglinide exert their effects by binding to ATP-sensitive potassium channels causing them to close and subsequently opening the voltage-sensitive calcium channels, causing a release of insulin from the β cells (Malaisse 2003). The big advantage meglitinides analogs offer over long acting SUs is a reduction in the risk of undesirable hypoglycemia due to a weaker binding affinity and faster dissociation from its binding site (Malaisse 2003).

#### 1.1.4.5 The incretin-based agents (Glucagon like peptide-1 agonists and dipeptidyl peptidase-4 inhibitors)

Incretins are gut hormones that are secreted from enteroendocrine cells into the blood within minutes after eating (Kim and Egan 2008). They enhance insulin secretion in a glucose-dependent manner. The combined incretin response accounts for 50 – 70 % of total postprandial insulin production. Glucagon like peptide-1 agonist (GLP-1) is one of two incretin hormones that stimulate insulin release and inhibits glucagon secretion, suppresses gastric emptying, and reduces appetite and food intake (Drucker and Nauck 2006). Due to the short half-life (1.5 - 2 min) of GLP-1 (as it is degraded by dipeptidyl peptidase-4 (DPP-4)), continuous administration is required for maintenance of glucose homeostasis (Kim and Egan 2008).

Several studies observed that GLP-1 is degraded rapidly by DPP-4 (Deacon et al. 1995; Kieffer et al. 1995; Mentlein 1999) which led to the development of specific protease inhibitors called dipeptidyl peptidase-4 inhibitors (DPP-4i). Similarly, to GLP-1 agonists, DPP-4i preserve β-cell mass through stimulation of cell proliferation, stimulate insulin secretion and inhibit glucagon secretion (Drucker and Nauck 2006).

GLP-1 agonists previously had to be injected subcutaneously, but recently, a new oral solid dosage form (semaglutide) has been approved by the FDA. DPP4i are administered orally (Kim and Egan 2008)but do not have as potent an effect on blood glucose as GLP-1 agonists. DPP-4i, such as sitagliptin, and GLP-1 agonists, such as liraglutide, are licensed as dual therapy but can be used as monotherapy when MET is contraindicated (medicines.ie 2018, 2019f).

#### 1.1.4.6 Sodium-glucose transporter 2 (SGLT2) inhibitors

Glucose cannot permeate through the walls of the nephron because it is made of lipids and glucose is a polar compound. Hence glucose transporters which utilize ATP help transport glucose across the membrane. Two glucose transporters are located along the proximal convoluted tubule (PCT) of the nephron, sodium-glucose transporter 1 (SGLT1) and sodium-glucose transporter 2 (SGLT2) (Brown 2000).SGLT inhibitors prevent the reabsorption of glucose through these transporters. Medicines in the SGLT2 inhibitor class include canagliflozin, dapagliflozin, and empagliflozin.

#### 1.1.4.7 Insulin

As type II diabetes mellitus can be a progressive disease, some patients will require the use of insulin, however, the often complex dosing seen with type I diabetes mellitus is rarely required (Inzucchi et al. 2012). Insulin is the most effective of any antidiabetic agent at lowering blood glucose levels and can potentially decrease any HbA1c

(glycosylated haemoglobin) level to any therapeutic goal. Compared to type I diabetes, relatively large doses of insulin may be needed to overcome the insulin resistance associated with type II diabetes (Nathan et al. 2006). The major issues associated with insulin are the complications associated with delivery, the increase in weight experienced by the patient, the increased cost of therapy, and the potential for hypoglycemia.

#### 1.1.4.8 Combination therapy in type II diabetes mellitus

As type II diabetes mellitus is characterised by decreased insulin secretion and decreased insulin sensitivity in target tissues, most medications used to treat the condition only target one of the underlying causes of the disease. It has been reported in several studies that individual oral glucose lowering medications have limited efficacy and, as a result, they are commonly used in combination resulting in better clinical outcomes due to synergistic effects of the chosen medications (Home et al. 2007; Nauck et al. 2007; Russell-Jones et al. 2009; UK Prospective Diabetes Study Group (UKPDS) 1998). The National Institute for Health and Care Excellence (NICE) recommends monotherapy with MET alone when lifestyle and dietary change have not been successful to achieve target HbA1c (Figure 1.4). If MET is contraindicated or not tolerated, then an alternative monotherapy is chosen to achieve target levels. Due to the progressive nature of diabetes, monotherapy alone is usually insufficient after a period of time. A review conducted by Turner et al (Turner et al. 1999), which looked at patients between 1977 and 1997 with type II diabetes mellitus who presented at outpatient diabetes clinics in 15 UK hospitals concluded that, after 3 years of starting monotherapy, 50 % of patients needed additional therapy to achieve target HbA1c levels (< 7 %). This increased further to 75 % of patients after 9 years. The report highlights that most patients need multiple therapies to attain glycemic target levels in the longer term.

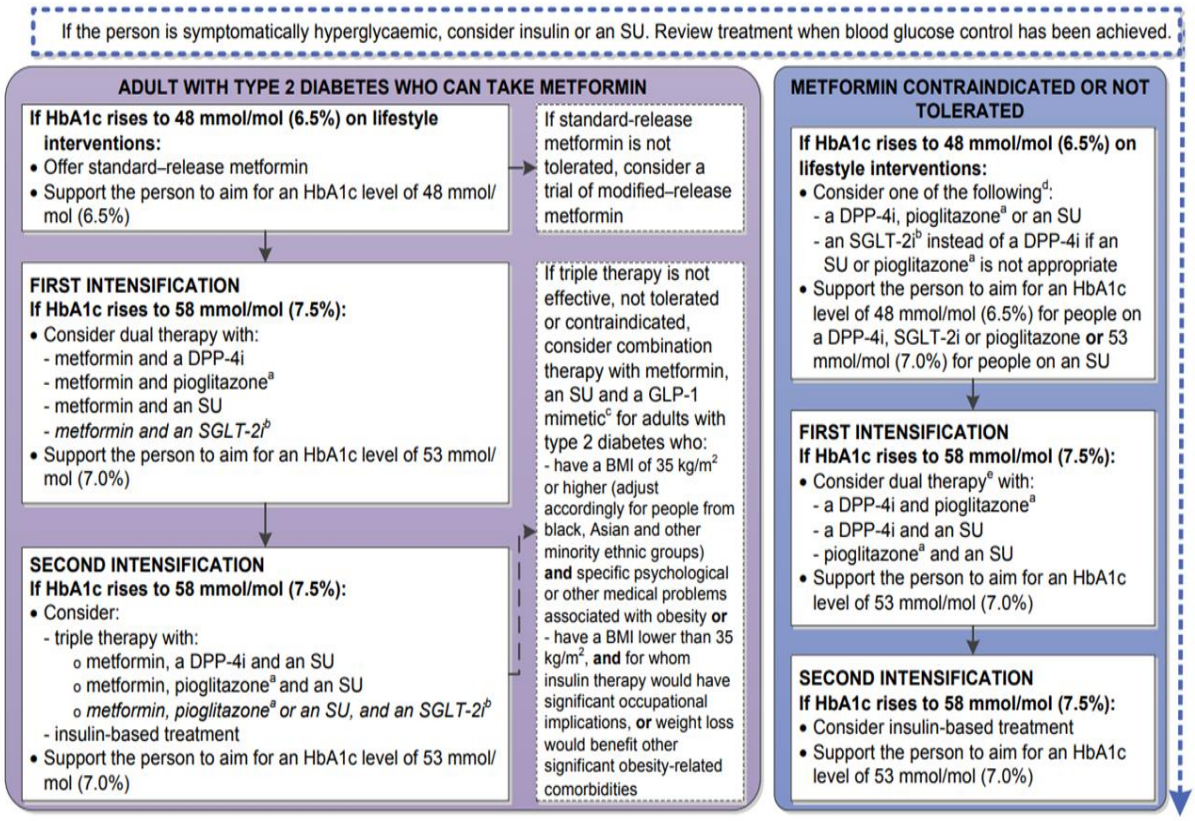


*Figure 1. 4: Management of type II diabetes in adults, NICE guideline NG28* (National Institute for Clinical Excellence 2018).

## 1.2 Cardiovascular Disease

Cardiovascular diseases (CVDs) refers to disorders of the heart and blood vessels and can include many specific diseases under this general heading. Such diseases may include, coronary heart disease, cerebrovascular disease, rheumatic heart disease and many other conditions. 17.7 million people die each year worldwide from CVDs which is an estimated 31 % of the total number of deaths (World Health Organisation 2017). Of these 17.7 million deaths, 80% are due to heart attacks and strokes. A heart attack (myocardial infarction) happens when the coronary arteries that supply blood to your heart muscle suddenly become blocked (Irish Heart Foundation 2019b). There are 2 different types of stroke; ischemic, which account for 80 % of strokes and which occurs when the arteries to the brain become narrowed or blocked causing severely reduced blood flow and hemorrhagic, which occurs when a blood vessel in the brain leaks or ruptures (Mayo Clinic 2019c). For both conditions, hypertension and hyperlipidemia are two of the main contributing factors.

## 1.3 Hypertension

Hypertension, which is more commonly known as high or raised blood pressure (BP), is a condition in which the blood vessels have constantly raised pressure (World Health Organization 2017b). BP tends to rise with age and therefore, because of increasing life expectancy in many countries, hypertension constitutes a major public health issue. For most people diagnosed (~ 95 %), there is no identifiable cause of the high BP. This type of high BP is called primary (essential) hypertension and tends to develop gradually over many years. For a minority of people (~ 5 %) they can attribute their high BP to an underlying condition. This type of high BP is called secondary hypertension and tends to appear suddenly. It is also usually associated with higher BP than that associated with primary hypertension. Some of the conditions associated with secondary hypertension include pheochromocytoma (tumor of the adrenal gland), hypothyroidism or hyperthyroidism, kidney disease, illicit or prescription drug use and chronic alcohol abuse.

### 1.3.1 Medical management of hypertension

First line management of people with elevated BP is education and advice on lifestyle activities and exercise. Patients should be offered advice on weight reduction, salt intake and reduced alcohol consumption to within recommended limits, as each of these factors are known to contribute to increased BP (Mancia and Grassi 2010). While lifestyle factors are important for BP reduction in mild to moderate hypertension, it must be remembered that their BP-lowering effect is generally modest and for some measures absent in the long term which means patients will need some form of pharmacological treatment. For example, restriction of sodium intake lowers BP in some patients with hypertension, but has no effect in others, and in rare cases actually triggers a BP increase due to stimulation of the sympathetic and the renin–angiotensin systems (Grassi et al. 2002).

When initiating people on antihypertensive medication, age, race and other medical conditions are factors that need to be considered when selecting an appropriate class of medication. Where possible, the recommended treatment should be initiated with a once daily regimen for convenience to the patient. Figure 1.5, adapted from NICE guideline 127 (National Institute for Health & Clinical Excellence 2019), outlines the preferred treatment regimens when starting on antihypertensive medication.

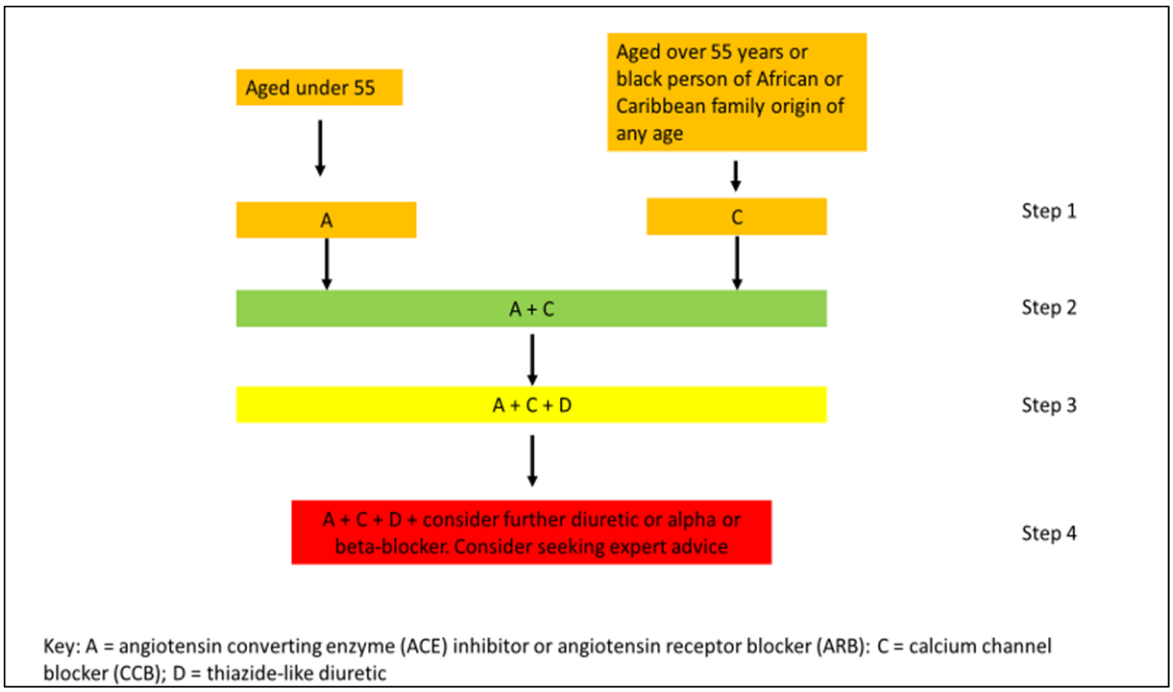


*Figure 1. 5:* Adapted from NICE clinical guideline 127 for treatment of hypertension. If a calcium channel blocker (CCB) is not tolerated in step 2, a thiazide-like diuretic may be considered instead (National Institute for Health & Clinical Excellence 2019).

#### 1.3.1.1 Renin–Angiotensin System (RAS)

The renin–angiotensin system (RAS), also known as the renin–angiotensin–aldosterone system (RAAS), is a hormone system that regulates blood pressure and fluid balance and it is here that angiotensin converting enzyme (ACE) inhibitors, angiotensin receptor blockers (ARBs) and renin inhibitors exert their desired antihypertensive effects. The RAS plays a major role in blood pressure regulation within the body.

##### 1.3.1.1.1 Angiotensin converting enzyme (ACE) inhibitors

In addition to targeting ACE in the RAS, resulting in decreased BP, ACE inhibitors also retard the degradation of bradykinin (Erdös 1977). The effects of ACE inhibitors on the RAS in humans is well documented. ACE inhibitors block the conversion of Ang I to Ang II resulting in decreased endogenous levels of Ang II and aldosterone and increased endogenous levels of Ang I (BRUNNER et al. 1979) due in part to loss of feedback inhibition (Vander and Geelhoed 1965). It has also been proposed that, due to the inhibition of ACE converting Ang I to Ang II, Ang I is converted to another metabolite, Ang-(1-7), a vasodilator (Ambühl et al. 1994), and it is thought to potentiate the antihypertensive effects of ACE inhibitors (Ferrario 1998).

The majority of ACE inhibitors are prodrugs converted by hepatic esterolysis to a major active diacid metabolite. For example, ramipril is converted to ramiprilat in the liver, which in turn, exerts the reduction in BP effects (Zisaki et al. 2015). The prodrug formulation allows for greater oral bioavailability. Depending on the half-life of the chosen ACE inhibitor, administration is recommended once or twice a day. Ramipril, captopril and enalapril are some of the most commonly prescribed ACE inhibitors.

#### 1.3.1.1.2 Angiotensin receptor blockers (ARBs)

ARBs exert their effects on the RAS. ARBs work by inhibiting the effects of Ang II, which causes constriction of blood vessels, increased salt and water retention and activation of the sympathetic nervous system, as previously described (Folkow et al. 1961). For Ang II to produce its effects in the body, it must bind to its receptor, in much the same way that a key must fit into a lock to open a door. ARBs prevent Ang II from binding to its receptor and thus reduce the effects of Ang II. All ARBs can be used to treat hypertension (Terra 2003).Valsartan, losartan and candesartan are some of the most commonly prescribed ARBs.

#### 1.3.1.1.3 Renin inhibitors

Renin inhibitors target the first and rate-limiting step of the RAS, namely the conversion of angiotensinogen to Ang I by binding to the active site of renin and this inhibits the binding of renin to angiotensinogen (Brown 2006). This leads to an absence of Ang II based on the rationale that renin only acts to inhibit this step, unlike ACE which is also involved in other biochemical reactions. Aliskiren is the first and only oral renin inhibitor on the market to be approved for the treatment of hypertension. It has been shown to be well tolerated over 6-12 months and effectively lowers BP (SICA 2006). Figure 1.6 gives an overview as to how the RAS is targeted at various steps to help reduce BP.

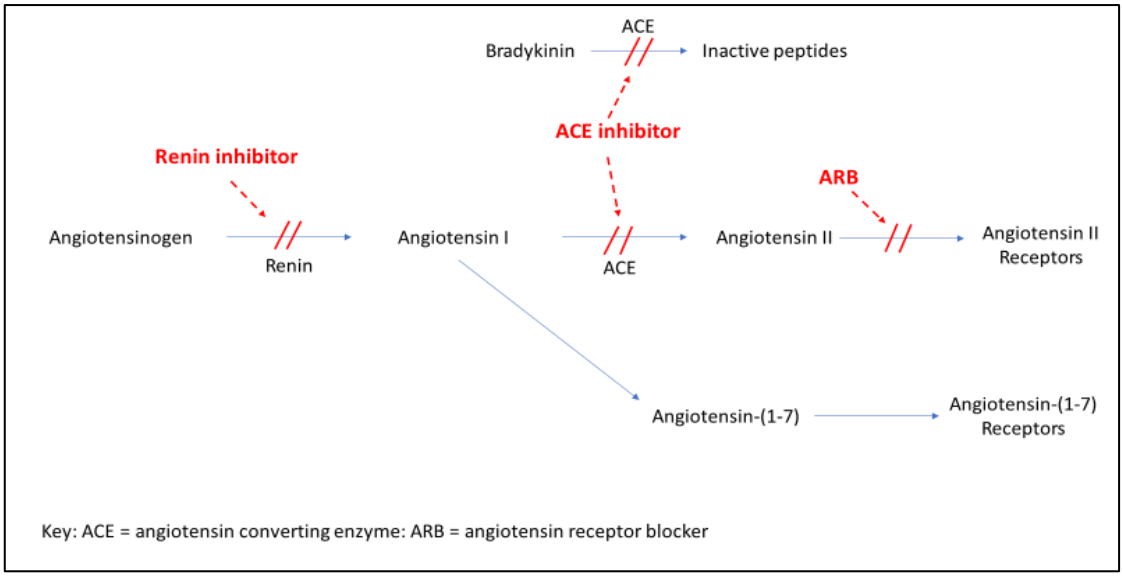


*Figure 1. 6:* Basic renin–angiotensin system (RAS) and target drug sites to reduce hypertension.

### 1.3.1.2 Calcium channel blockers (CCBs)

Calcium channels blockers (CCBs) are used for the treatment of many CVDs, including hypertension. They fall into two different classes depending on their chemical structure and target therapeutic area: the dihydropyridine CCBs and the non-dihydropyridine CCBs. CCBs inhibit the flow of extracellular calcium through ion-specific channels that span the cell wall. Currently available CCBs inhibit the $_{L}$-type channels in humans. Blockade of $_{L}$-type channels in vascular tissues results in the relaxation of vascular smooth muscle and in cardiac tissue results in a negative inotropic effect (Abernethy and Schwartz 1999). The non-dihydropyridine CCBs, such as verapamil and diltiazem, target the cardiac calcium channels causing cardiac depression more than targeting the vascular smooth muscles that cause vasodilation. They have negative effects at the sinoatrial (SA) and atrioventricular (AV) nodes, and cause reductions in heart rate and contractility (Regier and Downey 1997). On the other hand, the dihydropyridine CCBs, such as amlodipine and nifedipine, are more vascular selective and have fewer cardiac effects as they do not suppress AV conduction or SA node automaticity (Regier and Downey 1997). Although both the dihydropyridine CCBs and the non-dihydropyridine CCBs bind to $_{L}$-type calcium channels, the reason they have different selectivity is due to them binding at different sites on the channel (Elliott and Ram 2011).

### 1.3.1.3 Thiazide and thiazide-like diuretics

Thiazide and thiazide-like diuretics are among the most frequently used medications for hypertension treatment and have been available for well over 50 years (Duarte and

Cooper-DeHoff 2010). Compounds falling into the thiazide class of diuretics, such as hydrochlorothiazide and chlorothiazide, contain the benzothiadiazine parent structure in their chemical makeup. Thiazide-like diuretics, such as indapamide and metolazone, have the same mechanism of action as the thiazides but do not have the benzothiadiazine core structure. These diuretics help to control hypertension by inhibiting reabsorption of sodium and chloride ions from the distal convoluted tubules in the kidneys by blocking the thiazide-sensitive sodium-chloride cotransporter (Ellison et al. 1987; Obermuller et al. 1995). By decreasing sodium reabsorption back into the interstitium, thiazide use acutely results in an increase in fluid loss to urine, which leads to decreased extracellular fluid and plasma volume. This reduction in volume results in diminished venous return, increased renin release and reduced cardiac output (Conway and Lauwers 1960). Total peripheral resistance is reduced resulting in a decreased BP.

#### 1.3.1.4 Beta-blockers (β-blockers)

β-blockers aren't usually prescribed for BP until other medications haven't worked effectively. β-blockers, also known as β-adrenergic blocking agents, are medications that reduce BP by blocking the effects of the sympathetic nervous system hormone epinephrine, also known as adrenaline i.e. they are competitive antagonists (Gorre and Vandekerckhove 2010). β-blockers prescribed for BP target $\beta_1$-selective adrenoreceptors which are mostly present in the heart. By blocking these receptors, epinephrine is unable to induce its effect resulting in reduced heart rate as well as reduced force of contraction (Gorre and Vandekerckhove 2010). Atenolol, bisoprolol and propranolol are some of the most frequently prescribed β-blockers for BP.

#### 1.3.1.5 Alpha-blockers (α-blockers)

α-blockers, also called α-adrenergic antagonists, can be prescribed to treat high BP when other treatments have failed to satisfactory reduce BP or are not suitable e.g. doxazocin. As with β-blockers, α-blockers act by blocking the effect of nerves in the sympathetic nervous system. Specifically, $\alpha_1$ receptors are targeted in the treatment of hypertension by α-blockers. $\alpha_1$ receptors can be found in most vascular smooth muscle, the heart, the prostate, and pilomotor smooth muscle. α-blockers work by keeping the hormone norepinephrine (noradrenaline) from binding with its target receptors which results in the relaxation of the muscles in the walls of smaller arteries and veins, which causes the vessels to remain open and relaxed. This improves blood flow and lowers BP (Mayo Clinic 2019a).

## 1.4 Hyperlipidemia

Hyperlipidemia, which is more commonly known as high cholesterol, is a condition where there is an abnormally high concentration of fats or lipids in the blood. While cholesterol is often viewed negatively, it is needed in the body to continue to produce healthy cells. It is when there is an excess amount of this waxy substance that problems can occur. Due to the excess, fatty deposits can develop in the blood vessels. These deposits can eventually make it more difficult for enough blood to flow through the arteries and veins meaning cells can be deprived of their required oxygen content, resulting in a heart attack or stroke. High cholesterol can be inherited but is more likely to be caused by a lack of exercise and a poor diet.

When referring to cholesterol in the body, we are referring to a substance made up of three different constituents; HDL cholesterol (High Density Lipoprotein); LDL cholesterol (Low Density Lipoprotein); and triglycerides.

### 1.4.1 Medical management of hyperlipidemia

Hyperlipidemia has no symptoms, therefore, the only way to diagnose the condition is to have a blood test undertaken (Mayo Clinic 2019b). Like other conditions, lifestyle advice and exercise are the first line treatments before initiating pharmacological management of the condition. Diet plays a crucial role in hyperlipidemia management. People are encouraged to increase the amounts of monounsaturated and polyunsaturated fats in their diet, as these fats help to reduce LDL cholesterol in the blood, and to avoid saturated and trans fats, as these increase LDL cholesterol concentrations. People are advised to eat more fresh fruit and vegetables, less fatty foods and eat oily fish such as salmon at least twice a week to achieve these fat consumption goals. Alcohol consumption should be reduced, and smoking stopped as it can damage the walls of blood vessels making it easier for fatty acid deposits to stick. Thirty minutes of exercise on at least 5 days per week should be undertaken as exercise has been shown to increase the amount of HDL cholesterol in the blood and reduce the concentrations of LDL cholesterol (Irish Heart Foundation 2019a; Mayo Clinic 2019b). If lifestyle advice and exercise are unsatisfactory in preventing hyperlipidemia, pharmacological interventions should be undertaken. The choice of treatment will depend on the composition of the three main cholesterol constituents and the target cholesterol levels of the patient being treated.

#### 1.4.1.1 3-hydroxy-3-methyl-glutaryl-CoA (HMG-CoA) reductase inhibitors (Statins)

Most mammalian cells can produce cholesterol even though the biosynthesis of cholesterol is a very complex process involving more than 30 enzymes (Tobert 2003). Figure 1.7 shows a simplified version of the cholesterol biosynthetic pathway and where statins enact their effects. HMG-CoA reductase is the rate-limiting enzyme in the cholesterol biosynthetic pathway. HMG-CoA is water soluble and there are alternative metabolic pathways for its breakdown when HMG-CoA reductase is inhibited, so that there is no build-up of the intermediate, meaning it is an appropriate step to target in the pathway. Statins are chosen as first line therapy for patients with high LDL-cholesterol as they have been shown to be very effective in reducing this type of cholesterol. Statins, such as simvastatin, fluvastatin and pravastatin are usually recommended to be taken at night due to the body's natural cycle of increased cholesterol synthesis at nighttime. Atorvastatin, another statin, may be taken at any time of the day as results have shown administration time does not affect the overall lipid reduction seen with this compound (Plakogiannis et al. 2005).

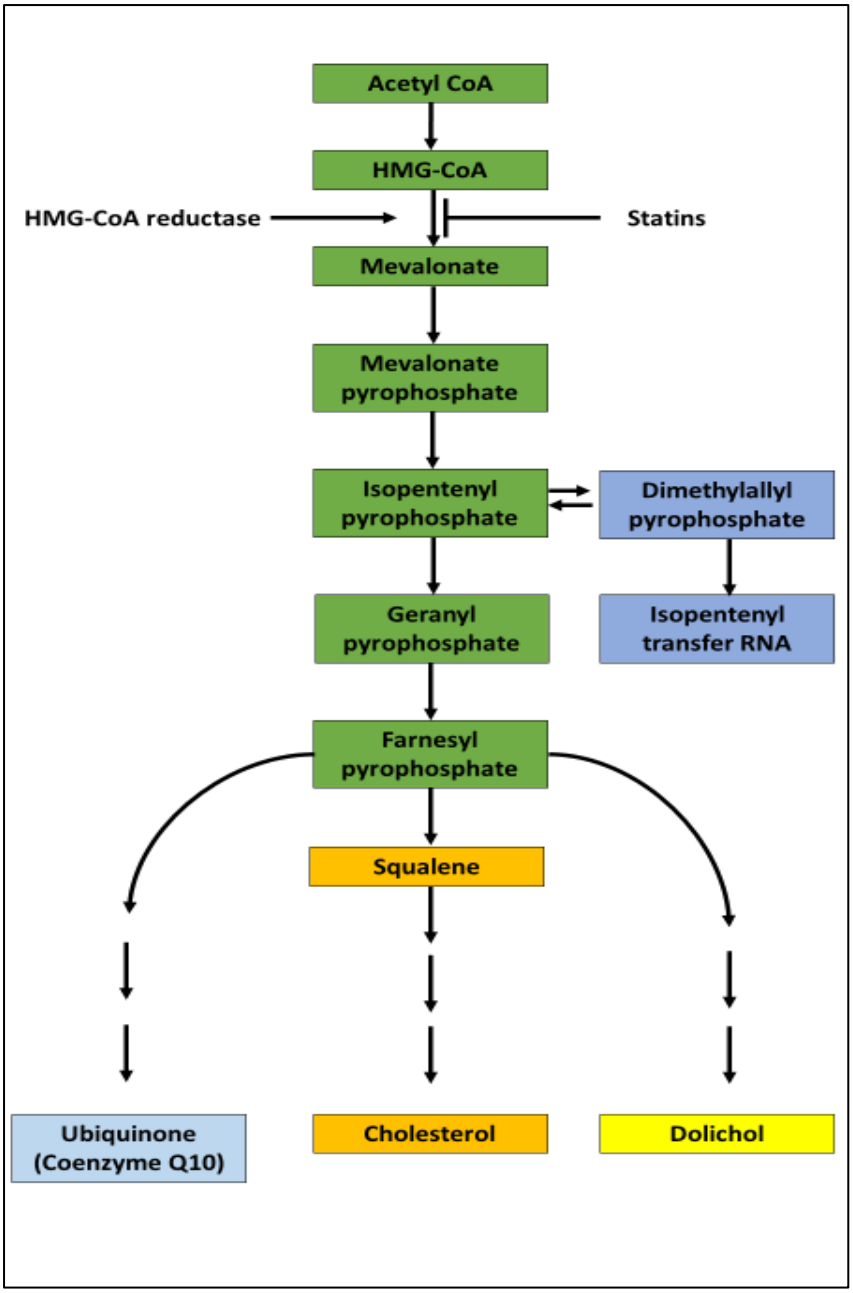


*Figure 1. 7:*The cholesterol biosynthesis pathway (Tobert 2003).

### 1.4.1.2 Fibric acid derivatives (Fibrates)

For patients suffering from high triglycerides or low HDL cholesterol concentrations, the fibrate class of therapeutic agents have been shown to be the best option for successful treatment e.g. fenofibrate. The fibrates exert their mechanism by activating the peroxisome proliferator-activated receptor alpha (PPAR-α) 1 receptor in the liver. This in turn, stimulates lipoprotein lipase and/or hepatic lipase activity resulting in increased oxidation of fatty acids and breakdown of lipoprotein production by the liver (Evans et al. 2003; Muscari et al. 2002). The primary clinical effect seen with fibrate therapy is a

reduction of triglycerides by 30 – 40 % and an increase in HDL cholesterol concentration by 8 – 15% (Evans et al. 2003).

#### 1.4.1.3 Cholesterol absorption inhibitors

Naturally occurring cholesterol absorption inhibitors include phytostanols and phytosterols. These compounds work by competing for incorporation into mixed micelles which absorb cholesterol from the gastrointestinal tract and as a result this reduces the amount of cholesterol absorbed. Irrespective of age, gender, ethnic background, body weight, background diet, or the cause of hypercholesterolemia, phytostanols and phytosterols at 2 g/day significantly lower LDL cholesterol concentration by 8 % – 10 % (Gylling and Simonen 2015). The first synthetic cholesterol absorption inhibitor, ezetimibe, has been approved for use in Ireland and the UK since 2003.

#### 1.4.1.4 Bile acid transport inhibitors

The bile acid transport inhibitors include both bile acid binding resins, such as cholestyramine, and specific inhibitors of ileal bile acid transport (IBAT), mediated by a specific apical $Na^+$ / bile acid transporter (Evans et al. 2003). The IBAT, is a key element in the enterohepatic circulation of bile acids. It is an integral brush border membrane glycoprotein mainly expressed in the distal ileum of the intestine, and is responsible for the reabsorption of about 95 % of the intestinal bile acids that are recirculated to the liver via portal venous blood (Graffner et al. 2016). About two to five grams of bile is continuously being recycled from the liver to the gut with relatively small amounts being lost in the stool. By blocking the reuptake process, faecal bile acid loss is increased. To replenish the supply of bile acids required, the liver converts cholesterol to bile which results in a reduction in hepatocyte cholesterol and an up regulation of LDL cholesterol receptors. Cholestyramine has proved an effective therapy to reduce LDL cholesterol concentration, however it is often poorly tolerated due to its mechanism of action (Williams et al. 1991).

#### 1.4.1.5 Nicotinic acid

Nicotinic acid (also known as niacin) is vitamin B3, which occurs naturally in food. Used as a medication for the treatment of hyperlipidaemia, it works by raising HDL cholesterol levels while also reducing LDL cholesterol and triglyceride concentrations. Niacin is more effective than fibrates at increasing HDL cholesterol and may be considered an alternative or an addition to fibrate treatment (Carlson 2005).

## 1.5 Pharmaceutical solids - Oral dosage forms

The majority of Active Pharmaceutical Ingredients (APIs) are formulated as solid oral dosage forms such as tablets and capsules. These dosage forms offer many advantages from a formulation and manufacturing point of view but also from a patient's perspective. They can be produced in a non-sterile environment and the process, equipment, and technology are well defined and known. Scale up from lab to industrial size manufacture is relatively straight forward and overall the costs associated with such dosage forms are generally lower when compared to other products for other routes of administration. For the patient, the oral route offers the most convenient and socially acceptable way of drug administration as it is non-invasive and easy to administer (Fasano 1998; Sastry et al. 1997, 2000). It is also possible to add additional excipients to be used as taste masking agents, such as sugar coatings, to encourage patient compliance for an otherwise non-pleasant tasting solid dosage form. The oral route also allows a vast number of different types of targeted drug releases to occur. It can be used to target the gastrointestinal tract locally or target systemic circulation through absorption. Antacids, such as magnesium carbonate and calcium carbonate, act locally within the stomach to reduce the amount of stomach acid present. Certain steroid compounds contained in solid dosage forms are released over time along the gastrointestinal tract to target inflammation in conditions such as ulcerative colitis and Crohn's disease e.g. budesonide modified release capsules. For many other medications administered by the oral route the goal is to enter systematic circulation, so once dissolved, they travel across the intestine into the circulatory system, exhibiting their effect elsewhere in the body.

Oral solid dosage forms are associated with some disadvantages also. Children, the elderly and any patient with swallowing difficulties can find it difficult to take solid oral forms and as a result may need alternative methods of administration (Lopez et al. 2015). To overcome these swallowing issues, novel formulations such as oral disintegrating films and mini-tablets are currently being developed to allow patients be administered their medications through the preferred oral route of administration (Preis 2015). From a manufacturing point of view, difficulties with tableting or capsule filling along with both physical and chemical instability of APIs can lead to unfavourable final products being produced. For example, amorphous or low-density APIs can be difficult to compress into tablets. The force needed to successfully compress these types of APIs may, as a result, cause changes to the desired physicochemical characteristics e.g. amorphous API crystallising to a different polymorph. Some of the most common problems associated with tableting are capping, sticking or poor flowability of the formulation. Ideally, avoiding a formulation change to overcome the challenge of capping

or sticking, would be preferable for most situations. By varying the pre-compression times and force, dwell times and the final compression force in the tablet press, these issues may be overcome without the need of additional excipients (Stahl 2014). If additional excipients are found to be required, the most common approach is to add a lubricant or glidant to the formulation. These substances can be used at low concentrations to prevent sticking to surfaces but also to increase flowability by reducing interparticular friction and decreasing surface charge. Some of the most common lubricants and glidants used are magnesium stearate, silica and microcrystalline cellulose. Additionally, newer technologies such as 3D-printing, hot melt extrusion, spray drying, spray coating etc. can help overcome some of these common manufacturing issues seen with older manufacturing technologies (Agrawal et al. 2013; Williams et al. 2010).

## 1.6 Crystalline and amorphous forms of the solid state

The solid state is the most commonly encountered and therefore the most relevant and important state for pharmaceutical development. Solid particles can show differences externally or internally. External differences are referred to as the shape, habit, or morphology of the particles, where the internal structures that make up the solid particles remain the same (Zhang and Zhou 2009). The internal solid state of a substance can, in effect, be divided into three categories depending on the structure of the degree of long-range order: crystalline, liquid crystalline and amorphous, as shown in figure 1.8.

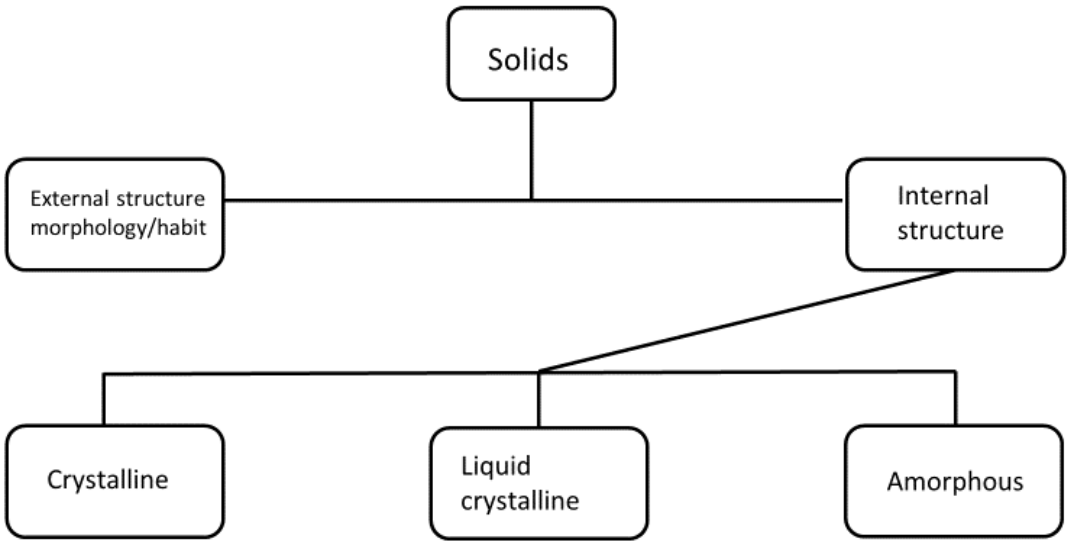


*Figure 1. 8: Solids can be categorised into three groups based on the degree of long-range order in their internal structure: crystalline, liquid crystalline and amorphous.*

### 1.6.1 Crystalline Solids

Crystalline solids exhibit a three-dimensional long-range order in which the structural units, termed unit cells, are repeated regularly and indefinitely in three dimensions in space. The unit cell has a definite orientation and shape defined by the translational vectors, *a*, *b*, and *c*, and hence has a definite volume, *V*, that contains the atoms and molecules necessary for generating the crystal. Different crystalline forms can exist, such as solvates and polymorphs.

Solvates, which can also be referred to as pseudopolymorphs, are crystalline solids containing solvent molecules incorporated into the crystal structure, either in stoichiometric or nonstoichiometric amounts giving rise to unique differences in the

pharmaceutical properties of the drug (Vippagunta et al. 2001). If the solvent molecule incorporated into the crystal structure is water, it is termed a hydrate. Solvates tend to crystallise more easily than single API molecules because the solvent can potentially form hydrogen bonds with the API molecules in the crystal lattice, or can contribute to adduct-induced conformational changes (Giron et al. 2004). Desolvated solvates are produced when a solvate loses its solvent molecules but the crystal retains the structure of the solvate (Byrn et al. 1994). Desolvated solvates are considered less ordered than their crystalline counterparts (due to an increase in the free volume within the crystal structure) and are difficult to characterize, because analytical studies indicate that they are unsolvated materials (or anhydrous crystal forms) when, in fact, they have the structure of the solvated crystal form from which they were derived (Byrn et al. 1995). These structural differences can lead to variations in solubility and dissolution from what otherwise would be expected of the anhydrous form.

As well as solvates, crystalline materials have the ability to exist as polymorphs. Polymorphism is the ability of solid materials to exist in two or more crystalline forms with different arrangements or conformations of the constituents in the crystal lattice (Raza 2014). In simple terms, crystal polymorphs have the same chemical composition but have different internal packing structures. This difference in structure allows for very different physicochemical properties to be present based on the polymorph. Overall, polymorphism can be divided into four categories: conformational polymorphism, packing polymorphism, synthon polymorphism and tautomeric polymorphism. Conformational polymorphs involve flexible molecules that can adopt more than one conformation in the solid state. Conformational polymorphism can be defined as molecular moieties with varied rotational degrees of freedom which can result in different conformations in the unit cell. Occasionally, more than one conformer is present in the same crystal structure (Nangia 2008). Packing polymorphism involves different packing arrangements of conformationally rigid molecules (Lee et al. 2011). In this structure, identical moieties pack into different periodic crystal structures resulting in differing physicochemical properties. Synthon polymorphism occurs when the primary synthons in the forms are different (Babu et al. 2010). These polymorphs can differ in their primary hydrogen-bond motifs. Interactions between molecules can occur via supramolecular synthons which can be assembled by known intermolecular interactions (Healy et al. 2017). Supramolecular synthons are spatial arrangements of intermolecular non-covalent interactions that frequently occur in supramolecular structures. They can, therefore, be relied upon to generate supramolecular functional materials. Molecules which have multiple hydrogen bonding sites are more inclined to form synthon polymorphs.

Tautomeric polymorphism exists when different tautomers of an API crystallise and co-exist in equilibrium in multiple crystal forms (Childs and Hardcastle 2007). A tautomer constitutes two or more isomers of a compound which exist together in equilibrium and are readily interchanged by migration of an atom or group within the molecule. Tautomers that interconvert in solution rapidly between isomers are considered to be the same compound, and therefore can be classed as polymorphs. However, tautomers that interconvert slowly are classed as different compounds (Bhatt and Desiraju 2007). This can, however, be subjective, as interconversion can be temperature dependent.

As different polymorphs and solvates result in different crystal packing, and/or molecular conformation, the differing lattice energy and entropy usually results in varying physicochemical properties being displayed. Density, melting point, enthalpy of fusion, solubility, dissolution, hardness, tabletability and even colour are some of the properties that can be affected (Grant 1999). These differences in physicochemical properties have an important effect on the processing of API into drug product for distribution to a patient population. Changes in solubility and dissolution properties may ultimately affect the desired clinical outcome for the patient and it is imperative that the appropriate screening for polymorphic forms of API are carried out prior to development (Miller et al. 2005). To prevent polymorphic changes occurring throughout processing and subsequently, during storage, the lowest energy polymorph is generally the most desirable as the polymorph for development, as it is the most stable solid state form of the API, although this is commonly the polymorph with the lowest dissolution rate and solubility (Miller et al. 2005). Even though polymorphism of drugs has been known since the 1960s and screening tools are available, there are several high-profile cases of drug products having to be withdrawn from the market due to polymorphism issues. Norvir® (ritonavir), used in the treatment of AIDS, was identified as having only one polymorphic form during the drug development stage (form I). However, in 1998, several lots of the product failed the dissolution test due to the appearance of a new polymorphic form (named form II) that had formed during the manufacturing process, which was more stable but not very soluble when compared to form I (Bauer et al. 2001; Chemburkar et al. 2000). Thus, the medication was removed from the market due to the inability to manufacture the desired polymorphic form (form I). A similar situation occurred with rotigotine (Neupro®), a drug used in the treatment of Parkinson's disease administered via a transdermal patch. Originally licensed as a polymorphism-free API, in 2008, rotigotine was removed from the market due to the transformation into a less soluble polymorphic substance that had crystallized and was not absorbed by the skin (Goldbeck et al. 2011).

### 1.6.2 Liquid Crystals

Liquid crystals are a state of matter which have properties between those of conventional liquids, such as fluidity and formation of droplets, and those of solid crystals, such as having a periodic arrangement of molecules in one or more spatial arrangements (Andrienko 2018). A mesophase is a liquid crystal state in which molecular groups are regularly oriented so as to show optical anisotropy. Depending on the arrangement of the molecules in a mesophase, or its symmetry, liquid crystals are subdivided into several groups e.g. nematics, cholesterics, smectics, and columnar mesophases (figure 1.9). In a nematic mesophase, molecules possess a long-range orientational order with molecular long axes aligned along a preferred direction. There is no long-range order in the positions of centres of mass of molecules. The cholesteric mesophase is similar to the nematic: it has a long-range orientational order, but no long-range positional order of the centres of mass of molecules. It differs from the nematic mesophase in that the director varies throughout the medium in a regular way even in an unstrained state. The important feature of a smectic mesophase is its stratification. The molecules are arranged in layers and exhibit some correlations in their positions in addition to the orientational ordering. Smectic mesophases can be further split into smectic A, B and C. Smectic A mesophases have molecules aligned perpendicular to the layers. In smectic B, there is a hexagonal crystalline order between the layers, while smectic C have a biaxial symmetry. The columnar mesophase is a class of liquid-crystalline phases in which molecules assemble into cylindrical structures. Originally, these liquid crystals were called discotic liquid crystals because the columnar structures are composed of stacked flat-shaped “discotic mesogens” which are typically composed of an aromatic core surrounded by flexible alkyl chains. (Oswald et al. 2005).

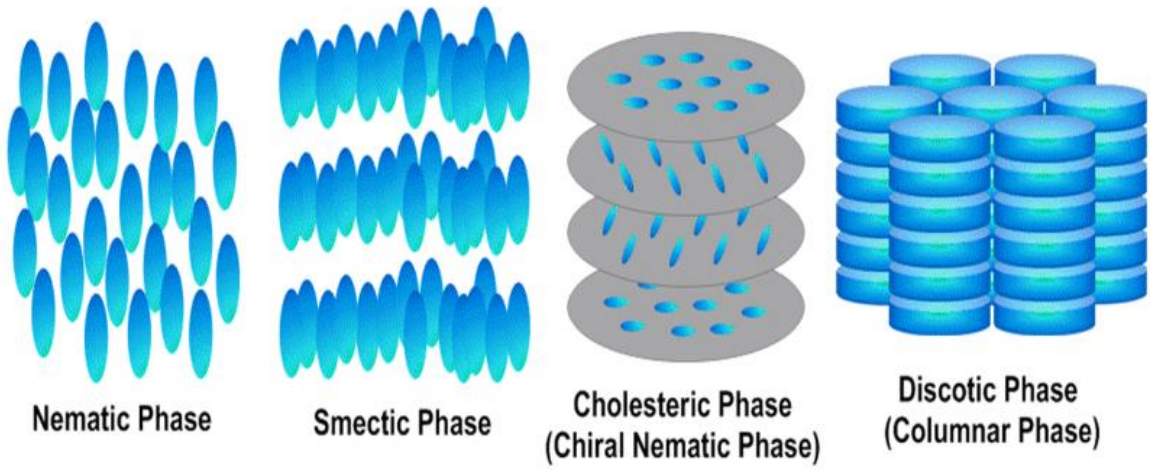


*Figure 1. 9: Visual representation of the different liquid crystal states* (Tokyo Chemical Industries 2015)

### 1.6.3 Amorphous Solids

As opposed to the crystalline state, where three-dimensional long-range order is seen, the amorphous state has no long-range repeating structures, with individual molecules randomly orientated relative to one another. As the amorphous state can exist in a variety of conformational states, each constituent molecule experiences slightly different inter and intra-molecular interactions (Hancock 2002). Amorphous materials do not display a melting temperature, instead they display a glass transition temperature ($T_g$) (figure 1.10). The $T_g$ is always lower than the melting temperature of the crystalline state of the material, if such a state exists. Below the $T_g$, the amorphous material exists in a nonequilibrium state (also known as a supercooled liquid or lower viscosity rubbery state) and behaves like a brittle solid or "glass" (Baghel et al. 2016). The $T_g$ is a temperature range over which the amorphous regions change from a brittle glassy state to a flexible rubbery state as they are heated. It is a second order thermodynamic transition characterized by a step change in the heat capacity which is also associated with change in thermodynamic properties such as entropy and enthalpy (Stillinger 1988). The amorphous form of a drug displays higher apparent solubility as it has a higher enthalpy, entropy, free energy, and volume as compared with the crystalline form (Baghel et al. 2016).

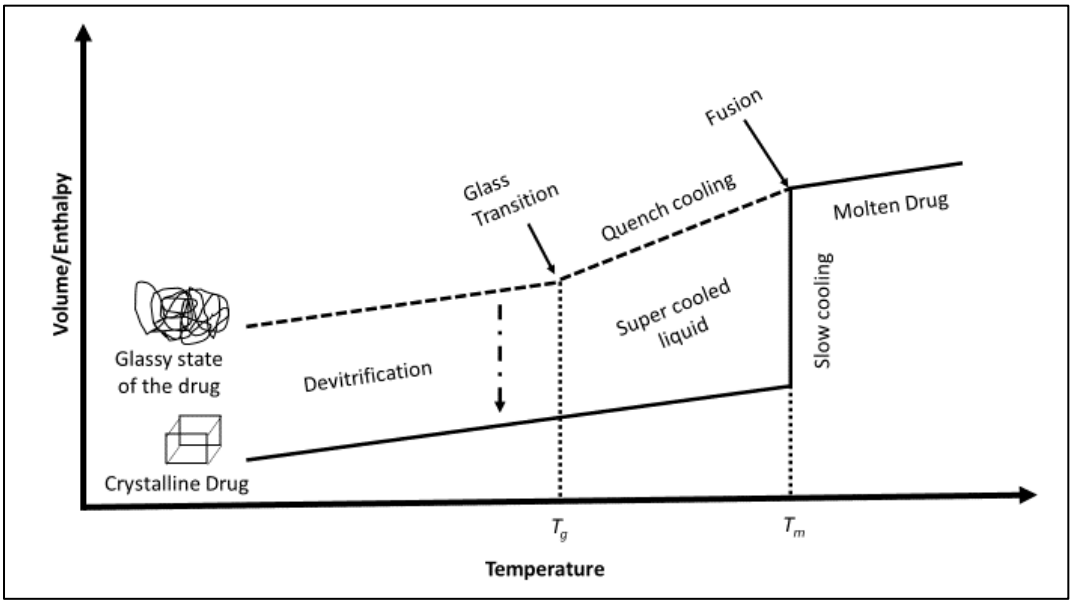


*Figure 1. 10: Enthalpy and volume of different state of drugs as a function of temperature; $T_g$ and $T_m$ are glass transition and melting temperature, note; diagram is not to scale* (Baghel et al. 2016).

In certain cases, along with higher solubility and dissolution rate, amorphous material can offer other advantages, such as better compression characteristics, relative to the crystalline form (Yu 2001). However, amorphous material can exhibit greater chemical instability relative to the crystalline form, likely due to the greater molecular mobility (Yoshioka and Aso 2007). As well as the amorphous form being chemically unstable, it can be physically unstable also, resulting in crystallisation during storage or during in vitro or in vivo dissolution. On adding an amorphous drug to a dissolution medium, dissolution can occur rapidly, when compared to the equivalent crystalline drug, which appears as a peak in the dissolution profile followed by a decrease in solubility and a drop in the drug concentration in solution due to devitrification. This is referred to commonly as a "spring and parachute effect," which can create considerable challenges during dissolution (figure 1.11) (Brough and Williams 2013).

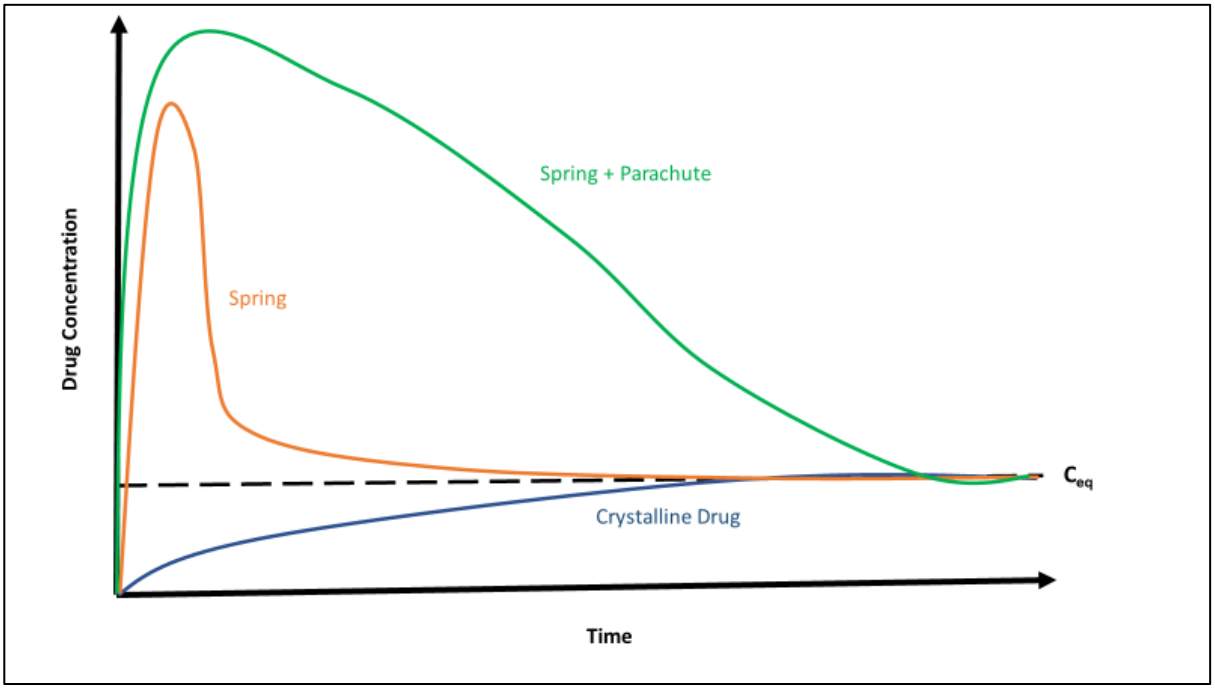


*Figure 1. 11: Drug dissolution profile based on the aqueous solubility of amorphous and crystalline forms of the drug, with max solid solubility ($C_{eq}$), note; diagram not to scale* (Brough and Williams 2013).

To prevent physical and chemical degradation of the amorphous form of the drug, polymers are often added as a carrier matrix in formulations, forming amorphous solid dispersions (ASD). Polymers are chemically composed of repetitive structural units known as monomers which are linked with each other forming an extended structural framework. They can be amorphous, semi-crystalline or crystalline materials. Polymers prevent devitrification of the amorphous drug state by lowering the chemical potential

and bringing it closer to that of the crystalline form. They manage to do this due to their complex three dimensional structures with numerous interchain or intrachain cross links and by incorporating amorphous drugs into these cross-linked networks, they hinder their molecular mobility (Donnelly et al. 2015). Polymers also increase the viscosity of the system which may alter the frequency of atomic/molecular transport at the surface of the nucleus which in turn causes an increase in plasticity or the "hardening" of a material (Tian et al. 2015). In thermodynamics, this increase in the system viscosity, is described as a phenomenon which leads to an increase in the $T_g$ of the material, which increases the free energy required by the amorphous drug to convert into the crystalline form. When two materials having different $T_g$s are mixed together and are miscible, the final $T_g$ of the mixture will be somewhere between the $T_g$s of both the materials. By mixing a low-$T_g$ amorphous drug with a high-$T_g$ polymer, an ASD with a $T_g$ in between the $T_g$ of the original components is formed, if they are miscible with one another. The resultant $T_g$ of the ASD can be calculated by using the Gordon-Taylor equation (Gordon and Taylor 1952):

$$T_g = \frac{W_1 T_{g1} + K_G W_2 T_{g2}}{W_1 + K_G W_2}$$

Where;

$T_g$, $T_{g1}$ and $T_{g2}$ are glass transition temperatures, in Kelvin, of the drug-polymer mixture, the amorphous drug, and the polymer, respectively;

$W_1$ and $W_2$ are the weight fraction of the drug and polymer, respectively;

$K_G$ is a constant the value of which depends on the level of interaction between the drug and the polymer and can be calculated using the equation below:

$$K_G = \frac{p_1 T_{g1}}{p_2 T_{g2}}$$

Where;

$p_1$ and $p_2$ are the densities of the amorphous drug and polymer, respectively.

Other equations such as Fox (Fox 1956), Couchman-Karasz (Couchman and Karasz 1978), or Kwei (Kwei et al. 1987) are also reported in the literature to estimate the resultant $T_g$ of the ASD. However, sometimes, experimentally obtained $T_g$ values deviate significantly from the theoretically predicted values from such equations. This is due to the volume nonadditivity resulting from nonideal mixing of the drug and polymer (Couchman 1978). Several homonuclear and heteronuclear interactions come into play

when a drug is dispersed in a polymer matrix and these can be represented as follows (Baghel et al. 2016):

Case 1. D-D + P-P > 2(D-P)

Case 2. D-D + P-P < 2(D-P)

Case 3. D-D + P-P = 2(D-P)

Where; D and P represent drug and polymer, respectively.

The final volume of ASDs is defined by the relative strength of these interactions. In case 1, the homonuclear interactions are stronger than the heteronuclear interactions. Thus, when a solid dispersion is formed, there would be a net contraction in the volume. Case 2 represents stronger heteronuclear interactions causing a net expansion of the volume. Case 3 is the preferred condition as there is no net increase or decrease in volume and volume additivity is perfect. This indicates complete miscibility between drug and polymer at a molecular level, allowing greater long term stability of the ASD than would be the situation with case 1 or 2 (Six et al. 2004). Ideally, the drug and polymer should be completely miscible with each other, and the drug should be evenly dispersed in the polymer carrier. However, in most cases, the drug-polymer mixture is not ideal, and this nonideal mixing causes deviation between experimental and theoretical $T_g$ values. A stronger drug-polymer interaction is generally preferred resulting in favourable exothermic mixing with increased configurational entropy (Paudel et al. 2010). For predicting the $T_g$ values of systems that are nonideal, the Schneider equation has been shown to be one of the most promising as it is based on combining the free volume rule and the thermodynamic origins of the $T_g$ (Tajber et al. 2005). It adds the effects of specific interactions to the factors already accounted for in the Gordon-Taylor equation to give a more accurate prediction (Schneider 1989);

$$\frac{T_g - T_{g1}}{T_{g2} - T_{g1}} = (1 - K_1)\emptyset - (K_1 + K_2)\emptyset^2 + K_2\emptyset^3$$

Where;

$\emptyset = \frac{KW_2}{(W_1 + KW_2)}$, where K = $K_G$ taken from the Gordon-Taylor equation,

The $K_1$ parameter depends mainly on the differences in interaction energy between the binary contacts of the components: D - D, P - P, and D - P, while $K_2$ accounts for the effects of the rearrangements in the neighbourhood of the contacts (Wunderlich 2005).

## 1.7 Solubility and Dissolution

One of the major issues associated with the development of new API compounds is their poor aqueous solubility. It has been reported that up to 70% of new drug candidates in development have a solubility of less than 100 µg/ml in water and consequently they are considered as practically insoluble (Ku and Dulin 2012). As the oral route is the preferred drug delivery route for APIs due to patient acceptance and ease of administration, formulation strategies must be developed to overcome the solubility challenge of these new APIs.

A true solution is a homogenous mixture of two or more components on a molecular level. Any sample collected from such a mixture will be representative of the entire bulk. In a two-component system, the component present in larger proportion is generally referred to as the solvent, and the other as the solute. Solubility is defined as the maximum amount of solute that can enter solution under defined conditions, such as temperature and pH. Dissolution is defined as the process of a solute disaggregating, dispersing and dissociating in a solvent to form a solution. While solubility is a thermodynamic concept, dissolution is a kinetic process and is usually expressed in terms of dissolution rate. The dissolution rate of a solute in a solvent is directly proportional to its solubility, as described by the Noyes-Whitney equation (Noyes and Whitney 1897):

$$\text{Dissolution rate} = \frac{dc}{dt} = K(Cs - Ct)$$

Where;

dc / dt is the rate of dissolution

K is a constant

$C_s$ is the saturation solubility of the drug

$C_t$ is the concentration of the drug at time (t).

Solubility is expressed in units of concentration including percentage on a weight or volume basis, mole fraction, molarity, molality, parts, etc. The US Pharmacopeia describes solubility as the number of millilitres of solvent required to dissolve 1 gram of the solute. The equilibrium solubility of a solute will depend on its relative affinities towards solvent molecules and fellow solute molecules. Thus, the strength of molecular interactions, both inter and intra, affect solubility. If a concentration in excess of the thermodynamic equilibrium solubility of a solute is achieved in solution, it is described as

supersaturation (Takano et al. 2010). This situation can occur if the temperature or volume of a solution is rapidly decreased or upon the addition of co-solvent in which the solute is less soluble. As a supersaturation state is thermodynamically unstable, eventually the excess solute will crash out of solution restoring equilibrium (Bevernage et al. 2012).

For new API products in development, dissolution profiles need to be established. These dissolution studies are usually undertaken in “sink conditions” which are related to the APIs solubility. Sink conditions means using a proportionate volume of solvent, usually about 5 to 10 times greater than the volume present in the saturated solution of the targeted API contained in the dosage form being tested. During the dissolution testing, "sink conditions"  are usually selected, otherwise, in non-sink conditions, when the concentration begins to get too close to the saturation point, even though the total soluble amount still remains constant, the dissolution rate will gradually begin to reduce in significant amounts, enough to effect the test results (Gibaldi and Feldman 1967).

## 1.8 Permeability

Permeability may be defined as the ability of a molecule to cross a cell, cell membrane, endothelium or epithelium. In order for a drug that has been administered orally to get into systematic circulation it must have a certain permeability. Permeability is usually described in terms of the rate at which it occurs, commonly expressed with units of cm/s (Fagerholm 2008). With regards to the intestinal epithelium, the movement of drugs across the membrane can occur by both passive and active transport. Passive transport is driven by a concentration gradient across the cell membrane and may occur through the enterocytes (transcellular) or between the enterocytes (paracellular). Active transport involves transmembrane proteins facilitating API going from the intestine to systematic circulation, frequently against a concentration gradient, requiring energy. Unlike passive absorption, carrier mediated transport across the membrane may be inhibited or can become saturated (Sugano et al. 2010).

During the last decade, a large number of published articles have discussed the existence and role of passive diffusion as a relevant mechanism across the biological membrane. The overall conclusion is that passive transcellular diffusion is the predominant mechanism for the transport of APIs but that it co-exists with carrier mediated transport processes (Kell et al. 2011, 2013; Sugano et al. 2010). Charged molecules can affect the surface potential of the lipid bilayer resulting in a non-linear concentration-permeation relationship (Sugano et al. 2010). The rate at which passive transport of a drug occurs is related to the lipophilicity, with the more lipophilic drugs diffusing through the cell membrane more quickly. However, passive drug absorption can also be reduced due to the presence of efflux transporters on the surface of enterocytes, such as P-glycoprotein, which work against the concentration gradient removing drug back into the intestinal lumen (Balimane et al. 2006). In general, efflux transporters will only have a significant effect on drugs with low passive permeability (Sugano et al. 2010).

Before reaching the intestinal cell membranes, drugs must pass through a 30 - 100 μm thick boundary layer which is comprised of water, mucus, and glycocalyx adjacent to the intestinal wall that is created by incomplete mixing of the luminal contents near the intestinal mucosal surface. This is also known as the unstirred water layer. While diffusion through this layer may be the rate limiting step for lipophilic compounds, it does not significantly affect the absorption of poorly permeable drugs (Lennernaäs 1998).

## 1.9 Biopharmaceutical Classification System (BCS)

The Biopharmaceutics Classification System (BCS) is used to classify drugs based on their aqueous solubility and intestinal permeability (FDA et al. 2017). The classification system was first proposed in 1995 by Amidon et al (Amidon et al. 1995). The BCS is divided into four classes as follows: Class I, High solubility-high permeability drugs, Class II, Low solubility-high permeability drugs, Class III, High solubility-low permeability drugs, and Class IV, Low solubility-low permeability drugs (figure 1.12).

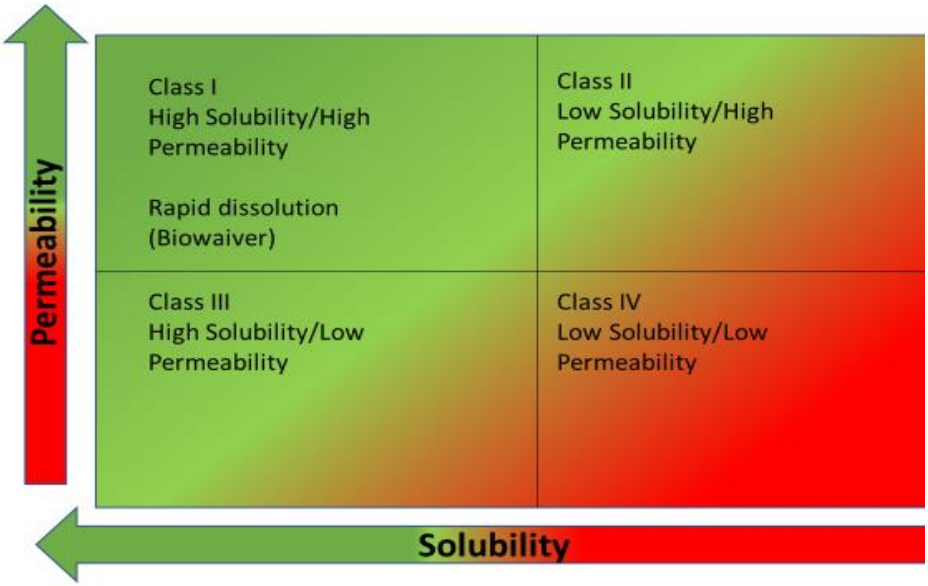


*Figure 1. 12: The Biopharmaceutical Classification System (BCS)*

A drug substance is highly soluble when the highest dosage strength is soluble in 250 ml or less of aqueous media within the pH range of 1 - 6.8 at 37 ± 1°C according to the Food and Drug Administration (FDA) definition (FDA et al. 2017). The European Medicines Agency (EMA) defines a drug substance as highly soluble when the highest dosage strength is soluble in 250 ml or less of aqueous media within the pH range of 1.2 - 6.8 at 37 ± 1°C (European Medicines Agency 2019). The 250 ml volume is derived from typical bioequivalence studies that prescribe administration of a drug product to fasting human volunteers with a glass of water.

Recently, both the EMA and the FDA have agreed consolidated definitions for highly permeable drug substances. A drug substance is considered to be highly permeable when the systemic bioavailability or the extent of absorption in humans is determined to be 85 % or more of an administered dose based on a mass balance determination or in comparison to an IV reference dose. Alternatively, non-human systems capable of

predicting drug absorption in humans can also be used (such as in-vitro culture methods) to determine permeability.

The EMA and FDA also utilise the BCS to allow the use of in vitro dissolution data for establishing the in vivo bioequivalence of drug products. BCS based biowaivers for drug products containing BCS class I drugs can be obtained by manufacturers of generic drug products when these products exhibit rapid dissolution, thus avoiding additional and unnecessary clinical trials (Davit et al. 2016; Kawabata et al. 2011). By definition, a drug product is considered rapidly dissolving when a mean of 85 percent or more of the labelled amount of the drug substance dissolves within 30 minutes, using United States Pharmacopeia (USP) basket apparatus type 1 at 100 rpm or paddle apparatus type 2 at 50 rpm (or at 75 rpm when justified) in a volume of 500 ml or less (or 900 ml when justified) in each of the following media: (1) 0.1 N HCl or Simulated Gastric Fluid USP without enzymes; (2) a pH 4.5 buffer; and (3) a pH 6.8 buffer or Simulated Intestinal Fluid USP without enzymes (European Medicines Agency 2019; FDA et al. 2017). Additionally, a drug product is considered very rapidly dissolving when a mean of 85 percent or more of the labelled amount of the drug substance dissolves within 15 minutes, using the previously mentioned conditions.

As BCS class I drugs exhibit high solubility and high permeability, the rate limiting step for absorption is often seen as gastric emptying due to the high rate of dissolution. Due to this high rate, class I drugs often behave like oral liquids (Sachan et al. 2014). Examples of BCS class I drugs include **ramipril**, propranolol and verapamil. BCS class II drugs have low solubility and high permeability and as a result, the dissolution rate becomes the rate limiting factor for absorption. Compounds in this class often exhibit variable bioavailability and often need enhancement in the dissolution rate by different methods such as the use of prodrugs, different polymorphs or solid dispersions (Sachan et al. 2014). Examples of BCS class II drugs include **simvastatin**, **gliclazide** and ketoconazole. BCS class III compounds have high solubility and low permeability meaning permeation through the intestinal membrane is the rate limiting step for absorption (Papich and Martinez 2015). Since absorption is permeation rate limited, bioavailability is independent of drug release from the dosage form. Interestingly, BCS class III drug products may also qualify for BCS based biowaivers. Products containing drugs in this class are subject to much stricter criteria however than those products with drugs in BCS class I. The drug products must be highly soluble, must have very rapid dissolution profiles (as defined previously) and the test product formulation is qualitatively the same and quantitatively very similar to the reference product. This is due to BCS Class III drug substances being more susceptible to the effects of excipients and

because they may have site-specific absorption, there are a greater number of mechanisms through which excipients can affect their absorption than for BCS Class I drugs (Wu and Benet 2005). Examples of BCS class III drugs are **metformin**, **sitagliptin**, **hydrochlorothiazide** and acyclovir. BCS Class IV drugs exhibit both low solubility and low permeability and as a result exhibit poor and variable BA. The BA can be significantly influenced by food, the efflux transporter, P-glycoprotein, and cytochrome P450 enzymes (especially CYP3A4), leading to considerable first pass metabolism (Ghadi and Dand 2017). As a result, the amount of BCS Class IV compounds absorbed into the systemic circulation can be erratic and unpredictable. BCS Class IV drugs include furosemide, ritonavir and chlorothiazide.

## 1.10 Fixed Dose Combination (FDC) products

Fixed dose combination (FDC) products have become an important alternative to monotherapies in the treatment of several diseases such as hypertension, diabetes, asthma and AIDS-HIV infections. Many different types of oral, parenteral, and inhalation FDC products are commercially available for the treatment of such diseases (Desai et al. 2013). A FDC product is defined as a combination product that includes two or more APIs combined in a single dosage form, which is manufactured and distributed in fixed doses (Gautam and Saha 2008). The ever-increasing role FDC products play in healthcare is evident from the increasing numbers available on the market. FDC approvals by the FDA in the United States increased from 12 in the 1980s to 59 in the 2000s (Hao et al. 2015). The World Health Organisation (WHO) has also increased the number of FDC products on their essential medication list, with 32 FDCs on the March 2017 (World Health Organization 2017c) published list, which is nearly double the number of products of the 2002 list.

### 1.10.1 Advantages of FDC products:

- Patient compliance

For the general population studies have repeatedly shown that by either reducing the frequency of dosing, or, by reducing the overall pill burden to treat targeted diseases, patient compliance rates increase, leading to better clinical outcomes (Cheong et al. 2008; Gerbino and Shoheiber 2007; Pan et al. 2008). FDC products reduce the “pill burden” by combining two or more APIs into one formulation.

- Synergistic or additive effects

Individual drug compounds can have an additive or synergistic effect when taken together to treat a target disease. For example, in severe pain management, combination products containing oxycodone hydrochloride/naloxone hydrochloride are often used. While oxycodone is absorbed through the intestine and carries out an analgesic effect throughout the body, the BA of naloxone is < 3% when taken orally. Naloxone acts as a competitive inhibitor of oxycodone at the opioid receptors in the intestine and this reduces the bowel function disorders that are typical for opioid treatment allowing for better patient tolerance (Leppert 2014). In the treatment of hypertension, angiotensin converting enzyme (ACE) inhibitors (e.g. ramipril and captopril) and thiazide diuretics (e.g. hydrochlorothiazide) in FDC products have been shown to reduce blood pressure more substantially than with individual therapy of the drugs alone (Ambrosioni, Borghi, and F. V Costa 1987; Brown et al. 1990; Chrysant 1994). Both have different mechanisms of action which, when combined, lead to better blood pressure control.

- Cost reduction

A reduction in costs is applicable to both the patient for whom the FDC is intended and indeed the manufacturers of the product. In general, FDC products at point of sale tend to be cheaper for patients to purchase when compared with buying two or more individual products to obtain the same APIs at the same strengths (Desai et al. 2013). For manufacturers, producing FDC products is cheaper than producing the individual API formulations separately, while at the same time simplifying the logistics of distribution. Pharmaceutical companies may also use FDC products as a way of extending proprietary rights leading to an increase in potential profits for the company. Since FDC products may be protected by patents, a company may obtain exclusive rights to sell a particular FDC or formulation thereof, even though the individual APIs may be off-patent (Hao et al. 2015).

### 1.10.2 Disadvantages of FDC products:

- Reduction in dosage flexibility

FDC products are manufactured at an established strength, which in turn reduces flexibility of dosing. To overcome this problem, several different strengths of the same combinations are often available. However, patients affected by some diseases often need frequent dosage adjustments to be carried out and FDC products may not be useful for such a cohort (Desai et al. 2013).

- Uncertainty over adverse effects

It is more difficult to accurately pinpoint the causative agent of an adverse drug event when several APIs are administered in the same dosage unit. For example, Inegy®, an FDC product that contains simvastatin and ezetimibe for the treatment of hypercholesterolemia, can cause an increase in liver enzyme activity. Both APIs in their respective individual formulations can also cause the same adverse effect and as a result it is difficult to pinpoint which API is causing it (Medicines and Healthcare products Regulatory Agency 2019b, 2019a).

- Large dosage form size

Since FDC products contain multiple drugs in the one tablet, it is a possibility that the tablet size may be too large to swallow, especially for paediatric and elderly patients. For example, in the case of, metformin, which is used in the treatment of type II diabetes, the usual unit dose is between 500 mg – 1000 mg. By adding an additional antidiabetic agent and excipients, the final tablet size may be too big to comfortably swallow.

## 1.11 Formulation design and development of FDC products

Formulation design and process development for FDC products are commonly more challenging than corresponding single entity products. In general, APIs are selected for FDC development based on several reasons and as a result a fundamental understanding of their pharmacological mechanisms, drug-drug interactions, pharmacokinetic profile and manufacturability are required for successful development. Synergistic therapeutic effects are desired when selecting APIs, but difficult to demonstrate (Desai et al. 2013). Various manufacturing processes and formulations have been used successfully to produce FDC products from a commercial point of view. Figure 1.13 shows a simplified decision tree on which a final formulation best suited to a potential FDC may be selected based on physicochemical properties of the APIs and desired dissolution profiles.

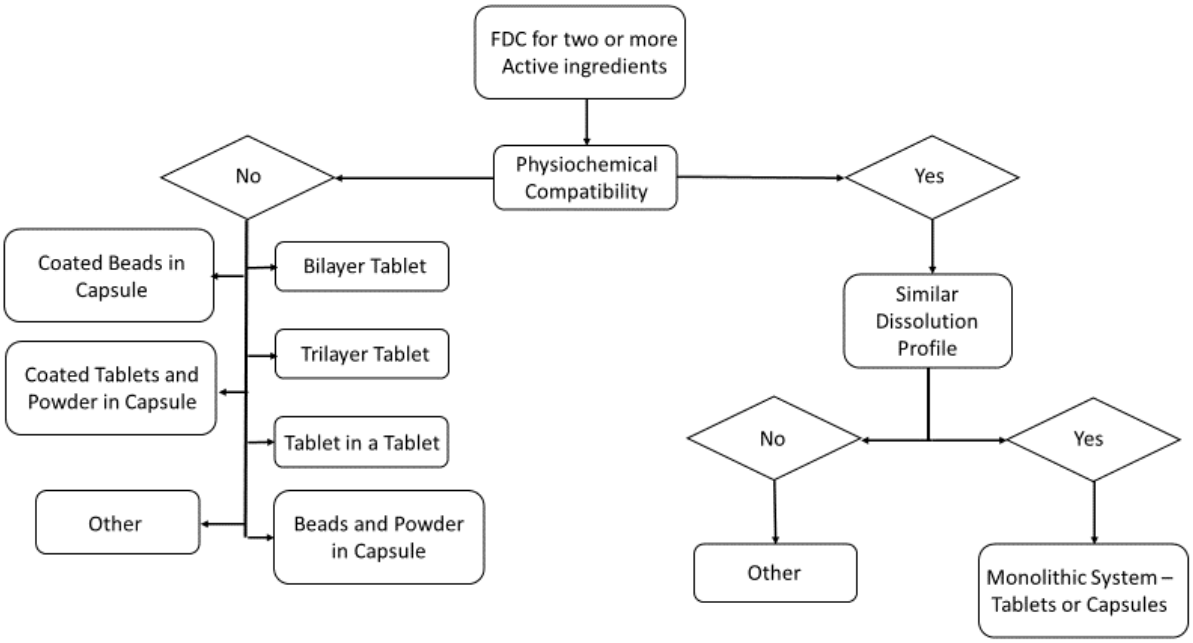


*Figure 1. 13: Decision tree of the formulation design of FDC products* (Siew 2014).

The simplest FDC formulation choice is the **monolithic system**. When two or more APIs are chemically compatible with each other and have a similar dissolution or targeted release profile, then the monolithic system in a solid oral dosage form is likely the most suitable option for manufacturing. However, achieving bioequivalence for the FDC APIs may prove difficult for some systems when comparing the individual formulations to the FDC product. For example, if a BCS class II drug and a BCS class III drug were formulated into one monolithic FDC, even though they may be chemically compatible,

the formulation matrix used for the BCS class III drug may impair the wetting and dispersion of the BCS class II drug making its bioavailability highly variable (Desai et al. 2013). Such examples highlight the need for adequate research to be undertaken prior to manufacturing.

**Multilayer tablets** are prepared by the repeated compression of powders. From a manufacturing point of view, they are a simple and convenient way of formulating incompatible drug compounds into a single solid dosage form. It is also a convenient way of enabling an immediate release formulation to be combined with a controlled release formulation. Drug compounds in the different layers may be the same API with different release profiles or, more commonly, contain two different APIs (Mandal and Pal 2008). Figure 1.14 shows some of the different multilayer tablets that may be manufactured. Figure 1.14 (a) shows the simplest multilayer tablet, a bilayer. During the tablet compaction process, layer 1 is filled into the tablet die and a compression takes place forming a relatively solid mass of the formulation. Next, layer 2 is filled into the die with another compression taking place to form the second solid layer. Finally, the desired compaction force is applied, and the bilayer tablet is produced. If the chemical stability of the APIs at the bilayer interface is not acceptable due to physicochemical interactions, a way to solve this problem is by adding in an additional layer known as a “buffer layer” as seen in figure 1.14 (b), to separate the two layers. For example, Bristol-Myers Squibb patented a multi-layered tablet of aspirin and pravastatin with a buffer layer between the two APIs because of possible physical interactions between the two. Aspirin is an acid whereas pravastatin is an alkali salt thus, the mixing of the two could result in aspirin hydrolysis as well as statin degradation (Benkerrour et al. 2004). The buffer layer between the two API layers prevents this from happening. Figure 1.14 (c) is another type of multi-layered tablet known as a “tablet in a tablet”. These types of formulations are only made possible through a sophisticated mechanism of tablet dies. Pre-compressed core tablets are centred over top of a die cavity by means of simple holders machined specifically to the core tablet features. This tablet in tablet compression press system has a continuous "chain and sprocket" mechanism, which reliably synchronizes incoming core tablets to the rotating press turret for accurate and repeatable core placement while the outer layer is filled around it and final compaction is undertaken.

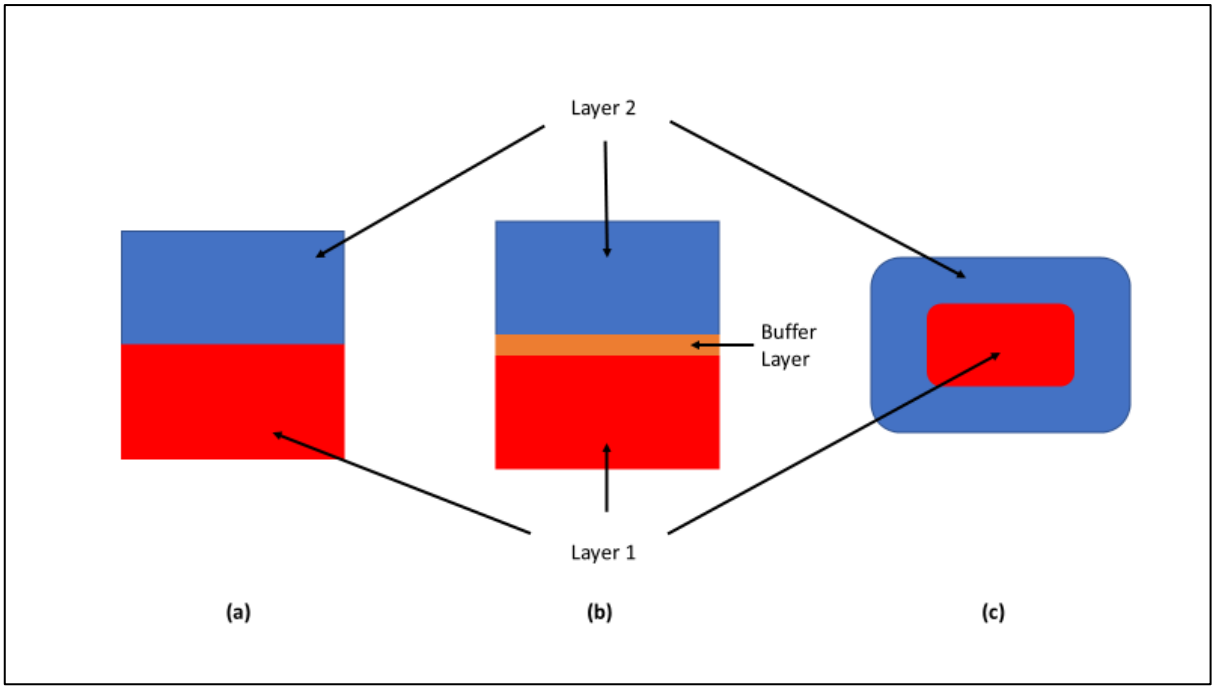


*Figure 1. 14: Visual representation of (a) bilayer tablet, (b) trilayer tablet and (c) tablet in a tablet.*

Once the chemical stability profiles of all drugs in multi-layered tablet FDCs are satisfactory, they can present some unique challenges in terms of obtaining acceptable tablet physical characteristics compared to conventional monolithic tablets. Some of the challenges associated with multilayer tablets may include insufficient overall tablet tensile strength, leading to excessive friability, delamination at the interface between layers, or capping within individual layers. Also, unsatisfactory weight control for the individual layers or the overall tablet, may lead to problematic content uniformity of the APIs (Abebe et al. 2014).

**Multiparticulate systems** intended for oral delivery, consist of numerous small discrete drug delivery units. Multiple units, beads, pellets, granules, spheroids or mini-tablets, are the various terminology used to describe these systems. In the literature the size of these units has been reported as being as small as 150 µm and as large as 2 - 3 mm in diameter (Rajabi-Siahboomi 2017). Multiparticulate systems may be made up with a single API or several, ranging from immediate release to modified release formulations. Multiparticulate systems are reliably administered as a single dose of the API/APIs using capsules, sachets or, after mixing with additional excipients and compression, in the form of tablets (Abdul et al. 2010). These types of systems offer many advantages including: flexibility for the choice of final dosage form e.g. capsules; flexibility in dose titration depending on how much API can be added individually; reduction in intra- and inter-

subject variability due to reduced variation in gastric emptying and; easier dose-weight proportionality as compared to single dosage forms (Rajabi-Siahboomi 2017). Pellets or spherical granules are usually made during an extrusion/spheronisation process, which has the advantage of having a narrower particle size distribution, and is the main manufacturing technology used in developing multiparticulate systems (Gandhi et al. 1999). They also have the advantage of being able to be coated with one or several layers of film coating after production. Even though the extrusion/spheronisation process and the film coating of pellets, is considered well established, they are far from simple, with small changes in the formulation or process leading to significant effects on the attributes of the final formulation (Wesdyk et al. 1993).

The film coating approach may be applied to produce various FDC products for several reasons. A simple film coat may provide protection of the API from light or moisture if these conditions have a detrimental effect on storage. Film coating may also be used for targeting drug release in a certain area of the gastrointestinal tract, such as a gastro-resistant film coating which prevents release in the stomach. Film coating technology may also be utilised to produce active film coats to prepare FDCs. The physical cores which are to be coated may be inert or may contain API. Layers of desired API may then be spray coated onto the core resulting in the FDC. The number of layers can vary from a single layer to several, depending on the number of APIs or the physicochemical interactions between the different layers that may be evident. One of the best examples of active film coating is in the product Claritin-D™. This product is composed of an extended release pseudoephedrine core which is film coated with an immediate release loratadine and pseudoephedrine formulation. Upon oral administration, the coating dissolves immediately to release loratadine and pseudoephedrine to provide the initial dose followed by an extended release of pseudoephedrine from the tablet core (Kwan and Liebowitz 1992). The main difficulties with the active final coating approach are determining the end point of coating and content uniformity when coating is complete. For determining the end point, traditionally it was based on either the amount of coating material sprayed, or the weight gain of the core material. Due to the nature of spray coating, the core material potentially can change shape due to colliding off the wall of the container or the core material colliding off itself. This potentially results in an uneven distribution of the coating material. To overcome these problems, periodical sampling to perform assays has been introduced to determine the end point and content uniformity (Desai et al. 2013).

## 1.12 Batch vs Continuous Manufacturing

General definitions of batch and continuous process can be described below (Felder et al. 2015).

*Batch process:* The raw material(s) is charged into the system at the beginning of the process, and the product is discharged all at once sometime later. No ingredients cross the system boundaries between the time the raw material(s) is charged and the time the product is discharged (figure 1.15).

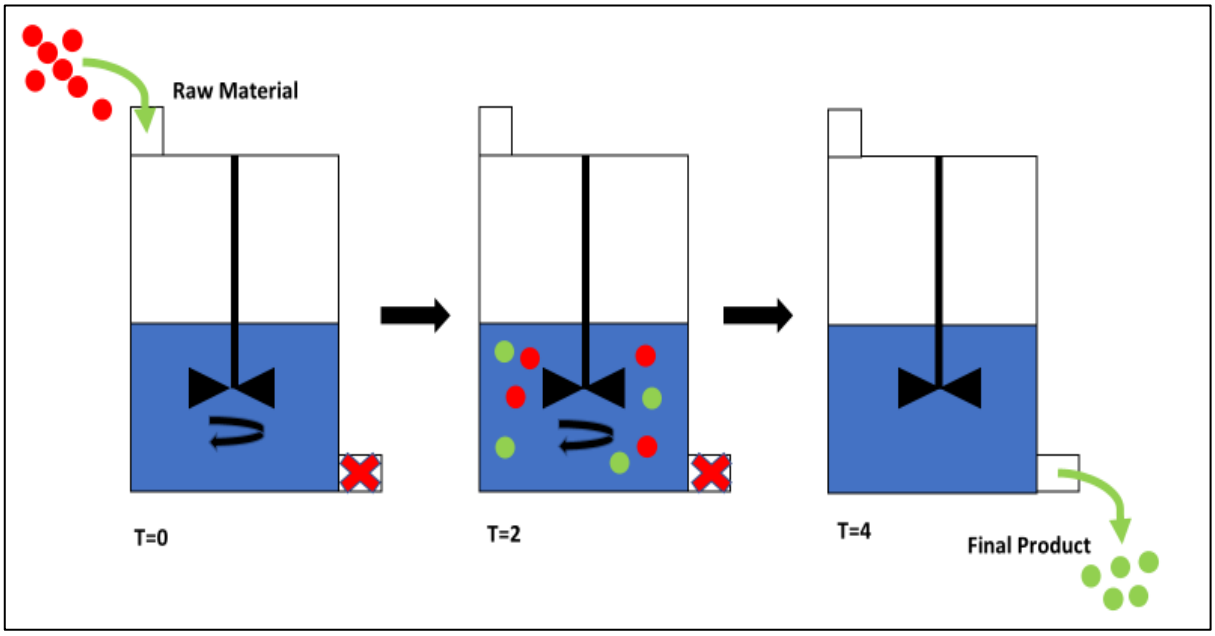


*Figure 1. 15: Batch manufacturing: the material(s) is charged before the start of processing and the product is discharged at the end of processing.*

*Continuous process:* The material(s) and product are continuously charged into and discharged from the system, respectively, throughout the duration of the process (figure 1.16).

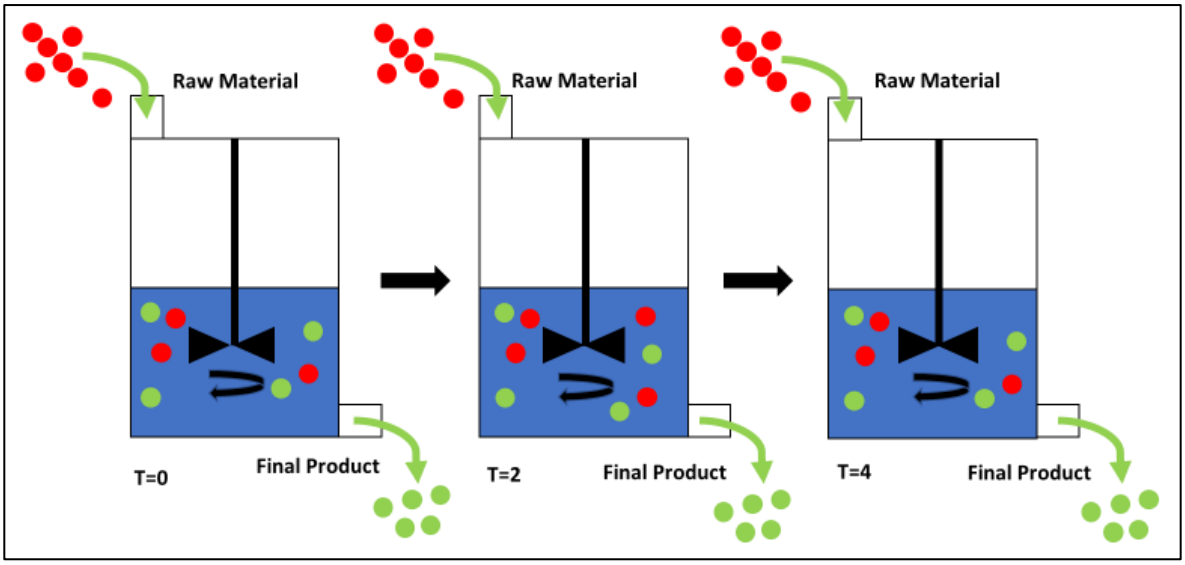


*Figure 1. 16: Continuous manufacturing: material(s) and the product are simultaneously charged and discharged from the process, respectively.*

Traditionally, batch manufacturing has been utilised to produce pharmaceutical products including, more recently, FDC products. In the batch process the main limitations for progressing from initial formulation to final product is the time it takes for offline testing to be completed. At each step of the batch process, the materials must be tested offline and stored appropriately before being sent to the next step of the manufacturing process (figure 1.17). The storage process may add days, weeks or even months to the processing time. Under a continuous operating mode, hold times between steps can be eliminated. This is a significant advantage for APIs or intermediates that can degrade over time or are sensitive to environmental conditions, directly improving the overall drug product quality.

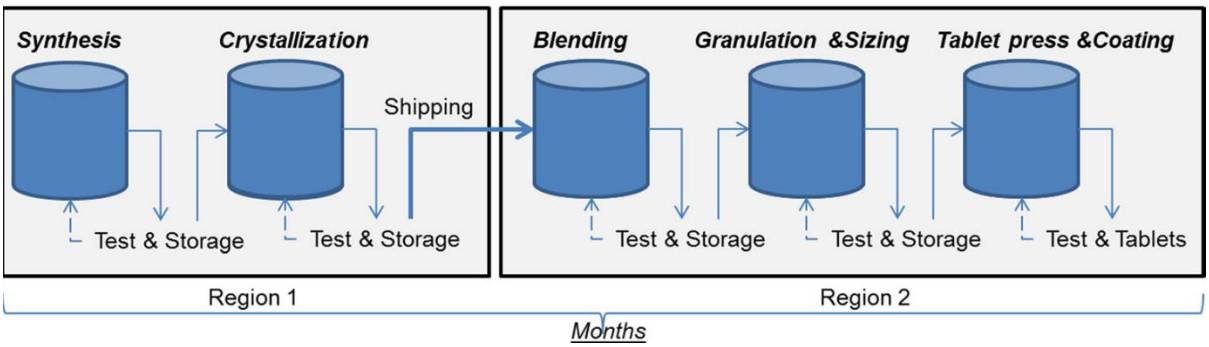


*Figure 1. 17: Typical schematic of a batch manufactured solid oral dose pharmaceutical product* (Lee 2015).

If the materials in question fail to meet quality expectations at any of the above steps when moving from one phase to the next, as shown in figure 1.17, then the material may be discarded or reprocessed before manufacturing can continue. Batch manufacturing is useful for producing pharmaceutical products for which the demand may be low, or which targets a very specific patient population. On the other hand, continuous manufacturing is more advantageous for pharmaceutical products for which demand remains high consistently. In continuous manufacturing, each material produced is directly and continuously sent to the next step for further processing without the lengthy holding times in between the different steps that is often seen in batch manufacturing (figure 1.18).

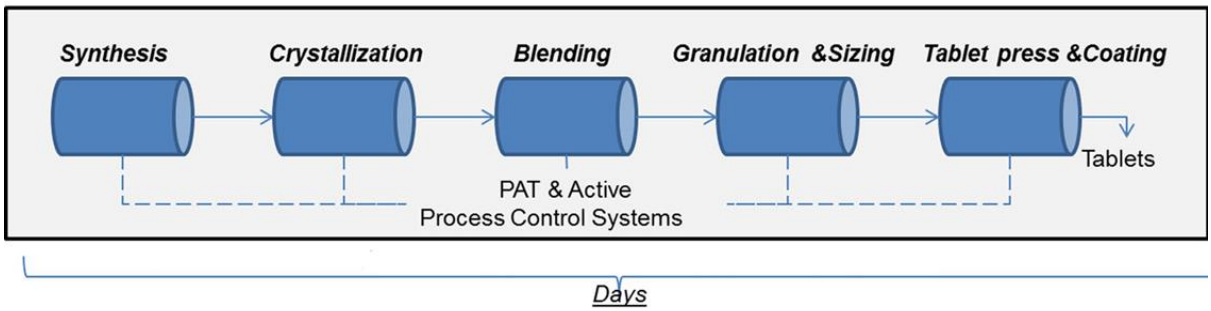


*Figure 1. 18: Typical schematic of a continuous manufactured solid oral dose pharmaceutical product* (Lee 2015).

In line Process Analytical Techniques (PAT) and Quality by Design (QbD) approaches ensure desired parameters are maintained throughout the continuous process, allowing manufacture to continue up to 24 hours per day if required. The in-line PAT and QbD also allow for consistent high-quality drug production to be maintained. While the continuous process is relatively new in drug product manufacturing, there is a push by companies to move towards it for future manufacturing developments for several reasons. The continuous manufacturing method is seen as a more integrated method of drug production. Less manual handling, shorter processing times and increased efficiency allow for higher quality products to be produced. Less initial capital investment is required as smaller equipment and facilities can produce large quantities of product over a given timeframe when previously large equipment for batch production would have been required. Once the continuous process has been established, overall production costs have been shown to be less expensive than the equivalent batch production technique (Schaber et al. 2011).

Some of the techniques that have employed in the continuous manufacturing process to date include Hot Melt Extrusion (HME) (Maniruzzaman and Nokhodchi 2017), Hot Melt

Co-Extrusion (HMCE) (Vynckier, Dierickx, Voorspoels, et al. 2014), Spray Drying (SD) (Hu et al. 2011) and 3D printing (Günther et al. 2014).

While both batch manufacturing and continuous manufacturing are subject to quality control standards, as monitoring tends to be automated in the continuous processes, sampling tends to be more frequent. As a result, continuous manufacturing may allow for more flexible tracking and tracing, which would be an advantage in the event of a product failure. The FDA define a batch as “a specific quantity of a drug or other material that is intended to have uniform character and quality, within specified limits, and is produced according to a single manufacturing order during the same cycle of manufacture” (FDA 2018). For batch manufacturing, the “batch” is the quantity produced according to the size of the equipment available at production. For continuous manufacturing however, the “batch” can be defined by a time stamp, amount of product produced or the amount of raw material that had been input into the process. These tracking methods along with the use of in-line PAT permit the manufacturer to isolate a smaller amount of defective material in the event of a process failure, which in turn leads to less waste and less chance of a product shortage (Lee 2017).

## 1.13 Manufacturing Methods used for Continuous/Semi-Continuous Manufacturing of Fixed Dose Combination Products.

### 1.13.1 Spray Drying (SD)

The SD process can be considered a continuous manufacturing method as a constant feed into the process results in a constant output. With regards to FDC products, SD is suitable to produce monolithic systems on a continuous basis. SD is a process that has been around for many years. The very first mention of the process comes from 1860 with the very first patent registered in 1872 (Percy 1872). Spray dryers of that time were quiet primitive and often had many problems associated with them and it wasn't until the 1920s that spray dryers underwent a degree of transformation that enabled their use in milk powder production, an application that still remains in use to this day (Cal and Sollohub 2010). The true boom in the technology was driven by World War II when large quantities of food were required to be transported over vast distances. SD allowed for a reduction in weight and volume and as a result was an ideal process to satisfy these needs. After the war, the pharmaceutical industry began to realise the potential this technique had and began to invest in developing the technology. Initially, the SD powders were characterised by poor flowability, chemical instability and were difficult to store (Cal and Sollohub 2010). Despite these drawbacks, the powders produced via this method of drying displayed more favorable properties, such as the ability to control particle size and residual solvent content, compared to products developed by other drying methods (Masters 2002). Even after all this time since the initial concept was developed, it provides a wide field for research and development. The SD process itself, begins with the atomization of a solution or suspension of the compound of interest, followed by mixing with a drying gas, evaporation of the solvent, and collection of the dried particles (Paudel et al. 2013). SD may be used to produce pure amorphous drugs, crystalline microparticles, as well as composite formulations, if the components are sufficiently soluble in a suitable solvent system. The solubility of the drug will determine whether SD is a practical method for producing the amorphous state, and whether a reasonable yield is possible (Paudel et al. 2013). However, using the SD method to produce amorphous samples can make them less stable than other production methods due to the powder's general low density. The presence of residual solvent in SD samples may also reduce their $T_g$ and thus stability. The physical properties of a SD formulation will depend on the process parameters chosen. These parameters (outlined in table 1.1) can be manipulated to achieve more desirable results if required.

*Table 1. 1: Effect of Spray Drying Conditions on Particle Properties* (Vasconcelos et al. 2016).

| PARAMETER (INCREASE) | PARTICLE SIZE | PARTICLE POROSITY | PRODUCT MOISTURE | PARTICLE SMOOTHNESS | POWDER YIELD |
|---|---|---|---|---|---|
| **INLET TEMPERATURE** | Increase | Decrease | Decrease | Decrease | Increase |
| **DRYING FLOW RATE** | Decrease | Increase | Decrease | Increase | Increase |
| **FEED RATE** | Decrease | Decrease | Increase | Increase | Decrease |
| **HUMIDITY** | Increase | Increase | Increase | Decrease | Increase |
| **SPRAY NOZZLES (INCREASE IN DROPLET SIZE)** | Increase | Increase | Increase | Decrease | Increase |
| **SOLID CONTENT IN SOLUTION** | Increase | Decrease | Decrease | Decrease | Increase |
| **SOLUTION VISCOSITY OR SURFACE TENSION** | Increase | Decrease | Increase | Decrease | Increase |

### 1.13.2 Hot Melt Extrusion (HME)

HME offers continuous manufacturing without the use of solvent. It is a process that is easy to scale-up and offers good batch reproducibility (Maniruzzaman and Nokhodchi 2017). Since the 1930s, the HME process has been used and developed in the plastic, rubber and food manufacturing industries. It is only within the last few decades that this manufacturing technique has been utilised in the pharmaceutical sector. The technique consists of converting a raw material into a product of uniform shape and density by forcing it through a die under controlled conditions. The HME manufacturing method is composed of three main zones in the extruder: feed zone, compression zone and metering zone. The feed zone is where the pre-mixed formulation enters into the extruder barrel. The pressure within the feed zone is very low allowing for consistent feeding from the hopper and gentle mixing of API and excipients. Zone two is seen as the area where, depending on screw element design and temperatures chosen, the formulation is heated, melted, homogenised and conveyed towards zone three, the metering zone where the formulation is in a suitable form for extrusion. Consequently, products are formed through the die. Depending on the die configuration, several shapes and sizes of pharmaceutical dosage forms can be produced for different routes of administration. For example, with an “annular” die, capsules can be made for the oral

route, or with a round die, tablets, granules, implants and inserts can all be prepared for oral, buccal, transdermal and ocular administration (Williams et al. 2010). The process allows for several forms of solid-state materials to be produced including co-crystals, amorphous solid dispersions and monolithic FDC products. HME is also seen as a current and future relevant technology in the pharmaceutical industry due to the ability to control the process parameters accurately. Monitoring of screw speed, feed rate, temperature barrel, type of screw(s) and its elements of conduction and conveying, permit residence time, mixing, melt viscosity and solid state to be managed in order to obtain the quality attributes expected (Lang et al. 2014). Thus, HME is particularly suitable to implement a PAT framework and QbD approach, assuring continuously product efficiency and security during all development steps (Simon et al. 2015).

### 1.13.3 Hot Melt Co-Extrusion (HMCE)

HMCE is the co-extrusion of two or more materials through the same die simultaneously, creating a multi-layered extrudate (Vynckier, Dierickx, Voorspoels, et al. 2014). It is regarded as an innovative continuous production technology that offers numerous advantages over other manufacturing techniques. As with HME, HMCE was a technique that first had application in the plastics and food industries. Along with continuity of the process, the major advantages of the technique include, fewer processing steps, no solvents needed and the possibility of improving drug performance (Vynckier, Dierickx, Saerens, et al. 2014). The added value of HMCE is that it allows the release of each drug from each of the two layers independently if desired, to enable simultaneous administration of non-compatible drugs and to produce FDCs in a continuous single-step process. On the other hand, HMCE can present some major difficulties during manufacturing. A specific challenge during HMCE is to establish a core/coat polymer combination fit for purpose considering required release characteristics of the incorporated drugs. Other challenges include requirements for similarity in extrusion temperature and appropriate adhesion between the layers. If there are major differences in the viscosity of the two layers of the co-extrudate, then it can become exceedingly difficult to form an acceptable extrudate product. At this moment in time, no HMCE product for oral use has made it to the market. However, at present there are two formulations made by HMCE which are marketed: Nexplanon®, a subdermal implant, and NuvaRing®, a vaginal ring (Fischer 2008).

### 1.13.4 Spray Coating (SC)/ Fluid Bed Coating (FBC)

While SC itself is not seen as a continuous manufacturing technique, it may be employed to coat materials that have been produced by a continuous process, making the overall method of manufacture a semi-continuous one. In contrast to SD, HME and HMCE, SC

originated in the pharmaceutical industry and has since found new applications in other industries such as food and cosmetics (Risch 1995). SC consists of dispersing droplets of a coating material onto a surface to produce a homogenous outer layer film. The sprayed liquid can be a solution, a suspension, an emulsion or a melt. For a SC application to be successful, it needs a solid support to produce the desired film. This solid support may be made up of inert beads or may be made up of a core API material to be coated. Of all the spray coating techniques, the FBC is the most commonly applied. This technique relies upon a nozzle spraying the coating material into a fluidized bed of core particles in a hot environment. Effective evaporation occurs after contact between spray droplets and the surface of the particles to be coated. This process allows high coating rates and it is suitable for particles with a diameter from 50 µm up to 5 mm. FBC is a three-step process. First, the particles to coat are fluidized in the hot atmosphere of the coating chamber. Secondly, the coating material is sprayed through a nozzle on to the particles and finally, the film formation begins with a succession of wetting and drying stages. It is possible to differentiate between the three types of coating processes available for FBC depending on the position of the spray nozzle: 1) the top spray, 2) the bottom spray (also known as the Wurster method) and 3) the tangential or rotary spray coating. However, for each type of coating device, the principle of particle coating remains the same. The quality of the final product is reliant on numerous variables that influence the process. Temperature, humidity and fluidised air/gas velocity affect the evaporation rate of the coating liquid droplets and consequently the film characteristics. The coating droplets must spread successfully over the target surface to form a successful film. The wettability of particles to be coated and the stickiness of the coating material impact the ability of the film to be formed.

## 1.14 Regulatory considerations for Fixed Dose Combination products

The FDA describes the fundamentals for FDC products in the Code of Federal Regulations 21 CFR 300.50 (FDA 2018). In these regulations, the FDA outlines the requirements drug manufacturers have to adhere to in order for a product to be granted approval to be labelled as an FDC product e.g. two or more active ingredients, single dosage form, therapeutic benefit to the patient etc. There are three filing pathways that companies can choose from when applying for FDA approval to bring their FDC to market, depending on the status of the APIs to be included in the formulation;

**505(b)(1) New Drug Application (NDA)** – is a full new application. This pathway is typically used for novel APIs that have not been studied or approved before. All studies that are required before submission have to be undertaken by the applicant and must demonstrate the safety and efficacy of the FDC.

**505(b)(2) NDA** – is a partial new application. It was designed in 1984 to prevent duplication of existing studies. This pathway must demonstrate safety and efficacy to the same standards as the 505(b)(1) NDA program. However, existing data from studies not conducted by or for the applicant, for which the applicant does not have the right of reference, may be used to meet some or all of the safety and efficacy requirements. This data may be obtained from published literature or from the FDA's finding of safety and effectiveness for an approved drug. Generally, for FDC products, this pathway is used when one API, which has been previously studied and approved, is formulated with a new novel API that has not been studied before. The 505(b)(2) pathway usually results in products being approved with lower cost and quicker timeframes than those being processed through the 505(b)(1) pathway.

**505(j) Abbreviated New Drug Application (ANDA)** – this pathway refers to APIs already approved and on the market. The applicant has to demonstrate bioequivalence to an innovator drug in lieu of replicating safety and efficacy studies. The bioequivalence studies are only sufficient if there is no change in dosing or proposed indication, otherwise additional clinical data is required. For FDC products, bioequivalence has to be shown for each of the individual APIs in the formulation. Usually, the individual product API already on the market is used as the reference.

The FDA have been encouraging companies towards developing FDCs for a variety of indications to improve clinical outcomes (FDA et al. 2006). They have also offered financial incentives to develop FDCs by allowing additional sales exclusivity for FDCs.

For example, to encourage development of FDCs for HIV treatment, the FDA has provided no-fee incentives (FDA et al. 2007).

The EMA has published guidance for the clinical development of FDC products that may be destined for the European market (EMA 2017). The basic scientific requirements for any FDC are:

1. Justification of the pharmacological and medical rationale for the combination.
2. Establishment of the evidence base for: (a) relevant contribution of all active substances to the desired therapeutic effect (efficacy and/or safety); (b) positive benefit-risk ratio for the combination in the targeted indication.
3. Demonstration that the evidence presented, if based on combined administration of separate APIs, is relevant to the FDC for which the application is made.

In relation to therapeutic use and indications, the EMA outlines three scenarios where FDC products may be developed for use:

1. “Add-on treatment” – Treatment of insufficiently responding patients; in this scenario the intended FDC product is for patients who are not responding adequately to existing therapy with one (or more of the) APIs in the FDC.
2. “Substitution” - Switch in patients adequately controlled with two or more active substances used in combination; the FDC is intended to be used in patients who are already stabilized on optimal doses of the combination of the same, but separately administered APIs, taken at the same dose interval and time. Patients discontinue taking the single API products and initiate therapy with the FDC product.
3. Initial combination treatment; The patient is to immediately begin taking the FDC, instead of the stepwise addition of the individual APIs.

Should any of the above FDC products contain an API that has not previously been authorised i.e. a new chemical entity, the pharmacokinetics, pharmacodynamics, safety and efficacy of the API have to be demonstrated.

## 1.15 Rationale for work undertaken in this thesis

While extensive work has been previously carried out and reported in the literature for all of the individual manufacturing techniques described in this thesis, the vast majority have focused primarily on the production of solid dosage forms containing a single API. As FDC products begin to play an ever-increasing important role in healthcare, along with an ever-increasing focus on continuous manufacturing, it is hoped that the work conducted in the thesis will help to improve the scientific literature and knowledge concerned with the production of FDC products with two or more APIs.

Currently, several different manufacturing techniques are employed in the manufacture of FDC products depending on the desired release profiles and/or as a means of reducing potential drug-drug interactions. Techniques include the manufacture of bilayer/multi-layer tablets (to keep APIs separate from one another), capsule filling of different pellets containing different APIs which are filled into capsules at the desired ratios, and the simple compression of multiple APIs with excipients into tablets. One of the limitations of these techniques is the batch manufacturing process associated with them, meaning there are long processing times and if there is a problem with the process, the whole batch may need to be discarded. The techniques in this thesis allow for continuous manufacturing to be built into the solid dosage form production process. It is hoped that in the long run, by implementing continuous manufacturing, supply chains can be improved, and waste can be reduced in instances where there is an issue with the manufacturing process.

# Chapter 2:

# Materials and Methods

## 2.1 Materials

| Material | Supplier |
|---|---|
| Ramipril (RAM) | Kemprotec (Carnforth, England) |
| Hydrochlorothiazide (HCTZ) | Kemprotec (Carnforth, England) |
| Sitagliptin Phosphate (SIT) | Kemprotec (Carnforth, England) |
| Metformin Hydrochloride (MET) | Tokyo Chemical Industry (TCI) UK Ltd. (Oxford, UK) |
| Simvastatin (SIM) | Fluorochem Ltd. (Hadfield, UK) |
| Gliclazide (GLZ) | Tokyo Chemical Industry (TCI) UK Ltd. (Oxford, UK) |
| Vinylpyrrolidone-vinyl acetate co-polymer (Kollidon® VA 64) | BASF (Ludwigshafen, Germany) |
| Polyvinylcaprolactam – polyvinyl acetate – polyethylene glycol graft copolymer (Soluplus®) | BASF (Ludwigshafen, Germany) |
| Polyethylene glycol (PEG 3350 g/mol) | Sigma-Aldrich (Dorset, UK) |
| Hydroxypropyl cellulose - A (HPC) (avg. molecular weight 1,150,000 g/mol) | Ashland (Kentucky, U.S.A.) |
| Hydroxypropyl cellulose - S (HPC) (avg. molecular weight 100,000 g/mol) | Sigma-Aldrich (Dorset, UK) |
| Microcrystalline cellulose (MCC), (Avicel® PH102) | IMCD Ltd. (Sutton, UK) |
| Eudragit® L100 | Evonik (Dortmund, Germany) |
| Eudragit® L100-55 | Evonik (Dortmund, Germany) |
| Eudragit® RSPO | Evonik (Dortmund, Germany) |
| Eudragit® RLPO | Evonik (Dortmund, Germany) |
| Triethyl citrate (TEC) | Sigma-Aldrich (Dorset, UK) |
| Hypromellose acetate succinate (HPMC-AS), MF grade | Shin-Etsu Chemical Co. Ltd (Japan) |
| D-α-Tocopherol polyethylene glycol 1000 succinate Bioextra (Vitamin E) | Sigma-Aldrich (Dorset, UK) |
| Low viscous Hypromellose/HPMC (Pharmacoat®), grade 603 | Shin-Etsu Chemical Co. Ltd (Japan) |

| | |
|---|---|
| Vivapur® microcrystalline cellulose (MCC) spheres 1 mm | JRS Pharma GMBH and Co. (Rosenburg, Germany) |
| Hydroxypropyl methylcellulose (Affinisol™ HPMC HME 100LV) | The Dow Chemical Company (Dewsbury, UK) |
| Meglumine | Sigma-Aldrich (Dorset, UK) |
| Water (HPLC grade) | Elix 3 connected to Synergy UV system, Millipore (Watford, UK) |
| Ethanol (96 %) | Corcoran Chemicals (Cooley, Ireland) |
| Methanol | Sigma-Aldrich (Dorset, UK) |
| Methanol (HPLC grade) | Fischer Scientific (Dublin, Ireland) |
| Liquid nitrogen | BOC (Dublin, Ireland) |
| Sodium perchlorate | ACROS (New Jersey, U.S.A.) |
| Acetonitrile (ACN) HPLC grade | VWR Chemicals (Dublin, Ireland) |
| Hydrochloric Acid (37 %) solution | Fischer Scientific (Dublin, Ireland) |
| Ammonium phosphate | Sigma-Aldrich (Dorset, UK) |
| Triethylamine | Sigma-Aldrich (Dorset, UK) |
| Phosphoric acid | Fischer Scientific (Dublin, Ireland) |

## 2.2 Unit Operations

### 2.2.1 Preparation of the Spray Dried (SD) formulations

All spray dried systems were prepared using a Buchi B-290 Mini Spray Dryer (BÜCHI Labortechnik AG, Flawil, Switzerland). A two-fluid nozzle with a 0.7 mm nozzle tip and a 1.5 mm diameter nozzle screw cap were used. All other conditions used were varied according to the system being produced and are stated in later chapters, where appropriate.

#### 2.2.1.1 Preparation of the RAM and HCTZ formulations

Drug(s) with or without polymer(s) were dissolved in 200 ml of premixed solvent with a composition of 95 % (v/v) ethanol, 5 % (v/v) deionised water. The inlet temperature, airflow, aspirator and feed rates at which the spray dryer was operated were kept at 78 °C, 667 Normlitres/h, 100 % (equivalent to 35 $m^3$/hr) and 20 % (~ 5 - 7 ml/min), respectively. The outlet temperature remained between 45 °C - 49 °C. The solution concentrations were kept constant at 5 % (w/v) for all formulations. Table 2.1 shows the composition of each formulation processed by SD and HME discussed in chapter 3.

*Table 2. 1: The composition of APIs and excipients in each of the formulations based on a % w/w*

| | HCTZ | RAM | Kollidon® VA 64 | PEG 3350 | Soluplus® |
|---|---|---|---|---|---|
| **Formulation 1 (F1)** | 12.5% | 5% | 82.5% | 0% | 0% |
| **Formulation 2 (F2)** | 12.5% | 5% | 74.25% | 8.25% | 0% |
| **Formulation 3 (F3)** | 12.5% | 5% | 0% | 0% | 82.5% |

#### 2.2.1.2 Preparation of the MET and SIT formulations

Drug(s) with or without polymer(s) were dissolved in a premixed solvent with a composition of 20 % (v/v) ethanol, 80 % (v/v) water. The inlet temperature, airflow, aspirator and feed rates at which the spray dryer was operated were kept at 120°C, 667 Normlitres/h, 100% (equivalent to 35 $m^3$/hr) and 20% (~ 5 - 7 ml/min), respectively. The outlet temperature varied between 72°C - 76 °C. The solution concentrations were varied between 1 % and 5 % (w/v) for the formulations, depending on the HPC polymer used.

### 2.2.2 Manufacture of extrudates and melt granules

All extrudates and melt granules produced by HME and MG were produced by a co-rotating, fully intermeshing twin-screw extruder (Microlab, Rondol Technology Ltd, France) with forward conveying elements only. The extruder details are outlined in table 2.2.

*Table 2. 2: Specification of Rondol 10 mm Microlab extruder*

| Specification | Value | Unit |
|---|---|---|
| Screw diameter | 10 | mm |
| Screw speed | 0 – 200 | rpm |
| Profile | Co-rotating, intermeshing | - |
| Number of barrel heating sections | 4 | - |
| Length of each barrel section | 5 : 1 | L/D |
| Overall barrel length | 20 : 1 | L/D |
| Minimum run size | 10 | g |
| Typical wastage | < 3 | g |
| Max processing temperature | 300 | °C |
| Materials of construction of the barrel | High strength carbon steel | - |
| Cooling water requirement | 1 | L/min |

The extruder die (Rondol Technology Ltd, France) was 2 mm in diameter, and was connected via screws to the end of the barrel. All heating zones were varied according to formulation, as was screw rpm. No die was attached during the MG process.

#### 2.2.2.1 Manufacture of the RAM and HCTZ extrudates

Formulations chosen for extrusion were premixed using an agate mortar and pestle for 5 min. The premixes were fed into the extruder using a twin-screw powder feeder (Rondol Technology Ltd, France) at a rate of 10 rpm. After air cooling, the cylindrical extrudates were manually cut into pellets with a length of 5 mm using a sterile scalpel and placed into a grinding jar for milling. The pellets were pulverised using a cryogenic ball-mill (Retsch Cryomill, Haan, Germany). A 50-litre liquid nitrogen pressurised tank, with a

pressure maximum of 1.2 bar was used to supply liquid nitrogen to the milling chamber. The milling jar was dipped into liquid nitrogen for 3 min prior to placing into the cryomill in order to cool the jar to liquid nitrogen temperature. A further precooling of 2 min was employed in the cryomill. Three cycles were employed consisting of 5 min of grinding (30 Hz) followed by a 2 min break. After cryomilling experiments, the temperature of the chamber was allowed to equilibrate to room temperature and the chamber opened under dry nitrogen atmosphere. The grinding jar material was composed of stainless steel and had a volume of 25 ml. Three stainless steel ball bearings with a diameter of 10 mm were used to pulverise the HME extrudates into a fine powder. Physicochemical analysis of the extrudates was conducted before and after cryo-milling. HME feed batch sizes were kept constant at 10 g. Table 2.3 shows the conditions used in the hot melt extruder at the various zones for the manufacture of the various formulations, discussed in chapter 3.

*Table 2. 3: Processing conditions used during hot melt extrusion of HCTZ/RAM pharmaceutical formulations.*

| Formulation | Feed rate (rpm) | Screw speed (rpm) | Feed Zone (°C) | Zone 1 (°C) | Zone 2 (°C) | Zone 3 (°C) | Die (°C) |
|---|---|---|---|---|---|---|---|
| **F1** | 10 | 20 | 90 | 110 | 140 | 140 | 120 |
| **F2** | 10 | 20 | 70 | 90 | 110 | 110 | 90 |
| **F3** | 10 | 20 | 90 | 110 | 140 | 140 | 120 |

#### 2.2.2.2 Manufacture of SIM extrudates/spherical pellets

Formulations chosen for extrusion were premixed using an agate pestle and mortar for 5 min. The premixes were fed into the extruder manually, using a spatula. After air cooling, the cylindrical extrudates were manually cut using a sterile scalpel into pellets with a length of 2 mm as the width was measured at 2 mm after extrusion (measured using digital callipers). To aid in the cutting process, heat was applied using a heat gun (Bosch PHG 600-3, Leinfelden, Echterdingen, Germany) until the extrudate was soft enough to easily and accurately cut. The cut extrudates were then placed into a Caleva spheroniser (GB Caleva Ltd, Dorset, UK), fitted with a 12 cm cross hatch friction plate, to try and make the extrudates as spherical as possible. Heat was applied, using a heat gun (Bosch PHG 600-3, Leinfelden, Echterdingen, Germany), to the spheroniser to aid in the process. Two min cycles of 3000 rpm in the spheroniser were followed by applying heat until the pellets were satisfactory spherical to be spray coated. HME feed batch sizes were kept constant at 11 g.

Table 2.4 shows the different polymers and API concentrations in the final product, with table 2.5 showing the final conditions used to produce the desired extrudate.

*Table 2.4: The composition of the optimised formulation for the simvastatin core material*

| Components | Weight | % |
|---|---|---|
| Simvastatin | 0.5g | 4.5 |
| HPMCAS-MF | 4.275g | 38.86 |
| Eudragit L100 | 2.1375g | 19.43 |
| Eudragit 100-55 | 2.1375g | 19.43 |
| d-α-Tocopheryl polyethylene glycol 1000 succinate (TPGS) | 0.950g | 8.64 |
| Triethyl Citrate (TEC) | 1g | 9.09 |
| **Total weight** | **11g** | **100%** |

*Table 2.5: Processing conditions used during hot melt extrusion of the simvastatin core material*

| Formulation | Feed rate (rpm) | Screw speed (rpm) | Feed Zone (°C) | Zone 1 (°C) | Zone 2 (°C) | Zone 3 (°C) | Die (°C) |
|---|---|---|---|---|---|---|---|
| **SIM core** | Manual | 20 | 80 | 130 | 150 | 130 | 110 |

### 2.2.2.3 Manufacture of GLZ extrudates

Formulations chosen for extrusion were premixed using an agate pestle and mortar for 5 min. The premixes were fed into the extruder manually, using a spatula. After air cooling, the cylindrical extrudates were manually cut using a sterile scalpel into pellets with a length of 2 mm as the width was measured at 2 mm after extrusion (measured using digital callipers). To aid in the cutting process, heat was applied using a heat gun (Bosch PHG 600-3, Leinfelden, Echterdingen, Germany) until the extrudate was soft enough to easily and accurately cut. The cut extrudates were then placed into a Caleva spheroniser (GB Caleva Ltd, Dorset, UK), fitted with a 12 cm cross hatch friction plate, to try and make the extrudates as spherical as possible. Heat was applied, using a heat gun (Bosch PHG 600-3, Leinfelden, Echterdingen, Germany), to the spheroniser to aid in the process. 2 min cycles of 3000 rpm in the spheroniser were followed by applying heat until the pellets were satisfactory spherical for to be spray coated. HME feed batch sizes were kept constant at 10 g

### 2.2.3 Manufacture of melt granules

#### 2.2.3.1 Manufacture of MET and SIT melt granules

Formulations were mixed for 5 min, using a mortar and pestle. Mixed powders were manually fed into a co-rotating 20:1 (screw length to diameter ratio), fully intermeshing twin-screw Rondol Microlab 10 mm extruder (Rondol Technology Ltd., France) with only forward conveying elements assembled and no die attached (open end). The ratio of MET to SIT was kept constant at 850:63, which corresponds to a dose ratio of 850 mg of MET and 50 mg of sitagliptin (as SIT). This is comparable to the already commercialised FDC product containing MET and SIT. PEG 3350 was used, when necessary, as an additional binding agent. The extruder barrel was divided into 4 heating zones (the feeding zone and zones 1-3). Processing temperatures were set at 130°C and incrementally increased up. Screw rotation speed was varied between 5-20 rpm during the development and optimisation stage of the study with 10 rpm being selected as the optimised screw rotation speed. MG feed batch sizes were kept constant at 5 g.

### 2.2.4 Spray coating using the Wurster method

A Mini-Glatt Fluidised Bed Dryer (Glatt, Weimar Germany) with a Wurster attachment was used to spray coat all spheronised extrudates.

#### 2.2.4.1 Spray coating of SIM spherical extrudates

In the preliminary spray coating studies, MCC beads of diameter 1 mm (largest commercially available from JRS pharma, Surrey, UK (VIVAPUR® MCC Spheres)) were used. The coating for the simvastatin extrudate contained RAM, HCTZ and Pharmacoat 603 dissolved in 200 ml of a solvent mixture which comprised of 50 % (v/v) water and 50 % (v/v) methanol with amaranth solution added for visual colouring effect. Pharmacoat 603 was dissolved in 100 ml of water and added to 100 ml of methanol in which RAM and HCTZ had been dissolved. Once preliminary testing with MCC beads was completed, spheronised extrudates were coated. The overall concentrations of RAM, HCTZ and Pharmacoat 603 were varied according to the run, however, the ratio remained constant at 1: 2.5: 6.5 when coating the extrudates. Nitrogen flow, atomiser pressure, inlet temperature and pump rate were optimised at 25 – 30 $m^3$/h, 1 bar, 80ºC and 0.8 (equivalent to 4 – 5 ml/min), respectively.

#### 2.2.4.2 Spray coating of GLZ spherical extrudates

The ratio of SIT : Pharmacoat 603 remained constant at 50 : 50 for all experimental runs. In the preliminary spray coating studies, MCC beads of diameter 1 mm (largest commercially available from supplier) were used. The initial solvent used comprised of

100 % water due to the solubility of both components. Subsequent runs comprised of a 50 % (v/v) water and 50 % (v/v) methanol solvent with amaranth solution added for visual colouring effect. The concentrations of SIT and Pharmacoat 603 varied according to runs. Nitrogen flow, atomiser pressure, inlet temperature and pump rate were optimised at 25 – 30 $m^3$/h, 1 bar, 80ºC and 0.6 (equivalent to 3 – 4 ml/min) respectively.

## 2.3 Solid State Characterisation

### 2.3.1 Thermogravimetric analysis (TGA)

TGA was conducted on a Q50 TGA (TA Instruments, Delaware, United States) apparatus. Aluminium pans were tared and samples (5 - 10 mg) were placed into the aluminium pans prior to analysis. Scans were recorded over a temperature range from 25 – 300 °C unless otherwise stated at a heating rate of 10°C/min. Universal Analysis software (TA Instruments) was used for data analysis. Analysis was performed in at least in triplicate.

#### 2.3.1.1 HCTZ and RAM formulation – TGA analysis of ramipril

To highlight the thermal degradation pathway of ramipril to ramipril diketopiperazine, samples of ramipril (5 – 10 mg) were placed in the TGA and heated to 140 °C at a heating rate of 10 °C/min. Samples were held at 140 °C for two hours to ensure complete conversion to the degradation product and then tested by HPLC as outlined in chapter 2, section 2.13.1. Analysis was performed in triplicate.

### 2.3.2 Differential scanning calorimetry (DSC)

The thermal behaviour of materials was analysed using a differential scanning calorimeter (Q200, TA Instruments, Leatherhead, UK). Nitrogen was used as the purge gas (60 ml/min). Calibration was performed with an indium standard every three months. Samples (3 – 10 mg) were analysed in crimped standard aluminium pans with a heating rate of 10 °C/min unless otherwise stated. DSC data was analysed using Universal Analysis software (TA Instruments). Melting temperatures of drugs were determined and reported as peak temperature. The $T_g$s were defined as the midpoint of the transition.

#### 2.3.2.1 MET and SIT formulation – DSC analysis of polymers

HPC polymers were heated to 150 °C, held for 5 min to remove any moisture present, cooled to – 40 °C, before being heated at a heating rate of 10 °C/min to determine the glass transition and melting temperatures. Analysis was performed in triplicate.

### 2.3.3 Modulated differential scanning calorimetry (mDSC)

Samples were directly filled into standard aluminium pans (3–8 mg) (TA Instruments, Leatherhead, UK) and analysed using mDSC (Q200, TA Instruments, Leatherhead, UK). Nitrogen was used a purge gas (60 ml/min). A heating rate of 5 °C/min, a modulation amplitude of 0.53 °C and a period of 40 s were used. Calibration was performed with an indium standard every three months. Analysis was performed in triplicate.

### 2.3.4 Powder x-ray diffraction (PXRD)

Powder x-ray analysis was performed using a Miniflex II Rigaku diffractometer (Rigaku™ Corporation, Japan) with Ni-filtered Cu Kα radiation (1.54 Å). The tube voltage and tube current used were 30 kV and 15 mA, respectively. The PXRD patterns were recorded in the angular range (2θ) ranging from 5 ° to 40 ° at a step scan rate of 0.02 ° per second. Rigaku Peak Integral software was used to determine peak intensity for each sample using the Sonneveld-Visser background edit procedure. Scans were performed in triplicate at room temperature. The programme Mercury (version 3.9, Cambridge Crystallographic Data Centre, Cambridge, UK) was used for calculation of PXRD patterns on the basis of the single crystal structure obtained from the Cambridge Crystallographic Data Centre. The crystallinity of API, physical mixtures and formulated products were all analysed using PXRD. Extrudates were crushed using an agate pestle and mortar to produce a fine powder for analysis.

## 2.4 Attenuated total reflectance Fourier transform infrared spectroscopy (ATR - FTIR)

Infrared spectra were recorded on a PerkinElmer Spectrum 1 FT-IR Spectrometer equipped with a UATR and a ZnSe crystal accessory. Each spectrum was scanned in the range of 650 – 4000 $cm^{-1}$ with a resolution of 4 $cm^{-1}$. Data were evaluated using Spectrum v 5.0.1. software. Four scans of each sample were taken. Analysis was performed in at least in triplicate.

### 2.4.1 ATR – FTIR of RAM and HCTZ formulations

The crystalline materials in the formulations were converted to their amorphous component counterparts by melt quenching (heating on a hotplate and subsequently dipping into liquid nitrogen) and these were mixed in the desired proportions using an agate pestle and mortar to obtain amorphous physical mixtures which were then subjected to FT-IR. Along with physical mixtures, the products produced by HME and SD were also subjected to FT-IR.

## 2.5 Scanning electron microscopy (SEM)

The surface images of the samples were captured at various magnifications by SEM using a Zeiss Supra Variable Pressure Field Emission Scanning Electron Microscope (Zeiss, Oberkochen, Germany) equipped with a secondary electron detector at 5 kV. Samples to be studied, were glued onto carbon tabs mounted on to aluminium pin stubs and sputter-coated with a gold/palladium mixture under vacuum prior to analysis.

### 2.5.1 SEM of HCTZ and RAM formulations

SEM was conducted on the raw materials, formulated products and the powder compacts compressed in the Wood's apparatus (for dissolution testing).

### 2.5.1 SEM of MET and SIT formulations

SEM was conducted on the raw materials, formulated granules and powders and caplet surfaces.

## 2.6 Particle size analysis (PSA)

### 2.6.1 PSA of HCTZ and RAM formulations

Particle size measurements were performed by laser diffraction using a Malvern Mastersizer 2000 particle sizer (Malvern Instruments Ltd, Worchester, UK) with Scirocco 2000 accessory. The dispersive air pressure used was 2.5 bar. Samples were run at a vibration feed rate of 50 %. The particle size reported is the median diameter d (0.5). The d (0.5) is the diameter where 50 % of the cumulative distribution is above and 50 % is below this size. The values presented are the average of at least three determinations. Mastersizer 2000 software (Version 5.61) was used for the analysis of the particle size.

### 2.6.2 PSA of MET and SIT formulations

Particle size measurements were performed by laser diffraction using a Malvern Mastersizer 3000 particle sizer (Malvern Instruments Ltd, Worchester, UK) with Aero M dry powder dispersion accessory. The dispersive air pressure used was 2 bar. Samples were run at a vibration feed rate of 50 %. The particle size reported is the median diameter d (0.5). The d (0.5) is the diameter where 50 % of the cumulative distribution is above and 50 % is below this size. The values presented are the average of at least three determinations. Mastersizer 3000 software (Version 3.50) was used for the analysis of the particle size.

## 2.7 Flowability measurements

### 2.7.1 MET and SIT formulations

The flowability behaviour of physical powder blends, the melt granules and SD formulations was determined using a FT4 powder rheometer (Freeman Technology, Tewkesbury, UK). Cohesiveness and angle of internal friction were determined by placing between 1 - 2 grams of samples in the 1 ml shear cell and applying a 24 mm shear head. The flowability for each sample following pre shearing at a pre-shear normal stress of 9 kPa was investigated by determining the angle of internal friction (AIF) cohesiveness and flow function (FF) (Freeman 2007). All samples were tested at least in triplicate and average values determined.

## 2.8 Caplet manufacture

### 2.8.1 MET and SIT formulations

Sample sizes of 1063 mg for each formulation (equivalent to 850 mg MET and 63 mg of SIT) were weighed and compressed using a Natoli NP-RD10A single punch laboratory tablet press (Natoli Engineering Company, Inc, USA) with an in-house designed punch and die (I Holland Ltd, Nottingham, UK). The die measured 21.37 mm in length and 10.45 mm in diameter. Two different compression forces, i.e. 5000 N and 8000 N were used to manufacture the caplets of each formulation.

## 2.9 Hardness measurements

### 2.9.1 MET and SIT formulations

A minimum of 6 individual caplets that were prepared at different compression forces were subjected to a crushing test using an EH-01 Electrolab manual tablet hardness tester (Electrolab, Mumbai, India). Thickness (internal and external), diameter and length of caplets were first measured, using a digital calliper, before placing at the moving jaw of the hardness tester. The long side of the caplet was oriented parallel to the direction of force. The force required to break the caplet was recorded in Newtons and tensile strength was calculated according to the equation proposed by Pitt and Heasley below (Pitt and Heasley 2013):

*Equation 2. 1*

$$\sigma_t = \frac{2}{3}\left(\frac{10P}{\pi D^2\left(2.84\frac{t}{D} - 0.126\frac{t}{w} + 3.15\frac{w}{D} + 0.01\right)}\right)$$

Where:

$\sigma_t$= Tensile strength (MPa)

*P*= Fracture load (N),

*D*= diameter (mm)

t= thickness (external) (mm)

w= thickness (internal) (height) (mm)

L= length of long axis (mm)

## 2.10 Friability studies

### 2.10.1 MET and SIT formulations

A sample of 10 caplets were carefully dedusted prior to testing, accurately weighed and placed in a Copley TA20 friability test drum (Copley Scientific, Nottingham, UK). The drum was rotated for 100 rpm at 25 rpm for 4 minutes. Caplets were dedusted and accurately weighed. Friability was calculated as per the equation below:

*Equation 2. 2*

$$\%\, F = \frac{W_0 - W_1}{W_0}\, X\, 100$$

Where:

$W_0$ = the initial total weight of caplets

$W_1$ = the total weight of caplets after the test.

## 2.11 Disintegration studies

### 2.11.1 MET and SIT formulations

A minimum of 6 caplets were placed in the basket rack of a Erweka ZT 44 disintegration tester (Novatech, Newcastle, UK) which was immersed in a bath of 0.1 M HCl, pH 1.2, held at 37 °C with a constant vertical agitation rate of 30 cycles per minute as per the European Pharmacopeia (European Pharmacopoeia 2020a). The volume of the fluid in the vessel was such that at the highest point of the upward stroke the wire mesh

remained at least 15 mm below the surface of the fluid and descended to not less than 25 mm from the bottom of the vessel on the downward stroke. At no time was the top of the basket-rack assembly submerged. The time required for all the caplets to pass through the mesh screen was recorded.

## 2.12 Forced degradation studies

### 2.12.1 SIM formulation

To fully convert the SIM lactone form to the SIM beta-hydroxy form, 5 mg of the raw material SIM lactone was dissolved in 100 ml of 0.1M HCl and left under constant agitation for 72 h in a volumetric flask to ensure full conversion to the beta-hydroxy form. HPLC analysis and LC-MS studies were conducted to confirm full conversion had occurred as outlined in chapter 2, sections 2.13.3 and 2.16. All analysis was done in triplicate.

### 2.12.2 GLZ formulation

5 mg samples of GLZ were dissolved in 100 ml of 0.1M HCl, 0.1M NaOH and pH 7.4 phosphate buffer and placed in water baths with a constant agitation of 60 rpm at 25 °C, 37 °C and 60 °C, respectively. Samples were taken at 24 h, 48 h and 72 h and tested for the degradation of GLZ to degradation product A through HPLC and LC-MS as outlined in chapter 2, sections 2.13.4 and 2.16. All analysis was done in triplicate.

## 2.13 High performance liquid chromatography (HPLC)

### 2.13.1 HCTZ and RAM HPLC method

The concentrations of HCTZ and RAM in solution were determined using an Alliance HPLC with a Waters 2695 Separations module system and Waters 2996 photodiode array detector (Waters, Milford, MA, USA). The HPLC mobile phases consisted of a 0.1 M sodium perchlorate solution adjusted to pH 2.5 (mobile phase A) and acetonitrile (mobile phase B). The mobile phase was vacuum filtered through a 0.45 µm membrane filter (Pall Supor® 0.45 µm, 47 mm) and bath sonicated for 5 min. Details of the gradient elution used are shown in Table 2.6. Separation was performed on a Kinetex® C18 column (150mm length, diameter 4.6 mm, particle size 5 µm) with UV detection at 210 nm. The column temperature was kept at 30 °C throughout. The elution times for HCTZ and RAM were 2.45 min and 6.4 min, respectively. Empower software was used for peak evaluation. Calibration curves were generated weekly, with freshly prepared samples, while studies were on-going. The linearity range was between 1 - 100 µg/ml for HCTZ and 1 – 25 µg/ml for RAM with regression coefficient ($r^2$) of 0.999 and 0.998, respectively. The limits of detection for the method were 0.15 µg/ml for HCTZ and 0.18

µg/ml for RAM. The HPLC method was validated for linearity, range, accuracy, precision and robustness as per ICH Q2 (R1) guidelines.

*Table 2. 4: Details of HPLC gradient elution method including time (min), mobile phase composition and flow rate (ml/min) (%).*

| Time (min) | Mobile phase A (%) | Mobile phase B (%) | Flow (ml/min) |
|---|---|---|---|
| 0 | 70 | 30 | 0.8 |
| 5 | 40 | 60 | 1.5 |
| 6 | 70 | 30 | 1 |
| 9 | 70 | 30 | 1 |
| 10 | 70 | 30 | 0.8 |

### 2.13.2 MET and SIT HPLC method

The concentrations of MET and SIT in solution were determined using an Alliance HPLC with a Waters 2695 Separations module system and Waters 2996 photodiode array detector (Waters, Milford, MA, USA). The HPLC mobile phase consisted of a 0.01 M ammonium acetate aqueous solution adjusted to pH 4.5 with acetic acid and acetonitrile in a 30:70 v/v ratio. The mobile phase was vacuum filtered through a 0.45 µm membrane filter (Pall Supor® 0.45 µm, 47 mm) and bath sonicated for 5 min. Separation was achieved using a Zorbax CN (4.6 mm i.d., 250 mm and 5 µm) column using a detection wavelength of 239 nm for MET and 267 nm for SIT, flow rate of 1.0 ml/min and an injection volume of 10 µL. The elution times for MET and SIT were 11.1 min and 13.6 min respectively. Empower software was used for peak evaluation. Calibration curves were generated weekly, with freshly prepared samples, while studies were on-going. The linearity range was between 1 - 100 µg/ml for MET and 1 – 75 µg/ml for SIT with regression coefficient ($r^2$) of 0.999 and 0.998, respectively. The limits of detection for the method were 0.6 µg/ml for MET and 1.1 µg/ml for SIT. The HPLC method was validated for linearity, range, accuracy, precision and robustness as per ICH Q2 (R1) guidelines.

### 2.13.3 SIM HPLC method

The concentration of SIM lactone and SIM beta-hydroxy in solution were determined using an Alliance HPLC with a Waters 2695 Separations module system and Waters 2996 photodiode array detector (Waters, Milford, MA, USA). The HPLC mobile phase consisted of a 0.1 % w/v phosphoric acid and acetonitrile in a 35:65 v/v ratio. The mobile phase was vacuum filtered through a 0.45 µm membrane filter (Pall Supor® 0.45 µm, 47

mm) and bath sonicated for 5 min. Separation was achieved using a Waters Spherisorb C8 column (250 mm length, diameter 4.6 mm, particle size 5 µm) column, detection wavelength was 238 nm, flow rate of 1.0 ml/min and an injection volume of 10 µl. The temperature of the column was kept constant at 25 °C. The elution times for SIM (beta-hydroxy) and SIM (lactone) were 4.95 min and 7.3 min respectively. Empower software was used for peak evaluation. Calibration curves were constructed weekly, with freshly prepared samples, while studies were on-going. The linearity range was between 1 - 30 µg/ml for SIM (beta-hydroxy) and 1 – 30 µg/ml for SIM (lactone) with regression coefficient ($r^2$) of 0.999 and 0.999, respectively. The limits of detection for the method were 0.19 µg/ml for SIM (beta-hydroxy) and 0.19 µg/ml for SIM (lactone). The HPLC method was validated for linearity, range, accuracy, precision and robustness as per ICH Q2 (R1) guidelines.

### 2.13.4 GLZ HPLC method

The concentrations of GLZ and GLZ degradation product A in solution were determined using an Alliance HPLC with a Waters 2695 Separations module system and Waters 2996 photodiode array detector (Waters, Milford, MA, USA). The HPLC mobile phase consisted of 5.751 g/l ammonium phosphate and 2 ml/L Triethylamine (pH adjusted to pH 2.4 with phosphoric acid) mixed with acetonitrile in a 50:50 v/v ratio. The mobile phase was vacuum filtered through a 0.45 µm membrane filter (Pall Supor® 0.45 µm, 47 mm) and bath sonicated for 5 min. Separation was achieved using a Waters Spherisorb ODS column (250 mm length, diameter 4.6 mm, particle size 5 µm) column, detection wavelength was 233 nm, flow rate of 1.2 ml/min and an injection volume of 10 µl. The temperature of the column was kept constant at 30 °C. The elution time for GLZ degradation product A was 3.4 min and the elution time for GLZ was 9.38 min. Empower software was used for peak evaluation. Calibration curves were constructed weekly, with freshly prepared samples, while studies were on-going. The linearity range was between 0.625 – 37.5 µg/ml for GLZ degradation product A and between 0.625 – 37.5 µg/ml for GLZ with regression coefficients ($r^2$) of 0.999 and 0.999 respectively. The limits of detection for the method were 0.48 µg/ml for GLZ degradation product A and 0.22 ug/ml for GLZ. The HPLC method was validated for linearity, range, accuracy, precision and robustness as per ICH Q2 (R1) guidelines.

## 2.14 Assay of drug content

### 2.14.1 HCTZ and RAM formulations

Fifty mg of each formulation was accurately weighed using a microbalance (Mettler-Toledo, Leicester, UK), added to a 100 ml volumetric flask and made up to the mark with

0.1 M HCl solution. The solution was sonicated for 10 min to ensure the formulation was fully dissolved before being analysed by HPLC (as described in chapter 2, section 2.13.1). Drug content was calculated by determining the area under the curve and comparing to area under the curve of standards of known concentration. Analysis was performed in triplicate.

### 2.14.2 MET and SIT formulations

Fifty mg of each formulation was accurately weighed using a microbalance (Mettler-Toledo, Leicester, UK), added to a 100 ml volumetric flask and made up to the mark with 0.1 M HCl solution. The solution was sonicated for 10 min to ensure the formulation was fully dissolved before being diluted suitably to fall within the concentrations of the calibration curves for the individual APIs and then analysed by HPLC (as described in chapter 2, section 2.13.2). Drug content was calculated by determining the area under the curve and comparing to area under the curve of standards of known concentration. Analysis was performed in triplicate.

### 2.14.3 SIM, HCTZ and RAM formulations

Before coating, a sample of spheronised pellets were crushed with a pestle and mortar to a powder. Fifty mg of the powder was added to 100 ml of acetonitrile and sonicated for 15 min to ensure all SIM had dissolved. The samples were then passed through a 0.45 µm membrane filter (Pall Supor® 0.45 µm, 47 mm) to remove the undissolved substances and were further suitably diluted with acetonitrile before being analysed by HPLC (as described in chapter 2, section 2.13.3). After coating, 490 mg of product (corresponding to one target dose) was weighed out and crushed with a pestle and mortar to a powder. Of this, 100 mg was added to a 100 ml volumetric flask and made up to the mark with 0.1 M HCl solution and sonicated for 10 min to ensure HCTZ and RAM had fully dissolved. The samples were then passed through a 0.45 µm membrane filter (Pall Supor® 0.45 µm, 47 mm) to remove the undissolved substances and were further suitably diluted with 0.1 M HCl before being analysed by HPLC (as described in chapter 2, sections 2.13.1 and 2.13.3). Drug content was calculated by determining the area under the curve and comparing to area under the curve of standards of known concentration. Analysis was performed in triplicate.

### 2.14.4 GLZ and SIT formulations

Before coating, a sample of spheronised pellets were crushed with a pestle and mortar to a powder. Fifty mg of the powder was added to 100 ml of acetonitrile and sonicated for 15 min to ensure all GLZ had dissolved. The samples were then passed through a 0.45 µm membrane filter (Pall Supor® 0.45 µm, 47 mm) to remove the undissolved

substances and were further suitably diluted with acetonitrile before being analysed by HPLC (as described in chapter 2, section 2.13.4). Drug content was calculated by determining the area under the curve and comparing to area under the curve of standards of known concentration. Analysis was performed in triplicate.

## 2.15 Surface topography

### 2.15.1 Surface topography of HCTZ and RAM formulations

The surface topography of compressed discs was assessed using a Filmetrics Profilm3D profilometer (San Diego, USA). Calibration was performed by using a VLSI surface topography reference step height standard with a height of 1.8 µm. The profilometer achieves measurements using vertical scanning interferometry (VSI) combined with high accuracy phase shifting interferometry (PSI) to provide access to surface topography from the sub-nanometre to millimetre scale. The profilometer was used to measure the surface roughness of the compressed discs and calculate Ra, the roughness average of a surface's measured microscopic peaks and valleys. Area scans of the disc surfaces were made. The transverse lengths were 1.92 mm in the X direction and 1.68 mm in the Y direction. The profilometer used has a spot size diameter of 0.88 µm. Roughness data was calculated by SPIP V5.1.5.0 software. Samples were sputter-coated with a gold/palladium mixture under vacuum prior to analysis. Scans and analysis were performed in triplicate. Statistical analysis was conducted using Minitab® 16 software. A two-sample t-test was carried out comparing the surface roughness of the SD formulation compressed discs with that of the cryomilled HME formulation compressed discs.

## 2.16 Liquid chromatography-mass spectroscopy (LC-MS)

The mass spectrometer used was an LTQ/Orbitrap XL Discovery Mass Spectrometer (Thermo Fisher) consisting of; Linear ion trap to collect, separate and detect ions; Orbitrap used for accurate mass detection (30,000 resolution); and Xcalibur software providing method setup, data acquisition, data processing and reporting. Mass scans were performed using Electrospray Ionization (ESI) under positive and negative modes. Nitrogen gas was used as the drying gas and to promote dissolution of sample as it was infused into the ion chamber. Temperature of the capillary needle through which sample flows was set to 300 °C. The following were the conditions used;

Sheath gas: 70 au Auxiliary gas: 5 au Sweep gas: 2 au

Capillary temp.: 300 °C Spray Voltage: 3.5 V

Capillary voltage: 31 V Tube Lens: 75 V

The liquid chromatography phase used corresponded to those used in the HPLC methods previously described in chapter 2 section 2.13.3 for SIM and section 2.13.4 for GLZ.

## 2.17 Dissolution

### 2.17.1 HCTZ and RAM formulations

#### 2.17.1.1 Intrinsic/constant surface area dissolution studies

The intrinsic dissolution rate of manufactured formulations and drug raw materials was determined using a Wood's apparatus (Quality Lab Accessories, Telford, PA, USA). 200 mg of drug raw material and 200 mg of each processed formulation (equivalent to 10 mg RAM and 25 mg HCTZ) was weighed and compressed in the 8 mm punch and die set of the Wood's apparatus, at a pressure of 3 tonnes for 1 min using a hydraulic press (Perkin Elmer, Shelton, USA). The Wood's apparatus was then attached to a Sotax AT-7 dissolution bath (Sotax, Wallbrunnstraße, Germany). The dissolution study was carried out using 0.1 M HCl as the dissolution medium (volume: 500 ml, temperature: 37 ± 0.5 °C, pH: 1.2) and a rotational speed of 100 rpm. A pH of 1.2 was chosen to mimic the acidic conditions of the stomach where the desired release of the formulations would occur. Five ml aliquots were withdrawn and were replaced with fresh media at the pre-determined time intervals. Samples were filtered through PTFE hydrophilic 0.45 µm filters (Fisher Scientific Ireland Ltd., Dublin, Ireland) and were analysed for drug content by HPLC. The dissolution study was terminated after 120 min. The intrinsic dissolution release rate was determined from the slope of the dissolution time profiles over the first 30 min. All studies were performed in triplicate.

### 2.17.2 MET and SIT formulations

#### 2.17.2.1 EP type I basket apparatus

In-vitro dissolution studies of the manufactured caplets were performed using an EP type I basket apparatus attached to a Sotax AT-7 dissolution bath (Sotax, Lörrach, Germany). The dissolution study was carried out using 0.68% w/v solution of potassium dihydrogen orthophosphate as the dissolution medium (volume: 900 ml, temperature: 37 ± 0.5 °C, pH: 6.8) and a rotational speed of 100 rpm. This dissolution method was chosen as it is the dissolution method detailed in the European Pharmacopoeia for MET immediate

release solid oral dosage tablets. Five ml aliquots were withdrawn and were replaced with fresh media at the pre-determined time intervals. Samples were filtered through PTFE hydrophilic 0.45 µm filters (Fisher Scientific Ireland Ltd., Dublin, Ireland) and were analysed for drug content by HPLC. The dissolution study was terminated after 120 min. All studies were conducted in triplicate.

### 2.17.3 SIM, HCTZ and RAM formulations

#### 2.17.3.1 EP type II paddle apparatus

In-vitro dissolution studies of the manufactured spray coated pellets were performed using an EP type II paddle apparatus attached to a Sotax AT-7 dissolution bath (Sotax, Lörrach, Germany). As the goal of the formulation was to manufacture a FDC product with delayed, targeted release of SIM and an immediate release of HCTZ and RAM, the pH conditions were varied throughout the dissolution to mimic gastrointestinal conditions (Evans et al. 1988). The dissolution conditions used were as follows, as detailed previously by Andrews et al (Andrews et al. 2019):

- 0.1 M HCl (pH 1.2) for two hours;
- pH adjusted to 6.8 by the addition of 0.2 M $Na_3PO_4$ and dissolution continued for a further 2 hours;
- pH adjusted to 7.5 by the addition of 2 M NaOH drops and dissolution continued for a further 2 hours;
- pH adjusted to 6.5 by the addition of 1 M HCl drops and dissolution continued for 18 hours until end.

The temperature was maintained at 37 ± 0.5 °C and a paddle stirring speed of 100 rpm was used. Five ml aliquots were withdrawn and were replaced with fresh media at the pre-determined time intervals. Samples were filtered through PTFE hydrophilic 0.45 µm filters (Fisher Scientific Ireland Ltd., Dublin, Ireland) and were analysed for drug content by HPLC. The dissolution study was terminated after 24 h. All studies were conducted in triplicate.

### 2.17.4 GLZ and SIT formulations

#### 2.17.4.1 EP type II paddle apparatus

In-vitro dissolution studies of the manufactured spray coated pellets were performed using an EP type II paddle apparatus attached to a Sotax AT-7 dissolution bath (Sotax, Lörrach, Germany). The dissolution study was carried out using phosphate buffer as the dissolution medium (volume: 900 ml, temperature: 37 ± 0.5 °C, pH: 7.4) with a rotational speed of 100 rpm as per the European Pharmacopeia method for gliclazide dissolution testing. 5 ml aliquots were withdrawn and were replaced with fresh media at the pre-determined time intervals. Samples were filtered through PTFE hydrophilic 0.45 µm

filters (Fisher Scientific Ireland Ltd., Dublin, Ireland) and were analysed for drug content by HPLC. The dissolution study was terminated after 24 h. All studies were conducted in triplicate.

## 2.18 Stability Studies

### 2.18.1 HCTZ and RAM formulations

Formulations produced by SD and HME methods were placed on short-term stability at two relative humidity (RH) conditions (25 °C/75% RH, and 25 °C/<10% RH) for 60 days. Sample storage conditions were monitored using the Amebis Stability Testing and Monitoring System (Amebis Ltd., Ireland). A suitable amount of test material was transferred to Amebis sample chambers containing a pre-prepared saturated salt solution to regulate the relative humidity. The sample chamber containing the test material and saturated salt solution was subsequently transferred to a temperature-controlled cabinet at the specified temperature. The integrated temperature and humidity sensor within the Amebis system wirelessly transmitted and logged data regarding the environmental conditions within each test chamber to the Amebis Control Software (Amebis Ltd., Ireland) at 30-minute intervals. The Amebis system allowed for remote monitoring of both temperature and relative humidity conditions without the need to remove the chamber for data retrieval/monitoring. Samples were taken and analysed periodically by PXRD, mDSC and HPLC over the course of 60 days to test for amorphous/crystalline nature and drug content.

## 2.19 Statistical analysis

### 2.19.1 HCZ and RAM formulations

Statistical analysis was conducted using Minitab® 16 software. A two-sample t-test was carried out comparing the particle size parameters for SD formulations and cryomilled HME formulations. A one-way analysis of variance (ANOVA) was carried out on the formulations comparing particle size d (0.5). The drug release profiles of manufactured formulations were compared using a one-way ANOVA at each individual time point with a two-sample t-test being used to compare the release rates of both active ingredients from the slope of the line for the first 30 min of each formulation. In all statistical analyses, $p < 0.05$ denoted significance.

### 2.19.2 MET and SIT formulations

Statistical analysis was conducted using Minitab® 16 software. A two-sample t-test was carried out comparing the particle size parameters between SD formulations and MG formulations. Another two-sample t-test was carried out comparing the particle size

parameters for SD formulations and MG formulations to MET raw material parameters. A one-way analysis of variance (ANOVA) was carried out on physical mixtures, spray dried formulations and melt granulation formulations for Angle of Internal Friction (AIF), cohesion and flow function (FF) parameters. A one-way analysis of variance (ANOVA) was carried out on physical mixtures, spray dried formulations and melt granulation formulations for heat of fusion DSC results to compare crystallinity. A two-sample t-test was carried out comparing the caplet size and caplet hardness between spray dried caplets and melt granulation caplets. In all statistical analyses, $p < 0.05$ denoted significance.

### 2.19.3 GLZ and SIT formulations

Statistical analysis of dissolution profiles was performed using DDSolver (Zhang et al. 2010). Dissolution similarity based using DDSolver is calculated using the mean-squared difference between a pair of profiles. An $f_2$ value between 50-100 indicates that dissolution profiles are similar.

# Chapter 3:

# A comparative study between hot-melt extrusion and spray-drying for the manufacture of anti-hypertension compatible monolithic fixed-dose combination products

## 3.1 Introduction

Hot Melt Extrusion (HME) and Spray Drying (SD) are two of most common processing techniques used in the continuous manufacturing of solid dispersions (Agrawal et al. 2016). Both techniques can be used to manufacture monolithic FDC products. In an industrial or lab setting, often one method of preparation of solid dispersions for production is arbitrarily chosen and then formulation scientists modify the formulation until the desired characteristics are achieved (Agrawal et al. 2016). However, solid dispersions prepared by different techniques can often display differences in their physicochemical properties (Agrawal et al. 2016; Riekes et al. 2014; Sethia and Squillante 2004). Therefore, during early stage development of a formulation, it may be important to understand the influence of the processing technique on the desired formulation. An understanding of the physicochemical properties of the active pharmaceutical ingredients (APIs) to be included in the formulation is crucial to avoid any degradation or formation of any unwanted products. For HME, thermolabile APIs may be difficult to work with due to the nature of the process which relies on thermal (and mechanical) energy input, which is normally supplied via heat conduction from barrel heating zones and the friction of the melt against the screw elements and interior wall of the extruder barrel, in order for the process to proceed (Huang, Donnell, et al. 2017). However, despite being challenging to work with, thermolabile APIs have been successfully processed via HME (Kulkarni et al. 2018; Repka et al. 1999). For APIs that thermally degrade at relatively low temperatures, SD may be more useful as it can be used to process solutions or suspensions (Aulton and Taylor 2013) at relatively low processing temperatures, due to the availability of a wide range of volatile solvents. While the wide range of solvents is advantageous for processing materials at low temperatures, the use of organic solvents can be controversial, due to the harmful environmental effects they can have. Residual solvents in manufactured products produced may also cause some issues, such as promoting the crystallization of amorphous material (Dunn et al. 2010)

Angiotensin converting enzyme (ACE) inhibitors and thiazide diuretics in fixed dose combination (FDC) products have been shown to reduce blood pressure more substantially than with individual therapy of the drugs alone (Ambrosioni, Borghi, and Costa 1987; Brown et al. 1990; Chrysant 1994). The diuretic causes intravascular volume depletion and increased sodium loss which causes reflex activation in the renin angiotensin system (RAS), thus potentiating the effects of an ACE inhibitor (Stanton and Reid 2002). Hydrochlorothiazide (HCTZ), a thiazide diuretic, and ramipril (RAM), an ACE inhibitor, are both recommended for the treatment of hypertension (World Health

Organization 2016). FDC products containing RAM and HCTZ have been previously shown to induce a significantly greater reduction in blood pressure than with individual monotherapies of the two APIs at the same dosages (Scholze et al. 1993).

Some authors have referred to HCTZ as a BCS class IV drug (Ghadi and Dand 2017; Sanphui et al. 2015), while others have classed it as a BCS class III (Klein and Shah 2008; Zaid et al. 2016). HCTZ has a reported $pK_a$ value of 7.9 (O'Neill 2013) and has been reported to have a solubility ranging from 60.8 mg to 103 mg per 100 ml within the pH range 1.0 to 7.4 (Blatnik et al. 2015). As the maximum daily dose of HCTZ is 100 mg (Brayfield 2014), HCTZ may be considered highly soluble according to the BCS system, as the maximum dose dissolves in less than 250 ml water over the stated pH range, and it may thus be classed as a BCS class III drug compound. RAM has a reported $pK_a$ value of 3.17 (O'Neill 2013). With a maximum daily dose of 10 mg (Brayfield 2014), RAM is classified as a BCS class I compound (Ramirez et al. 2010; Zaid et al. 2016). RAM is, however, a thermolabile drug compound, degrading on melting at a relatively low temperature (~ 117 °C).

The literature contains many examples of research conducted to gain an understanding of the effect of the manufacturing technique on the physicochemical properties of solid dispersions containing a single API (Agrawal et al. 2016; Badens et al. 2009; Guns et al. 2011). There is, however, a lack of discussion in the literature of the influence of different continuous manufacturing processes on the solid state and performance characteristics of systems containing more than one API (i.e. FDCs). The main objective was to produce monolithic FDCs for the treatment of hypertension using continuous manufacturing techniques and to investigate how these techniques affect the physicochemical properties of the products. A further aim was to understand how these properties can affect manufacturability, product performance and physical stability.

## 3.2 Results and discussion

Both Kollidon® VA 64 and Soluplus® were evaluated in this investigation as carriers for oral immediate release formulations. When incorporated into other formulations, these polymers have been shown to significantly increase the drug dissolution rate (Fule et al. 2016; Shamma and Basha 2013; Song et al. 2013). Table 2.1, chapter 2 shows the composition of each formulation in the current study processed by SD and HME, with table 2.3, chapter 2, showing the conditions used in the hot melt extruder at the various zones.

The lowest possible extrusion temperature was used to produce an extrudate of the formulations. One extrudates were formed, they were placed in a cryomill and pulverized until a power was formed as detailed in chapter 2 section 2.2.2.1. PEG 3350 was included as a plasticiser for HME experiments (and the same formulation was then also processed by SD for comparison purposes as detailed in chapter 2 section 2.2.1.1).

As well as including PEG 3350 to act as plasticiser, allowing HME to be conducted at lower processing temperatures, it has been reported previously in the literature that low molecular weight PEG can improve handling and processing (Repka et al. 1999; Schilling et al. 2007, 2010; Wu and McGinity 2001).

### 3.2.1 Physicochemical characteristics

Thermal analysis is utilized in the pharmaceutical industry to obtain information about substances' glass transition ($T_g$), melting and degradation temperatures. Thermogravimetric analysis (TGA) was used to analyse the thermal degradation of the APIs and polymers used in this study. As can be seen in figure 3.1, HCTZ is thermally stable up to at least 300 °C which corresponds well to previous reports in the literature (Valladao et al. 1996). RAM starts to thermally degrade at a much lower temperature at around 124 °C (figure 3.1).

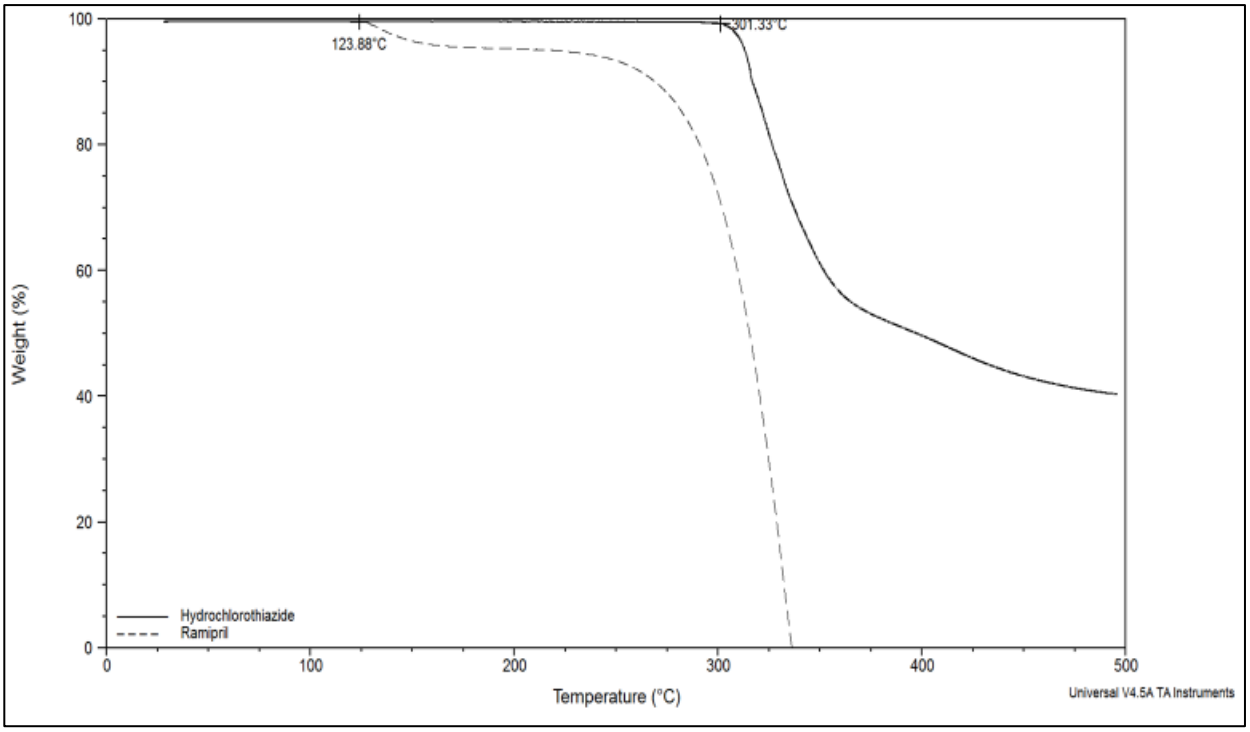


*Figure 3. 1: TGA thermogram of API raw materials with a heating ramp from 25 °C to 500 °C at 10 °C/ min, showing HCTZ and RAM.*

Polymers used in the study are thermally stable under the process conditions used in this study – PEG 3350 exhibits less than 1% weight loss up to 300 °C, while Soluplus® and Kollidon® VA 64 start to degrade just over 280 °C (figure 3.2).

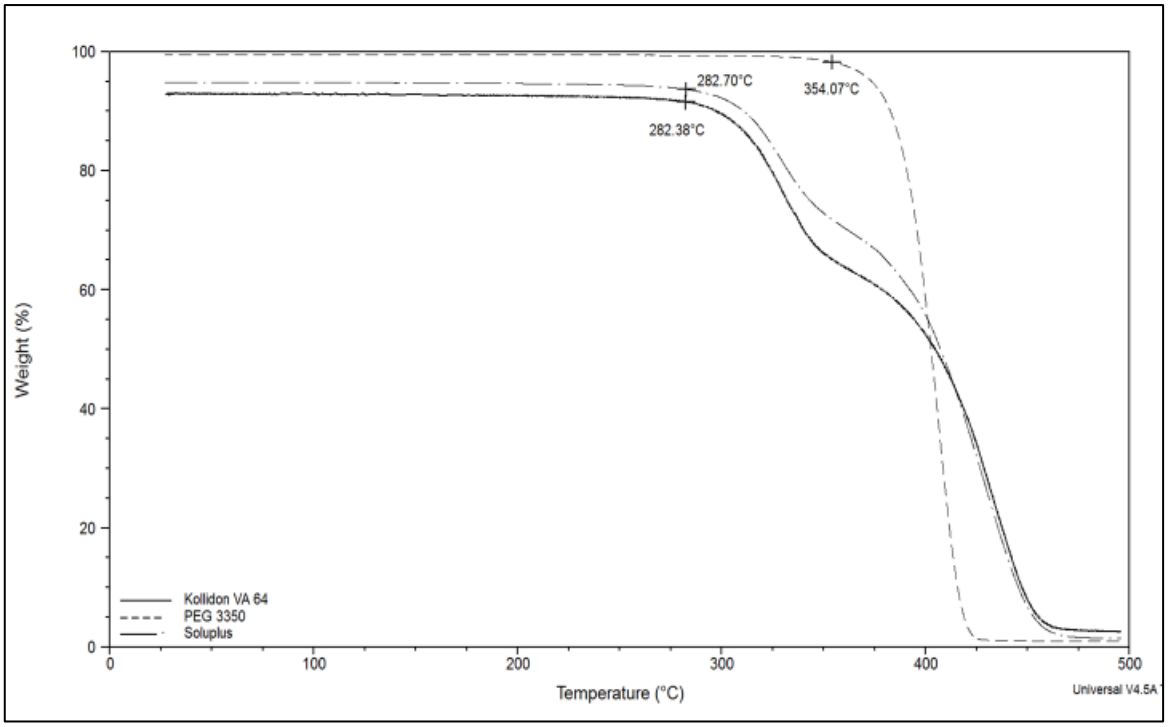


*Figure 3. 2: TGA thermogram of polymers/plasticiser used in formulations. Heating ramp from 25 °C to 500 °C at 10 °C/ min, showing PEG 3350 degradation at ~354 °C, Soluplus® degradation at ~283 °C and Kollidon® VA 64 degradation at ~282 °C.*

Differential scanning calorimetry (DSC) (detailed in chapter 2, section 2.3.2) and powder X-ray diffraction (PXRD) (detailed in chapter 2, section 2.3.4) were used to determine the physical state of the starting materials. As shown in figure 3.3, both HCTZ and RAM displayed sharp melting endotherms at 270.10 ± 2.86 °C and 115.99 ± 1.23 °C, respectively, while Kollidon® VA 64 exhibited a $T_g$ at 107.89 ± 1.81 °C and Soluplus® had a $T_g$ at 61.55 ± 2.34 °C. PEG 3350 is a semi-crystalline plasticiser that exhibits a melting endotherm at 59.81 ± 1.20 °C.

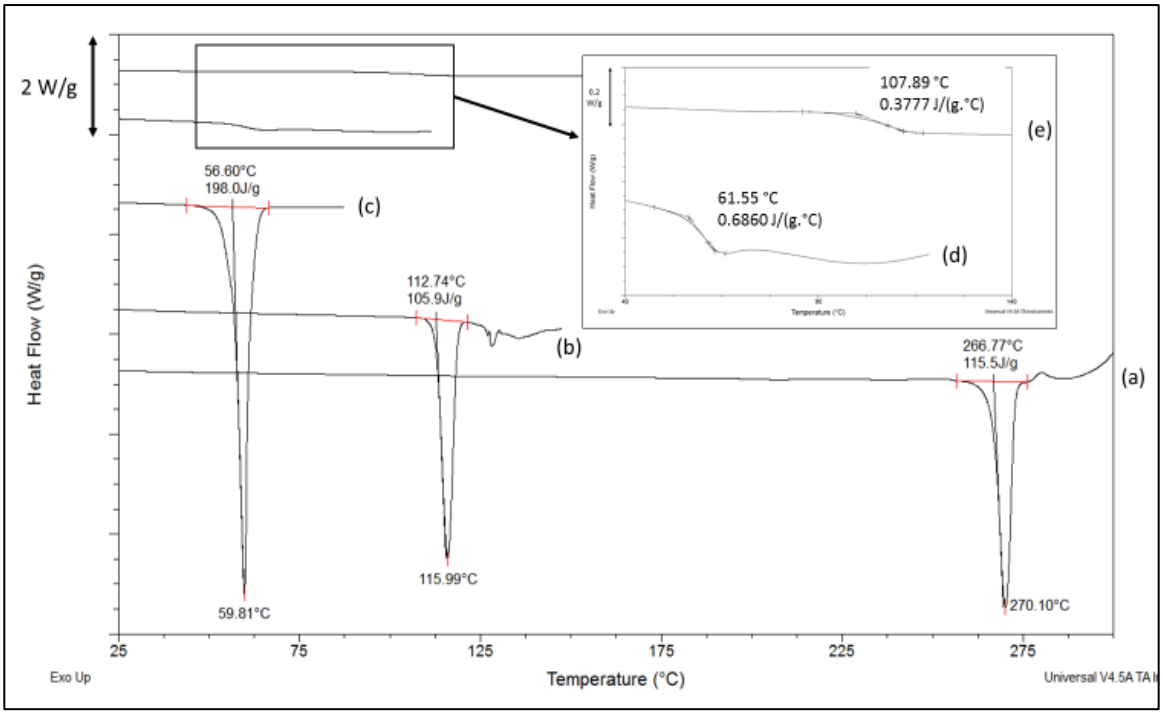


*Figure 3. 3: DSC thermogram of API raw materials, polymers and plasticiser with a heating rate of 10 °C/min showing (a) HCTZ, (b) RAM, (c) PEG 3350, (d) Soluplus® and (e) Kollidon® VA 64.*

With regards to HME, the extrusion temperature required is usually set to 15–60 °C above the glass transition of the system (Crowley, Michael M. 2007). This is to allow the smooth operation of the HME equipment to produce a satisfactory extrudate and avoid the equipment stalling during the operation. RAM starts to thermally degrade soon after its melting point, loses a water molecule and converts to ramipril diketopiperazine (figure 3.4). As a result, the operating temperature conditions of the extruder for the formulations chosen, need to be relatively low to avoid this degradation from occurring during processing.

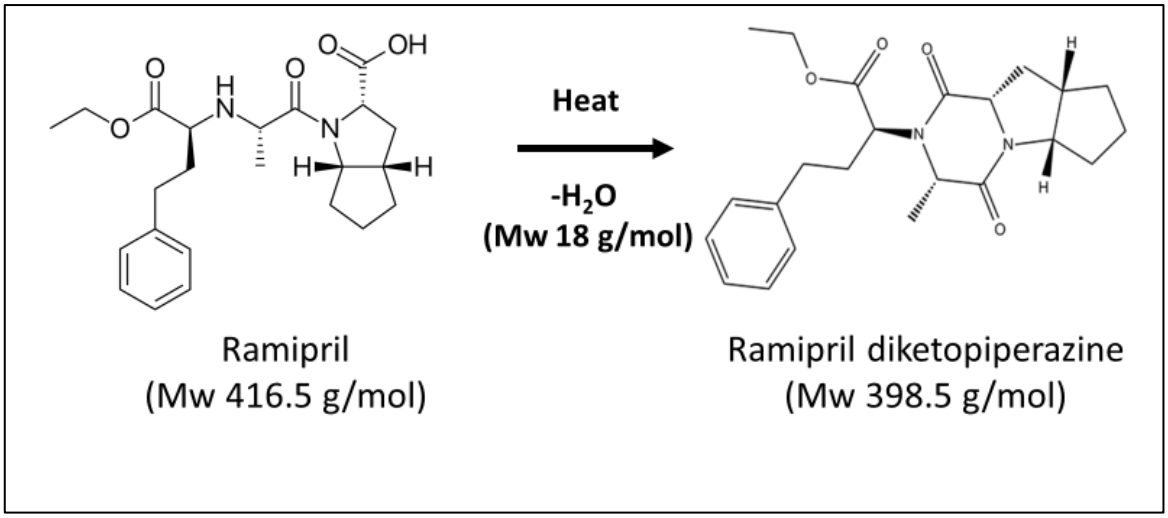


*Figure 3. 4: Thermal degradation pathway of ramipril to ramipril diketopiperazine* (Hanyšová et al. 2005)

To highlight the conversion of RAM to ramipril diketopiperazine, a sample of RAM was held at 140 °C for two hours (detailed in chapter 2, section 2.3.1.1) and tested via HPLC (detailed in chapter 2, section 2.13.1) for the presence of ramipril diketopiperazine (figure 3.5) and the presence of the product was confirmed via LC-MS (detailed in chapter 2, section 2.16) (figure 3.6). The same HPLC method was used to quantify HCTZ and RAM (Appendix 1).

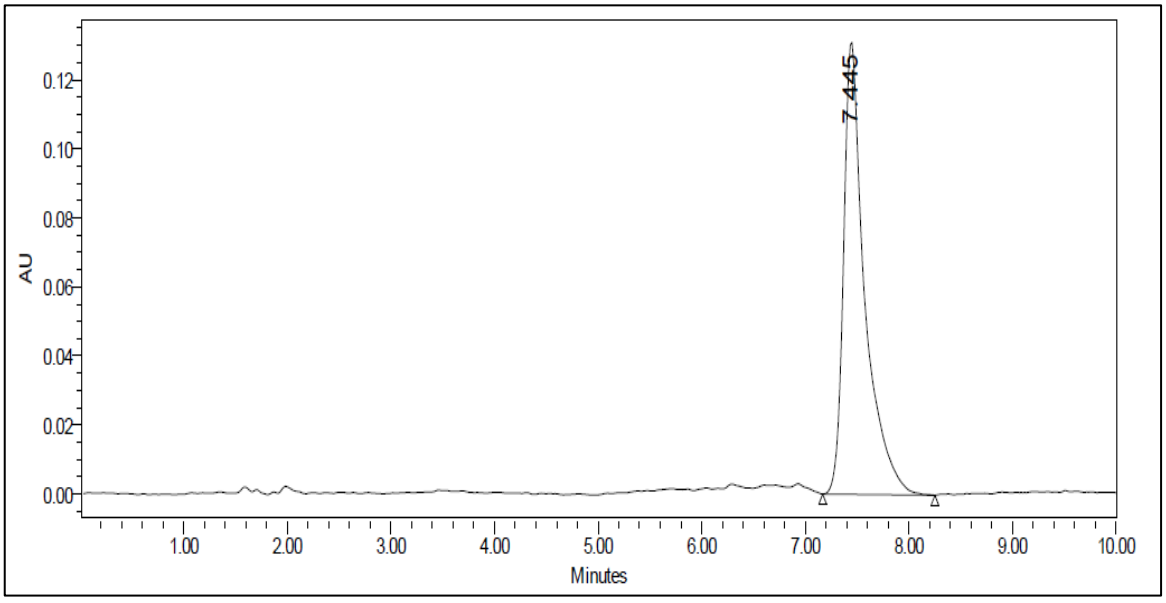


*Figure 3. 5: HPLC chromatogram of the main thermal degradation product of ramipril, ramipril diketopiperazine.*

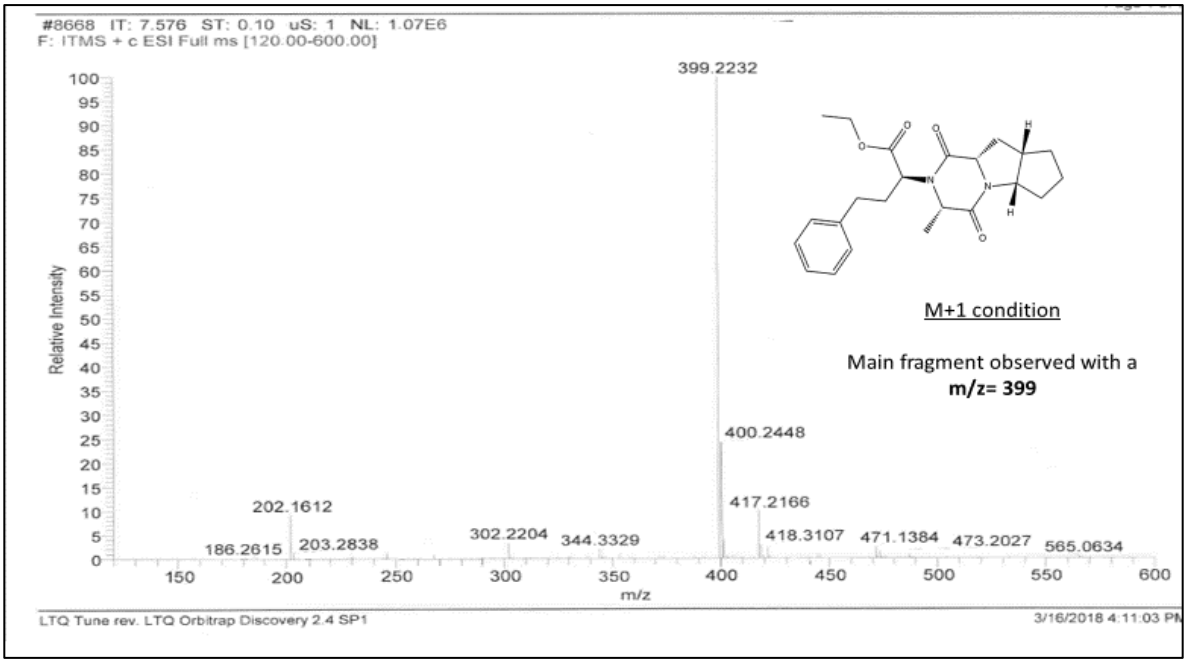


*Figure 3. 6: LC-MS of the main thermal degradation product of ramipril, ramipril diketopiperazine.*

PXRD diffractograms for all raw materials are shown in figure 3.7. Both Kollidon® VA 64 and Soluplus® are amorphous polymers, and lack crystalline peaks, instead showing a smooth halo. For crystalline materials, characteristic peaks can be seen in PXRD diffractograms. As it is a crystalline material, HCTZ shows characteristic peaks at 16.65°(2θ), 18.75°(2θ), 21.40°(2θ) and 24.65°(2θ), which is consistent with the published literature (De Jaeghere et al. 2015; Panneerselvam et al. 2010). RAM also shows characteristic diffraction peaks at 7.60°(2θ), 8.05°(2θ), 19.30°(2θ) and 21.25°(2θ), consistent with the published literature (Jagdale et al. 2013; Madhavi et al. 2016). PEG 3350 has two clear peaks at 19.20°(2θ) and 23.35°(2θ).

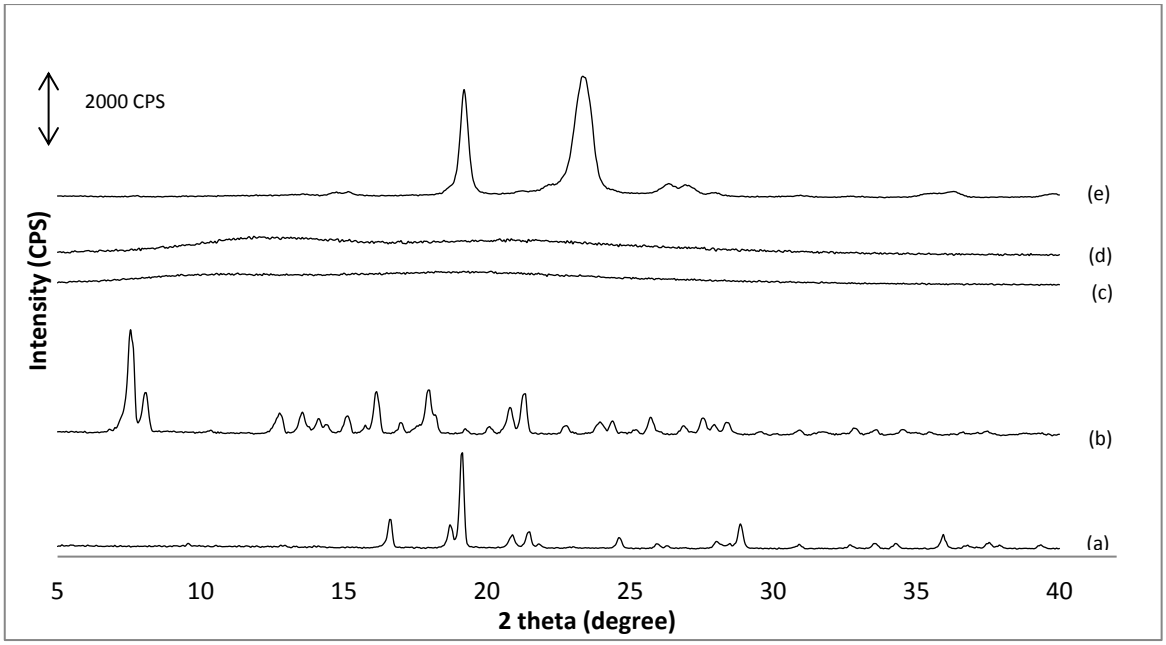


*Figure 3. 7: PXRD of raw materials over the range of 5–40° 2θ of (a) HCTZ, (b) RAM, (c) Kollidon® VA 64, (d) Soluplus®, (e) PEG 3350.*

Unique characteristic peaks for HCTZ, RAM and PEG 3350 can be seen in the PXRDs of physical mixtures of each of the formulation constituents (figure 3.8). For HCTZ, unique characteristic peaks are seen at 16.65°(2θ), 20.9°(2θ) and 24.65°(2θ) in F1, F2 and F3. For RAM, unique characteristic peaks are seen at 7.60°(2θ) in F1, F2 and F3. For PEG 3350 a unique characteristic peak can be seen at 23.35°(2θ) in F2 (which is the only formulation that contains PEG 3350). Formulations processed by SD show no characteristic peaks in the diffractograms (figure 3.8), indicating that these formulations are completely PXRD amorphous. Formulations processed by HME followed by cryomilling, on the other hand, show characteristic peaks for HCTZ at 16.65°(2θ) and 20.9°(2θ) and thus are partially crystalline.

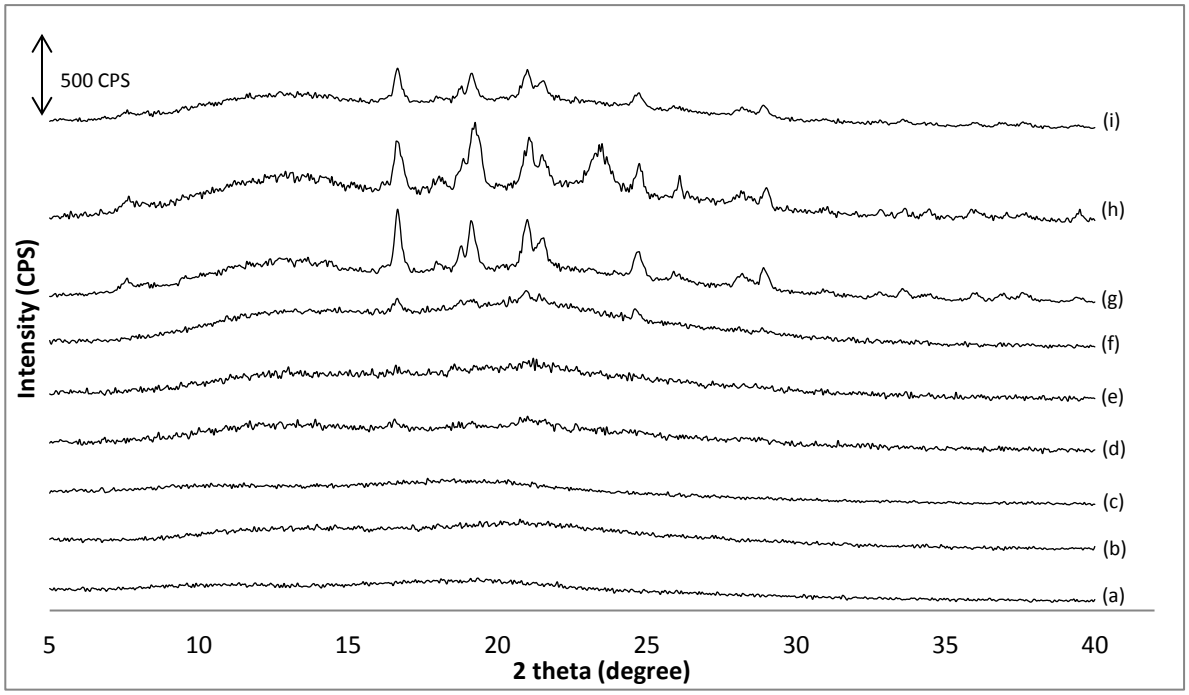


*Figure 3. 8: PXRD of Spray Dried (SD), Hot Melt Extruded (HME) and Physical Mixtures (PM) of formulations (F1, F2, F3) from Table 3.1 over the range of 5–40° 2θ (a) SD-F1, (b) SD-F2, (c) SD-F3, (d) HME-F1, (e) HME-F2, (f) HME-F3, (g) PM-F1, (h) PM-F2, (i) PM-F3.*

Due to several different materials being present in the formulations, the standard DSC methods are less sensitive and the results more difficult to interpret than the more modern modulated DSC (mDSC) methods that are available. mDSC is also known to be more sensitive when determining the $T_g$, by studying the reverse heat flow of materials rather than just the total heat flow which may overlap with several thermal events thus masking the $T_g$ event (Craig 1995; Reading et al. 1994). mDSC was performed on all formulated products (detailed in chapter 2, section 2.3.3) (figure 3.9 and 3.10). Figure 3.9 shows the reverse heat flow recorded for spray dried (SD) formulations (F1, F2 and F3). SD-F1 (figure 3.9 (a)) has a clear single $T_g$ at 114.28 ± 0.52 °C, which indicates a homogenous molecular mix of all the formulation components in the amorphous system. SD-F2 and SD-F3 (figure 3.9 (b) and (c)), which are also shown to be PXRD amorphous, show two clear $T_g$s in the reverse heat flow. This suggests a phase separation of the formulation components, and unlike SD-F1, they are not homogenously mixed at a molecular level even though they are as per PXRD, fully amorphous.

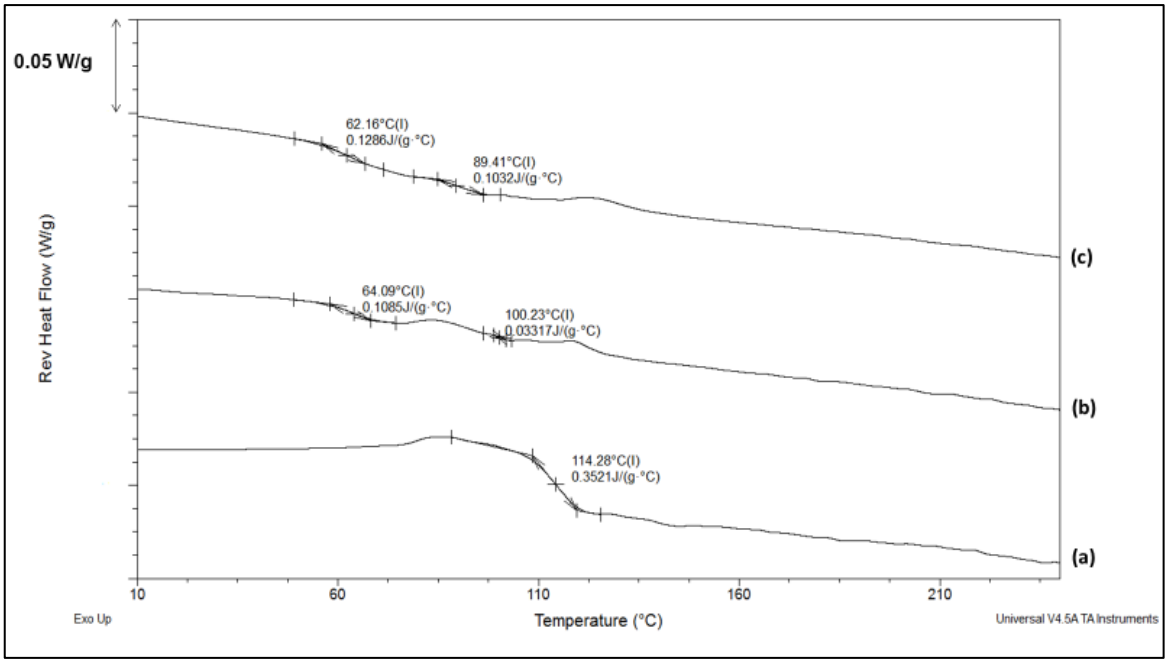


*Figure 3. 9: DSC thermograms showing the reverse heat flow (W/g) signal for (a) SD-F1 (b) SD-F2 and (c) SD-F3*

Hot melt extrusion (HME) formulations (F1, F2 and F3) produced similar results to the equivalent SD formulations. HME-F1 (figure 3.10 (a)) shows one clear $T_g$ at 104.35 ± 1.25 °C, with HME-F2 and HME-F3 (figure 3.10 (b) and (c)) showing two separate $T_g$s, which again suggests a phase separation. Formulations which undergo phase separation, show more than one $T_g$ (Lin and Huang 2010); in our case the two distinguishable $T_g$s are presumed to be due to a RAM/polymer rich zone and a HCTZ/polymer rich zone. The higher Tg is related to HCTZ ($T_g$ of 113.53 ± 1.25 °C, see appendix 2) as it has a higher $T_g$ than RAM ($T_g$ of 2.80 ± 0.43 °C, see appendix 2). Unfortunately, it was not possible to detect any endothermic peak for HCTZ at 270.10 °C. This was due to the fact, the formulations started to thermally degrade before this temperature and, as a result, distorted the heat flow signal, meaning if any endothermic peak for crystalline HCTZ was present, it was not possible to record it.

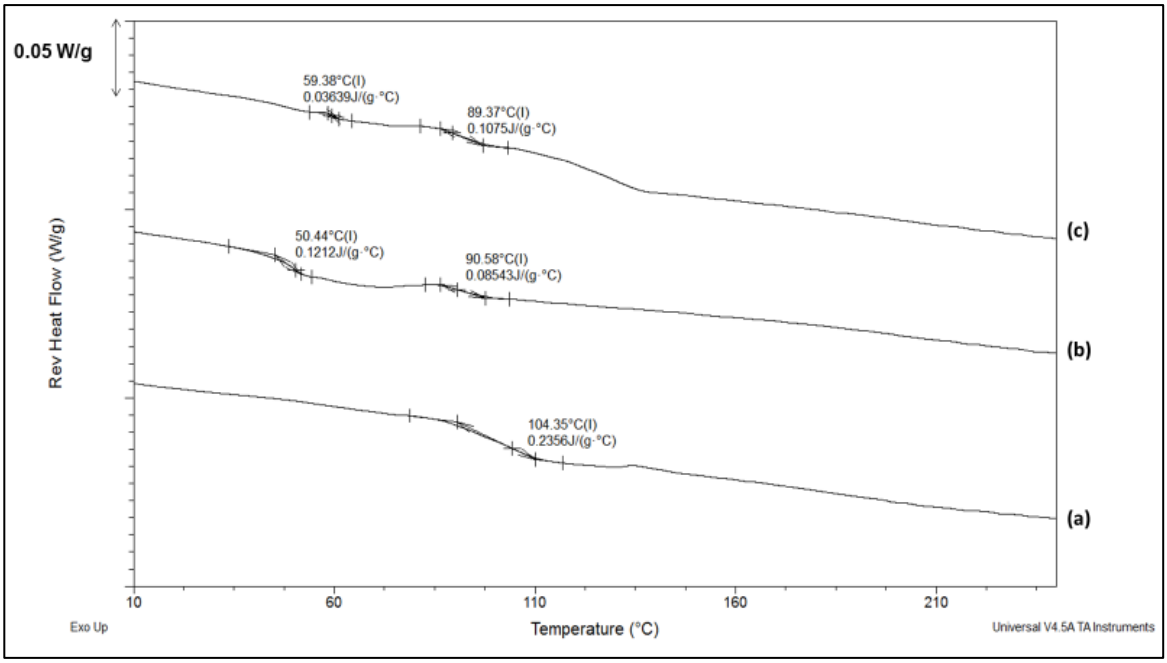


*Figure 3. 10: DSC thermograms showing the reverse heat flow (W/g) for (a) HME-F1 (b) HME-F2 and (c) HME-F3.*

As can be seen by a comparison of figures 3.9 and 3.10, the $T_g$s determined for all three formulations produced by HME are lower than those observed for identical formulations produced by SD. This is due to the increased crystalline HCTZ content in the HME formulations when compared to the fully PXRD amorphous systems produced by SD. According to the Gordon-Taylor equation (Gordon and Taylor 1952), the weight fraction and density of individual amorphous components plays a critical role in the overall $T_g$ of compatible amorphous blends. As HCTZ remains partially crystalline in the HME formulations, the weight fraction of RAM and the polymer carriers (both of which have lower $T_g$ values than HCTZ) in the amorphous complex increase and have a greater influence over the overall $T_g$/$T_g$s, thus causing a $T_g$ reduction relative to equivalent SD systems which have fully amorphous components.

With respect to the production of amorphous solid dispersions through the different manufacturing processes, the most important factors are the solid state of the drug and its miscibility in the carrier system (Singh and Van den Mooter 2016). All three SD formulations were amorphous, indicating sufficient component miscibility and intermolecular interactions to ensure molecular level mixing and ASD production. However, since all HME formulations were processed below the melting point of HCTZ, the formation of ASDs relies on the solubilization of the API components in the other formulation excipients (DiNunzio et al. 2010). Due to limitations in the HME

manufacturing process temperature due to the degradation of RAM above its melting point, the incomplete solubilization of HCTZ results in partially crystalline products.

When comparing the SD formulations to the HME formulations (post cryomilling), there were significantly smaller particles for each spray dried formulation. As is to be expected with SD, the particles were in the micrometre size range. Once the extrudates for HME were pulverised into a powder, the milling process was stopped to minimise the impact it would have on the solid-state properties of the formulation. Particle size can decrease exponentially with time when milled (Suryanarayana 2001) but this also increases the chances of milling changing the physical and solid-state characteristics, such as amorphous content, of the HME formulation. While milling was undertaken at cryogenic temperatures to maintain amorphous content, local “hot spots” can develop due to the violent impact of balls during the milling process (Casale and Porter 1979) which can promote crystallisation. For this reason, the milling process was conducted using the shortest timeframe possible (described in chapter 2, section 2.2.2.1).

Fourier transform infrared spectroscopy (FT-IR) is one of the most widely used methods to detect the intermolecular interactions in ASDs, such as hydrogen bonds between API and polymer excipients (Van Eerdenbrugh and Taylor 2011). For this reason, it was used to probe the presence of hydrogen bonding in the SD formulations. In the HCTZ molecules, the N - H and N - $H_2$ groups may act as hydrogen donors which can form hydrogen bonds with appropriate acceptor groups, such as a carbonyl (C = O) groups. For the RAM molecule, the N - H group and O - H group are potential hydrogen donors. Kollidon® VA 64 contains two hydrogen acceptors, which are derived from the C = O groups of the pyrrolidone ring and the acetate structure. Hydrogen bonding of the API donor groups should preferentially involve the C = O group of the pyrrolidone group, because this group is a stronger hydrogen bond acceptor than the acetate group (Kestur and Taylor 2010; Taylor et al. 2001). For Soluplus®, the C = O groups of the caprolactam and acetate groups can act as hydrogen acceptors, with the O - H groups acting as potential hydrogen donors. The amorphous form of a given drug may give rise to a different IR spectrum than that obtained from the crystalline counterpart (Van Eerdenbrugh and Taylor 2011). The crystalline form of HCTZ has clear peaks for its N - H group stretching at 3165 $cm^{-1}$, 3264 $cm^{-1}$ and 3360 $cm^{-1}$ (figure 3.11 (a)).

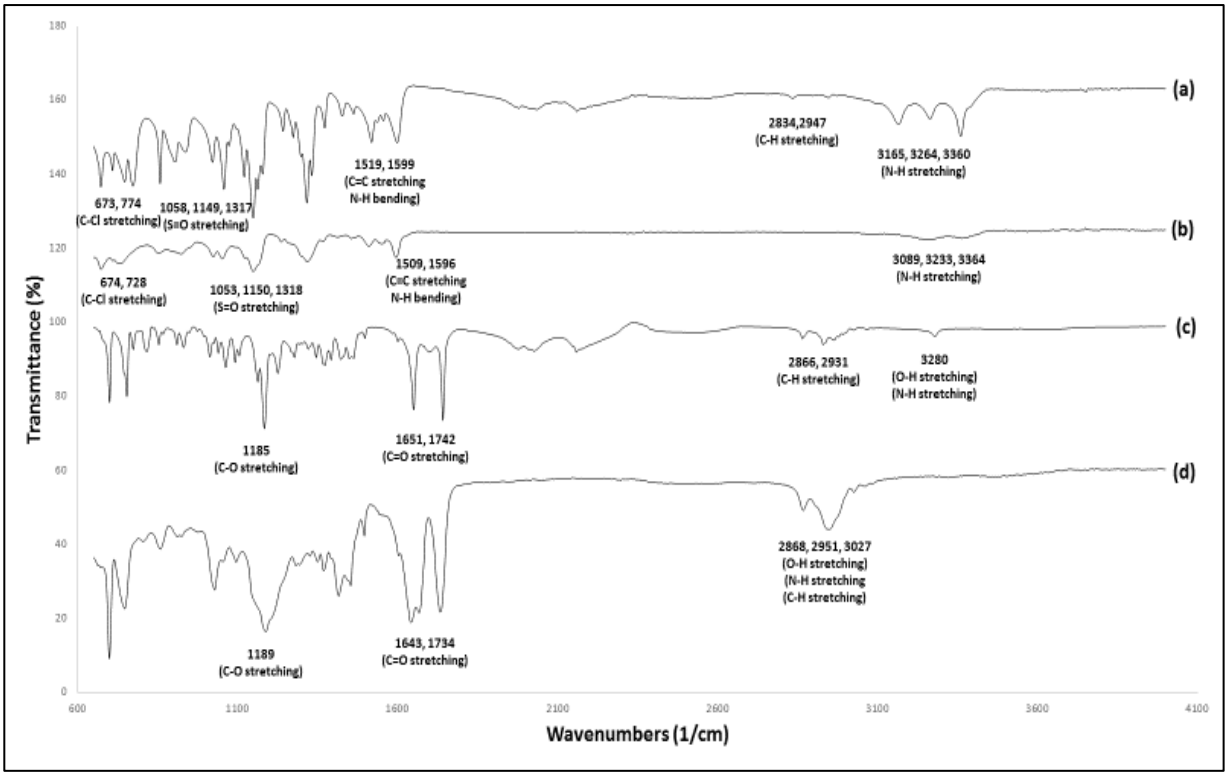


*Figure 3. 11: FTIR analyses of (a) crystalline HCTZ, (b) amorphous HCTZ, (c) crystalline RAM, and (d) amorphous RAM*

In the amorphous form, we can see a downward shift in these bands with peak broadening. With crystalline RAM, O – H and N - H group stretching can be attributed to the peak seen at 3280 $cm^{-1}$; however, this peak is shifted to 3027 $cm^{-1}$ in the amorphous form. Similarly, the C - O stretch peaks in the amorphous form of RAM shift downwards to 1643 $cm^{-1}$ and 1734 $cm^{-1}$ and broaden compared to the crystalline RAM peaks at 1651 $cm^{-1}$ and 1742 $cm^{-1}$. The reason for these differences between crystalline and amorphous API relate to both the wider range of conformations typically present in an amorphous solid and differences in intermolecular interactions (Van Eerdenbrugh and Taylor 2011). Hence, when comparing physical mixtures to SD formulations, it is important that the physical mixtures contain amorphous excipients and amorphous APIs, rather than crystalline API raw materials. This has been shown previously by Taylor and Zografi (Taylor and Zografi 1997) who demonstrated that for amorphous systems that contain more than one compound, the spectra of both the pure amorphous drugs and the amorphous excipients are needed in order to conclude the presence or absence of drug-polymer hydrogen bonds.

For F1 and F2, the N - H stretching of HCTZ at peaks 3165 $cm^{-1}$, 3264 $cm^{-1}$ and 3360 $cm^{-1}$, which are seen in the amorphous HCTZ, are not detected in the IR spectra for

either the PM of amorphous components or the SD formulations (figure 3.12) (described in chapter 2, section 2.4.1).

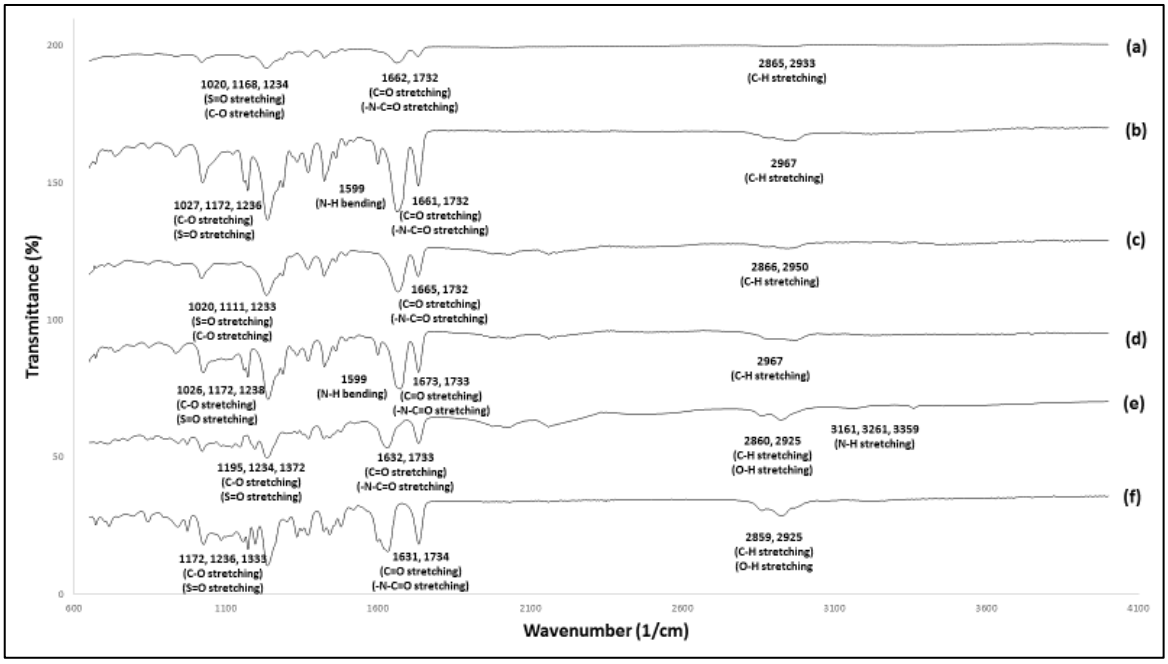


*Figure 3. 12: FTIR analyses of Physical Mixtures (PM) of amorphous form of materials (prepared by melt quenching) found in different formulations and Spray Dried (SD) formulations (a) PM of amorphous form of materials (prepared by melt quenching) comprising F1, (b) SD-F1, (c) PM of amorphous form of materials (prepared by melt quenching) comprising F2, (d) SD-F2, (e) PM of amorphous form of materials (prepared by melt quenching) comprising F3 and (f) SD-F3.*

N - H stretching may downshift due to hydrogen bonding between drug and polymer components and be hidden by the C - H stretching peaks, which are seen between 2860 $cm^{-1}$ and 2970 $cm^{-1}$ for both the PM and SD systems. Another possible explanation for the absence of the peak attributable to N - H stretching of HCTZ in F1 and F2 PM and SD systems, may be that, due to the large polymer content, the signal is too weak to be detected. For the F1 and F2 formulations, peaks relating to the carbonyl groups of the pyrrolidone and acetate structures are at the same wavenumbers, i.e. 1662 $cm^{-1}$ and 1732 $cm^{-1}$, respectively, for both SD and PM systems. However, in the case of the SD formulation peaks are broader and of a higher intensity than their corresponding PM, which indicates the presence of hydrogen bonding with the APIs hydrogen donors. Interestingly, for both SD-F1 and SD-F2 an additional peak is seen at 1599 $cm^{-1}$, which is not present in the corresponding PM systems, and this is thought to correspond to an aromatic C = C stretch or N - H bending, which suggests a strong interaction taking place between the aromatic ring structures of both HCTZ and RAM. For F3, N - H stretching seen in the amorphous HCTZ can be detected in the PM but, like SD-F1 and SD-F2, this

is not detectable in the SD-F3 system. Again, as with SD-F1 and SD-F2, the C - H stretching peaks seen between 2860 $cm^{-1}$ and 2925 $cm^{-1}$ are broader and more intense than for the PM, which may be due to an overlap with N - H stretching which may downshift due to hydrogen bonding. The carbonyl group (C = O) peaks seen at 1631 $cm^{-1}$ and 1734 $cm^{-1}$ in the SD-F3 spectrum are broader than the corresponding peaks in the PM equivalent system. The broadened peak at 1631 $cm^{-1}$ is also split, indicating hydrogen bonding interaction between the carbonyl groups and the hydrogen donor groups in the APIs. As Soluplus® also contains hydrogen donors in its structure it can be clearly seen that evidence of an interaction between the sulfonyl groups (O = S = O) in HCTZ and the alcohol donor groups in Soluplus® occurs, with a downshift peak movement in the SD formulation compared to the PM (figure 3.12).

### 3.2.2 Scanning electron microscopy (SEM)

The SEM images of HCTZ raw material exhibit particles with irregular shapes with clearly defined edges (figure 3.13 (a)). The SEM images of RAM raw material display flat broken needles of varying sizes (figure 3.13 (b)).

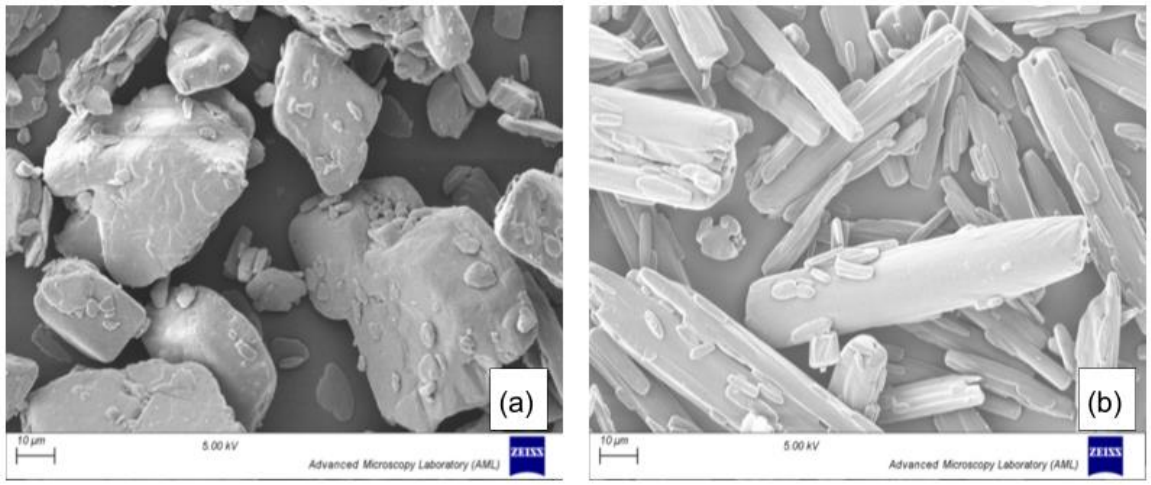


*Figure 3. 13: SEM micrographs of (A) HCTZ raw material, (B) RAM raw material*

SD-F1, SD-F2 and SD-F3 show partially spherical particles where the sphere surface is smooth with concave depressions (figure 3.14 (a) – (c)) of the type previously seen when PVP (Paradkar et al. 2004) and Soluplus® (Homayouni et al. 2015) were spray dried. Once compressed into a disc for intrinsic dissolution studies, SD-F1 and SD-F2 (figure 3.14 (d) & (e)) display a surface with more crevices/voids than SD-F3 (figure 3.14 (f)), most probably due to the different polymer viscoelastic properties. Polymers, in general, are viscoelastic materials and usually deform once sufficient pressure is applied.

Kollidon® VA 64 (Dashevsky et al. 2004; Kolter and Flick 2000) and Soluplus® (Hughey et al. 2013; Zhong et al. 2016) polymers have been shown to be compressible into tablet formulations, which in turn enables discs to be successfully prepared in the Wood's apparatus for intrinsic dissolution studies. Kollidon® VA 64 displays very good plastic properties and for this reason, it is often used as a binder in direct compression. Soluplus® on the other hand, has more elastic behaviour (Gupta et al. 2015) due to the storage modulus being greater than the loss modulus at temperatures below and close to its $T_g$ (Gupta et al. 2016). The plastic properties of the Kollidon® VA 64 account for the cracks/voids forming, as the material will remain deformed, differing from its original configuration after compression force is applied. However, the elastic properties of the Soluplus® (Hughey et al. 2013; Zhong et al. 2016) account for fewer cracks/voids as the material tries to revert to its original configuration.

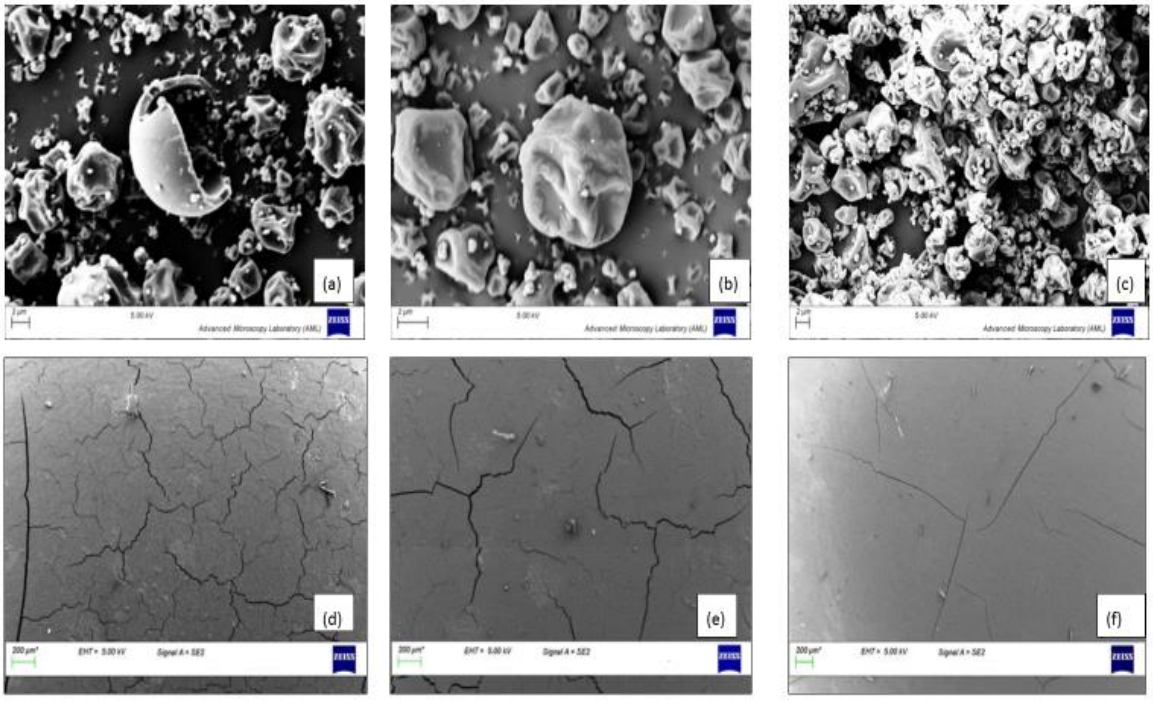


*Figure 3. 14: SEM micrographs of (a) SD-F1, (b) SD-F2, (c) SD-F3, (d) compressed disc SD-F1, (e) compressed disc SD-F2, (f) compressed disc SD-F3.*

As one of our objectives was a direct comparison between products, it was decided that the extrudates would be cryomilled for the shortest amount of time that completely pulverised the extrudates to a powder using the cryomill (described in chapter 2, section 2.2.2.1). PXRD and mDSC analysis was conducted on HME formulation material to test for any potential physicochemical changes that may occur during the milling process. Cryomilling was chosen as previous studies have shown that, by milling at temperatures

below the $T_g$, amorphous components of formulations retain their amorphous content (Descamps et al. 2007). Post milling, PXRD and mDSC showed no statistical difference in peak intensity of crystalline components or change in $T_g$s present (figure 3.15 and figure 3.16).

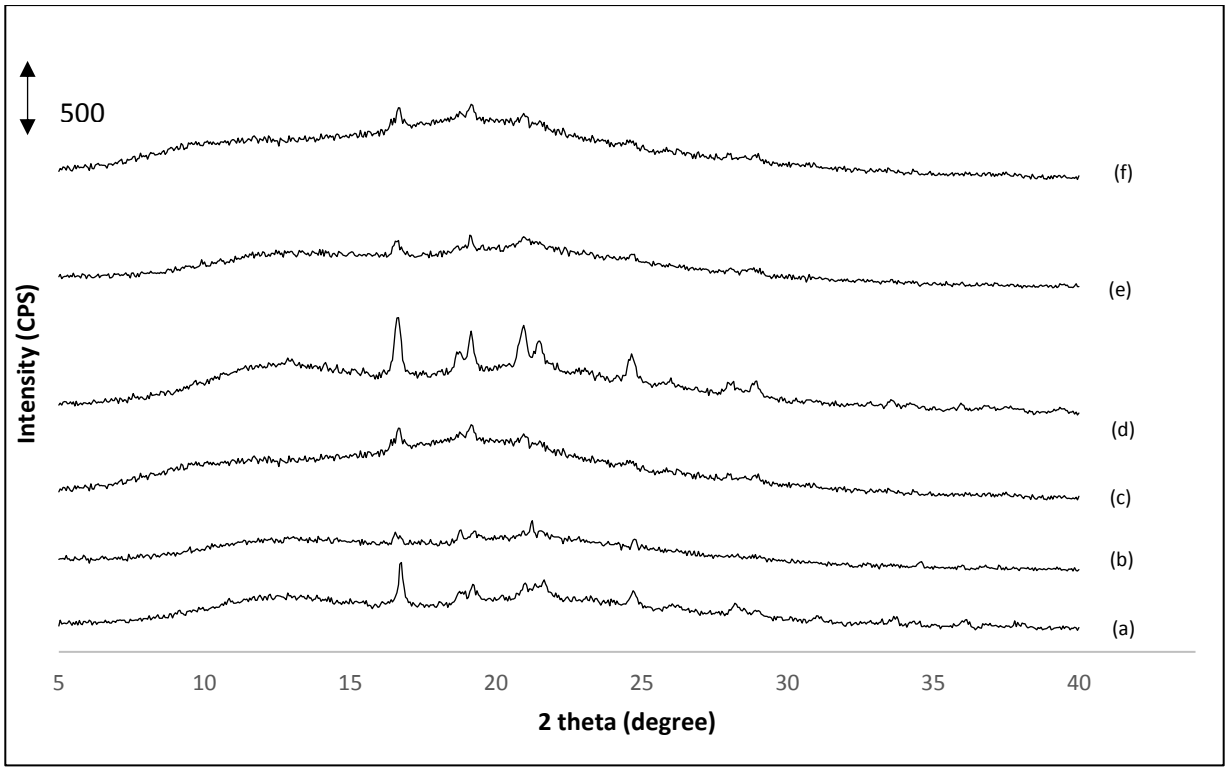


*Figure 3. 15: PXRD over the range of 5–40° 2θ of (a) HME – F1 pre milling, (b) HME – F2 pre milling, (c) HME – F3 pre milling, (d) HME – F1 post milling, (e) HME – F2 post milling and (f) HME – F3 post milling.*

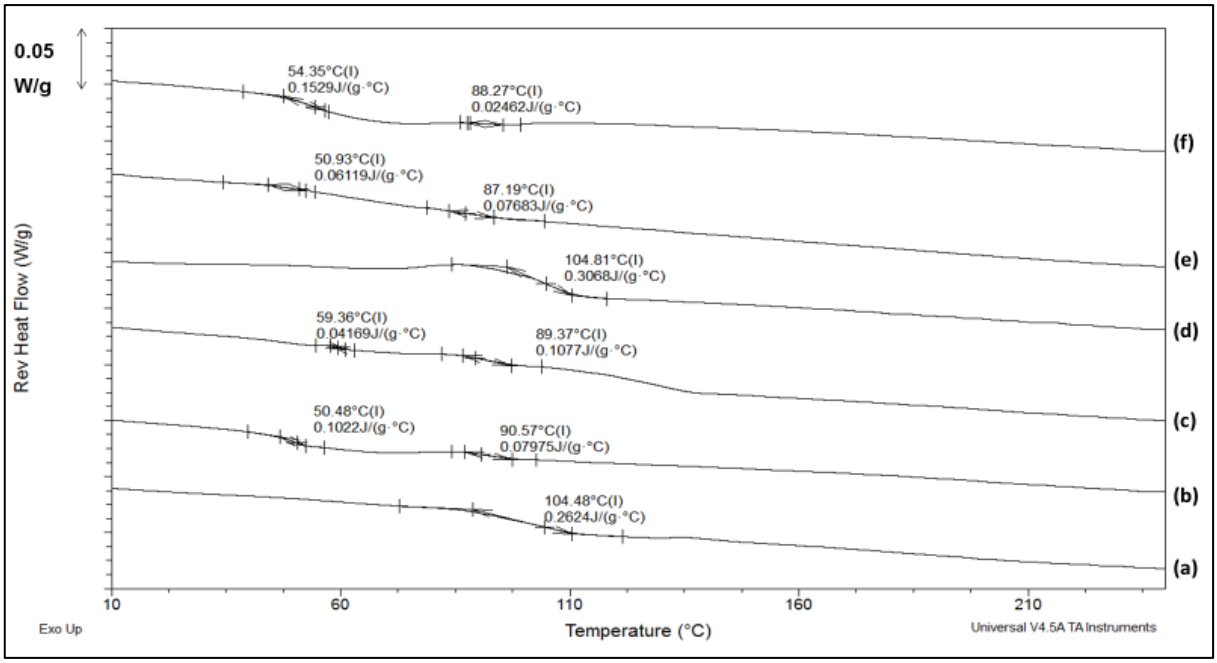


*Figure 3. 16: DSC thermograms showing the reverse heat flow (W/g) for (a) HME – F1 pre milling, (b) HME – F2 pre milling, (c) HME – F3 pre milling, (d) HME – F1 post milling, (e) HME – F2 post milling and (f) HME – F3 post milling.*

HME-F1, HME-F2 and HME-F3 post milling show particles with asymmetrical shapes (figure 3.17 (a) - (c)). Once compressed into a disc for intrinsic dissolution studies, HME-F1 and HME-F2 (figure 3.17 (d) & (e)) exhibit a surface with more crevices/voids than HME-F3 (figure 3.17 (f)) on the scale displayed. As with the SD formulations, the visual differences can most probably be attributed to the different viscoelastic properties of the polymers used in the formulations.

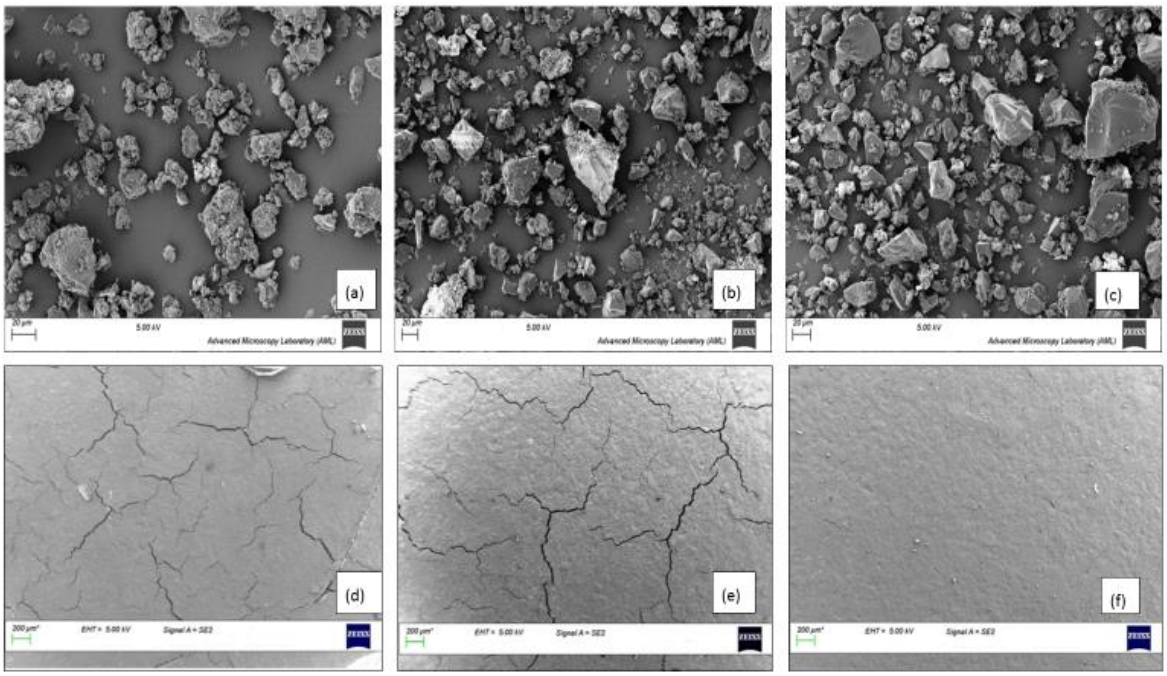


*Figure 3. 17: SEM micrograph of (a) HME-F1, (b) HME-F2, (c) HME-F3, (d) compressed disc HME-F1, (e) compressed disc HME-F2, (f) compressed disc HME-F3.*

### 3.2.3 Particle size analysis (PSA)

PSA results for SD-F1, SD-F2 and SD-F3 were compared to the results of PSA for HME-F1, HME-F2 and HME-F3 systems post cryo-milling (table 3.3). The SD-F1, SD-F2 and SD-F3 median particle size are statistically different from one another (95%CI, $P < 0.05$, F-value 181.37), which may be attributed to the different polymers and polymer compositions used. While SD parameters and solution concentrations remained constant, the only variable for SD formulations was the composition. It has been previously shown that formulation composition can result in varying particle size distribution when other conditions remain constant (Costantino et al. 2002; Oneda and Ré 2003). The molecular weight of Kollidon® VA 64 is between 45,000–70,000 g/mol (BASF 2008) on average whereas the average molecular weight for Soluplus® is between 90,000–140,000 g/mol (BASF 2010). PEG 3350 has an average molecular weight of 3350 g/mol. The greater the molecular weight, the longer the chain length resulting in more stiffness in the polymer structure, leading to larger particle size post SD processing (Gupta et al. 2016). The results in table 3.1, show the formulation with the largest molecular weight polymer (SD-F3) produced the largest particle size.

HME-F1 and HME-F2 were not statistically different from one another post-milling. However, HME-F3 was statistically different from HME-F1 and HME-F2 (95%CI, P <

0.05, F-value 25.05). It is thought that the reason HME-F1 and HME-F2 are different to HME-F3 is due to the formulation composition, as described above for SD formulations. HME-F1 and HME-F2 contain Kollidon® VA64 in both formulations with the addition of PEG 3350 in F2 not affecting the overall particle size post milling at its formulation concentration of 8.25 %. As HME-F3 contains a different polymer, namely Soluplus®, it is thought that it behaves differently (due to its more elastic properties when compared to Kollidon® VA 64) in the cryo-mill, resulting in a different median particle size distribution.

*Table 3. 1: Overview of particle size analysis (PSA) results of API raw materials and processed formulations.*

| Sample | Particle Size (µm) (d50) |
|---|---|
| HCTZ (Raw) | 28.48 ± 0.13 |
| RAM (Raw) | 8.79 ± 0.22 |
| HME-F1 | 50.48 ± 2.45 |
| HME-F2 | 49.16 ± 4.00 |
| HME-F3 | 36.16 ± 0.74 |
| SD-F1 | 3.41 ± 0.11 |
| SD-F2 | 3.00 ± 0.02 |
| SD-F3 | 3.98 ± 0.01 |

### 3.2.4 Drug assay

Drug assays of pharmaceutical formulations are of great importance, as actual drug content must fall within specific limits of the manufacturer's label claims. Specific individual monographs exist in the European Pharmacopoeia for both HCTZ and RAM in relation to acceptable limits for tablet drug content, although a monograph for a combination of the two APIs in a single oral tablet does not exist in the European Pharmacopoeia. HCTZ content is considered acceptable if the drug content is found to be between 92.5 and 107.5 % of the stated amount (European Pharmacopoeia 2020c) and RAM content is considered acceptable if the drug content is found to be between 90.0 and 105.0 % of the stated amount(European Pharmacopoeia 2020e). It was decided that these drug content ranges would be acceptable for our formulations as ultimately, our target final dosage form will be an oral tablet. From the assays conducted, both HCTZ and RAM content fall within the desired ranges for each of the SD formulations (table 3.4). For HME formulations, HCTZ content is also within the desired ranges of the European Pharmacopoeia, however for HME-F1 and HME-F3, RAM content falls outside the desired ranges. As previously described, RAM starts to

thermally degrade above its melting point of 116 °C. Both formulations are subjected to a maximum temperature of 140 °C for a period (found to be the lowest temperature processing was possible at for these formulations), which causes the degradation to occur. As PEG 3350 was added to act as a plasticiser to F2, the maximum temperature HME-F2 is subjected to is 110 °C avoiding excessive thermal degradation of RAM. While some degradation of RAM does occur (RAM content was not 100% of theoretical content), this may be due to the formation of excess thermal energy that can be generated due to mechanical energy being generated by the extruder elements and materials during the process (Crowley et al. 2007).

*Table 3.2: Summary of drug content for processed formulations and intrinsic drug dissolution rates from compressed discs in 0.1M HCl pH 1.2 @ 37 °C over 120 min.*

| Formulation | HCTZ content (%) | HCTZ dissolution rate (mg/ min/ $cm^2$) | RAM content (%) | RAM dissolution rate (mg/ min/ $cm^2$) |
|---|---|---|---|---|
| **HME-F1** | 101.44 ± 1.45 | 0.240 ± 0.03 | 90.71 ± 0.65 | 0.087 ± 0.01 |
| **HME-F2** | 101.88 ± 2.10 | 0.384 ± 0.04 | 96. 07 ± 0.01 | 0.136 ± 0.02 |
| **HME-F3** | 99.64 ± 0.46 | N/A | 85.93 ± 0.33 | N/A |
| **SD-F1** | 100.69 ± 0.57 | 0.165 ± 0.02 | 99.54 ± 0.20 | 0.072 ± 0.01 |
| **SD-F2** | 100.33 ± 0.74 | 0.239 ± 0.04 | 101.89 ± 1.25 | 0.110 ± 0.01 |
| **SD-F3** | 101.25 ± 1.64 | N/A | 100.08 ± 0.26 | N/A |

### 3.2.5 Dissolution testing

Intrinsic dissolution is described as particle size independent (Hendriksen 1991; Wood et al. 1965) and is based on measurements taken from compacted powder discs of known surface area under controlled hydrodynamic conditions (Healy et al. 2002). The area exposed to the dissolution media remains constant over time. Therefore, the intrinsic dissolution rate/constant surface area dissolution rate depends on the solubility of the powder compact, the hydrodynamics of the system and the diffusion coefficient of the dissolving substance in the dissolution medium (Hendriksen 1991; Wood et al. 1965). The intrinsic/constant surface area dissolution studies for all formulations were carried out over a 120 min period in 0.1 M HCl at 37 °C to mimic the targeted stomach release

environment (detailed in chapter 2, section 2.17.1.1). The intrinsic dissolution rates were calculated from the slope of the line for the first 30 min of the study as this is where a linear response was observed for F1 and F2 (figure 3.18 and 3.19). After 30 min, a nonlinear response was observed for the release of HCTZ, possibly due to the recrystallization of HCTZ in-situ. RAM continued to display linear release profiles up to 120 min. For F1, the intrinsic dissolution rate for both HCTZ (T-value = -8.99, $p < 0.05$) and RAM (T-value = -3.61, $p < 0.05$) were significantly higher for the HME formulations when compared to the SD formulations. Similarly, for F2, the dissolution rates for both HCTZ (T-value = -4.51, $p < 0.05$) and RAM (T-value= 3.46, $p < 0.05$) were higher for the HME formulations when compared to the SD formulations.

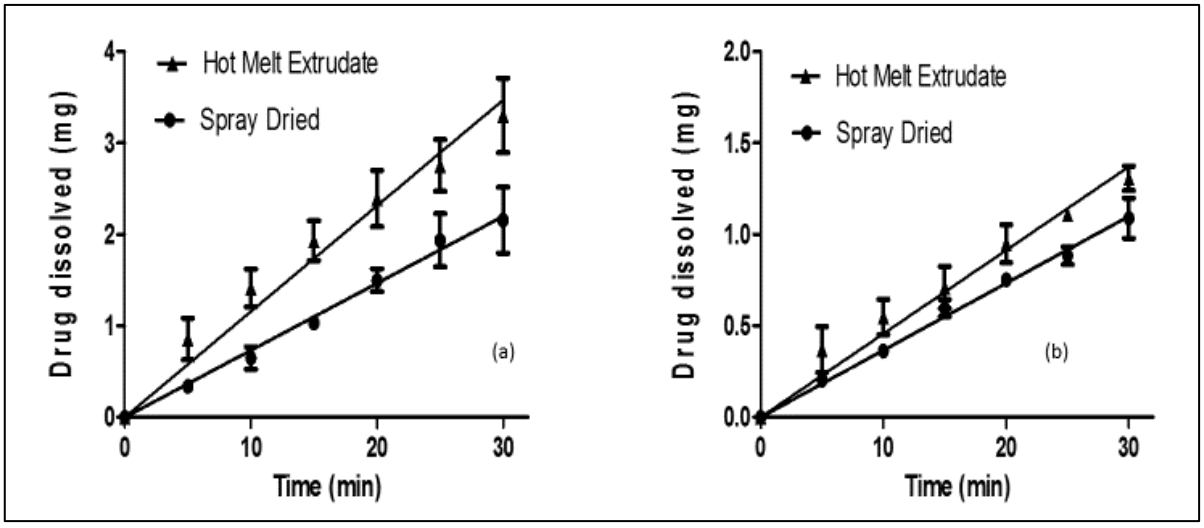


*Figure 3. 18: Intrinsic/constant surface area dissolution profiles of (a) HCTZ from SD-F1 and HME-F1 showing the higher dissolution rate of the HME formulation (n=3, t-value = -8.99, $p < 0.05$) and (b) RAM from SD-F1 and HME-F1 showing the higher dissolution rate of the HME formulation (n=3, t-value = -3.61, $p < 0.05$).*

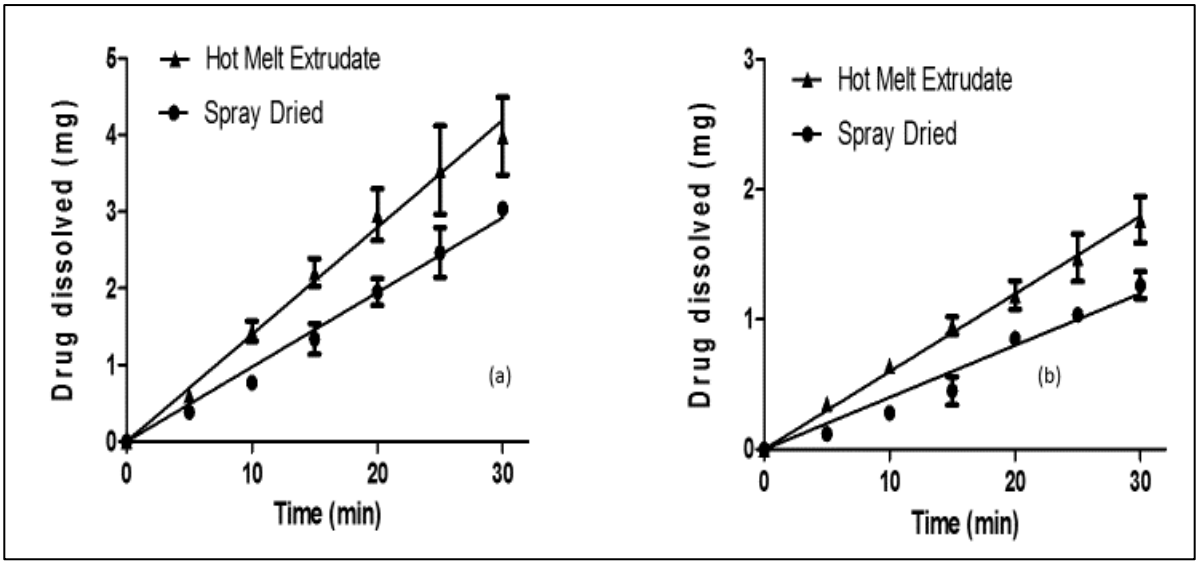


*Figure 3. 19: Intrinsic/constant surface area dissolution profiles of (a) HCTZ from SD-F2 and HME-F2 showing the higher dissolution rate of the HME formulation (n=3, t-value = -4.51, $p < 0.05$) and, (b) RAM from SD-F2 and HME-F2 showing the higher dissolution rate of the HME formulation (n=3, t-value = 3.46, $p < 0.05$).*

The Wood's apparatus experiments were repeated for the SD particles and surface scrapings of the pellets were taken at 10 min time point intervals up to 30 min to test for any recrystallisation at the pellet surface which may influence the rate of release. All SD pellets surfaces remained fully XRD amorphous up to the 30 min time point (figure 3.20). Surface scrapings of the HME formulations were not taken as the original formulations were already partially crystalline.

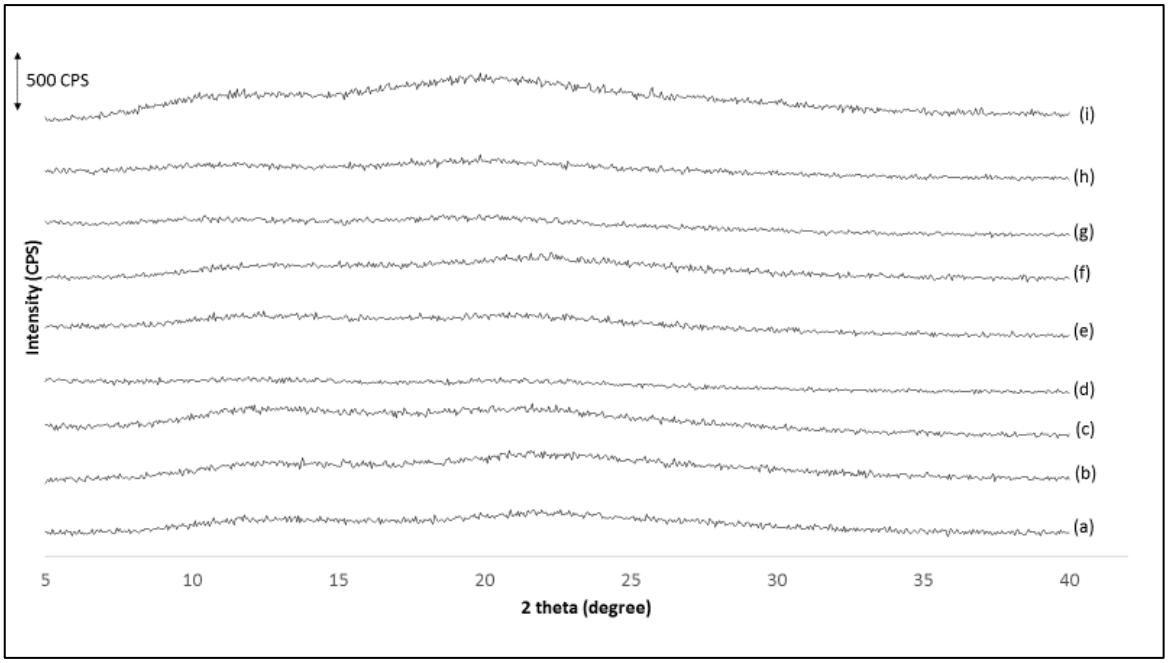


*Figure 3. 20: PXRD of disk surface scratchings of Spray Dried (SD) formulations, compressed in Wood's apparatus, after dissolution up to different time points - (a) SD-F1 10min, (b) SD-F1 20 min, (c) SD-F1 30 min, (d) SD-F2 10 min, (e) SD-F2 20 min, (f) SD-F2 30 min, (g) SD-F3 10 min, (h) SD-F3 20 min and (i) SD-F3 30 min.*

In general, amorphous formulations usually display a higher dissolution rate when compared with the equivalent crystalline formulation. As the SD formulations produced fully amorphous formulations, it would be expected they would display a higher dissolution rate when compared to the semi-crystalline HME formulations. However, as can be seen from the intrinsic dissolution results (figure 3.18 and 3.19, table 3.4), the HME formulations showed a statistically significantly greater dissolution release rate for F1 and F2 for both HCTZ and RAM from the compressed discs in the Wood's apparatus.

With regards to F3, no release was observed from either the SD or HME products over the timeframe studied. It is thought the lack of drug release from SD-F3 and HME-F3 can be attributed to Soluplus® portion of the formulation. Soluplus® is comprised of three different monomer components, namely, polyvinyl caprolactam, polyvinyl acetate and polyethylene glycol (Kolter et al. 2012). It should be noted that Soluplus® has been previously shown to be soluble at pH 1.2 (Sun and Lee 2015), however, one component monomer, polyvinyl caprolactam, which is soluble in cold water, is no longer water soluble above 35 °C (Kroker et al. 1995) which may result in reduced solubility of the polymer at the experimental temperature (37 °C). Soluplus® has also displayed properties of extensive swelling in dissolution media (Taupitz et al. 2013) resulting in a very slow dissolution rate of test material and, in our studies, polymer swelling was

evident when discs were removed post dissolution. On contact with aqueous dissolution medium, Soluplus® is known to enter the solution as single polymer chains which then organize into uni-chain polymer micelles (BASF 2010). As the concentration of Soluplus® increases, the uni-chain micelles join together to form multi-chain ones. The lower critical solution temperature has been reported to be between 37 °C (Ali et al. 2009) and 40 °C (Cavallari et al. 2016) for Soluplus® and at these temperatures the aspect of multi-chain polymer micelles forming is more relevant as the chains lose the hydration crown and progressively associate, decreasing their solubility and forming a cloudy suspension that can precipitate. This behavior is responsible for the gel forming property of Soluplus® (Cavallari et al. 2016). Due to the polymer gelling and swelling it is possible that the intrinsic dissolution/constant surface area model is not suitable for dissolution testing with Soluplus® polymer even though it has been reported in the literature that Soluplus® has been shown to increase the solubility and dissolution rate of some APIs (Djuris et al. 2013; Homayouni et al. 2015; Linn et al. 2012; Shamma and Basha 2013; Zhang et al. 2014).

### 3.2.6 Surface topography

As previously stated, all formulations produced by SD were amorphous in nature while formulations produced by HME remained partially crystalline. It is generally accepted that amorphous material has a higher solubility and dissolution rate than equivalent crystalline material, and thus the higher dissolution rates observed for HME systems was surprising. From SEM images of the discs, the surface of HME discs appeared rougher than SD discs. It was hypothesized that this could lead to an increased turbulence in the hydrodynamic boundary layer for the HME compressed discs, resulting in a higher dissolution rate than for smoother SD compressed discs (Healy and Corrigan 1996; Healy et al. 1995). Surface topography analysis was conducted to study the surface roughness of the compressed discs (detailed in chapter 2, section 2.15.1). Surface roughness, which may be quantified by several parameters including Ra, the surface roughness average, is a measurement of surface finish – it is topography at a scale that might be considered “texture” on the surface. The roughness average is a quantitative calculation of the relative roughness of a linear profile or area, expressed as a single numeric parameter. Table 3.3 outlines the surface roughness average (Ra) for each of the compressed discs.

*Table 3. 3: Roughness average (Ra) of the surface of compressed discs for intrinsic dissolution. The Ra difference between SD F1 and HME F1 ((T-value = −11.85, p < 0.05) and SD F2 and HME F2 (T-value = −8.38, p < 0.05) were statistically significant. The Ra difference between SD F3 and HME F3 (T-value = −1.78, p > 0.05) was not statistically significant.*

| Formulation | Roughness average (Ra) (nm) |
|---|---|
| **SD F1** | 121897 ± 4857 |
| **SD F2** | 171079 ± 8641 |
| **SD F3** | 148757 ± 24077 |
| **HME F1** | 171314 ± 5350 |
| **HME F2** | 215656 ± 3188 |
| **HME F3** | 174651 ± 7573 |

The Ra values for SD formulations were compared to the Ra values for equivalent HME formulations. There is a statistically significant difference in Ra between SD-F1 and HME-F1 (T-value = −11.85, p < 0.05) and SD-F2 and HME-F2 (T-value = −8.38, p < 0.05). There is no statistically significant difference between the Ra of SD-F3 and HME-F3 (T-value = −1.78, p > 0.05). While the Wood's apparatus is designed to minimize the effects particle size can have on the dissolution rate, it can be clearly shown from the results in Table 3.5 and graphs in figure 3.21, that the surface texture differs after compression between the SD and HME formulations. It is hypothesized the differences in surface texture give rise to varying turbulence levels at the hydrodynamic boundary layer and as a result, the dissolution rates differ. Figure 3.21 provides a visual representation of the surfaces of the compacted discs and shows how the difference in manufacturing techniques and particle size leads to differences in the Ra of compacted discs.

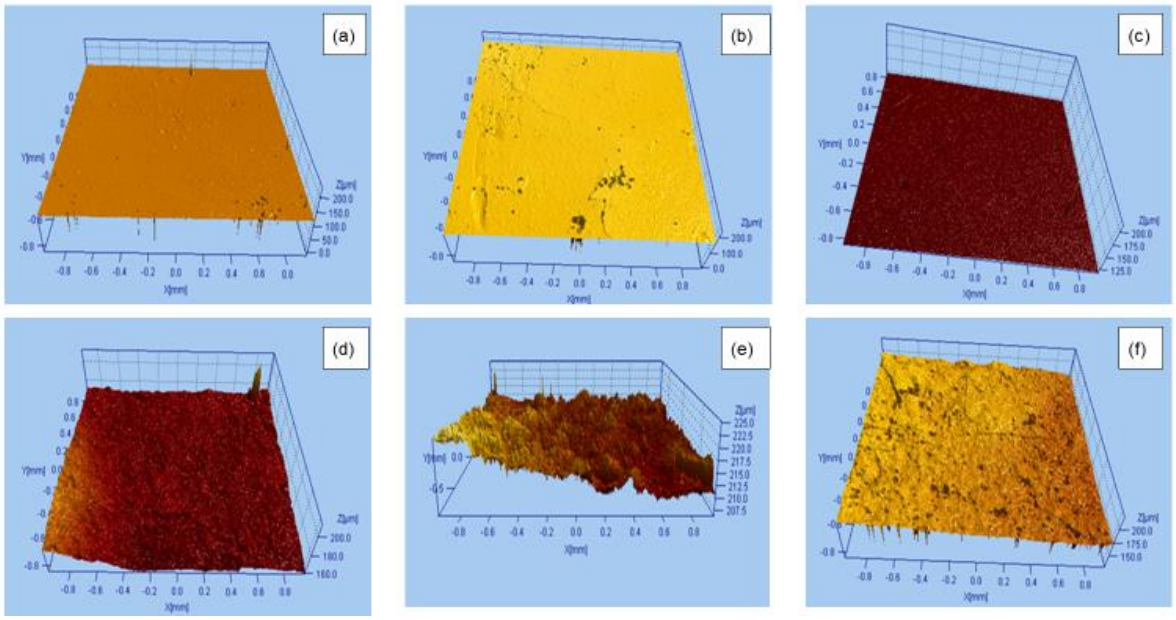


*Figure 3. 21: 3D graphs following surface topography measurements of (a) SD-F1, (b) SD-F2, (c) SD-F3, (d) HME-F1, (e) HME-F2 and (f) HME-F3.*

### 3.2.7 Stability studies

As molecular mobility allows for physical ageing and recrystallization (Yoshioka et al. 1994) of glasses below their $T_g$, the $T_g$ is unsatisfactory as an indicator for the temperature below which mobility stops (Hancock et al. 1995). As a general guide, it is accepted that the $T_g$ -50 Kelvin rule should apply to allow for physical stability on long term storage (Hancock et al. 1995). Practically, the higher the $T_g$ of an amorphous system, the longer it would be expected to remain stable in an amorphous state at relevant pharmaceutical temperatures (Hancock et al. 1995). As well as temperature, moisture can also induce crystallization of amorphous formulations (Konno and Taylor 2008; Makower and Dye 1956). Water can absorb and adsorb onto polar functional groups of hydrophilic polymers (Thibert and Hancock 1996). The interaction of the water with the amorphous material lowers the $T_g$ of the formulation due to its universal activity as a plasticiser (Szakonyi and Zelkó 2012) – water molecules may be able to penetrate into the hydrophilic polymer matrix, increasing the distance between polymer chains and thus resulting in greater free volume for molecular movement to occur (Abiad et al. 2009). SD and HME products were tested for stability at two different relative humidities, as described in chapter 2, section 2.18.1.

All SD formulations remained completely PXRD amorphous at stability conditions < 10 % RH / 25 °C throughout the entire stability study (t = 60 days) as can be seen in figure 3.22 (a) – (c). HME formulations remained partially crystalline at < 10 % RH / 25 °C storage conditions, however there was an increase in peak intensity for peaks

corresponding to HCTZ, indicating partial crystallization of the previously amorphous segment of the API (figure 3.22 (d) – (f)). PXRD also revels the partial crystallization of PEG 3350 in HME-F2 with a peak seen at 23.35 °(2θ).

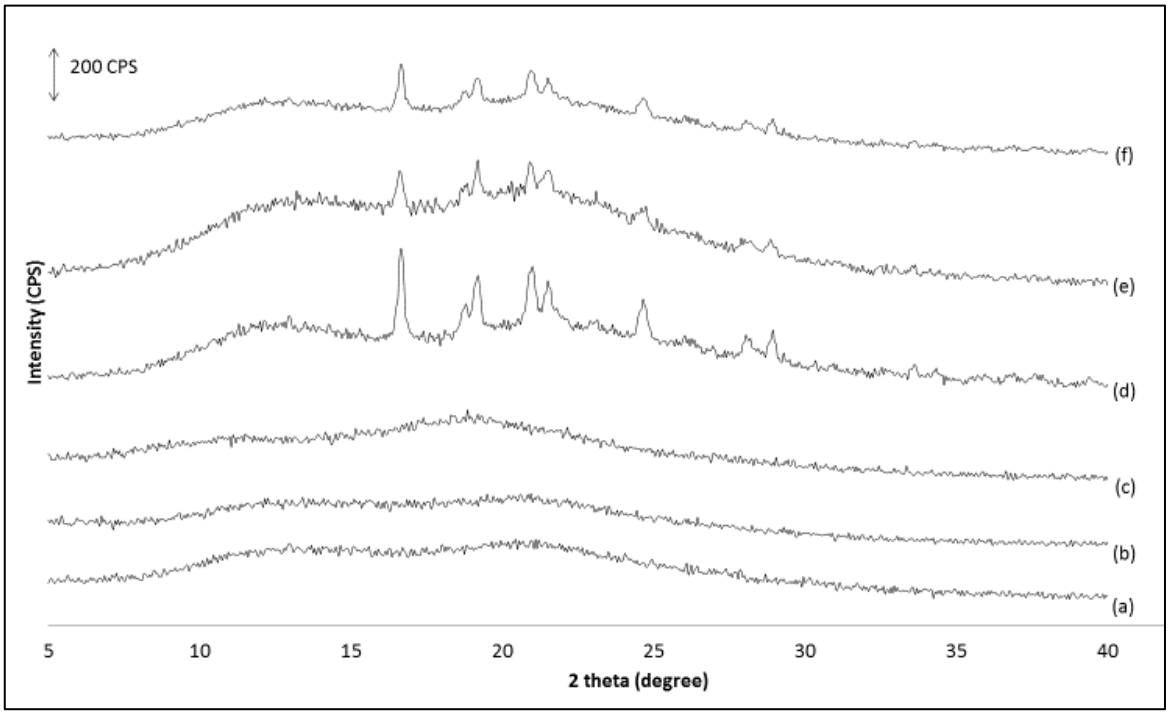


*Figure 3. 22: PXRD of Spray Dried (SD) and Hot Melt Extruded (HME) formulations at time point 60 days and samples stored at < 10 % RH, 25 °C - over the range 5~40 °2θ (a) SD-F1, (b) SD-F2, (c) SD-F3, (d) HME-F1, (e) HME-F2 and (f) HME-F3*

For SD formulations, mDSC studies showed similar results as for the initial products tested (at t = 0), with SD-F1 displaying one clear $T_g$ at 112.74 ± 0.25 °C, SD-F2 displaying two clear $T_g$s at 52.29 ± 1.13 °C and 93.70 ± 0.88 °C and SD-F3 displaying two $T_g$s at 58.81 ± 2.02 °C and 88.88 ± 1.29 °C, respectively (figure 3.23) after 60 days on stability. For SD-F2 and SD-F3, phase separation was evident at the initial analysis time point and this remains the case at time point t = 60 days, however, the formulations remain in an amorphous state. As previously stated, a homogenous molecularly dispersed system may be seen as favorable for long term stability of amorphous products due to the higher $T_g$ value obtained but, below the $T_g$ should phase separation be thermodynamically favored, the characteristics of the system may offer significant barriers to recrystallization resulting in a stable system over pharmaceutical relevant time frames (Tian et al. 2013). HPLC analysis revealed both drugs remained within 100 ± 5% of the stated drug content in each of the SD formulations over the stability study, with no degradation products present. For HME formulations, the endothermic peak seen at

54.78 ± 0.27 °C in HME-F2 confirms the crystallization of PEG 3350 during storage (figure 3.23 (e)). HPLC analysis for both APIs indicted no further degradation occurred during storage than that seen initially after manufacture via HME.

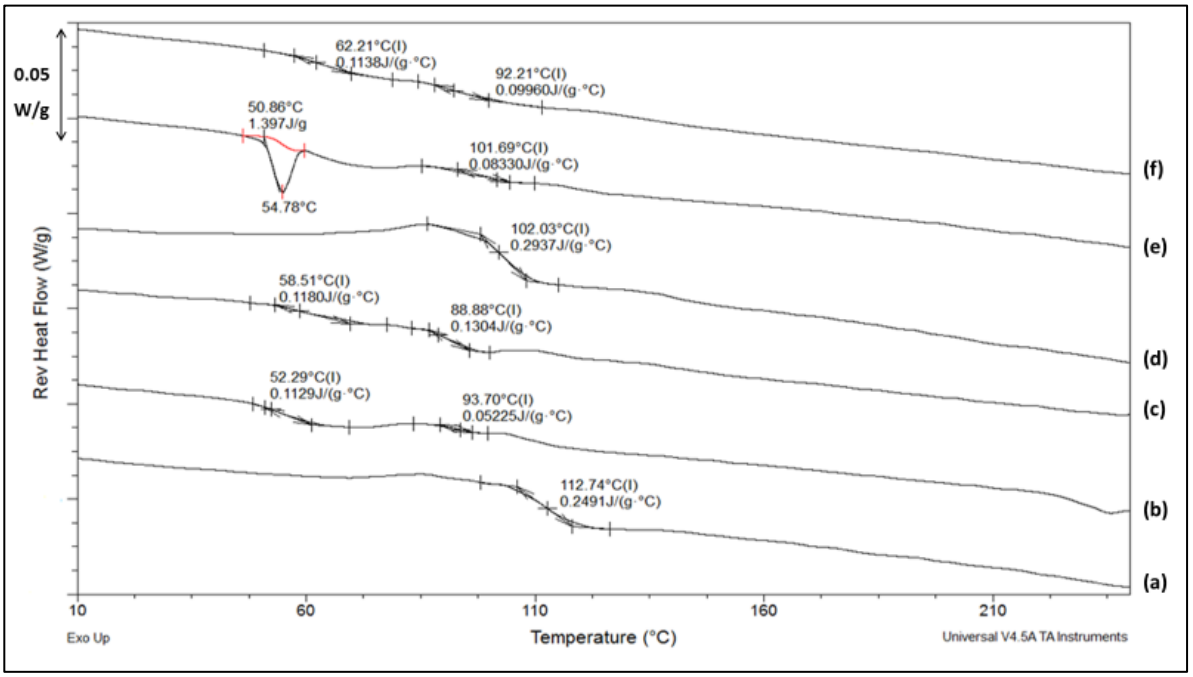


*Figure 3. 23: DSC thermograms showing the reverse heat flow (W/g) at time point 60 days and samples stored at < 10 % RH, 25 °C of (a) SD-F1, (b) SD-F2, (c) SD-F3, (d) HME-F1, (e)HME-F2 and (f) HME-F3*

SD-F1 and SD-F3 remained completely PXRD amorphous at stability conditions 75 % RH / 25 °C throughout the entire stability study (figure 3.24 (a) and (c)). SD-F2 remained PXRD amorphous up to t = 30 days, however by the final time point (t = 60 days), the PEG 3350 in the formulation had partially recrystallized, which is evident by a unique PEG 3350 peak at 23.35 °(2θ) (figure 3.24 (b)) in the diffractogram. HME formulations at stability conditions 75 % RH / 25 °C, as seen with the HME formulations stored at stability conditions < 10 % RH / 25 °C, remain partially crystalline on the PXRD with PEG 3350 recrystallizing in HME-F2 (figure 3.24 (e)).

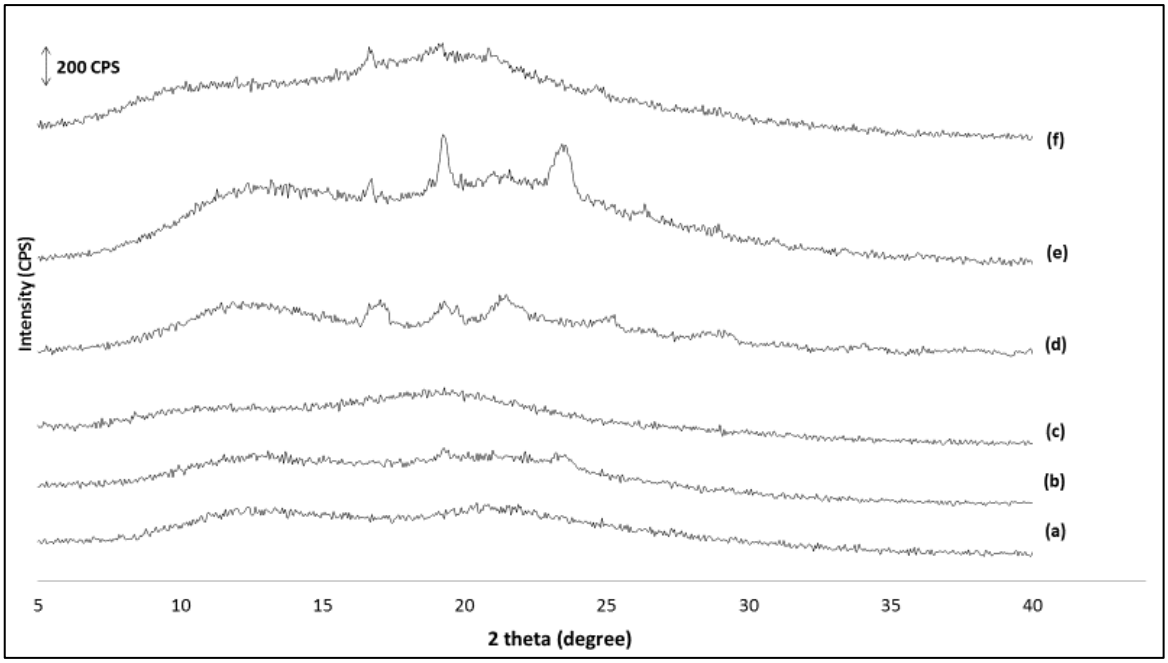


*Figure 3. 24: PXRD of Spray Dried (SD) and Hot Melt Extruded (HME) formulations at time point 60 days and samples stored at 75 % RH, 25 °C -over the range 5~40 °2θ (a) SD-F1, (b) SD-F2, (c) SD-F3, (d) HME-F1, (e) HME–F2 and (f) HME-F3.*

mDSC at time point t = 60 days for SD-F2 also revealed an endothermic peak at 55.27 ± 1.36 °C (figure 3.25 (b)) in the reverse heat flow corresponding to PEG 3350 melting, which confirms partial crystallinity. mDSC showed similar results to the initial products tested (at t = 0) with SD-F1 displaying one clear $T_g$ at 113.98 °C and SD-F3 displaying two $T_g$ s at 58.03 ± 0.62 °C and 89.32 ± 1.20 °C, respectively. HPLC analysis revealed both APIs remained within 100 ± 5% of the stated drug content in each of the SD formulations over the 60-day study. For HME formulations, partial PEG 3350 crystallization for HME–F2 at stability condition 75 % RH / 25 °C is confirmed with the presence of endothermic peaks in the mDSC at 54.69 ± 0.78 °C (figure 3.25 (e)). HPLC analysis revealed both APIs remained at the initial drug content in each of the HME formulations with no increase in degradation products present.

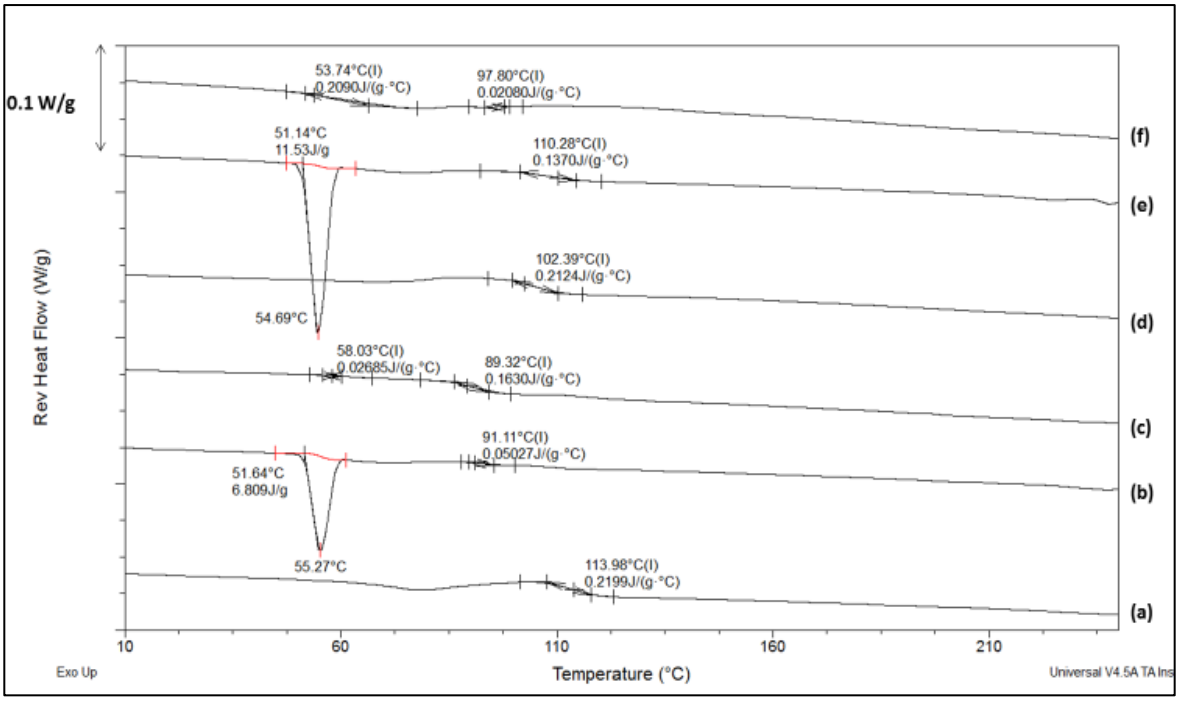


*Figure 3. 25: DSC thermograms showing the reverse heat flow (W/g) at time point 60 days and samples stored at 75 % RH, 25 °C of (a) SD-F1, (b) SD-F2, (c) SD-F3, (d) HME-F1, (e)HME-F2 and (f) HME-F3*

From the PXRD and mDSC data we can see that the SD formulations offer greater long-term amorphous stability than the HME formulations under the stability test conditions chosen. As the initial PXRD analysis demonstrated SD products to be completely PXRD amorphous and the HME products to be partially crystalline, the crystal components may encourage further crystal growth to occur throughout the product as time progresses, leading to decreased amorphous stability in the HME products when compared to SD products. Initial $T_g$s were also relatively lower for HME products when compared to SD products, which can result in decreased amorphous stability. Generally, a system with a higher $T_g$ results in longer-term amorphous stability when compared to a system with a lower $T_g$.

## 3.3 Conclusions

The pharmaceutical industry is moving towards continuous manufacturing to produce pharmaceutical products rather than the traditional batch-based processes, and two continuous manufacturing techniques – HME and SD – were employed in this study to produce FDC products. Depending on the desired characteristics of the final formulation, the method of manufacture has a critical impact upon the outcome. Both SD and HME may be used to produce monolithic FDC products with an immediate release dissolution profile. However, SD may be a more suitable option if a thermolabile API is being processed due to the vast array of volatile solvents available, allowing processing to be conducted at a lower temperature than may be required in HME with the same formulation. On the other hand, required processing temperatures can be reduced if the addition of a plasticiser is feasible and appropriate for HME, potentially avoiding the degradation of the thermolabile API. While the Wood's apparatus allows for comparison of release rates from a constant surface area, the surface roughness of the compacted disc may have a significant effect on the release rate. Also, formulations that contain polymers prone to swelling under the test conditions used may not be suited to a Wood's apparatus dissolution test. The present study demonstrates the importance of selecting the manufacturing method as well as polymer selection in the manufacture of stable monolithic fixed dose combination products.

# Chapter 4:

# A comparative study between melt granulation and spray-drying for the manufacture of large dose anti-diabetic compatible monolithic fixed-dose combination products

## 4.1 Introduction

Melt granulation (MG) and spray drying (SD) are two continuous manufacturing techniques that can be employed to manufacture monolithic FDC products which contain high drug loads. A requirement for high drug load oral solid dosage forms, is to use the minimum amounts of excipients as is possible during processing, in order to keep the overall tablet size small enough to allow ease of swallowing. Both MG and SD techniques allow for high drug dose formulations to be processed this way, with minimal amounts of excipients used to improve the manufacturability of such formulations.

MG, which is also often referred to as thermoplastic granulation, is a technique that facilitates the agglomeration of powder particles, using excipients, which melt or soften at relatively low temperatures, to form granules (Shanmugam 2015). The most common production technique for MG uses extruders, but MG in high-shear mixers has also been extensively described in the literature. In this process, the necessary energy to melt the binder is provided either by the mixer arm or by a heated jacketed vessel (Schaefer 1992). Another alternative for MG is if the binder used absorbs microwaves (e.g. PEG). Microwaves can be used to melt the binder much quicker than other processes, as the energy produced penetrates the product faster than heat energy travelling by conduction (Parikh 2010). The process usually incorporates a high shear processor with microwave input in order to carry out the granulation. The mechanism of MG is essentially like that of wet granulation with the main difference being, unlike wet granulation, no solution or liquid, such as water, is added to the powder bed before or during processing (Vasanthavada et al. 2011). Instead, the API is subjected to temperatures below its melting temperature but above the $T_g$ or melting temperature of the solid excipients used as polymeric binders. Once the melting of the binders and mixing with the API/APIs has occurred, the mixture is then subjected to lower temperatures, where, in an extruder, the mixture solidifies and produces granules at the end of the extruder barrel. MG using extruders has the advantage over other types of granulators in being designed for continuous processing. Additionally, MG has been reported to be beneficial in enhancing compactability, densifying granules, enhancing flowability, reducing segregation, and decreasing the generation of dust of pharmaceutical materials (Repka et al. 2007; Vasanthavada et al. 2011). It also has the advantage of being seen as a “green technology” as no solvents are required and it is easily scaled up (Vaingankar and Amin 2017).

Metformin (MET) is a good example of a high dose drug that is commonly used for the treatment of type II diabetes. The usual dosage ranges from 500 mg once daily to 1000

mg three times daily. It is a highly water soluble drug but has significant processing challenges due to its poor compressibility and moisture sensitivity (Lakshman et al. 2011; Vaingankar and Amin 2017). In addition, MET is often manufactured with other anti-diabetic agents to develop FDC products. Sitagliptin phosphate (SIT) is one such agent that is formulated with MET and marketed under the brand name Janumet®. Janumet® is available as 850/50 mg and 1000/50 mg metformin/sitagliptin film-coated tablets (850/1000 mg metformin hydrochloride and 50 mg sitagliptin as sitagliptin phosphate monohydrate). It is recommended for use in patients who are taking both drugs as independent products simultaneously where their blood glucose levels are not adequately controlled by one drug alone. The use of Janumet® tablets has resulted in significantly improved reduction in blood glucose levels in patients compared to either MET or SIT alone (Bell 2006; Reynolds et al. 2008).

Both MG and SD techniques have been successfully employed to improve the compressibility of high drug load tablets of MET and reduce the overall excipient amount to produce satisfactory oral tablets (Al-Zoubi et al. 2017; Barot et al. 2010; Lakshman et al. 2011; Vaingankar and Amin 2017). However, as far as the author is aware, there has been no previous work undertaken to investigate the use of MG or SD as a continuous technique to produce a monolithic high dose FDC product of MET and SIT. The main objective of the current work is to investigate the use of MG and SD as continuous processing techniques to produce a monolithic high dose FDC product of MET and SIT. Additionally, the study aims to investigate the effect of different polymer grades and processing conditions on the performance of the manufactured solid dosage form. HPC was chosen as the preferred binder as HPC based polymers have been successfully employed in previous MG studies for high dose drugs, including MET (Vaingankar and Amin 2017; Vasanthavada et al. 2011), because of their high binding ability behavior (Arndt and Kleinebudde 2018; Grymonpré et al. 2018; Lakshman et al. 2011). Lakshman et al. also reported that MET was compatible with HPC (Lakshman et al. 2011). Once suitable granules were achieved via MG, the same formulations were processed via SD and the physicochemical properties of each product were investigated to see how the different manufacturing processes affect the properties of the product. Granules produced via MG and powders produced via SD were compressed into caplets, using an in-house design, to produce a final solid oral dosage form. These caplets were then tested for friability, tablet hardness, disintegration time and dissolution.

## 4.2 Results and discussion

### 4.2.1 Physicochemical characterization of raw materials

As is the case with hot melt extrusion (HME), it is important to know the thermal degradation points of each of the components to be added to the formulations for MG studies. Figure 4.1 shows the various thermal degradation temperatures by TGA for the different components used in developing the final formulations. MET has previously been reported to be thermally stable over a wide range of temperatures (Sarkar et al. 2017) and was found by TGA to be thermally stable up to approximately 230 °C (figure 4.1 (a)). SIT also showed thermal stability up to 216 °C (figure 4.1 (b)), which was consistent with a previous report (Priyadarshini et al. 2016). It is worth noting that there was some weight loss in SIT samples at approximately 126 °C, which corresponds to 3.34 % w/w of the initial sample weight; this loss in weight can be attributed to the single water molecule within the initial starting monohydrate material.

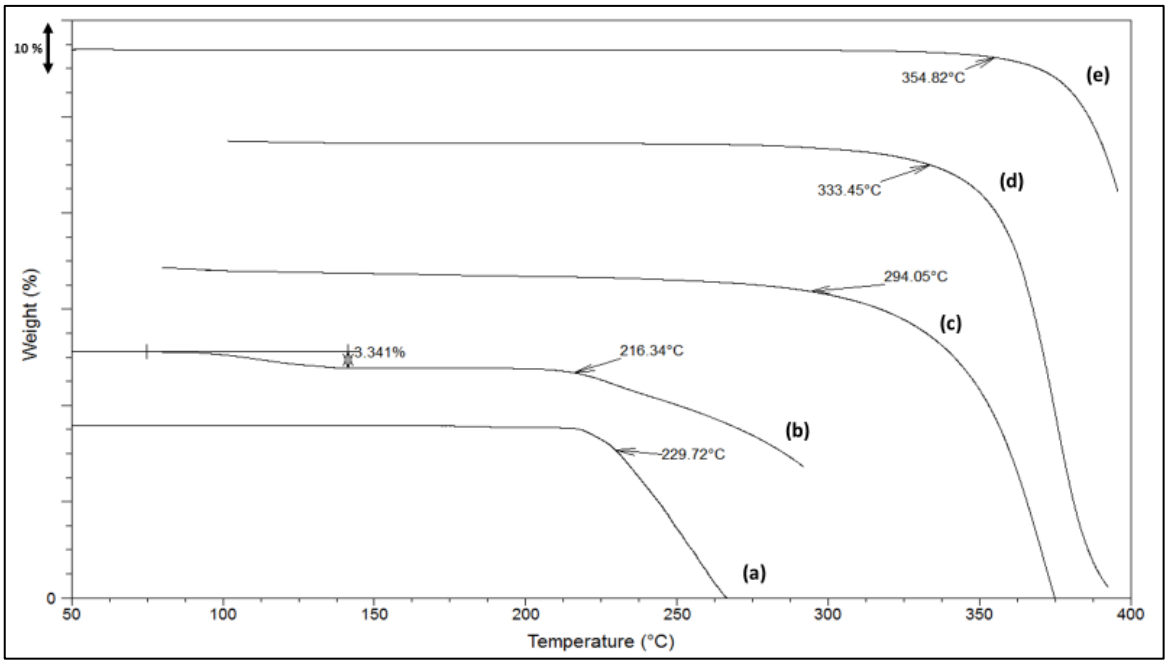


*Figure 4. 1: TGA thermogram of APIs and polymers/plasticiser used in formulations. Heating ramp from 50 °C to 400 °C at 10 °C/ min, showing, (a) MET thermal degradation at ~230 °C, (b) SIT dehydration at ~130 °C and thermal degradation at ~216 °C, (c) HPC-S thermal degradation at ~294 °C, (d) HPC-A thermal degradation at ~ 334 °C and (e) PEG 3350 thermal degradation ~ 355 °C.*

TGA studies of HPC samples indicated that their thermal degradation occurs at higher temperatures than the APIs. The HPC-S grade showed a thermal stability up to 294 °C, whereas HPC-A started to thermally decompose at approximately 334 °C. PEG 3350 started to thermally degrade at approximately 355 °C, as shown in figure 4.1.

The two HPC polymers, display different characteristics that are summarised in table 4.1 below. As HPC is a semi crystalline polymer it has both amorphous and crystalline domains within the structure (Sarode et al. 2013). The polymer itself is very hygroscopic, and as a result the $T_g$ of the amorphous domain varies greatly with moisture content (Picker-Freyer and Dürig 2007). Based on work conducted by Picker-Freyer and Dürig, crystallinity for the various grades of HPC is estimated to be between 7 % and 9 % (Picker-Freyer and Dürig 2007).

*Table 4. 1: Physicochemical properties of HPC polymers used in the study* (Ashland 2017; Sigma Aldrich 2019).

| | Hydroxypropoxy content (%) | Viscosity (mPA.s) in $H_2O$ @ 25 °C | Moles of substitution* | Molecular weight (g/mol) |
|---|---|---|---|---|
| HPC-A | 75 | 1500-3000 @ 1 % w/v | 3.8 | 1,150,000 |
| HPC-S | 65 | 75-150 @ 5 % w/v | 3.0 | 100,000 |

*Degree of substitution (DS) are the number of moles of hydroxypropyl groups per glucose unit. Complete substitution would provide a DS of 3. Because the hydroxypropyl group added contains a hydroxyl group, this can also be etherified during preparation of HPC. When this occurs, the number of moles of hydroxypropyl groups per glucose ring, moles of substitution, can be higher than 3.

Figure 4.2 below, shows the second heating cycle of a heat cool heat cycle of both HPC -A and HPC-S to highlight the thermal characteristics of the polymers without any water content (as detailed in chapter 2, section 2.3.2.1). The results correspond well to previous reports by Picker-Freyer and Dürig, that the $T_g$s of the amorphous portion of HPC polymers are around 0 °C and the crystalline domains display melting endotherms in the range of 180 °C to 220 °C. The higher the molecular weight of the HPC polymer, the higher the melting endotherm that is evident as is the case in figure 4.2 where HPC -A has a higher melt at 207.31 ± 1.23 °C compared to HPC-S at 197.71 ± 0.40 °C (Picker-Freyer and Dürig 2007).

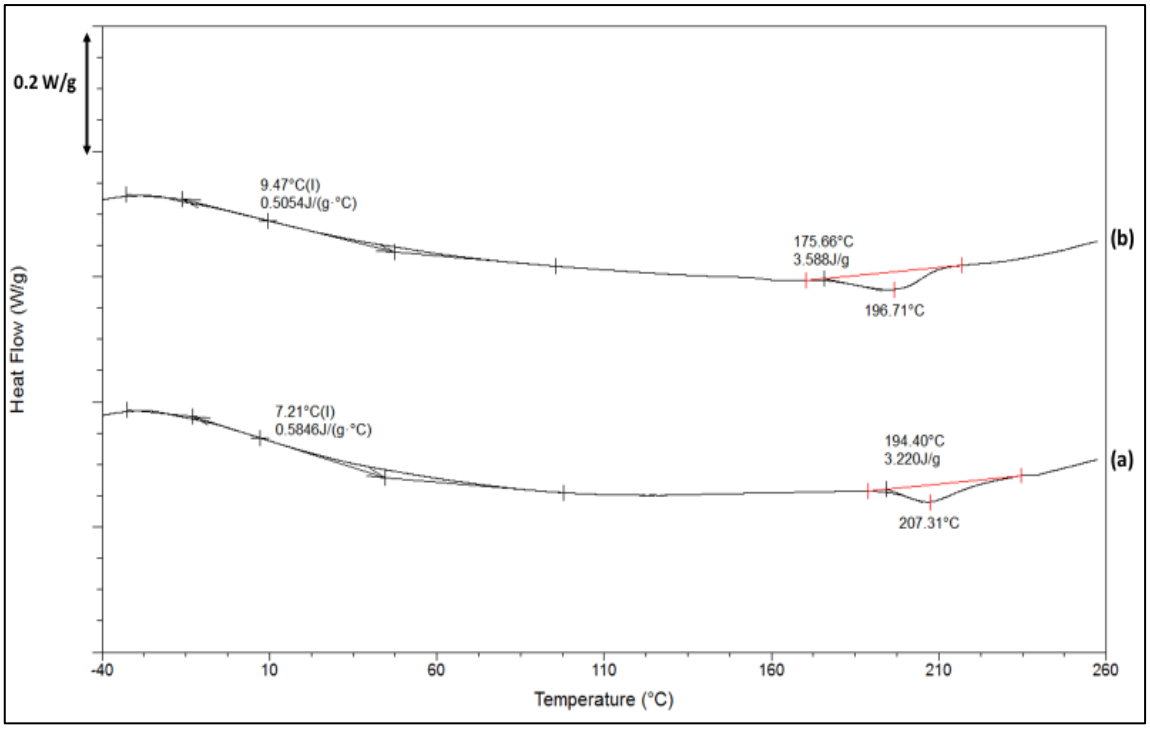


*Figure 4. 2: DSC thermogram of the second heating cycle in a heat cool heat cycle as described in chapter 2, section 2.3.2.1 showing (a) HPC - A and (b) HPC – S.*

Standard DSC runs (as detailed in chapter 2, section 2.3.2) showed the starting API materials were crystalline in nature with sharp melting endotherms at 232.65 ± 0.52 °C and 213.92 ± 0.98 °C for MET and SIT, respectively (figure 4.3). With regards to the endotherm seen with SIT at 137 °C, this can be attributed to the loss of a water molecule consistent with the TGA data. PEG 3350 is a semi-crystalline plasticiser that exhibits a melting endotherm at 59.81 ± 1.20 °C (figure 4.3 (a)). As both MET and SIT start to thermally degrade near their melting temperatures, this information has to be considered when determining the processing conditions for MG and SD.

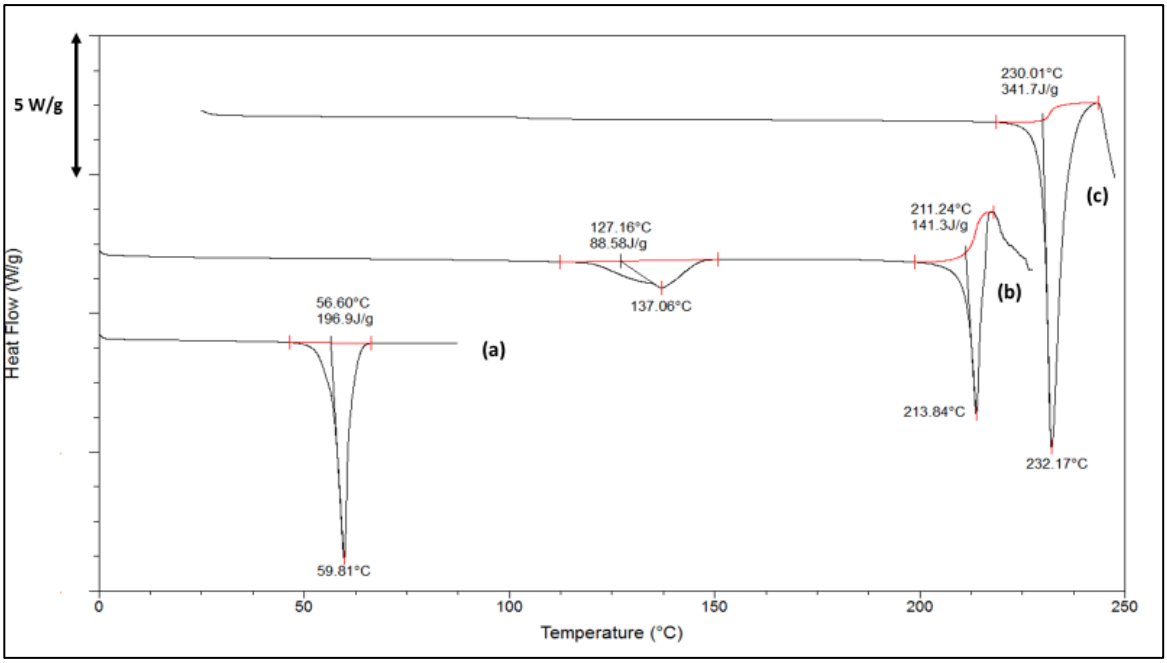


*Figure 4. 3: DSC thermogram of API raw materials and plasticiser with a heating rate of 10 °C/min showing, (a) PEG 3350 shows a melting endotherm at 59.81 ± 1.20 °C, (b) SIT shows an endotherm at 137 °C corresponding to the loss of a water molecule and shows a melting endotherm at 213.92 ± 0.98 °C and (c) MET shows a melting endotherm at 232.65 ± 0.52 °C*

PXRD data (figure 4.4) supported the data obtained from DSC analysis that the starting API materials were in the crystalline state. MET showed characteristic Bragg peaks at 12.25 °(2θ), 17.65 °(2θ), 22.40 °(2θ) and 39.5 °(2θ), which are consistent with the literature (Ige and Gattani 2012; Rebitski et al. 2018). SIT showed characteristic Bragg peaks at 13.90 °(2θ), 16.1 °(2θ), 18.65 °(2θ), and 21.25 °(2θ), which are also consistent with the literature (Shantikumar et al. 2014). PEG 3350, which was used as a plasticiser in the study, showed characteristic Bragg peaks at 19.2 °(2θ) and 23.3 °(2θ), consistent with previous reports in the literature (Baird et al. 2010). The PXRD diffractograms for HPC-A and HPC-S are very similar displaying “halo” patterns, which are characteristic of amorphous material, centred at 8.55 °(2θ) and 20.35 °(2θ). While cellulose polymers consist of both crystalline and amorphous domains, the crystalline domain content is, presumably so small, the PXRD is not sensitive enough to pick out these peaks, so the amorphous halo dominates the PXRD pattern.

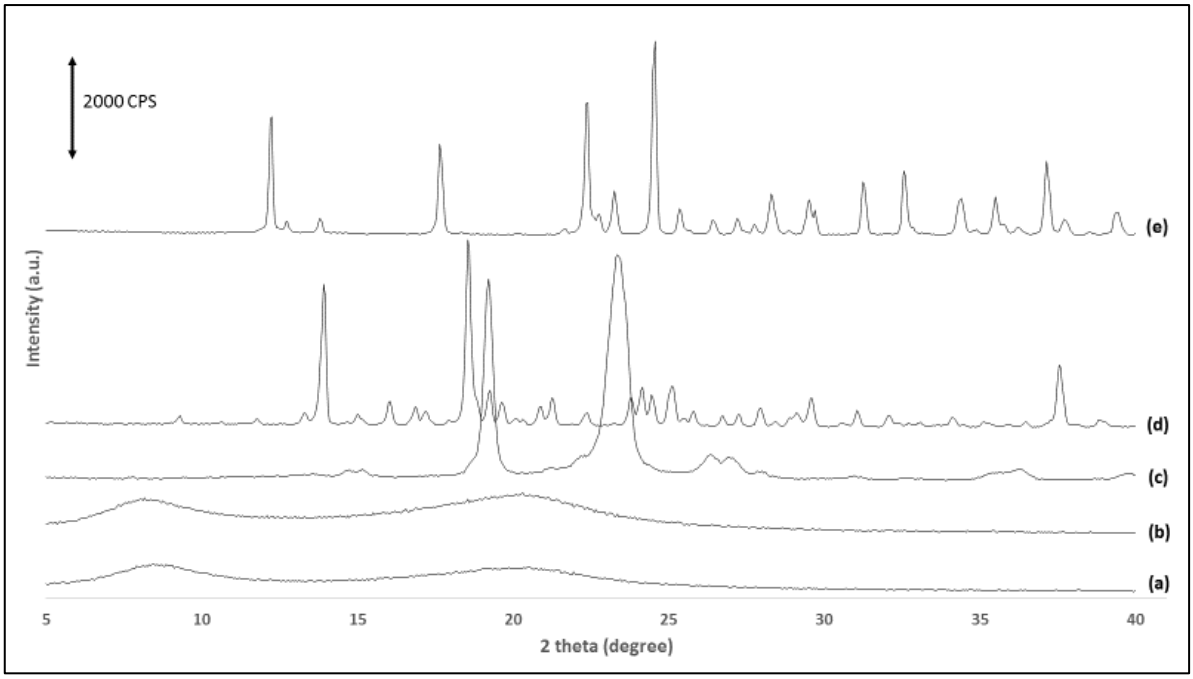


*Figure 4. 4: PXRD of raw materials over the range of 5–40° 2θ of (a) HPC-S, (b) HPC-A, (c) PEG 3350, (d) SIT, and (e) MET.*

### 4.2.2 Manufacture of melt granules

The initial visual characterisation of melt granules is essential when processing materials using a melt granulation technique (Parikh 2010; Repka et al. 2007). Optimised melt granule formulations are expected to be solid, uniform in particle size distribution, show acceptable flow properties and have no charred spots (Passerini et al. 2002; Shimpi et al. 2004). During the course of this study, during method development and optimisation, a range of processing parameters (screw rotation speed and processing temperatures), HPC grade and proportions were investigated to optimise the final melt granule formulation so that it exhibited acceptable visual characteristics upon manufacture. The minimum amount of HPC was used to ensure the dosage size remained as small as possible.

The extruder barrel was divided into 4 heating zones (the feeding zone and zones 1-3). The final temperatures chosen are displayed in table 4.2. The temperature throughout remains below the melting temperatures of both APIs but above the HPC $T_g$ and melting temperature of PEG 3350. This allows for granules to form successfully. The temperature increases from the feed zone through to zone 3 to allow the complete melting of the excipients while also allowing adequate time for the components to mix with one another during the process.

A disadvantage associated with working with FDC products is that that ratio of drugs needs to remain constant, in this case, for every 850 mg of MET we need 63 mg of SIT (equivalent to 50 mg of sitagliptin). For this reason, the only variation in formulation can come from the excipients added. Ideally, we want the final formulation to contain as little excipients as possible due to the already large API content required. HPC-S and HPC-A were successfully employed to produce granules which, from initial visual inspection, were larger in size compared to the physical mixtures fed into the extruder. Initial studies consisted of MET and HPC only as these components made up most of the formulation. It was possible to process MET drug loadings as high as 85 % w/w using either of the two grades of HPC. However, the manufactured granules were slightly fragile and tended to break apart after they were cooled. While other studies have shown that MET may be successfully melt granulated up to 90 % w/w with HPC and other polymers using larger melt extruders (Batra et al. 2017; Lakshman et al. 2011), it is likely that this is because of the ability of larger extruders to exert relatively higher pressures and torque required for granule formation in comparison to the 10 mm lab-scale extruder used in this study. To overcome this problem, PEG 3350 was added to the formulation, as it was hypothesised that the melting of the waxy hydrophilic substance would allow for better granule formation. PEGs are well suited to work as binders in granulation and have been successfully used for many years in various granulation techniques (Van Melkebeke et al. 2006; Schæfer and Mathiesen 1996). Low molecular weight PEGs have been shown to produce more spherical particles than high molecular weight PEGs owing to differences in viscosity exerted during the MG process (Schæfer and Mathiesen 1996). The addition of the PEG at low concentrations had the desired effects visually, with granules appearing freer flowing and less fragile. Finally, the second API, SIT, was added to the formulation and the final % w/w of each component is displayed in table 4.2 below. The optimised screw rotation speed was 10 rpm.

*Table 4. 2: Summary and composition and processing temperature for optimised formulations.*

| Proportion (% w/w) of components in MG formulation | | | |
|---|---|---|---|
| MET | SIT | PEG 3350 | HPC-A or HPC-S |
| 80 | 6 | 4 | 10 |
| Processing Temperature (°C) | | | |
| Zone 3 | Zone 2 | Zone 1 | Feed Zone |
| 180 | 170 | 150 | 130 |

### 4.2.3 Spray drying of formulation

Once successful MG had taken place, the two optimised formulations (detailed in Table 4.2) were spray dried (as detailed in chapter 2 section 2.2.1.2), so that the manufactured products could be compared to one another. The formulation containing HPC-S was spray dried at 5 % w/v. The formulation containing HPC-A was spray dried at 1 % w/v. Higher concentrations of both formulations were trialled; however, it was found the solution viscosity was too high for successful spray drying.

### 4.2.4 Characterisation of Manufactured Granules

#### 4.2.4.1 Particle size analysis (PSA)

Particle size plays an important role in many aspects of the manufacturing process. In general, smaller particles demonstrate stronger interparticular cohesive forces compared to larger particles, which in turn affects the flowability. Typically, granulation aims to increase particle size of formulations to form granules (usually between 200 µm and 4000 µm) by creating bonds between particles by compression or by using binding agents. Particle size analysis (PSA) results are presented in table 4.3 for the APIs, MG and SD formulations (detailed in chapter 2, section 2.6.2). As MET comprised the majority of the formulations (80 %), the particle size of the MET raw material was compared to the MG and SD formulations particle size. The median particle size of MG formulations were statistically larger than the MET or SIT raw material ($p < 0.05$). As the MG process resulted in particles larger than the MET raw material and were larger than 200 µm, the process conditions resulted in successful granule manufacture for both HPC grades. With regards to the SD formulations, all SD formulations were statistically smaller than the MET raw material ($p < 0.05$) which is expected due to the spray drying conditions selected during the initial experimental design. The SD formulations are in solution before processing with all materials fully dissolved. As spray drying solutions usually result in materials with median particle size less than 10 µm, the results of the SD materials is as expected (Saleem et al. 2017).

*Table 4. 3: Overview of particle size analysis (PSA) results of API raw materials and processed MG and SD formulations*

| Sample | Particle size (d50) (µm) |
|---|---|
| MET | 115.08 ± 10.88 |
| SIT | 28.64 ± 0.80 |
| MG-A | 221.67 ± 13.80 |
| MG-S | 281.67 ± 55.05 |
| SD-A | 7.45 ± 0.47 |
| SD-S | 8.72 ± 1.71 |

#### 4.2.4.2 Flowability measurements

Flowability measurements are essential, as poorly flowing particles or powder blends are problematic in the manufacturing of solid dosage forms, such as compressed tablets or powder-filled hard gelatin capsules (Lindberg et al. 2004). Powder flow characteristics are determined by both the physical properties of the powders such as particle size, distribution and shape and are also determined by several environmental factors such as temperature, humidity and the stresses applied during storage and processing, such as gravity, vibrations, air pressure, and external loading from filling devices (Freeman et al. 2009). As the products being tested varied in particle size and shape, the initial state of the products before testing is particularly important and so “conditioning” to ensure a reproducible packing condition is essential if the data is to be reproducible, repeatable and comparable (Freeman 2007). Once consolidation has been completed and shear testing has been performed, several different results are displayed, including the measured Angle of Internal Friction (AIF) and cohesion, which can be directly used to measure the product’s flowability. The AIF is defined as a measure of the ability of a unit of product to withstand a shear stress. It is the angle (φ), measured between the normal force and resultant force that is attained when failure just occurs in response to a shearing stress. The AIF values have been shown to be directly related to particle size and shape (Freeman 2007; Guo et al. 2015). Previously, it was reported that the AIF plays a significant role in determining the flow function (FF) of powders and granules (Freeman 2007; Guo et al. 2015; Podczeck and Mia 1996). Recently however, Wang et al (Wang, Koynov, et al. 2016) reported that, while by definition FF requires the AIF be

known, in practice the AIF plays a very limited role and cohesive factors are much more critical. Correlation between FF and cohesion can be sustained as long as the AIF at incipient flow is not significantly larger than the AIF at steady-state flow, a condition covering almost all pharmaceutical powders. These findings were confirmed by Leung et al (Leung et al. 2017) when the experimental conditions were undertaken using a much larger sample size. As a result, determining a product's cohesiveness is much more critical than the AIF.

Results of AIF, cohesiveness and FF are shown in table 4.4 for all manufactured products and the corresponding physical mixtures (detailed in chapter 2, section 2.7.1). For HPC - S formulations, statistically there is no difference between the PM, MG and SD formulations in their respective AIF results ($p > 0.05$). For cohesiveness, there is no difference between the PM and MG however, the SD formulation is statistically more cohesive ($p < 0.05$). For HPC-A formulations, the same observation was made with no difference between the products AIF ($p > 0.05$), but the SD formulation is more cohesive than the MG and PM formulations ($p < 0.05$). The reason for increased cohesiveness of the SD formulations in comparison to PM and MG formulations is primarily due to the smaller particle size. Smaller particle size leads to an increase in cohesiveness due to an increase in surface area per unit mass of powder allowing greater area for those cohesive forces to occur such as hydrogen bonding and electrostatic forces (Fitzpatrick et al. 2004; Ratanatriwong and Barringer 2007).

*Table 4. 4: Summary of flow parameters of physical mixtures (PM), manufactured melt granules (MG) and manufactured spray dried (SD) materials.*

| Sample | AIF, º | Cohesion, kPa | FF |
|---|---|---|---|
| PM MET SIT HPC-S PEG | 32.01 ± 2.55 | 0.84 ± 0.18 | 5.57 ± 0.85 |
| PM MET SIT HPC-A PEG | 31.45 ± 1.06 | 0.81 ± 0.13 | 5.61 ± 0.84 |
| MG MET SIT HPC-S PEG | 34.30 ± 1.28 | 0.79 ± 0.18 | 5.38 ± 1.32 |
| MG MET SIT HPC-A PEG | 32.00 ± 1.56 | 1.05 ± 0.13 | 4.74 ± 0.69 |
| SD MET SIT HPC-S PEG | 36.95 ± 0.49 | 2.20 ± 0.06 | 2.04 ± 0.06 |
| SD MET SIT HPC-A PEG | 32.35 ± 2.19 | 4.22 ± 0.33 | 1.11 ± 0.11 |

Several other factors can have significant effects on the flowability of products such as moisture content, storage conditions and hopper angle. Jenike (Jenike 1964) used FF to classify powder flowability with higher values representing easier flow as shown in Table 4.5. Both the PM and MG formulations are considered to be easy flowing based on the classification, with the SD formulations being very cohesive with poor flowability.

*Table 4. 5: Jenike classification of flowability by flow function* (Jenike 1964)

| **Flowability** | **No flow** | **Very cohesive** | **Cohesive** | **Easy flow** | **Free flowing** |
|---|---|---|---|---|---|
| **Flow function** | <1 | <2 | <4 | <10 | >10 |

#### 4.2.4.3 Powder X-Ray Diffraction (PXRD)

The PXRD patterns for PM, MG and SD formulations are shown in figure 4.5. Bragg peaks displayed in patterns of the PMs (figure 4.5 (a) and (b)) are peaks associated with crystalline MET. Due to the high MET content in the formulations and the strong Bragg peaks associated with it, unique Bragg peaks associated with SIT and PEG 3350 (displayed in figure 4.4) are not detectable in the PMs. As a method of determining the solid state of SIT and PEG 3350 post processing, PXRD is unsuitable. However, it remains a suitable technique to determine the solid state of MET. For MG and SD formulations, MET remains in the crystalline state post processing as is evident with characteristic Bragg peaks remaining. Two MET polymorphs have previously been reported in the literature, the stable form A and a metastable form B (Bretnall and Clarke 1998; Childs et al. 2004). The MET raw material used during the study was form A. The positions of the strong diffraction peaks at the x-axis are the same for all PM, MG and SD formulations indicating the same crystal lattice, implying no MET polymorph form change in MET during processing.

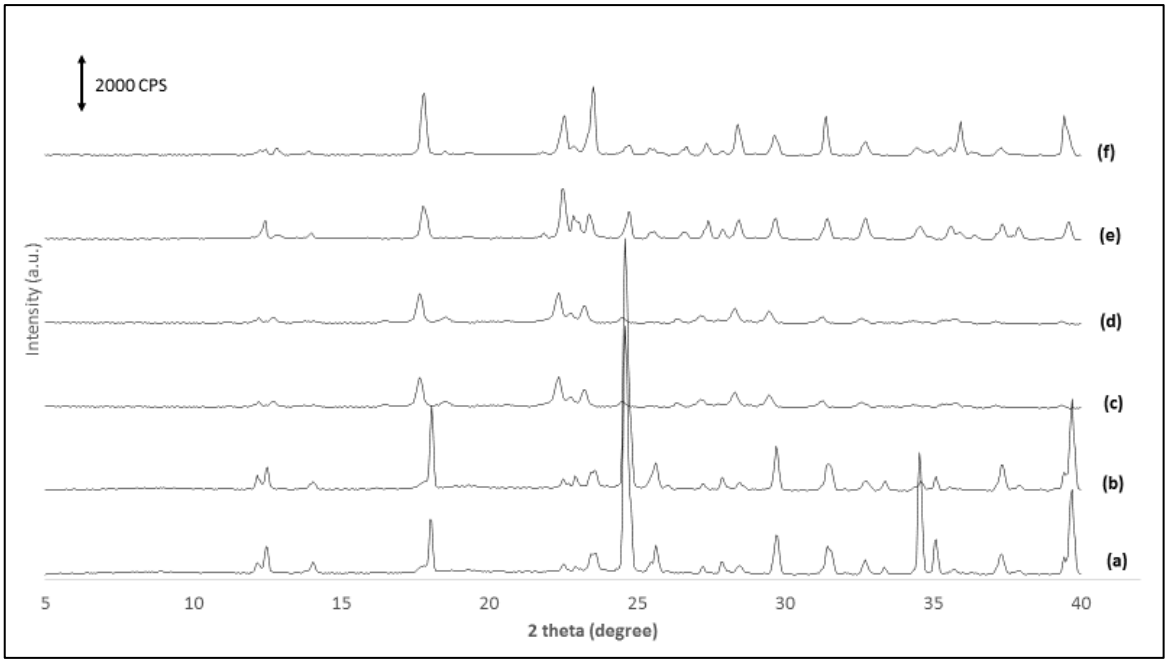


*Figure 4. 5: PXRD over the range of 5–40° 2θ of (a) Physical mixture of HPC-S formulation (b) Physical mixture of HPC-A formulation (c) Spray Dried HPC-S formulation (d) Spray Dried HPC-A formulation (e) Melt granulation HPC-S formulation and (f) Melt granulation HPC-A formulation.*

While we see a difference in peak intensity for the different formulations, this may be explained by the preferential orientation of the crystals within the sample holder (Garekani et al. 1999). The lower intensities of the processed formulations compared to the PMs may also be due to some loss of crystallinity. Thermal analysis was conducted to assess the level of crystallinity pre and post processing.

#### 4.2.4.4 Differential Scanning calorimetry (DSC)

The lack of endothermic peaks for PEG 3350 and SIT in the MG and SD formulations, indicate that post processing, both components are present in a non-crystalline state, most likely in their amorphous states instead. When spray dried using the conditions as for the SD formulations, SIT alone produces an amorphous form with a clear $T_g$ evident at 27.49 ± 1.01 °C and the absence of an endotherm at 213.92 ± 0.98 °C (Appendix 2). Due to this finding, we can conclude SIT is amorphous in the SD formulations also. For MG formulations, the absence of a melting endotherm for SIT, which is evident in the PMs, can be explained primarily due to the API melting. While the melting point of pure SIT is 214 °C, strong intermolecular interactions exist between SIT and MET causing a melting point depression to occur for both APIs. As can be seen in figures 4.6 (c) and 4.7 (c), the melting endotherm for SIT has been depressed to 186 °C in both PMs. As the melting point is evident in the PMs, if SIT remained crystalline after MG then it would be

expected to see the same endotherms post processing. It also suggests the quantity of SIT is not soluble in the other excipients which have melting points and $T_g$s are lower than 186 °C. If SIT was soluble in these excipients, we would most likely not see any endotherm at 186 °C in the PMs also. Even though the highest temperature on the extruder during processing was 180 °C, local hot spots can form causing increases in temperature above the set point on the thermostats. These hot spots may allow SIT to melt forming an amorphous form during processing. MET remains fully crystalline in both MG and SD formulations with no statistical difference between the heat of fusion for any of the samples compared to the PMs ($p > 0.05$).

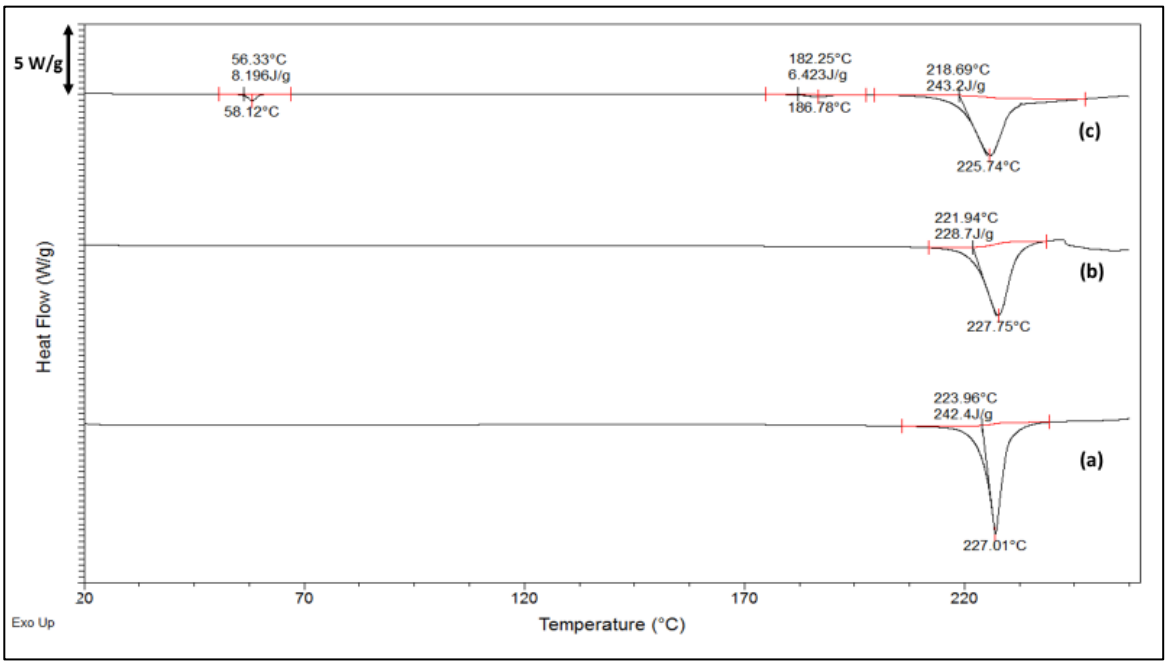


*Figure 4. 6: DSC thermogram with a standard heating rate of 10 °C/min. of (a) Spray dried HPC - S formulation, (b) Melt granulation HPC – S formulation and (c) Physical mixture of HPC – S formulation.*

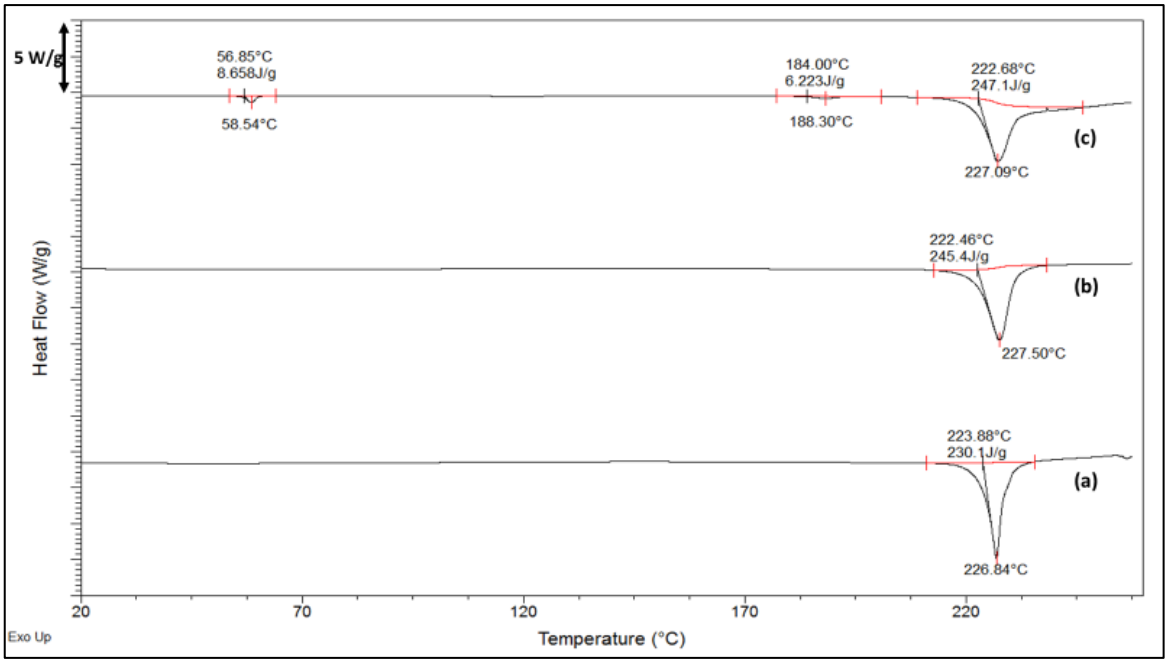


*Figure 4. 7: DSC thermogram with a standard heating rate of 10 °C/min. of (a) Spray dried HPC - A formulation, (b) Melt granulation HPC – A formulation and (c) Physical mixture of HPC – A formulation constituents.*

### 4.2.4.5 Content assay

During processing, degradation of APIs may occur and as a result it is important to investigate the final API content to comply with regulations. During MG, thermal degradation is a potential hazard for APIs due to excess thermal energy generation, whereas with SD, the potential hazards can include solvent composition and thermal degradation due to excess heat within the spray dryer. Due to the design of the experiments, however, the possibility of degradation occurring due to these processes was considered to be low. Acceptable limits of API content are usually stipulated in the monographs of pharmacopoeias. In the European Pharmacopoeia, no monograph currently exits for FDCs containing both MET and SIT. For individual monographs of MET and SIT, the requirement for content assay tests to be successful is to have drug content not less than 95.0 % and not more than 105.0 % of the stated amount(European Pharmacopoeia 2020d, 2020f). Table 4.6 shows content assay for MET and SIT for all processed formulations, with all results complying with the required content of APIs and indicating no significant degradation in processing.

*Table 4. 6: Content assay (%) of melt granulation (MG) and spray dried (SD) formulations.*

| Formulation | MG MET SIT HPC-S PEG | MG MET SIT HPC-A PEG | SD MET SIT HPC-S PEG | SD MET SIT HPC-A PEG |
|---|---|---|---|---|
| **MET (% of max theoretical amount)** | 98.12 ± 0.84 | 98.84 ± 0.46 | 99.25 ± 0.45 | 100.12 ± 1.15 |
| **SIT (% of max theoretical amount)** | 99.14 ± 0.35 | 98.47 ± 0.74 | 100.45 ± 0.35 | 98.95 ± 0.56 |

#### 4.2.4.6 Scanning electron microscopy (SEM)

SEM images for API raw materials (MET and SIT) show both APIs to consist of orthorhombic-shaped crystals (figure 4.8 (a) and (b)). Figures 4.8 (c) and 4.8 (d) show SEM images for the MG formulations containing HPC-A and HPC-S, respectively. The formulations appear as round agglomerates of smaller particles, with the loss of the longitudinal orthorhombic structures of the individual API raw materials. This corresponds well to the increase in the particle size discussed previously for the MG formulations in comparison to the API raw materials. Figures 4.8 (e) and 4.8 (f) show smooth spherical particles which correspond well to the literature reports of SD materials containing large doses of MET (Al-Zoubi et al. 2017; Barot et al. 2010).

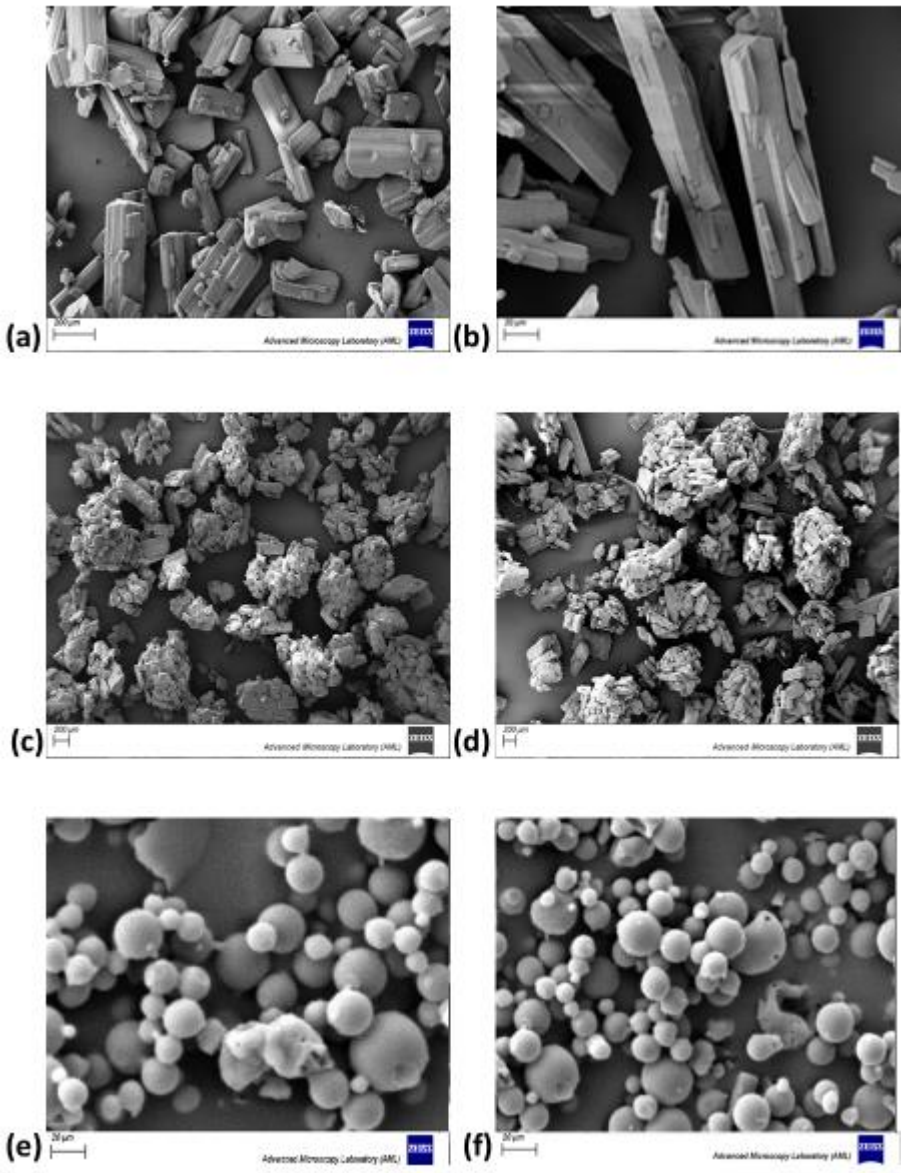


*Figure 4. 8: SEM micrographs of (a) MET raw material, (b) SIT raw material, (c) MG MET SIT HPC-A PEG, (d) MG MET SIT HPC-S PEG, (e) SD MET SIT HPC-A PEG and (f) SD MET SIT HPC-S PEG.*

### 4.2.5 Caplet manufacturing and characterisation

Due to the large therapeutic dosage of the APIs, conventional circular tablets with flat faces are unsuitable for patients to swallow easily. As the market product Janumet®, is manufactured to produce an elongated tablet, otherwise known as a caplet, it was decided that our in-house caplet die would be used to produce a similarly shaped product for ease of swallowing. Figure 4.9 (a) shows an example of the dimensions of manufactured caplets post compaction using the in-house caplet die. The average

weight of the equivalent marketed product (Janumet®) is 1142 ± 2.65 mg in comparison to the SD and MG manufactured products target weight of 1063 mg.

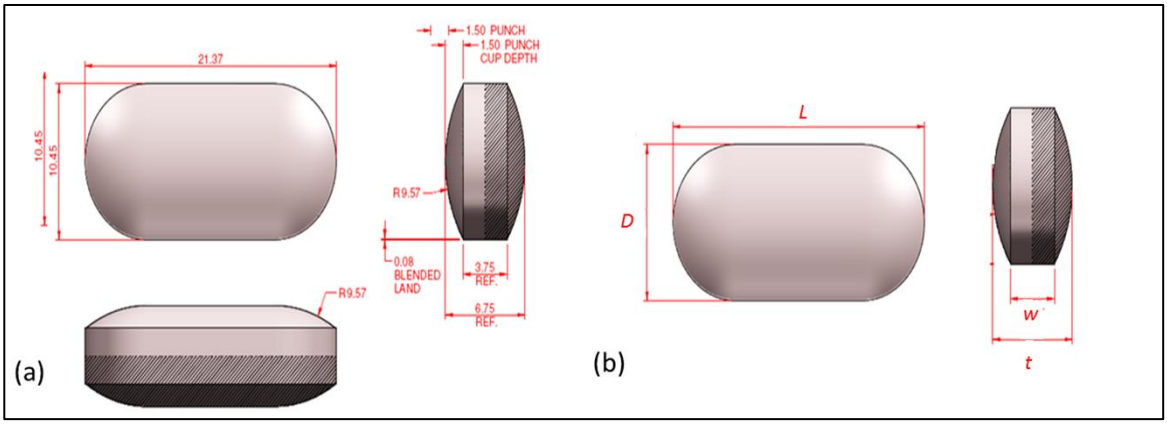


*Figure 4. 9: Diagram of (a) In-house design of manufactured caplets and (b) caplet shape and dimensions for equation 1(chapter 2, section 2.9.1)* (Pitt and Heasley 2013).

Two different compression forces were selected for caplet formation and the manufactured caplets were subjected to evaluation according to the common compendial tests for oral tablets (i.e. hardness, friability, disintegration and in-vitro dissolution). SEM imagery of the caplet surfaces was also recorded.

### 4.2.5.1 Scanning electron microscopy (SEM)

SEM images of the caplet surfaces highlight the differences between the compressibility of the different formulations. MG images show rough uneven surfaces highlighting the more plastic nature of the larger MG granules under different compression forces compared to the SD powders. Figure 4.10 (e) – (h), show smooth surfaces of the compressed SD materials. Given the particles shape and size, SD powders contain more elastic crystals of MET than the equivalent crystals in the MG granules giving the smoother, less porous looking surface.

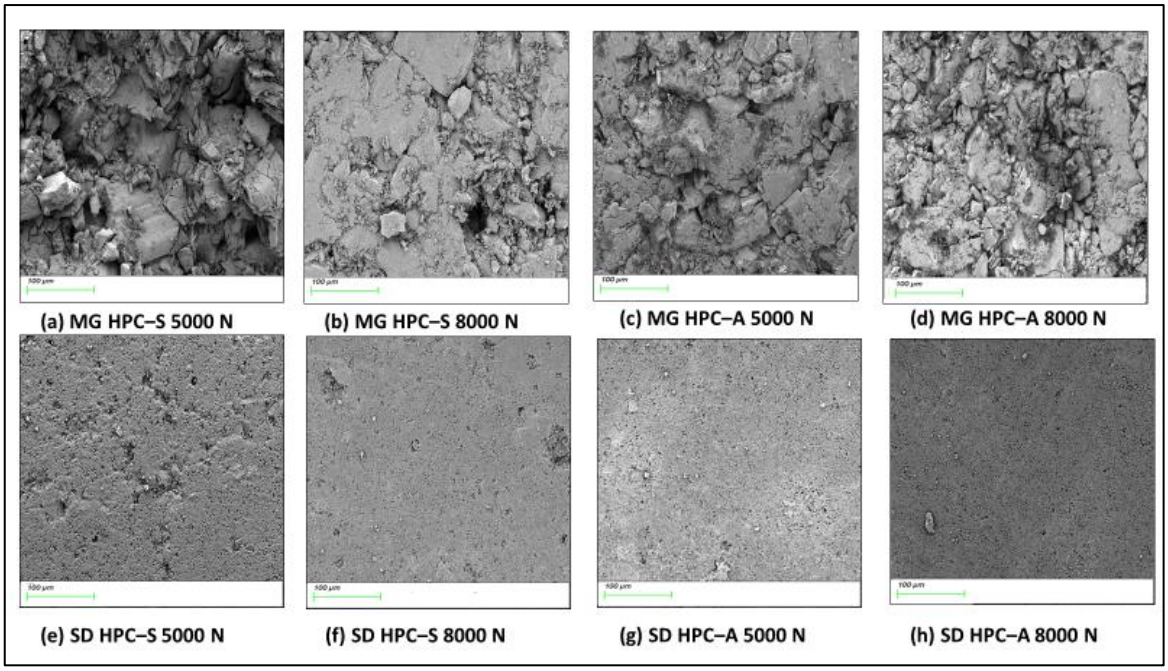


*Figure 4. 10: SEM micrographs of the surface of melt granulation (MG) and spray dried (SD) caplets, compressed at different compression forces (5000 N and 8000 N).*

### 4.2.5.2 Hardness measurements

The strength of manufactured caplets can be defined in terms of the compression force required to fracture a specimen across its diameter, which is commonly determined by conducting a hardness test (Fell and Newton 1970). The hardness of complex dosage forms, such as elongated caplets, may be determined using a crushing method, however, the breaking load does not take into consideration all dimensions and shape of such complex geometries. Thus, converting fracture loads to tensile strength, allows the determination of resistance to crushing while also taking into consideration the geometry of the tablets being tested (Pitt and Heasley 2013). Table 4.7 and table 4.8 show the measured dimensions of the MG and SD manufactured caplets compressed under different compression forces. The length of the short axis (D) and the length of the long axis (L) show no statistical differences ($p > 0.05$) regardless of the formulation or compression force used. However, for overall thickness (t) and tablet wall height (w), all SD formulations displayed larger dimensions when compared to the equivalent MG formulations compressed at the same force ($p < 0.05$). It has been shown previously in the literature that larger particles can display higher densification compared to finer particles due to easier packing (Al-Zoubi et al. 2017). In general, spray dried powders have larger bulk densities due to a smaller particle size and narrower particle size distribution when compared to other manufacturing methods. The larger size distribution of the MG formulations allows for smaller particles to fill in the interstices between the

coarser particles allowing for greater compaction when compression forces are applied. HPC has also previously been described as being a visco-elastic material (Picker-Freyer and Dürig 2007), SD formulations are therefore more likely to revert back to their larger bulk density in comparison to the MG formulations once the compression force is removed.

*Table 4. 7: Dimensions of melt granulation (MG) manufactured caplets post compression at different compression forces.*

| **Sample** | **MG HPC – S formulation** | | **MG HPC – A formulation** | |
|---|---|---|---|---|
| Compression force to form caplets (N) | 5000 | 8000 | 5000 | 8000 |
| L (mm) | 21.41 ± 0.02 | 21.44 ± 0.02 | 21.39 ± 0.02 | 21.43 ± 0.03 |
| D (mm) | 10.52 ± 0.02 | 10.51 ± 0.03 | 10.52 ± 0.02 | 10.52 ± 0.02 |
| t (mm) | 6.14 ± 0.02 | 5.93 ± 0.06 | 6.32 ± 0.01 | 6.03 ± 0.06 |
| w (mm) | 3.58 ± 0.08 | 3.23 ± 0.09 | 3.93 ± 0.01 | 3.59 ± 0.08 |

*Table 4. 8: Dimensions of spray dried (SD) manufactured caplets post compression at different compression forces.*

| **Sample** | **SD HPC – S formulation** | | **SD HPC – A formulation** | |
|---|---|---|---|---|
| Compression force to form caplets (N) | 5000 | 8000 | 5000 | 8000 |
| L (mm) | 21.46 ± 0.02 | 21.46 ± 0.01 | 21.39 ± 0.05 | 21.37 ± 0.03 |
| D (mm) | 10.53 ± 0.02 | 10.51 ± 0.01 | 10.49 ± 0.01 | 10.50 ± 0.02 |
| t (mm) | 6.99 ± 0.02 | 6.45 ± 0.06 | 6.81 ± 0.08 | 6.20 ± 0.03 |
| w (mm) | 4.40 ± 0.05 | 3.88 ± 0.04 | 4.31 ± 0.04 | 3.83 ± 0.04 |

In addition to the physical properties of the powders/granules during compaction discussed previously in relation to caplet geometry size, the molecular interactions that occur during processing play a major role in the final tablet hardness. Statistically, each

of the SD caplets have a significantly higher tablet hardness compared to the equivalent MG caplets ($p < 0.05$) due to their higher hydrogen bonding capabilities (table 4.9). During the SD process, all components of the formulations are in solution allowing for all components to interact with one another as the process is undertaken. As HPC-A is a higher Mw polymer and has increased hydroxypropyl binding sites compared to HPC-S, MET creates a higher degree of hydrogen bonding, resulting in increased tablet hardness when compressed at the same compression force. This corresponds well to the literature where it is reported an increase in intermolecular bonds, such as hydrogen bonding, can lead to an increase in tablet hardness (Wawer 2008). For MG caplets, we see the opposite results seen with the SD caplets, with the HPC-S formulations showing higher tablet hardness than the HPC-A formulations at the same compression forces. HPC-A has a higher Mw resulting in higher viscosity when molten during the MG process (Paradkar et al. 2009) reducing the exposure time MET has to potentially hydrogen bond with the hydroxypropyl binding sites when compared to the potential binding time MET has with the lower Mw (and hence lower viscosity) HPC-S. Although containing more potential sites to hydrogen bond than the HPC-S, the higher viscosity of HPC-A and the short process time prevent them from occurring.

*Table 4. 9: Results of the tablet hardness test for MG and SD formulations compressed into caplets at different compression forces. SD caplets manufactured with HPC-S compressed at 5000 N (n=6, t-value= -5.55, $p < 0.05$) and 8000 N (n=6, t-value= -9.01, $p < 0.05$) resulted in significantly harder tablets compared with the corresponding MG formulations. SD caplets manufactured with HPC-A compressed at 5000 N (n=6, t-value= -48.73, $p < 0.05$) and 8000 N (n=6, t-value= -21.18, $p < 0.05$) resulted in significantly harder tablets compared with the corresponding MG formulations.*

| **Sample** | **HPC-S formulation** | | **HPC-A formulation** | |
|---|---|---|---|---|
| Compression force to form caplets (N) | 5000 | 8000 | 5000 | 8000 |
| Tensile strength of Spray Dried products (MPa) | 0.35 ± 0.04 | 0.60 ± 0.04 | 0.67 ± 0.02 | 1.94 ± 0.19 |
| Tensile strength of Melt Granulation products (MPa) | 0.28 ± 0.03 | 0.44 ± 0.05 | 0.22 ± 0.01 | 0.31 ± 0.01 |

### 4.2.5.3 Friability studies

Friability is the tendency of a solid dosage from (e.g. caplet) to crumble, chip or break following compression, which could be caused by many factors such as: caplet design, insufficient excipients (e.g. binder) and low compression force during pressing. Caplets should be hard enough to withstand packaging and transport conditions, but also need to disintegrate in a reasonable time to allow for drug dissolution to occur (Chowhan 1979; Seitz and Flessland 1965). The European Pharmacopoeia sets the standard for friability testing, with a maximum loss of mass (obtained from a single test or from the mean of 3 tests) not greater than 1.0 % considered acceptable for most products(European Pharmacopoeia 2020b). Friability results for SD and MG caplets are shown in table 4.10. For SD caplets, SD HPC-S formulation, compressed at 5000 N, is the only formulation to fail the friability test, due to insufficient compression force being applied during manufacture. All other SD caplets passed friability testing. For MG caplets, MG HPC-S, compressed at 8000 N, is the only MG caplet formulation to pass friability. All other MG caplet formulations failed friability due to insufficient compression force being used during manufacture.

*Table 4. 10: Friability test results for SD and MG caplets compressed at different compression forces.*

| Sample | HPC-S formulation | | HPC-A formulation | |
|---|---|---|---|---|
| Compression force to form caplets (N) | 5000 | 8000 | 5000 | 8000 |
| Friability of Spray Dried caplets (%) | 96.30 % (Fail) | 99.21 % (Pass) | 99.82 % (Pass) | 99.90 % (Pass) |
| Friability of Melt Granulation caplets (%) | 91.96 % (Fail) | 99.25 % (Pass) | 65.53 % (Fail) | 81.08 % (Fail) |

### 4.2.5.4 Disintegration studies

Disintegration refers to the mechanical break up of a compressed tablet into small granules upon ingestion and therefore it is characterised by the breakdown of the interparticulate bonds, which were forged during the compaction of the tablet (Markl and Zeitler 2017). Oral solid dosage forms are required to break apart or disintegrate in a reasonable period of time when brought into contact with a liquid medium to allow for the APIs contained in the dosage forms to be released (Caramella et al. 1988; Quodbach

and Kleinebudde 2015). In addition to the solubility of components of the solid dosage form and the type of disintegration medium, it is well documented that the more compact the solid dosage form the more the time it needs to disintegrate, and hence very compressed caplets may show longer disintegration times (Caramella et al. 1988; Radwan et al. 2014). Table 4.11 shows disintegration times for each of the manufactured caplets compacted at different compression forces. For uncoated oral tablets with an immediate release profile, the European Pharmacopoeia states, tablets must be fully disintegrated within 15 min in order to comply with standards(European Pharmacopoeia 2020a). All MG caplets passed the disintegration test with caplets fully disintegrated within 15 min. MG HPC-A caplets disintegrated statistically quicker ($p < 0.05$) than the equivalent MG HPC-S due to differences in tablet hardness, tablet size, porosity and differences in intermolecular bonding as previously described. Each of these factors has previously been described as having an influence on the disintegration times of oral solid dosage forms (Markl and Zeitler 2017). All SD caplets failed the disintegration test with no caplets disintegrating fully within 15 min. No data is available for SD HPC-A caplets as the test was stopped after two hours with caplets not fully disintegrated. SD caplets, as previously described, have stronger intermolecular bonds between constituents, are less porous, more compact and are harder when compared to the MG equivalent caplets.

*Table 4. 11: Disintegration times of MG and SD caplets compressed at different compression forces. Disintegration test was conducted according to European Pharmacopoeia disintegration testing conditions* (European Pharmacopoeia 2020a) *SD caplets manufactured with HPC-S compressed at 5000 N (n=6, t-value= -77.14, p < 0.05) and 8000 N (n=6, t-value= -28.90, p < 0.05) resulted in significantly longer disintegration times compared with the corresponding MG formulations.*

| **Sample** | **HPC-S formulation** | | **HPC-A formulation** | |
|---|---|---|---|---|
| Compaction force to form caplets (N) | 5000 | 8000 | 5000 | 8000 |
| Disintegration of Spray Dried caplets (sec) | 1209 ± 14 | 1323 ± 32 | N/A | N/A |
| Disintegration of Melt Granulation caplets (sec) | 235 ± 35 | 748 ± 28 | 70 ± 12 | 257 ± 55 |

### 4.2.5.5 In-vitro dissolution studies

Dissolution studies were undertaken as per dissolution guidelines in the European Pharmacopoeia for MET oral tablets. No dissolution guidelines exist for the combination of MET and SIT in the European Pharmacopoeia so as MET was the majority constituent of the formulations, it was decided to follow European Pharmacopoeia guidelines for MET oral tablets. Figure 4.11 and figure 4.12 show the release profiles for MET and SIT from MG caplets and SD caplets respectively. Janumet® is also include in both figures as the reference product. All MG caplets fully release both MET and SIT within 10 min and 5 min respectively (figure 4.11). All SD HPC-S caplets release > 85 % MET and SIT after 30 min and SD HPC-A caplets failed to fully release 100 % MET and SIT within the two-hour dissolution test timeline. Interestingly, the compression force applied to manufactured caplets had no influence on rate of release of both drugs.

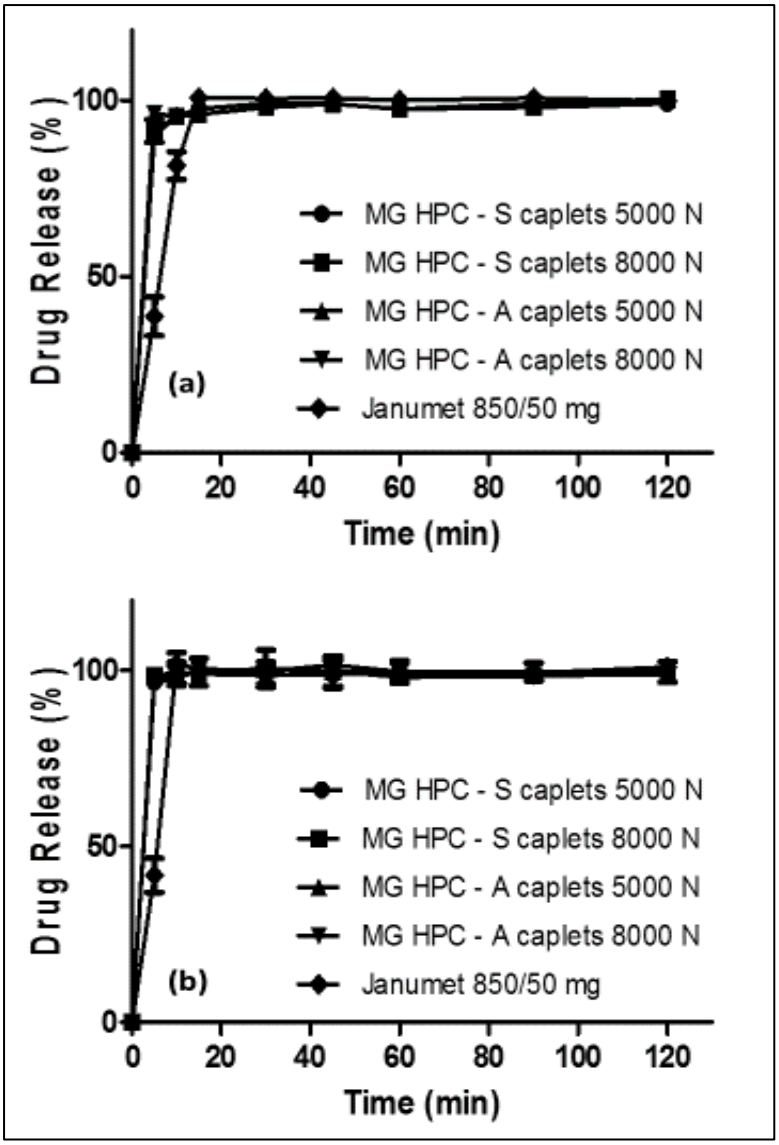


*Figure 4. 11: Dissolution of melt granulation (MG) caplets in pH 6.8 using EP type 1 basket apparatus at 100 rpm showing (a) MET release profile and (b) SIT release profile.*

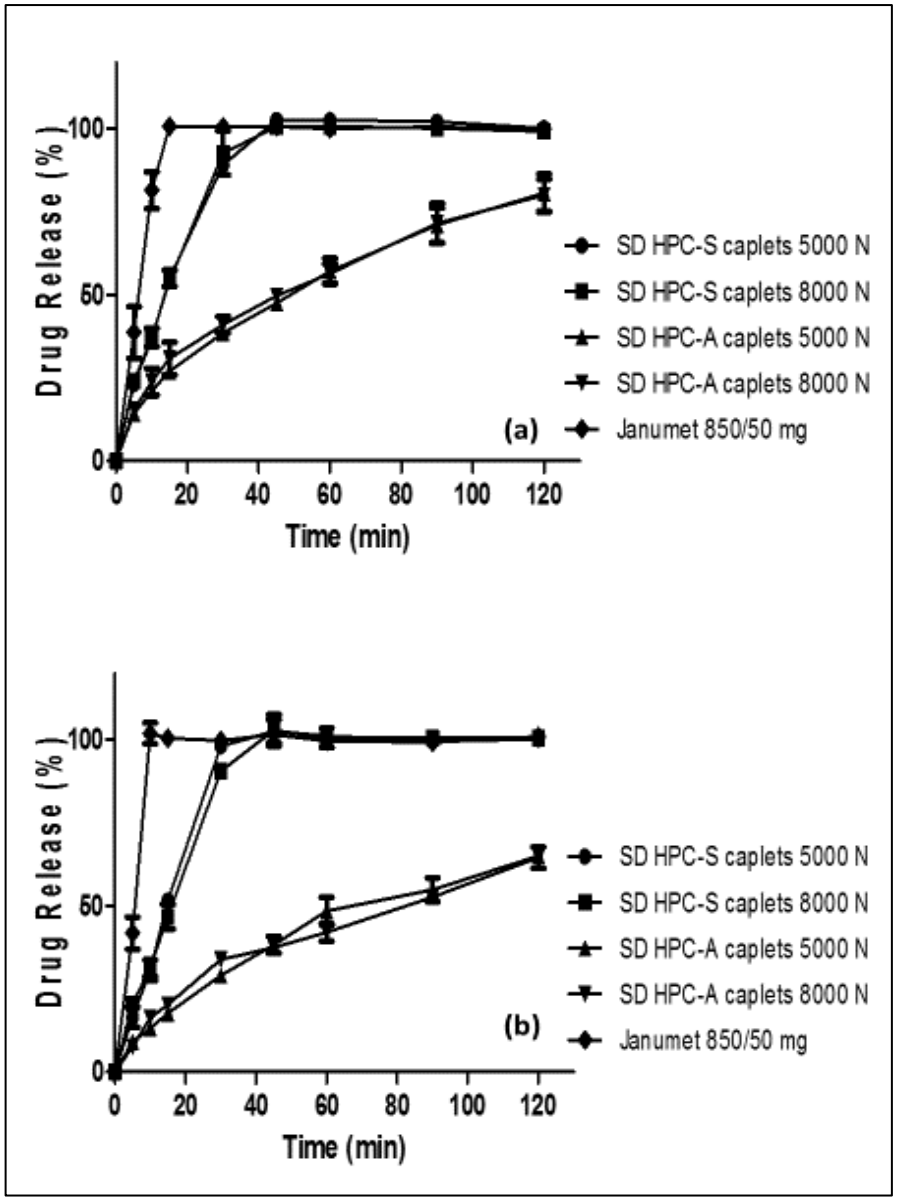


*Figure 4. 12: Dissolution of spray dried (SD) caplets in pH 6.8 using EP type 1 basket apparatus at 100 rpm showing (a) MET release profile and (b) SIT release profile.*

## 4.3 Conclusions

The continuous manufacturing of FDC products is beneficial in pharmaceutical manufacturing, where there has been increased interest in recent years in moving away from batch-based processes due to their limitations. Both MG and SD techniques can be used in the continuous manufacturing of monolithic FDC products. Both techniques were employed in this study to produce large dose immediate release formulations of FDC products for the treatment of type II diabetes. While both techniques can be used, only the MG HPC-S formulation compressed at 8000 N passed all the common compendial tests for immediate release oral tablets. The two selected HPC polymers chosen, varied in molecular weight and degree of hydroxypropoxy substitution which lead to differences in caplet characteristics irrespective of manufacturing technique. The current work highlights how manufacturing method, polymer composition and subsequent compression forces significantly impact caplet characteristics. MG may be a more suitable manufacturing technique for high dose combination products, when compared to SD, due to being more environmentally friendly (due to no solvents being used), products having better flow characteristics and when suitably compressed, pass all common compendial tests for immediate release formulations.

Additionally, as MET is indicated for treatment in type II diabetes in combination with several other APIs, further work could be done to assess the suitability of MG to produce FDC products of MET and other APIs.

# Chapter 5:

# Manufacture of a fixed dose combination product of simvastatin, hydrochlorothiazide and ramipril using hot melt extrusion, spheronisation and spray coating for the management of cardiovascular disease

## 5.1 Introduction

Cardiovascular diseases (CVDs) are the leading cause of morbidity and mortality worldwide according to the World Health Organization (WHO) (World Health Organization 2017a). Hyperlipidemia and hypertension are two of the major risk factors associated with CVDs. Diabetic patients in particular, have an increased risk of developing CVDs from these factors and are in general recommended to take medication for primary and secondary prevention of both conditions (National Institute for Clinical Excellence 2016). Previous studies have shown the benefit of targeting both conditions with a fixed dose combination (FDC) product that can be administered once daily (Kim et al. 2016; Kirchhoff et al. 2008).

Simvastatin (SIM) is a 3-hydroxy-3-methylglutaryl coenzyme A (HMG-Co-A) reductase inhibitor used in the treatment of hyperlipidemia. SIM is considered a Biopharmaceutical Classification System (BCS) class II drug due to its poor solubility in gastrointestinal fluids (Ambike et al. 2005; Kang et al. 2004). Being a BCS Class II drug, SIM often shows dissolution rate-limited oral absorption and high variability in pharmacological effects. Therefore, enhancing the solubility of SIM using enabling technologies represents an exciting means of improving the pharmacokinetics and hence bioavailability of this drug (Andrews et al., 2019).

SIM is available on the market as a prodrug in the lactone form (Zocor®) and can be converted to the active β-hydroxy acid form in the gastrointestinal tract or in the liver by hydrolysis (Medicines and Healthcare products Regulatory Agency 2019b). As well as being poorly soluble, SIM (in both the lactone and β-hydroxy acid form) is rapidly cleared by enzymatic oxidation carried out by cytochrome P450 3A (CYP3A) enzymes. The availability of the active β-hydroxy acid to the systemic circulation following an oral dose of SIM was found to be less than 5% of the dose administered, consistent with extensive hepatic first-pass extraction (Medicines and Healthcare products Regulatory Agency 2019b). As well as residing in the liver, CYP3A enzymes are contained in enterocytes, which are located mainly in the villi tips of the small intestine. Moreover, the concentration of CYP3A enzymes in the gut varies significantly, with higher levels in the jejunum, slightly decreased levels in the duodenum, and significantly decreased levels in the ileum, cecum, and colon. By protecting the drug from the hostile environment of the upper gastrointestinal tract, it is hypothesized that SIM therapeutic activity can be enhanced while also reducing adverse events associated with SIM such as muscular myopathy or rhabdomyolysis (Tubic-Grozdanis et al. 2008).

Hydrochlorothiazide (HCTZ), a thiazide diuretic, and ramipril (RAM), an angiotensin converting enzyme (ACE) inhibitor, are both recommended for the treatment of hypertension (World Health Organization 2016). FDC products containing RAM and HCTZ have been previously shown to induce a significantly greater reduction in blood pressure than with individual monotherapies of the two APIs at the same dosages (Scholze et al. 1993). Both APIs are manufactured as immediate release formulations.

Hot melt extrusion (HME) is one of the most common processing techniques used in the continuous manufacture of solid dispersions (Agrawal et al. 2016). Previous studies have shown that SIM can be converted to its amorphous form, increasing its solubility, via HME (Javeer et al. 2013) and hot melt co-extrusion (HMCE) may be used to manufacture formulations of amorphous SIM to target specific sites of the gastrointestinal tract (Andrews et al. 2019). HMCE is associated with several challenges which can make formulating a successful FDC difficult via this technique. Layer nonuniformity is a problem in polymer co-extrusion and can be caused by many process factors such as different melt temperatures between layers, variation in pressure and varying velocities of the different layers. Careful selection of polymers is essential for overcoming these issues as incorrect velocity matches can result in encapsulation rather than layering (Vynckier, Dierickx, Voorspoels, et al. 2014). Layer adhesion is another difficulty that is commonly encountered during formulation development. Adequate adhesion between the layers is essential to avoid separation during downstream processing. Adhesion is defined as the tendency of dissimilar particles or surfaces to cling to one another or as the molecular attraction that holds the surfaces of two dissimilar substances together. If adhesion does not occur between the layers, then separation occurs. Other considerations include miscibility of the layers, delamination of individual layers and influence of die design, all of which can lead to product failure (Vynckier, Dierickx, Voorspoels, et al. 2014).

An alternative approach to the challenging technology of HMCE is to spray coat a core formulation of one API with a coating comprising a second or multiple other APIs. Spray coating using the Wurster method is undertaken in a fluidised bed dryer (FBD) and uses differential airflow to create a cyclic movement of material to be coated. The location of the spray nozzle at the bottom of the fluidized bed of particles is what sets the Wurster process apart from other coating methods. Differential air streams move the bed of materials upward in a cyclic motion inside the chamber as it is coated with an atomised material to create a core-shell structure. This configuration ensures that the coating material can be applied efficiently to individual particles while controlling for agglomeration. The process can be continued until the desired uniform film thickness

and dosages are achieved through depositing one or more layers to the core material. No matter the shape of the core material, the Wurster process is capable of creating a unique formulation to achieve the desired properties of the coating material.

In this study, HME was used to produce a delayed/extended release formulation of SIM followed by heat aided spheronisation to produce spherical pellets. These spherical pellets were then spray coated using a FBD with an immediate release formulation containing HCTZ and RAM to manufacture a final FDC product to treat CVD.

## 5.2 Results and discussion

### 5.2.1 Simvastatin core manufacture

During the initial developmental stages of the SIM core material several polymers were selected based on their characteristic release profiles. These polymers included ethyl cellulose, microcrystalline cellulose, hydroxypropyl methylcellulose and low substituted hydroxypropyl cellulose. While successfully extruding products that contained an amorphous form of SIM, these polymers proved too brittle to manufacture into spherical pellets, while also failing to deliver the desired delayed release profile. As a result, these polymers were excluded from further investigation in this study. Along with our colleagues in Queen's University Belfast (who were, in tandem, developing a co-extrudate formulation), a suitable SIM core formulation was selected and processed by HME, followed by spheronisation to produce a product with the desired physical characteristics and release profiles. Tables 2.3 and 2.4, chapter 2 outline the final formulation of the core material and the conditions used in the extruder, respectively.

As the ultimate goal of formulating SIM was to delay its release until it reaches the small intestine, polymer selection is critical. Table 5.1 highlights the pH threshold and targeted gastrointestinal tract (GIT) site of delivery for the polymers used in the optimized formulation.

*Table 5.1: pH threshold and targeted site of GIT release for polymers used in optimised formulation* (Friesen et al. 2008; Patra et al. 2017).

| Polymer | pH threshold for dissolution | Targeted site for GIT delivery |
|---|---|---|
| HPMCAS-MF | 6 | Jejunum |
| Eudragit L100 | 6 | Jejunum |
| Eudragit 100-55 | 5.5 | Duodenum |

Thermal degradation points of the API and the formulation excipient polymers are important to determine due to the HME process that is used to produce the core material. Figure 5.1 shows the thermal degradation points of SIM and the polymers used in the formulation (as determined using the method described in chapter 2, section 2.3.1).

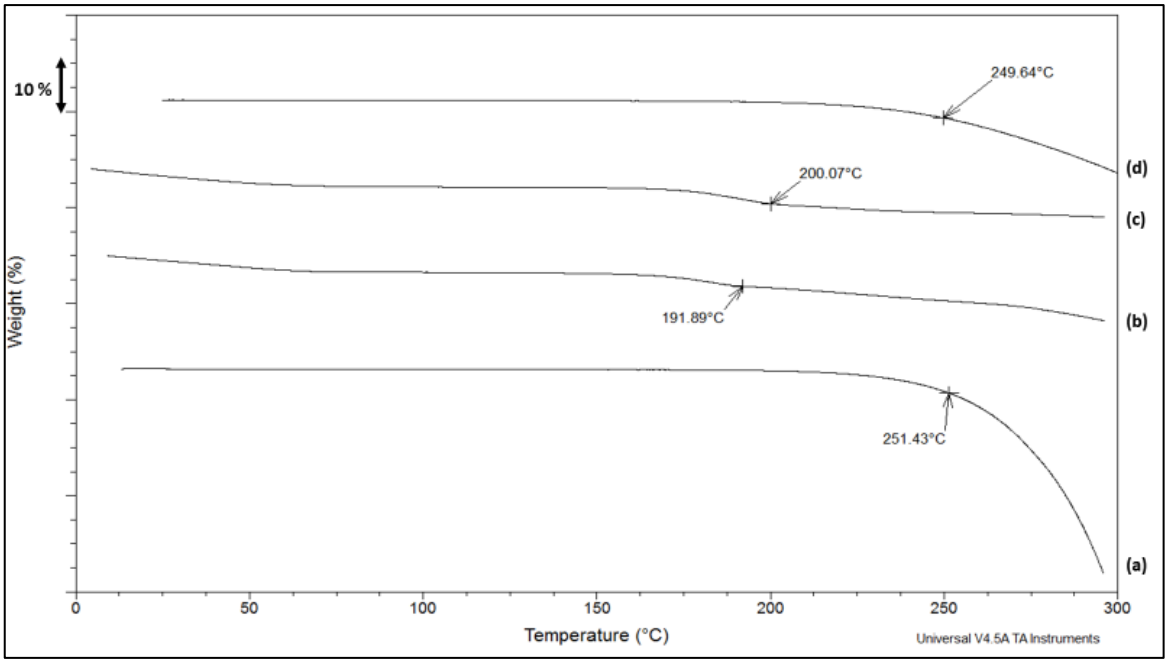


*Figure 5. 1: TGA thermogram of SIM and polymers used in optimised formulation. Heating ramp from 20 °C to 300 °C at 10 °C/ min, showing, (a) SIM thermal degradation at ~251 °C, (b) Eudragit L100-55 thermal degradation at ~192 °C, (c) Eudragit L100 thermal degradation at ~200 °C and (d) HPMCAS MF thermal degradation at ~250 °C.*

Triethyl citrate (TEC) was added to the formulation as a plasticiser to increase the processability of the formulation extrudates. TEC also offers the advantage of increasing the flexibility of the extrudates, enabling them to be spheronised once extrudates are cut into pellets. TEC has previously shown to be compatible with HPMCAS (Siepmann et al. 2006) and Eudragit (Qiao et al. 2013) polymers as a plasticiser, and so is suitable for the proposed blend of polymers in the optimized formulation.

The incorporation of d-α-tocopheryl polyethylene glycol 1000 succinate (TPGS), a water-soluble vitamin E derivative, plays several important roles in the formulation; it prevents the oxidation reaction of the carboxylic acid groups in HPMCAS-MF during extrusion by entrapping compounds which are prone to oxidation (Cagno et al. 2012) and, owing to the amphiphilic nature of the compound which allows it to solubilize poorly water soluble drug compounds (Moneghini et al. 2010; Soon Ahn et al. 2011), it was found that the release of SIM was significantly improved when compared to those formulations without TPGS. TPGS is also a P-glycoprotein inhibitor, which may allow greater amounts of SIM to enter the systemic circulation (Guo et al. 2013; Holtzman et al. 2006) reducing the dose required to achieve the desired therapeutic outcomes.

The PXRD diffractograms of the raw materials are shown in figure 5.2. SIM raw material is a crystalline API as can be seen by characteristic Bragg peaks at 9.40° (2θ), 15.65° (2θ), 17.35° (2θ) and 22.65° (2θ), which are consistent with the literature (Jun et al. 2007; Rao et al. 2010). Eudragit L-100, Eudragit L-100 55 and HPMCAS MF are amorphous polymers with characteristic PXRD amorphous "halos". TPGS is a waxy crystalline material with 2 clear Bragg peaks at 19.20° (2θ) and 23.40° (2θ), consistent with the literature (Gao et al. 2010). TEC is not represented in the PXRD figures as it is in a liquid state at room temperature.

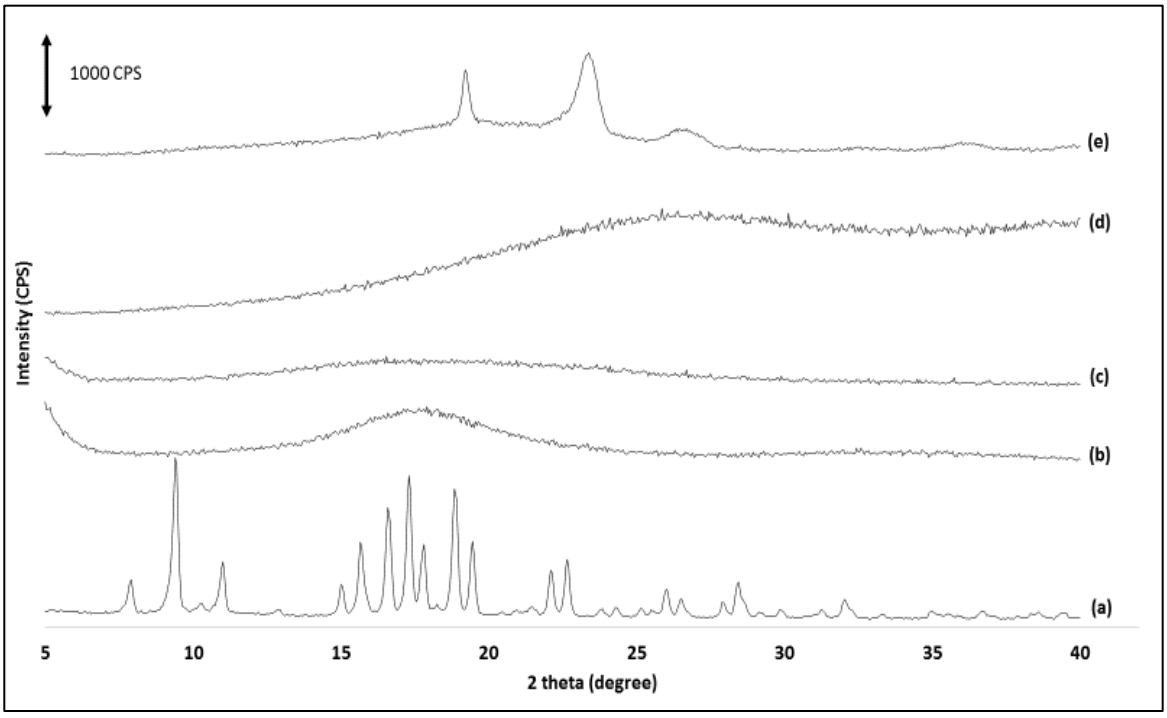


*Figure 5. 2: PXRD over the range of 5–40° 2θ of (a) SIM, (b) Eudragit L-100 55, (c) Eudragit L-100 (d) HPMCAS MF and (e) TPGS*

Standard DSC runs (undertaken as detailed in chapter 2, section 2.3.2) were completed on raw materials and results are shown in figure 5.3. The three amorphous polymers, namely Eudragit L-100 55, Eudragit L-100 and HPMCAS MF, display $T_g$s at 124.79 ± 3.31 °C, 110.66 ± 1.53 °C and 123.38 ± 2.34 °C respectively. TPGS displays a melting point at 34.79 ± 0.34 °C and SIM displays a melting point at 140.34 ± 1.56 °C, both consistent with previously published literature, while also confirming the crystalline solid state of the API raw material, consistent with the PXRD data described above.

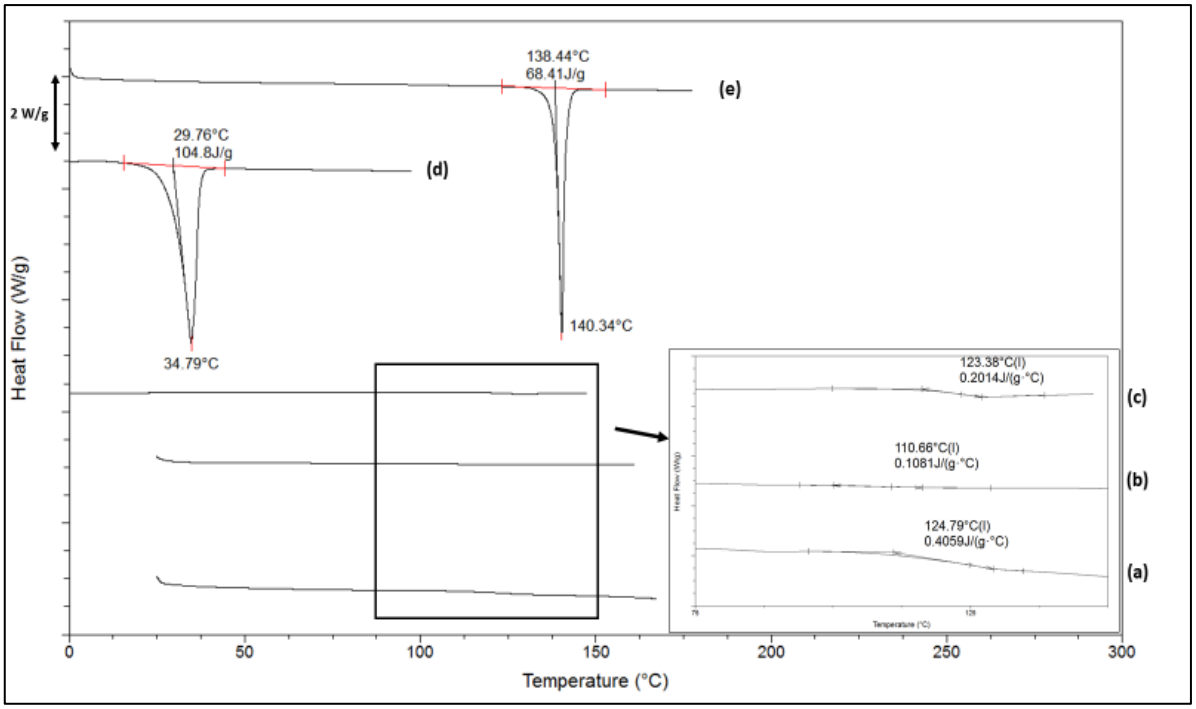


*Figure 5. 3: DSC thermogram of API raw material and excipients with a heating rate of 10 °C/min showing, (a)Eudragit L100-55, (b) Eudragit L100, (c) HPMCAS MF, (d) TPGS and (e) SIM*

As the temperature of the processing conditions for the optimized formulation described in table 5.2 go above the melting point of SIM, intermolecular interactions between SIM and the other excipients are expected to be critical to forming a stable amorphous solid dispersion when SIM solidifies following melting and subsequent cooling, as is the inherent glass stability of SIM.

Figure 5.4 (a) shows the PXRD of the physical mixture of the optimized formulation constituents, with Bragg peaks clearly evident for the crystalline SIM raw material at 9.40° (2θ), 15.65° (2θ), 17.35° (2θ) and 22.65° (2θ). Figure 5.4 (b) shows the amorphous PXRD of the optimized formulation post extrusion (as described in chapter 2, section 2.3.4).

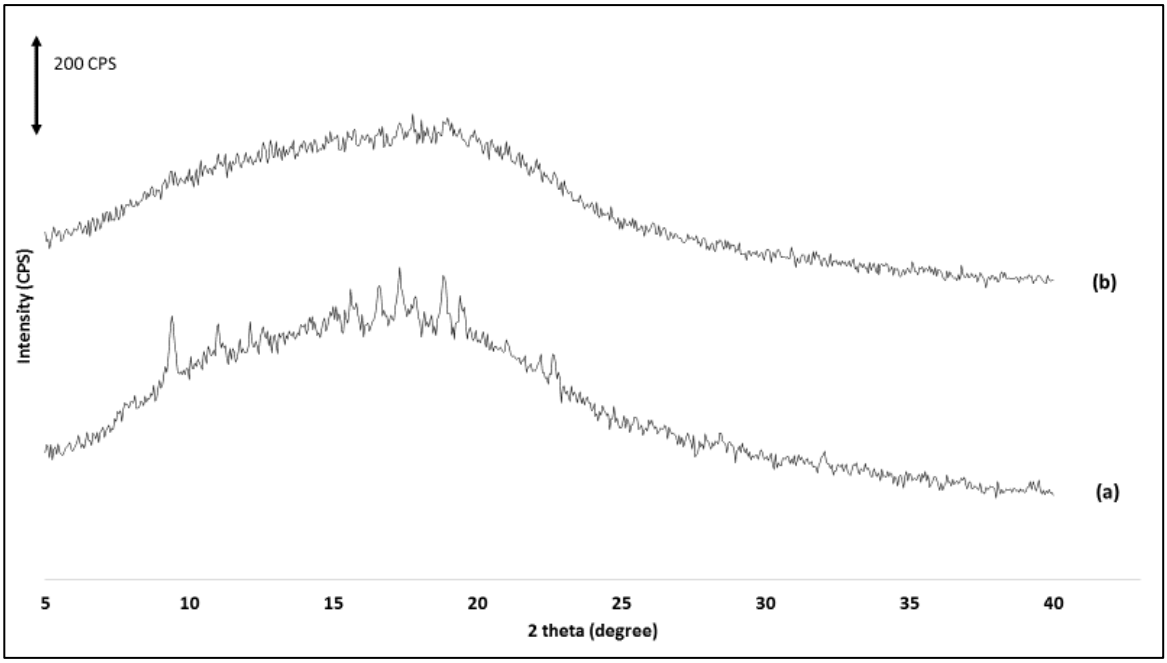


*Figure 5. 4: PXRD over the range of 5–40° 2θ of (a) physical mixture of optimized formulation and (b) extrudate of optimized formulation post hot melt extrusion.*

While PXRD can confirm if a sample is amorphous, it cannot confirm if the formulation is fully miscible or if phase separation has occurred within the amorphous material. To confirm miscibility, DSC scans (as described in chapter 2, section 2.3.2) were obtained for both the optimized formulation physical mixture and the optimised formulation extrudate, post HME. Figure 5.5 (a) shows the standard DSC results for the physical mixture of the optimised formulation. Melting endotherms can be seen for both the TPGS and SIM constituents at 36.42 ± 0.65 °C and 136.87 ± 1.05 °C, respectively. Figure 5.5 (b) represents the thermogram for the optimised formulation extrudate. A single $T_g$ at 54.75 ± 1.41 °C is evident, which is an intermediate temperature between that of amorphous SIM ($T_g$ of 32.44 ± 0.68 °C, see Appendix 2) and the other excipient constituents, indicative of miscible single-phase amorphous system.

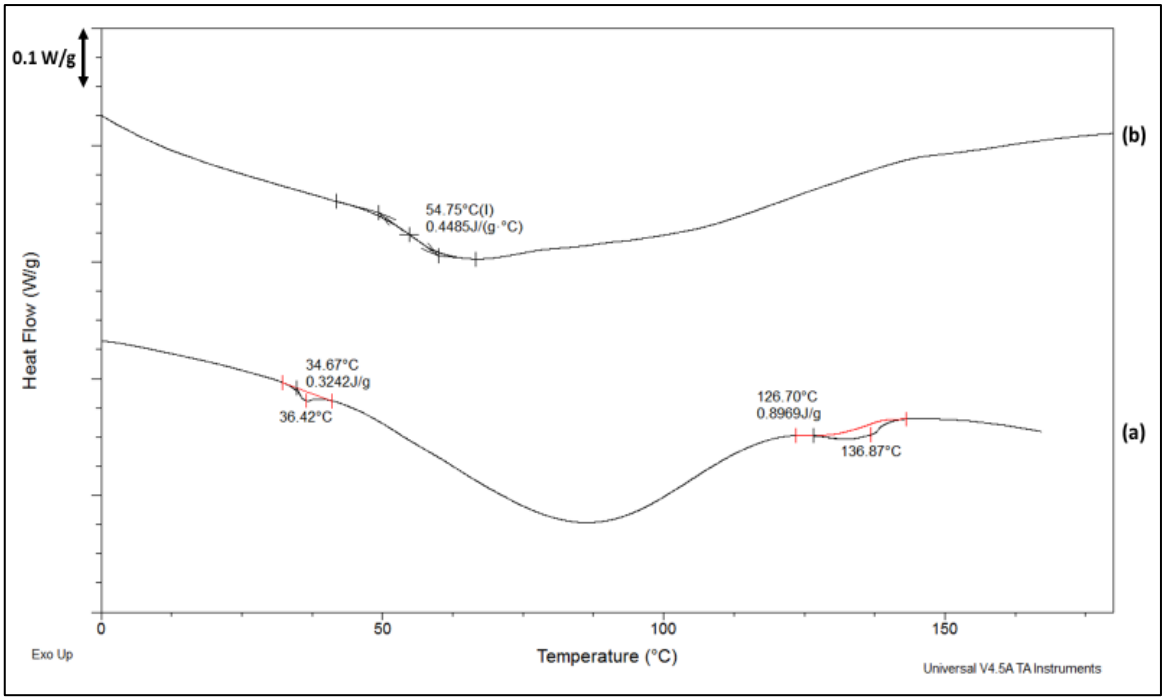


*Figure 5. 5: DSC thermogram with a heating rate of 10 °C/min showing (a) physical mixture of optimised formulation and (b) optimized formulation extrudate.*

Once the extrusion was completed, the next part of the processing was to spheronise the pellets that were collected by cutting the extrudate (as described in chapter 2, section 2.2.2.2). Figure 5.6 shows the results of the spherisation process.

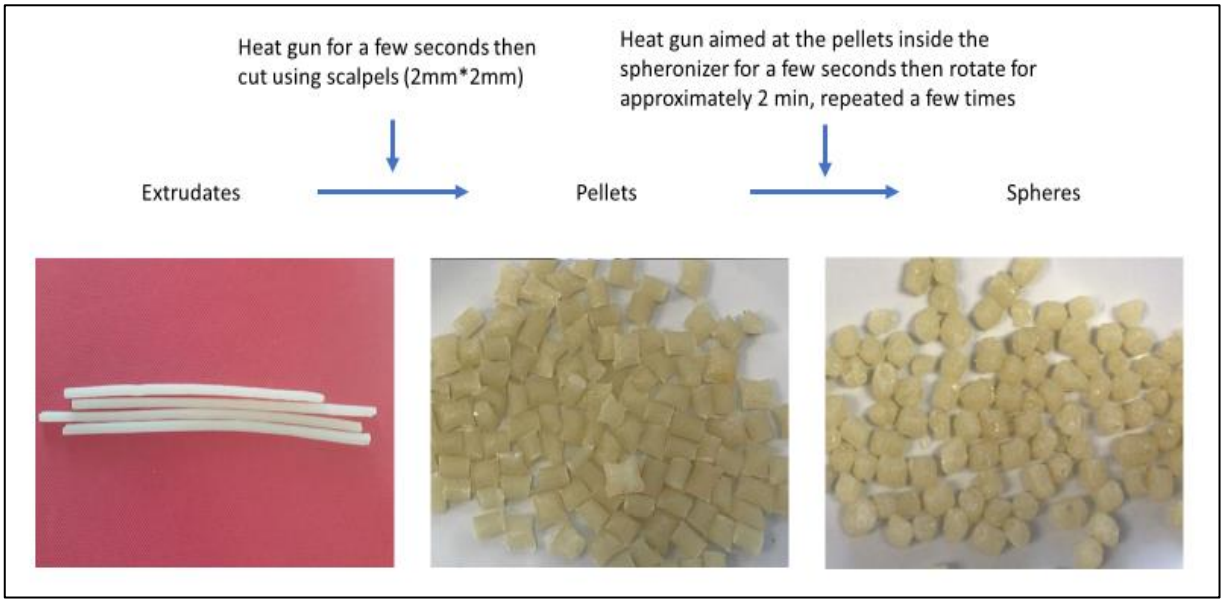


*Figure 5. 6: Photographs of the optimised formulation extrudates following extrusion. The extrudates are cut into 2 mm x 2 mm pellets before being spheronised while heat is applied from a heat gun. The spheres seen on the right are the final core materials to be transferred for coating.*

### 5.2.2 Hydrochlorothiazide and ramipril coating of simvastatin cores

Once SIM core spherical pellets had been successfully manufactured, the next step in the process was to use a FBD to add an additional layer, comprising HCTZ and RAM, to create the final FDC product. Immediate release of HCTZ and RAM is required, in contrast to the delayed release profile required for SIM. Kollidon® VA 64 (PVP vinyl acetate) (Dangel et al. 2000), Metolose® (HPMC and Methylcellulose) (Marek et al. 2007) and Pharmacoat 603 (HPMC) (Perfetti et al. 2012) were the polymers chosen initially for spray coating in conjunction with HCTZ and RAM. These three polymeric excipients were chosen due to their immediate release profiles, film forming abilities and because they are among the most commonly used polymers for spray coating (Bharadia and Pandya 2014). Due to the amount of time required to manufacture the core material, preliminary studies were conducted on MCC beads as a surrogate for the SIM cores, as described in chapter 2, section 2.2.4.1. The concentration of formulations (% w/v), solvent composition, inlet temperature and pump rate were varied and trialed until a suitable coating method was established.

Polymers were spray coated at different concentrations, with the ratio of HCTZ to RAM remaining constant at 2.5:1, onto MCC beads. Kollidon® VA 64 and Metolose® containing formulations were unsuccessful as they caused MCC beads to agglomerate at the various concentrations trialed (figure 5.7). Formulations containing Pharmacoat 603 proved successful, and this polymer was chosen as the main polymer for spray coating going forward.

Pharmacoat 603 has many of the desired coating polymer properties: it forms a transparent, tough and flexible film that protects fragile tablets/cores, masks the unpleasant taste of drug and improves the appearance, tolerates the presence of colorants and other additives and is resistant to abrasion. Pharmacoat 603 is stable in the presence of heat, light, air and moisture in room conditions, although it is moderately hygroscopic, so it is a good candidate to use for spray coating (Nagai et al. 1997).

*Figure 5. 7: Images highlighting the agglomeration of MCC beads during preliminary coating studies undertaken with Kollidon® VA 64 and Metolose® in the Mini-Glatt fluidized bed dryer.*

Figure 5.8 shows the PXRD for the raw materials used in the spray coating formulations. For crystalline materials, characteristic Bragg peaks can be seen in PXRD diffractograms. HCTZ shows characteristic peaks at 16.65° (2θ), 18.75° (2θ), 21.40° (2θ) and 24.65° (2θ), which is consistent with the published literature (De Jaeghere et al. 2015; Panneerselvam et al. 2010). RAM also shows characteristic diffraction peaks at 7.60° (2θ), 8.05° (2θ), 19.30° (2θ) and 21.25° (2θ), consistent with the published literature (Jagdale et al. 2013; Madhavi et al. 2016). Pharmacoat 603 is an amorphous polymer and displays the characteristic “halo” associated with amorphous materials. As Pharmacoat 603 is a cellulose derived polymer, it contains low amounts of crystalline material (Picker-Freyer and Dürig 2007), however, PXRD is not sensitive enough to pick up Bragg peaks associated with it, and, as a result, it appears PXRD amorphous.

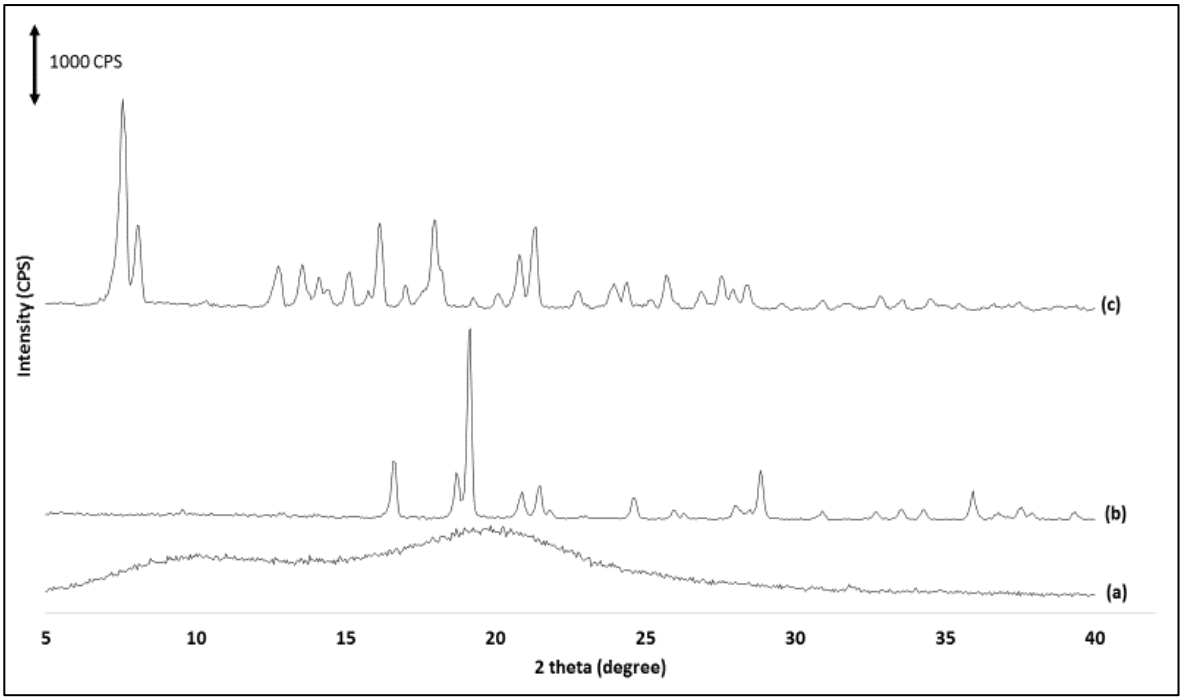


*Figure 5. 8: PXRD over the range of 5–40° 2θ of (a) Pharmacoat 603, (b) HTCZ and (c) RAM.*

Figure 5.9 shows DSC thermograms of the raw materials used in the optimized spray coating formulation. Both HCTZ and RAM displayed sharp melting endotherms at 271.99 ± 2.67 °C and 115.99 ± 1.12 °C, respectively, while Pharmacoat 603 exhibited a $T_g$ at 97.14 ± 0.98 °C for the amorphous component of the polymer and a melt endotherm at 205.95 ± 2.01 °C for the crystalline content of the polymer. As Pharmacoat 603 is a cellulose derived polymer, it contains low amounts of crystalline material as well as the amorphous content (Picker-Freyer and Dürig 2007). The crystalline content is highlighted by the melting endotherm at 205.95 ± 2.01 °C.

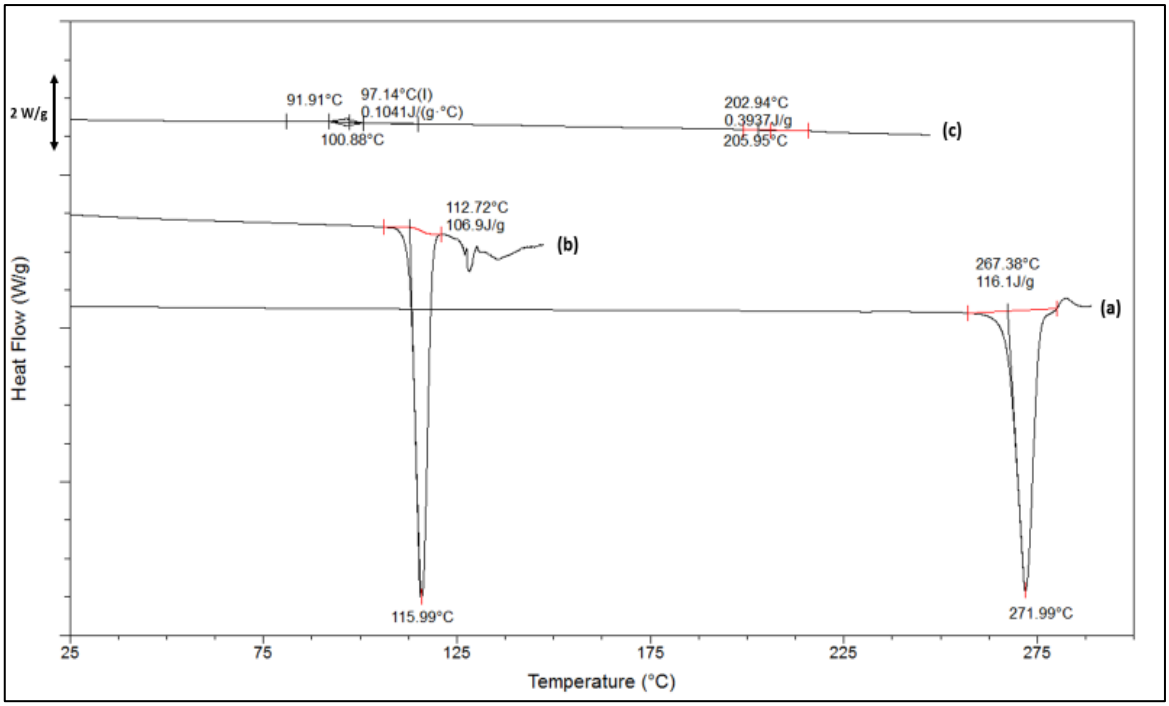


*Figure 5. 9: DSC thermogram with a heating rate of 10 °C/min showing (a) HCTZ, (b) RAM and (c) Pharmacoat 603*

In the process of spray coating using the Wurster method, a certain amount of the intended spray coating material is invariably lost to the filters during the process (figure 5.10). With larger batch sizes to be spray coated, this is usually not a major issue, as the loss of product is minimal due to the efficiency of the coating process and the large batch size to be coated. However, as we are dealing with smaller batch sizes, larger amounts of material are lost (percentagewise), requiring larger initial amounts of coating material to achieve the desired API concentrations in the final product.

*Figure 5. 10: Filters of the Mini-Glatt fluidized bed dryer before (left) and after (right) spray coating, highlighting material lost to the filters during the process due to small batch sizes.*

The final solvent mixture chosen for the formulations to be dissolved in was a 50:50 mixture of methanol and water. Other solvent/solvent mixtures trialled included various ratios of ethanol : water, ethanol alone, methanol alone and water alone. However, these solvents proved unsuccessful due to solubility issues and clumping of the material to be coated. Once the final solvent was selected, the various mixtures were then spray coated onto MCC beads as described in chapter 2 section 2.2.4.1. Table 5.2 gives the formulation concentrations in the preliminary studies carried out, with table 5.3 giving the final concentrations of the theoretical maximum of APIs on MCC beads. Figure 5.11 gives a visual representation of the final preliminary study products (based on MCC beads).

*Table 5.2: Formulations used in preliminary studies of spray coating of MCC beads with Pharmacoat 603 polymer, HCTZ and RAM.*

| | | **Dissolved in 100 ml water** | **Dissolved in 100 ml methanol** | | |
|---|---|---|---|---|---|
| **Formulation** | **MCC 1 mm beads (g)** | **Pharmacoat 603 (mg)** | **HCTZ (mg)** | **RAM (mg)** | **Amaranth solution (drops)** |
| **1** | 4.4 | 150 | 250 | 100 | 2 |
| **2** | 4.4 | 350 | 250 | 100 | 2 |
| **3** | 4.4 | 650 | 250 | 100 | 2 |

By increasing the Pharmacoat 603 content in the formulations, there was a statistically significant increase in the amount of API retained on the MCC beads as shown in table 5.3.

*Table 5.3: % of theoretical max of HCTZ and RAM on MCC beads post spray coating.*

| **Formulation** | **HCTZ recovery (%)** | **RAM (%)** |
|---|---|---|
| **1** | 73.70 ± 1.23 | 73.89 ± 1.14 |
| **2** | 75.75 ± 0.98 | 74.00 ± 1.23 |
| **3** | 79.09 ± 1.64 | 78.19 ± 0.98 |

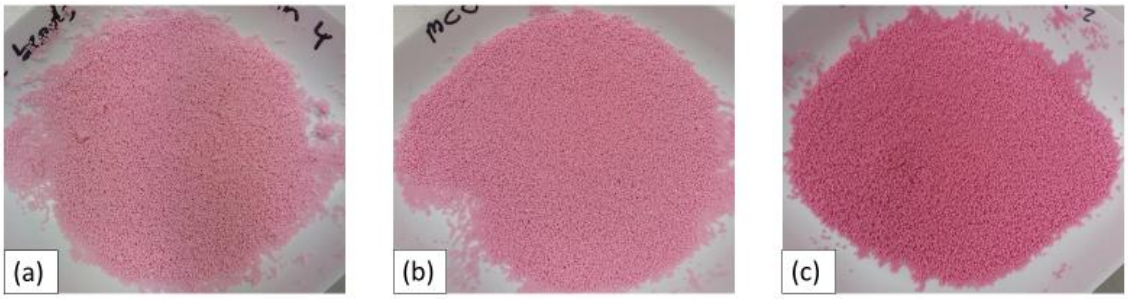


*Figure 5. 11: MCC beads coated with (a) Pharmacoat 603; HCTZ; RAM in ratio 1.5; 2.5;1, (b) Pharmacoat 603; HCTZ; RAM in ratio 3.5;2.5;1 and (c) Pharmacoat 603; HCTZ; RAM in ratio 6.5; 2.5;1.*

Film formation from the polymer/API solution occurs through a series of phases. When the polymer/API solution hits the surface of the MCC beads, cohesion forces from a bond between the coating polymer/API molecules on the surface of the MCC beads. To obtain high cohesion, the cohesive strength of polymer/API molecules must be relatively high, and the surface of the film material must coalesce. Coalescence of adjacent polymer/API molecular layer or surfaces occurs through diffusion. When the majority of the solvent evaporates, the viscosity of the solution increases and leaves the polymer chains in close proximity to each other and deposited over a previous polymer layer (Ghebre-Sellassie et al. 1987). If there is adequate cohesive attraction between the molecules and sufficient diffusion and coalescence upon the more complete evaporation of the residual solvent, the individual polymer chains align themselves to form a cohesive film. As Pharmacoat 603 concentrations increase, the viscosity of the initial solution increases, which in turn increases the film forming properties of the polymer/API mixture due to greater coalescence of mixture upon evaporation of the solvent on the surface of the MCC beads (Bharadia and Pandya 2014).

Once the preliminary studies were completed with MCC beads, the formulation of Pharmacoat 603; HCTZ; RAM in the ratio 6.5:2.5:1 was carried forward to be used in coating the spherical core pellets manufactured via HME, pelletisation and spheronisation. Figure 5.12 (a) shows the PXRD of the physical mixture of the formulation constituents, with diffraction peaks at 7.60° (2θ) and 8.05° (2θ) evident for RAM, and diffraction peaks at 16.65°(2θ) and 18.75°(2θ) evident for HCTZ.

Samples of the spray coating formulation were obtained from the FBD chamber post spray coating and analysed to test for the final solid state of the spray coated material. Due to the difficult nature of removing the spray coated layer from the final FDC formulation, it was thought the spray coated material collected from the chamber would

give an accurate representation of the coated layers solid state characteristics. Figure 5.12 (b) shows the PXRD of the spray coating formulation, and it is completely PXRD amorphous with no diffraction peaks evident for either of the APIs that are seen in the physical mixture.

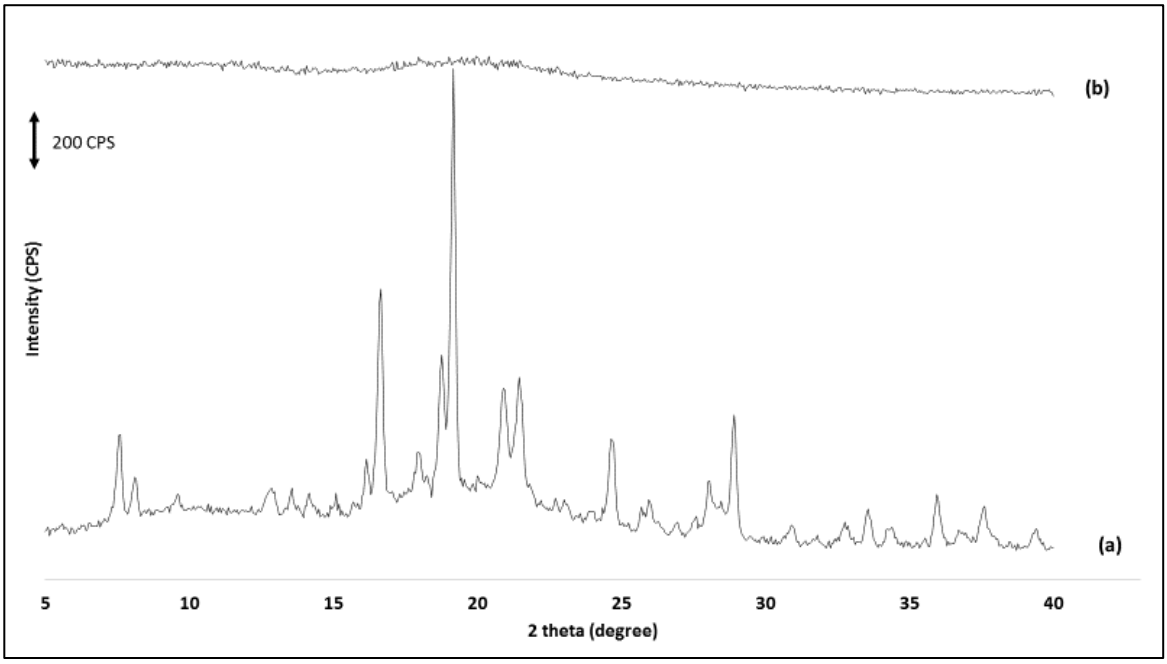


*Figure 5. 12: PXRD over the range of 5–40° 2θ of (a) physical mixture of Pharmacoat 603, HCTZ and RAM in the ratio of 6.5: 2.5: 1 (b) spray coating of optimised formulation.*

To confirm the amorphous state of the spray coating formulation, DSC was conducted as described in chapter 2, section 2.3.2. Figure 5.13 (a) shows the DSC thermogram for the physical mixture of the spray coating formulation constituents, with a melting point at 113 ± 1.20 °C attributed to RAM. The DSC was stopped at 250 °C so as to avoid contamination of the DSC furnace, as the signal started to become distorted due to degradation of the mixture. As a result, the melting point of the crystalline HCTZ cannot be seen in the thermogram for this formulation. The amorphous nature of the spray coated formulation can be confirmed by the lack of the melting endotherm, which was seen in the physical mixture at 113 ± 1.20 °C, and the presence of a single $T_g$ at 102 ± 1.32 °C. As is the case with the physical mixture, the spray coated formulation DSC thermogram was stopped at 250 °C due to the signal become distorted. As the $T_g$ at 102 ± 1.32 °C is an intermediate temperature between the $T_g$s of the amorphous phases of HCTZ ($T_g$ of 114 °C, Appendix 2), RAM ($T_g$ of 3 °C, Appendix 2) and Pharmacoat 603 ($T_g$ of 97 °C), the DSC of the spray coated formulation is indicative of a fully amorphous miscible system.

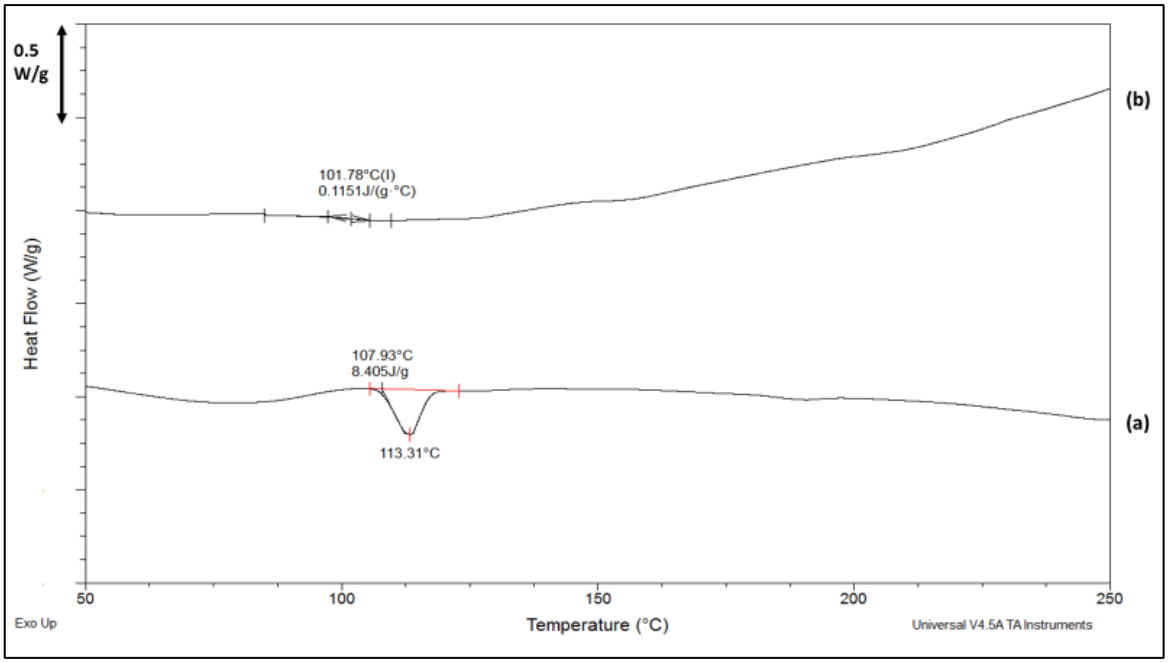


*Figure 5. 13: DSC thermogram with a heating rate of 10 °C/min showing (a) physical mixture of Pharmacoat 603, HCTZ and RAM in the ratio of 6.5: 2.5: 1 (b) spray coating of optimized formulation.*

The target individual doses for SIM, HCTZ and RAM for the final FDC product are 20 mg, 12.5 mg and 5 mg, respectively. As a result, 4.4 g of the core spherical beads corresponds to 10 dosage units of SIM. Based on the target individual doses, the final weight of the spray coated material should be 4.9 g. Table 5.4 shows the different concentrations (% w/v) used in the coating of the core spherical beads while maintaining the 6.5:2.5:1 ratio of Pharmacoat 603; HCTZ: RAM from the preliminary studies involving MCC beads.

*Table 5.4: Formulations used for spray coating of SIM core spherical beads maintaining the 6.5: 2.5: 1 ratio of Pharmacoat 603; HCTZ: RAM. Conditions used as described in chapter 2, section 2.2.4.1.*

| | | Dissolved in 100 ml water | Dissolved in 100 ml methanol | | |
|---|---|---|---|---|---|
| **Formulation** | **SIM spheronised pellets (g)** | **Pharmacoat 603 (mg)** | **HCTZ (mg)** | **RAM (mg)** | **Amaranth solution (drops)** |
| **1** | 4.4 | 325 | 125 | 50 | 2 |
| **2** | 4.4 | 1300 | 500 | 200 | 2 |
| **3** | 4.4 | 2600 | 1000 | 400 | 2 |

One of the major factors that has to be considered when moving from the MCC beads to the spherical core material when spray coating is the difference in surface area available to be coated. The MCC beads used in the preliminary studies are smaller and hence have a larger surface area for coating when compared to the spheronised core pellets using the same mass during coating. Formulation 1, as per table 5.6, was undertaken under the assumption that the coating process developed in preliminary studies was 100% efficient. Of course, due to the small initial weight of the material to be coated and the spray coating process itself, this was not true. However, it provided a base run, which would enable us to optimize the process and eventually spray coat the desired amount.

Table 5.5 shows the results for the different formulations used and their final coating potency, with figure 5.14 showing images of the resulting products. Formulation 3 provided the desired drug loading of HCTZ and RAM.

*Table 5.5: Results of final spray coated formulations weight and final % API dosage target amount.*

| | Formulation 1 | Formulation 2 | Formulation 3 |
|---|---|---|---|
| Weight of pellets pre spray coating (g) | 4.4 | 4.4 | 4.4 |
| Weight of pellets post spray coating (g) | 4.45 ± 0.02 | 4.61 ± 0.03 | 4.88 ± 0.03 |
| HCTZ dosage target (%) | 11.2 ± 1.5 | 46.5 ± 2.4 | 101.2 ± 4.5 |
| RAM dosage target (%) | 11.8 ± 0.6 | 45.7 ± 1.2 | 100.4 ± 3.9 |

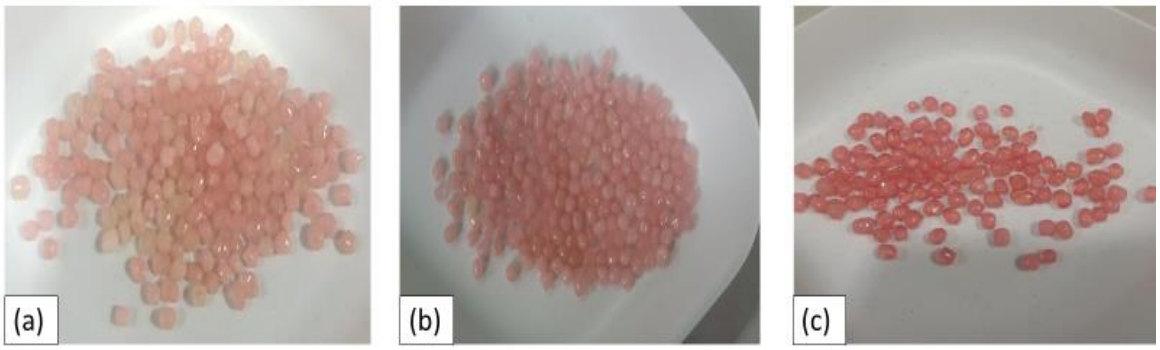


*Figure 5. 14: Images of the final fixed dose combination products after (a) formulation 1, (b) formulation 2 and (c) formulation 3 as outlined in table 5.6.*

### 5.2.3 Dissolution of coated pellets

Dissolution of the final coated product was conducted as described in chapter 2, section 2.16.3.1. The pH of the gastrointestinal tract progressively increases from the stomach (pH 1 – 3, average of 1.8) to the terminal portion of the ileum (pH 7 – 8, average of 7.5), followed by a decrease to a mean of pH 6.5 in the cecum and distal colon (Dressman 1986; Dressman and Krämer 2005; Evans et al. 1988). The average transit time for the stomach is generally accepted to be 2 hours, while that for the small intestine is 3 – 4 hours. The small intestine is further divided into two subsections, the proximal small intestine with an average pH of 6.8 and the distal small intestine with an average pH of 7.5. The dissolution studies were conducted on 490 mg of coated pellets which was the equivalent of one dosage unit of the FDC product i.e. 20 mg of SIM, 12.5 mg of HCTZ and 5 mg of RAM.

While HCTZ and RAM are immediately released in pH 1.2 and undergo no chemical modification at this pH, SIM potentially undergoes a hydrolysis reaction, as shown in figure 5.15, throughout the dissolution. As a result, calibration curves for both the lactone and β-hydroxy acid forms were constructed (appendix 1). As SIM undergoes this reaction, it impacts the analysis of the release profile during dissolution as both forms have to be tested for. Chapter 2, section 2.12.1 describes how the raw lactone material was fully converted to the β-hydroxy acid form in order to construct the calibration curve. Figure 5.15 shows the hydrolysis reaction between the lactone and β-hydroxy acid form of SIM.

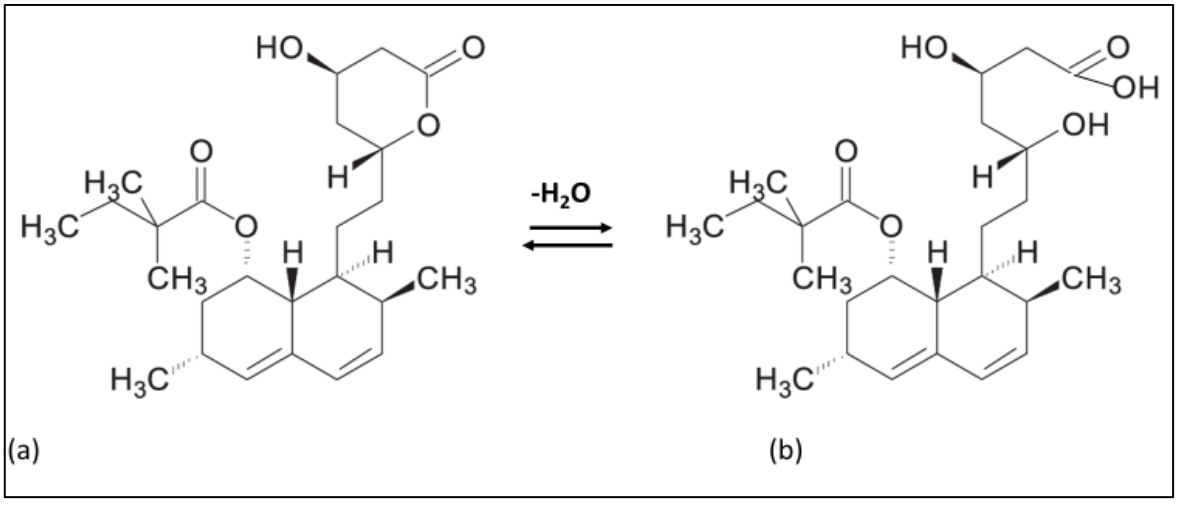


*Figure 5. 15: Hydrolysis of (a) simvastatin (lactone) to (b) simvastatin β-hydroxy acid.*

Figure 5.16 shows the dissolution results (via HPLC analysis, chapter 2, sections 2.13.1 and 2.13.3, respectively') for the final FDC product produced. 100 % of both the HCTZ and RAM are released within 15 min of the start of the dissolution study. For the core material, the release of SIM is delayed, as desired, for the first 2 hours, with release beginning when the pH of the dissolution medium increased to pH 6.8. Further release of SIM was observed when the pH was increased to 7.5 with 100 % of SIM being successfully released from the formulation.

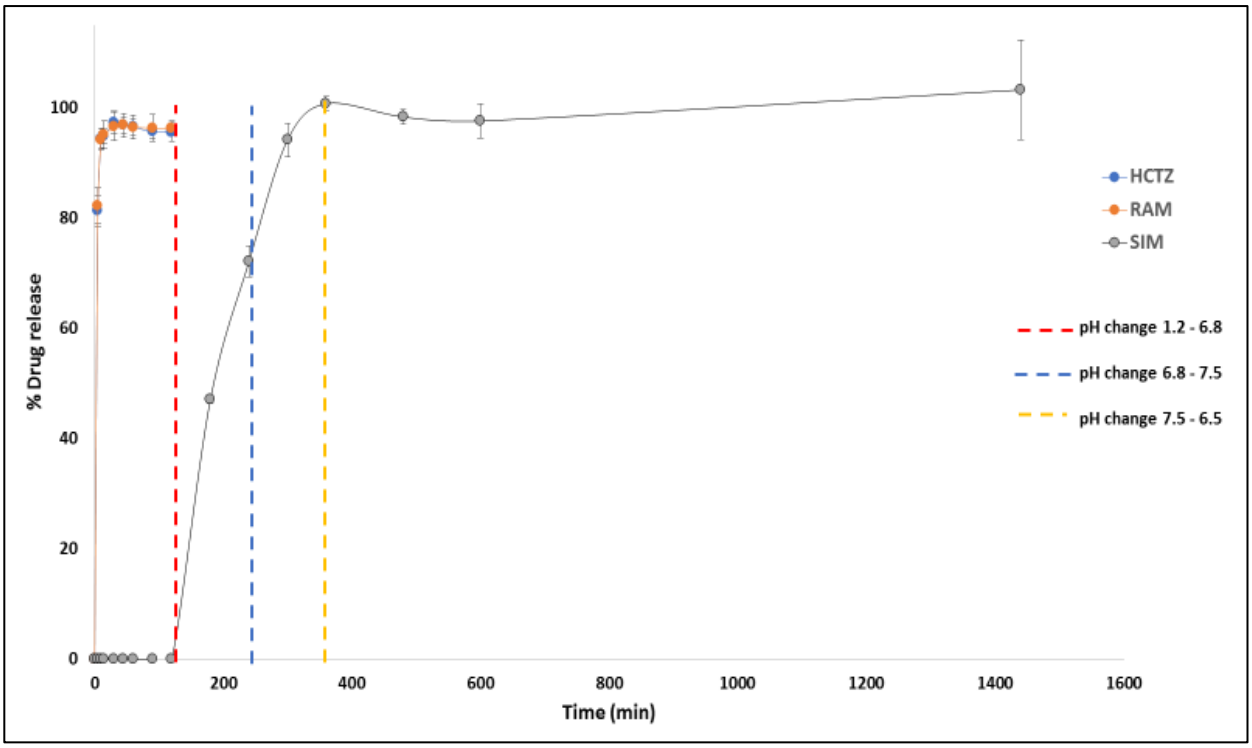


*Figure 5. 16: Dissolution behaviour of the final spray coated spheronised pellets combining an immediate release HCTZ and RAM formulation and a delayed release SIM formulation.*

## 5.3 Conclusions

An optimised formulation tested for dissolution performance clearly demonstrated an ability to delay the release of simvastatin. In addition, an immediate release layer based on Pharmacoat 603 was successfully developed to deliver hydrochlorothiazide and ramipril. Both formulations were then manufactured as a bilayer drug delivery system, and the release performance was examined. Based on the obtained results, these formulations may be used as a platform for delivering a wide range of medications in a biphasic manner.

# Chapter 6:

# Manufacture of a fixed dose combination product of gliclazide and sitagliptin using hot melt extrusion, spheronisation and spray coating for the management of type II diabetes

## 6.1 Introduction

Type II diabetes mellitus is associated with diminished insulin secretion, impaired insulin action and increased hepatic glucose production (Stumvoll et al. 2005). It is seen as a complex condition, involving genetic and environmental factors and is often accompanied by other symptoms of metabolic syndrome, such as dyslipidemia and hypertension (Lin and Sun 2010). Type II diabetes mellitus accounts for about 90 % of all diabetes cases and is characterised by insulin resistance at target cells and a relative, rather than absolute deficiency in insulin activity which is associated with type I diabetes mellitus (Zimmet et al. 2001). Sulphonylureas (SUs) are the oldest oral antidiabetic agent and have been available since the early 1950s. As SUs act by reducing blood glucose levels by stimulating insulin secretion from the β-cells of the islets of Langerhans, hypoglycemia is the most common side effect associated with this class of drugs (Binder and Bendtson 1992; Marks and Teale 1999). Metformin (MET) is recommended as first line treatment for type II diabetes, however, when MET is contraindicated or not tolerated, SUs are recommended as first line treatment (National Institute for Clinical Excellence 2018). If further intensification of treatment is required in addition to SUs, dipeptidyl peptidase-4 inhibitors (DPP-4i) are recommended as the next additional line of treatment. DPP-4i preserve β-cell mass through stimulation of cell proliferation, stimulating insulin secretion and inhibiting glucagon secretion (Drucker and Nauck 2006). Both SUs and DPP-4i have the advantage of being suitable for administration as solid oral dosage forms.

Gliclazide (GLZ) is a SU that is currently available on the market in two different oral solid dosage forms: an immediate release (IR) 80 mg formulation and a modified release (MR) formulation available in either 30 mg or 60 mg strengths. As the 30 mg MR formulation is comparable to the 80 mg IR formulation due to the pharmacokinetics of the different formulations (they have been shown to have the same efficacy), the MR formulations are often favored due to the lower active pharmaceutical ingredient (API) concentration, resulting in less adverse effects being observed (medicines.ie 2019d). The MR formulations also offer the advantage of maintaining effective GLZ plasma concentrations over 24 h, whereas the IR formulations see a peak plasma level between 2 – 6 hours after administration (medicines.ie 2019c). GLZ is classified as a Biopharmaceutics Classification System (BCS) class II drug, as it is highly permeable and poorly soluble (Grbic et al. 2011). It is also considered to be a thermolabile drug, due to degradation occurring upon melting (Huang, O'Donnell, et al. 2017). Sitagliptin phosphate (SIT) is a DPP-4i that is available on the market as an IR formulation in strengths of 25 mg, 50 mg and 100 mg alone, or in combination with MET. SIT is a BCS class III drug compound, as it is highly soluble and poorly permeable (Shakya 2015).

Hot melt extrusion (HME) is a manufacturing technique that has gained popularity in the pharmaceutical industry due to its application as a continuous process (Maniruzzaman and Nokhodchi 2016), ability to enhance solubility of BCS class II and IV drug compounds (Javeer et al. 2013) and to produce controlled release formulations (Lang et al. 2014). Thermal energy input during the extrusion process is normally supplied by heat conduction from the barrel and the friction of the material against the kneading elements and interior wall of the extruder barrel. As thermal energy is involved, it can make dealing with thermolabile materials difficult. As well as thermal degradation during the process, APIs and excipients may be susceptible to different degradation pathways during the process, such as hydrolysis, oxidation and photo degradation (Blessy et al. 2014). These chemical degradation pathways can be caused during the HME process by elevated temperature, presence of oxygen, moisture and pH level (Huang, O'Donnell, et al. 2017).

Spray coating using the Wurster method is undertaken in a fluidized bed dryer (FBD) and uses differential airflow to create a cyclic movement of material to be coated. The location of the spray nozzle at the bottom of the fluidized bed of particles is what sets the Wurster process apart from other coating methods. Differential air streams move the bed of materials upward in a cyclic motion inside the chamber as it is coated with an atomized material to create a core-shell structure. This configuration ensures that the coating material can be applied efficiently to individual particles, while controlling for agglomeration. The process can be continued until the desired uniform film thickness and dosages are achieved through depositing one or more layers to the core material. No matter what the shape of the core material is, the Wurster process is capable of coating formulations onto the core material to achieve the desired properties of the coating material. More recently, the spray coating process has been incorporated into the continuous manufacturing production line (Process Worldwide 2019). As the pharmaceutical industry moves towards the continuous manufacturing model, and away from the traditional batch model, spray coating can now be incorporated into process.

In this study, HME, followed by heat aided spheronisation to produce spherical pellets, was used to produce a sustained release formulation of GLZ with a similar release profile to the commercially available tablets. These spherical pellets were then spray coated using a FBD with an immediate release formulation containing SIT to manufacture a final fixed dose combination (FDC) product. As this combination is not currently available on the market, it represents a novel FDC product with potential for the treatment of type II diabetes mellitus.

## 6.2 Results and discussion

### 6.2.1 Gliclazide core material manufacture

As one of the objectives is to manufacture an extended release formulation of GLZ, the thermal degradation pathway of the API is important to consider. Huang et al. (Huang, O'Donnell, et al. 2017) described the thermal degradation of GLZ through the hydrolysis of the amide group (figure 1).

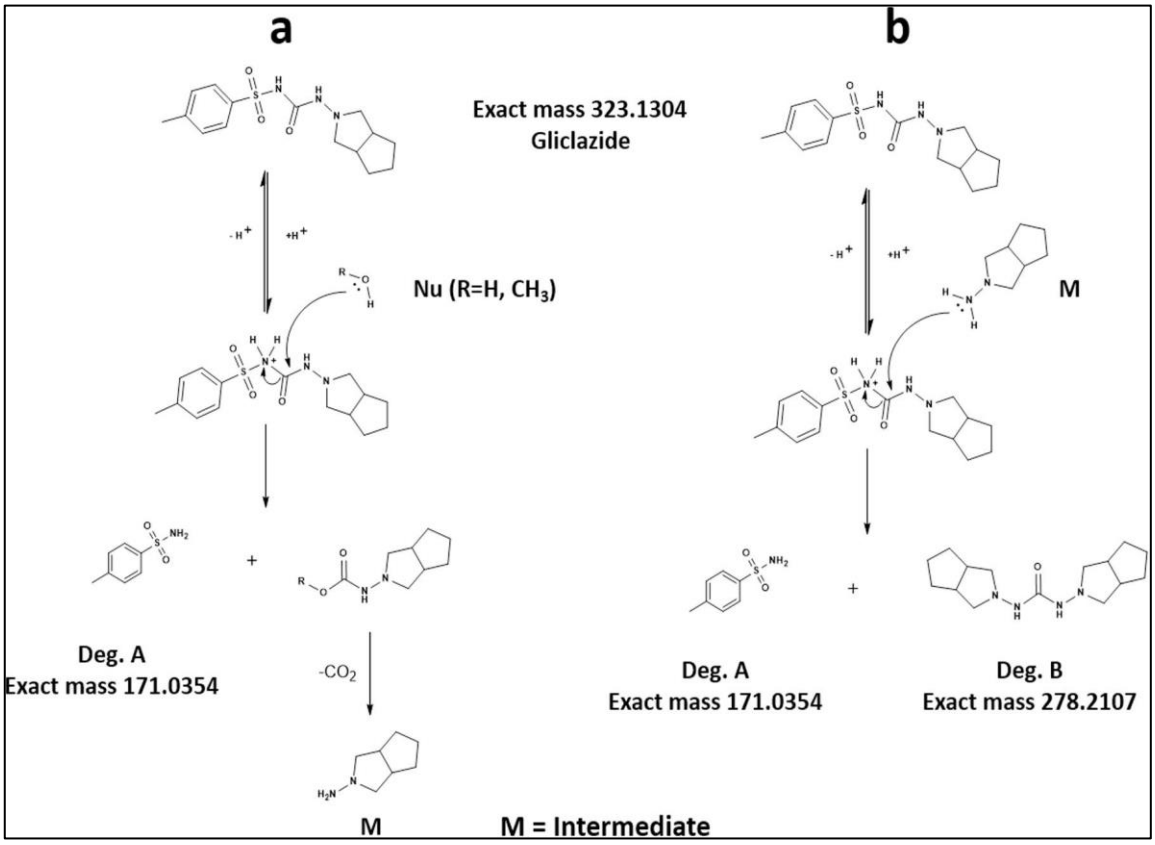


*Figure 6. 1: Thermal degradation of gliclazide by the hydrolysis of the amide group generating two major degradants* (Huang, O'Donnell, et al. 2017)*. Importantly, both hydrolysis pathways proposed in this scheme lead to degradation product A (Deg. A), which means that gliclazide molecules will end up with the same amount of Deg. A molecules after hydrolysis.*

Forced degradation of GLZ, as described in chapter 2, section 2.12.2, highlights the hydrolysis of the amide group and the influence that pH and temperature have on the degradation process of GLZ (figure 6.2). From the results seen in figure 6.2 we can see that increasing temperature results in an increased degradation of gliclazide, regardless of the solution in which it is dissolved. Another interesting finding is that at 25 °C and 37 °C, the basic pH environment provided by NaOH results in no degradation over 72 h, indicating that, at lower temperatures, a more basic environment may prevent the degradation of GLZ.

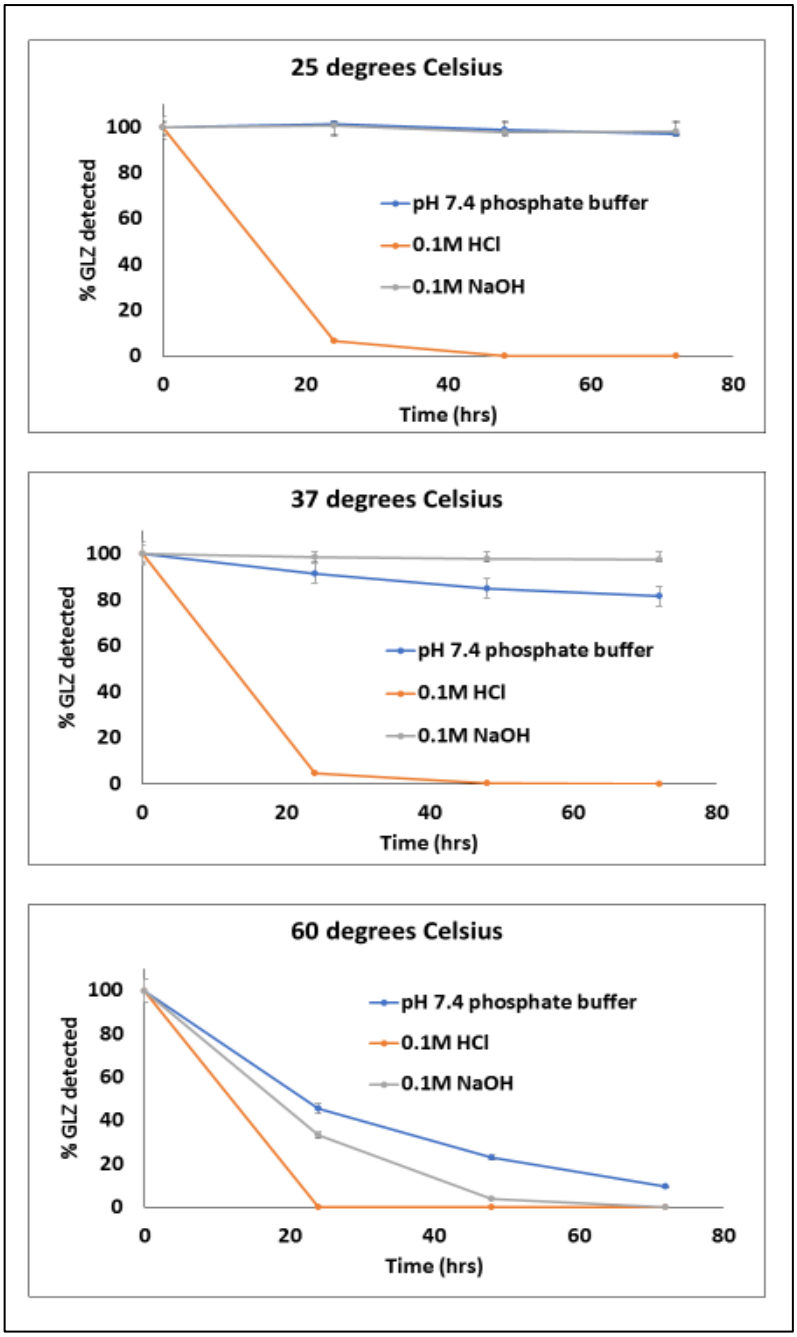


*Figure 6. 2: Forced degradation studies of GLZ in pH 7.4 phosphate buffer, 0.1M HCl and 0.1M NaOH at different temperatures over 72 h.*

Figures 6.3 and 6.4 show the liquid chromatography – mass spectroscopy (LC-MS) results for GLZ and GLZ degradation product A, respectively (following the method described in chapter 2 section 2.16). The figures highlight the main degradation product produced as previously reported by Huang et al. (Huang, O'Donnell, et al. 2017).

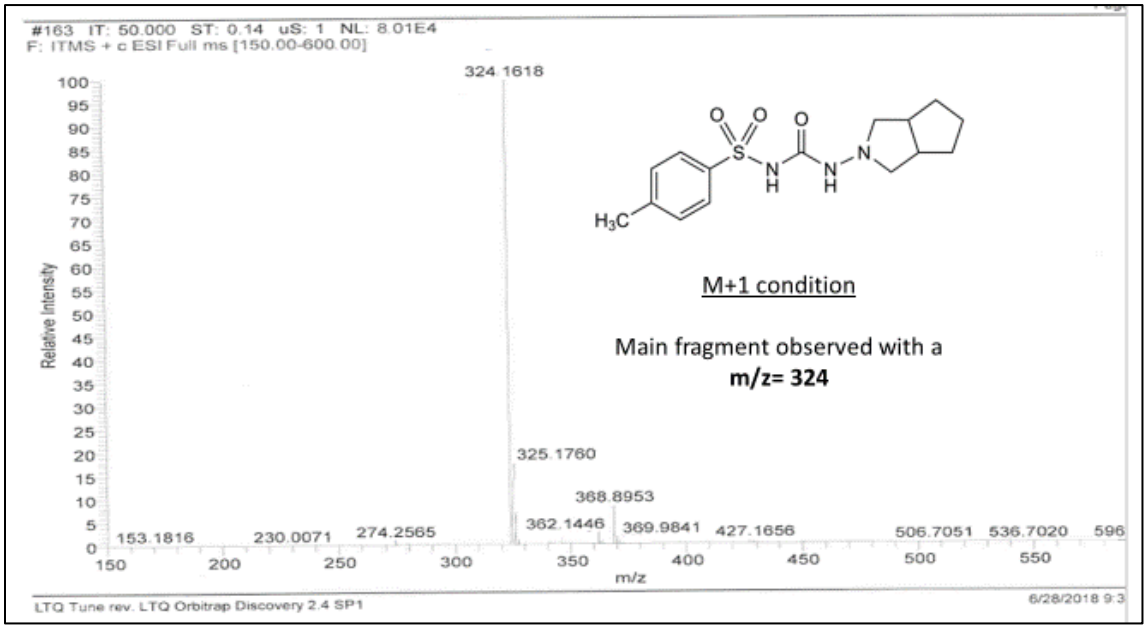


*Figure 6. 3: LC-MS of gliclazide.*

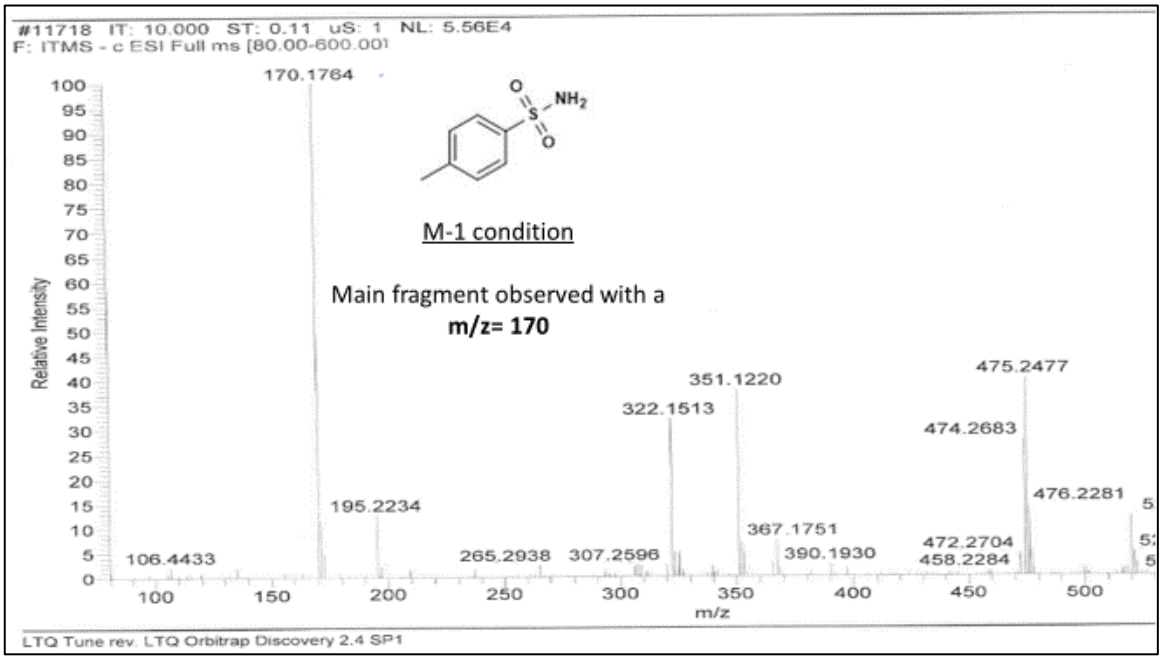


*Figure 6. 4: LC-MS of the main thermal degradation product of gliclazide, 4-methylbenzenesulfonamide (degradation product A).*

Several generic products of the 30 mg modified release dosage form of GLZ are available on the market. When tested using the drug release dissolution method detailed in chapter 2, section 2.17.4.1, both Diamicron® and Vitrile® brands were found to release > 90 % of the GLZ API over the first 12 h, with the Diaclide® brand releasing just over 80

% (figure 6.5). Knowing the release profiles of the generics already available, allows us to target a similar release profile for GLZ from the HME formulations.

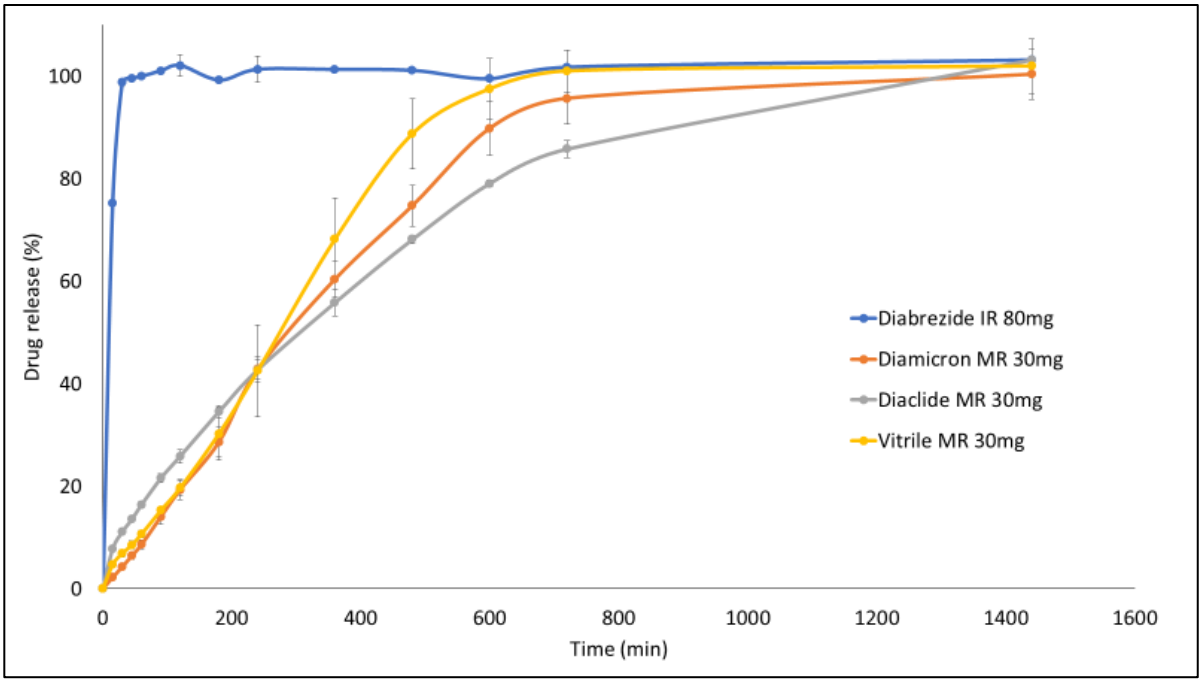


*Figure 6. 5: Dissolution of gliclazide marketed products in pH 7.4 over 24 hours.*

Due to the degradation of GLZ at its melting point (171.12 ± 1.09 °C) (figure 6.6), the thermal nature of the HME process, and, the desired release profile of the final formulation, polymer selection plays a vital role in the development of the formulation. It has also previously been shown that GLZ's melting point is significantly depressed in the presence of polymers due to molecular interactions (Huang, O'Donnell, et al. 2017) which has to be taken into account when the process parameters for the HME are being chosen.

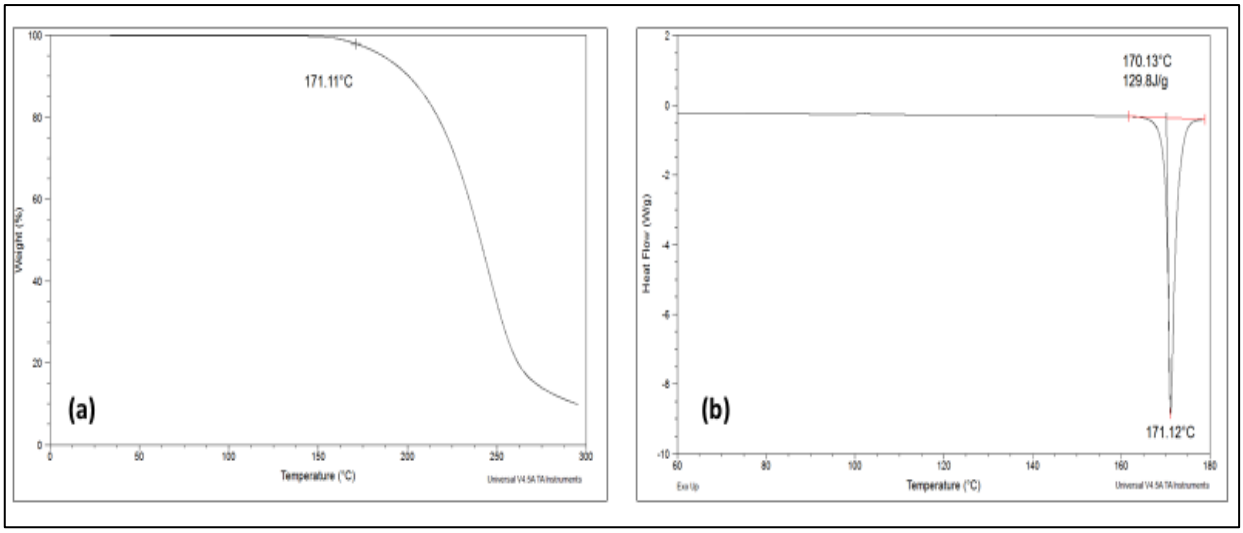


*Figure 6. 6: TGA (a) and DSC (b) images showing the thermal degradation of GLZ upon melting.*

Eudragit® RSPO and Eudragit® RLPO are both amorphous, insoluble polymers with relatively low glass transition temperatures ($T_g$s) (figure 6.7). Both are copolymers of ethyl acrylate, methyl methacrylate and a low content of methacrylic acid ester with quaternary ammonium groups. The ammonium groups are present as salts, which allows the polymers to be permeable, i.e. the solvent in to which the polymers are placed can penetrate the polymer layers, allowing the API to be dissolved and then released from the formulation (Patra et al. 2017). Eudragit® RLPO is described as being more permeable than Eudragit® RSPO (Thakral et al. 2013). Both polymers are suitable for sustained release formulations and, depending on the concentrations of each used, can vary the drug release profiles. Both polymers are miscible with one another and have been used and extensively reported in the literature for sustained release formulations (Boza et al. 1999; Sahoo et al. 2007, 2009).

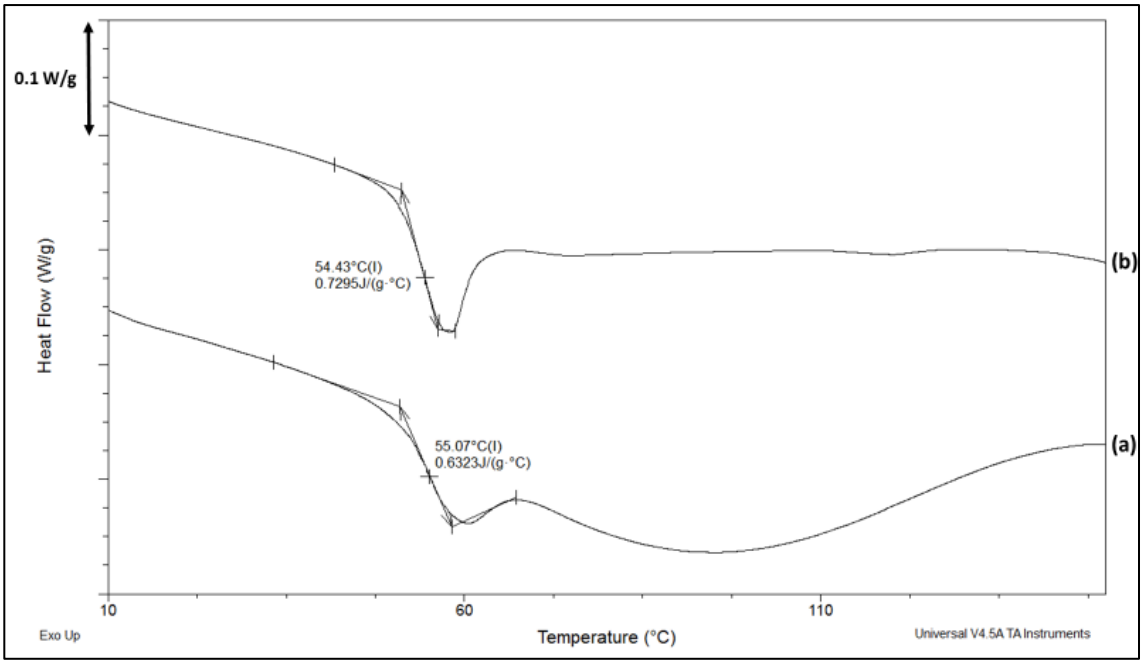


*Figure 6. 7: DSC thermograms at a heating rate of 10 °C/min of (a) Eudragit® RLPO showing a $T_g$ at 55 °C and (b) Eudragit® RSPO showing a $T_g$ at 54 °C*

Initial HME studies were conducted using various ratios of Eudragit® RSPO and Eudragit® RLPO, as shown in table 6.1. Triethyl citrate (TEC) was added as a plasticiser in order to reduce torque and pressure during the HME process. TEC was chosen as a plasticiser as previous studies have shown it to be compatible with acrylic polymers (Pearnchob and Bodmeier 2003; Zhu et al. 2002). The conditions used in the extruder are detailed in table 6.2.

*Table 6. 1: Composition of formulations 1 - 6 extruded as described in chapter 2 section 2.2.2.3.*

| Formulation | Gliclazide (% w/w) | Eudragit ® RSPO (% w/w) | Eudragit ® RLPO (% w/w) | Triethyl Citrate (% w/w) | PXRD amorphous |
|---|---|---|---|---|---|
| **1** | 10 | 76 | 9 | 5 | No |
| **2** | 10 | 69.5 | 15.5 | 5 | No |
| **3** | 10 | 62 | 23 | 5 | No |
| **4** | 10 | 42.5 | 42.5 | 5 | No |
| **5** | 10 | 25.5 | 59.5 | 5 | No |
| **6** | 10 | 17 | 68 | 5 | No |

*Table 6. 2: Processing conditions used during hot melt extrusion of the gliclazide core formulation.*

| Feed rate (g/min) | Screw speed (rpm) | Feed Zone (°C) | Zone 1 (°C) | Zone 2 (°C) | Zone 3 (°C) | Die (°C) |
|---|---|---|---|---|---|---|
| 3.5 | 20 | 80 | 90 | 100 | 110 | 105 |

During the extrusion process, residence time, maximum torque and maximum pressure observed were recorded, and are shown in table 6.3. Long residence time, high torque and high pressure resulted in large amounts of degradation product (A) being formed during the process (which were quantified using the methods described in chapter 2, section 2.13.4). Once extrusion had taken place, the extrudates were cut and spheronised as described in chapter 2, section 2.2.2.3. While the extrudates were easily cut and spheronised, it was noted that, due to the liquid state of the TEC, feeding the formulations into the extruder proved difficult.

*Table 6. 3: Extruder readings and degradation product detected for formulations 1 to 6*

| Formulation | Residence time (min) | Max Torque ($Nm^{-1}$) | Max Pressure (bar) | Degradation product detected (%) |
|---|---|---|---|---|
| **1** | 14.50 ± 1.45 | 2.87 ± 0.12 | 24.30 ± 2.50 | 10.25 ± 1.56 |
| **2** | 13.67 ± 2.78 | 3.14 ± 0.08 | 27.87 ± 1.63 | 15.26 ± 4.55 |
| **3** | 14.21 ± 2.04 | 2.97 ± 0.25 | 26.41 ± 4.74 | 12.53 ± 4.66 |
| **4** | 12.36 ± 1.04 | 2.73 ± 0.13 | 23.45 ± 3.43 | 11.21 ± 2.72 |
| **5** | 13.96 ± 2.78 | 3.11 ± 0.27 | 21.32 ± 1.54 | 12.56 ± 1.47 |
| **6** | 11.45 ± 0.65 | 2.74 ± 0.28 | 19.50 ± 2.34 | 14.69 ± 3.48 |

Figure 6.8 shows the release profiles of the formulations trialled from formulations 1 to 6 (Table 6.1). We can see from the figure that none of the formulations proved satisfactory due to incomplete release of the API over the 24-hour timeframe.

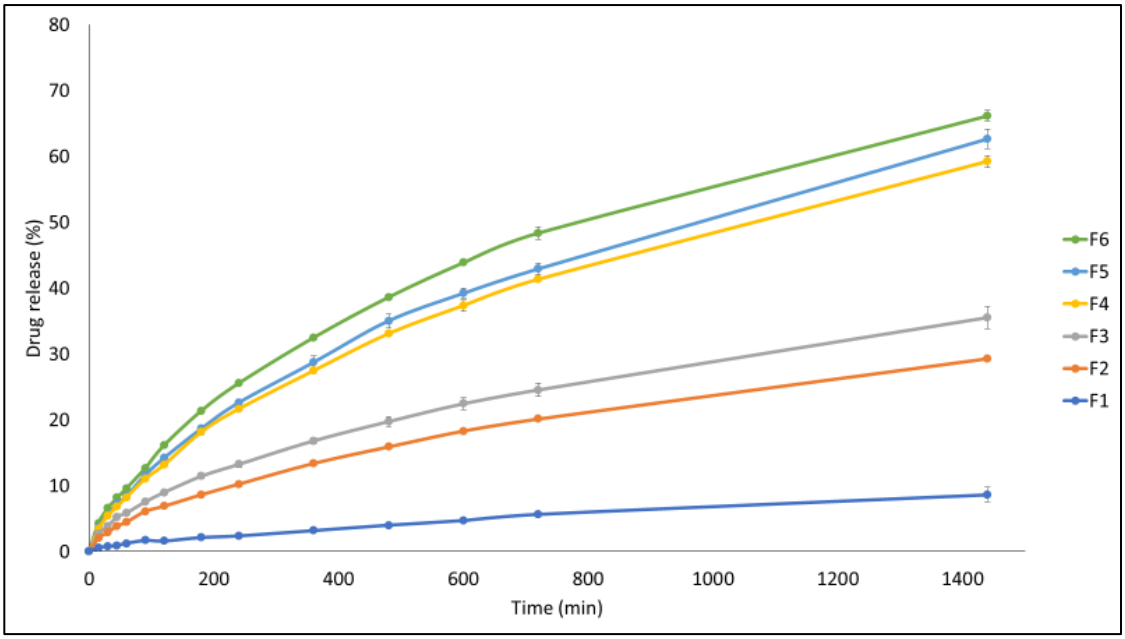


*Figure 6. 8: Dissolution of formulations 1 – 6 in pH 7.4 over 24 hours (using the drug release method detailed in chapter 2, section 2.17.4.1).*

Several issues were noted with the initial formulations which were addressed on review. The first issue, as mentioned previously, was the difficulty associated with the feed mixture being fed from the pestle and mortar into the extruder. The plasticiser was changed from the liquid TEC to the solid PEG 3350. This allowed the powders to be homogenously mixed, while also allowing much easier transfer from the mortar into the extruder. The changing of plasticiser also had a knock-on effect for residence time of the mixtures in the extruder. Due to the thermolabile nature of GLZ, the amount of time it is exposed to higher temperatures should be reduced in order to minimise the potential degradation of the API. While F1 to F6 all had residence times of greater than 10 minutes under the conditions described (table 6.3), formulations which contained PEG 3350 as the plasticiser instead of triethyl citrate had much reduced residence times (tables 6.5 and 6.7).

The second issue addressed related to the formulation composition with respect to the Eudragit® polymers. As Eudragit® RSPO content decreased and Eudragit® RLPO content increased, the release rate of the formulations increased, while also maintaining a sustained release profile. As a result, it was decided that Eudragit® RLPO (the more permeable of the two polymers) alone would form the basis of future formulations.

To further increase the rate of release from the polymer matrix, Kollidon® VA 64 and Affinisol™ HPMC HME 100LV were trialled as potential pore formers. Polyvinyl acetate-

based polymers, such as Kollidon® VA 64, have been used extensively throughout the literature as pore formers to increase the rate of release of sustained release formulations (Kolter et al. 2001, 2013). Although the $T_g$ of Kollidon® VA 64 is 108 °C (figure 6.9) and the maximum temperature the formulations are subjected to is 110 °C, the miscibility of the polymer with Eudragit® RLPO and the presence of a plasticiser allow the formulations to be extruded. Affinisol™ HPMC HME 100LV is a brand of HPMC specifically developed for HME, allowing processing to occur at lower temperatures than other HPMC brands (Huang et al. 2016). It has a $T_g$ of 104 °C (figure 6.9) and has previously been shown to be compatible with GLZ (Huang, O'Donnell, et al. 2017).

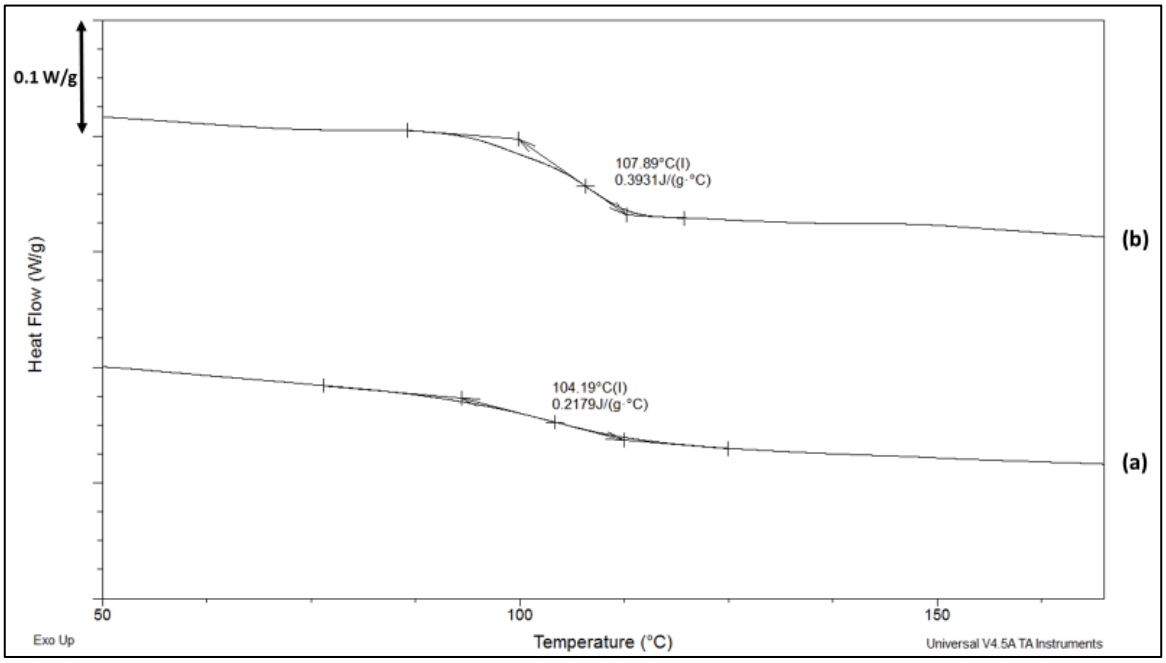


*Figure 6. 9: DSC thermograms at a heating rate of 10 °C/min of (a) Affinisol™ HPMC HME 100LV showing a $T_g$ at 104 °C and (b) Kollidon® VA 64 showing a $T_g$ at 108 °C.*

Table 6.4 shows the formulations trialled for the next stage of the formulation development.

*Table 6. 4: Composition of formulations 7 - 13 extruded as described in chapter 2 section 2.2.2.3.*

| Formulation | Gliclazide (% w/w) | Eudragit ® RLPO (% w/w) | Kollidon ® VA 64 (% w/w) | Affinisol ™ HPMC (% w/w) | PEG 3350 (% w/w) | PXRD amorphous |
|---|---|---|---|---|---|---|
| **7** | 10 | 75 | 10 | 0 | 5 | No |
| **8** | 10 | 65 | 20 | 0 | 5 | No |
| **9** | 10 | 55 | 30 | 0 | 5 | No |
| **10** | 10 | 45 | 40 | 0 | 5 | No |
| **11** | 10 | 65 | 0 | 20 | 5 | No |
| **12** | 10 | 75 | 0 | 10 | 5 | No |
| **13** | 10 | 80 | 0 | 5 | 5 | No |

The change in plasticiser and addition of pore formers had the desired effects on the formulation development. Table 6.5 shows reduced residence time, reduced maximum torque and reduced maximum pressure for formulations 7 – 13 when compared to formulations 1 – 6. The amount of degradation product produced during the process was also reduced, as can be seen by the results shown in table 6.5. However, the quantities of degradation product still exceeded the desired maximum of 5 %.

*Table 6. 5: Extruder readings and degradation product detected for formulations 7 to 13*

| Formulation | Residence time (min) | Max Torque ($Nm^{-1}$) | Max Pressure (bar) | Degradation product detected (%) |
|---|---|---|---|---|
| **7** | 2.30 ± 0.65 | 1.31 ± 0.12 | 13.10 ± 0.94 | 8.45 ± 1.21 |
| **8** | 2.55 ± 0.72 | 1.35 ± 0.08 | 12.67 ± 1.52 | 7.75 ± 1.23 |
| **9** | 3.08 ± 1.15 | 1.46 ± 0.94 | 13.56 ± 3.32 | 7.20 ± 1.52 |
| **10** | 5.20 ± 1.30 | 1.54 ± 0.17 | 11.63 ± 2.52 | 6.59 ± 1.06 |
| **11** | 2.41 ± 0.52 | 1.61 ± 0.08 | 16.40 ± 4.41 | 7.15 ± 0.65 |
| **12** | 2.21 ± 0.40 | 1.39 ± 0.02 | 13.32 ± 2.30 | 6.46 ± 1.25 |
| **13** | 2.25 ± 0.15 | 1.77 ± 0.12 | 17.54 ± 3.55 | 6.82 ± 1.68 |

Figure 6.10 shows the release profiles for formulations 7 – 13. A sustained release profile can be seen for the formulations, however, as with the initial formulations 1 – 6, the rate of release is slower than desired and 100 % of the API is not released over 24 hours.

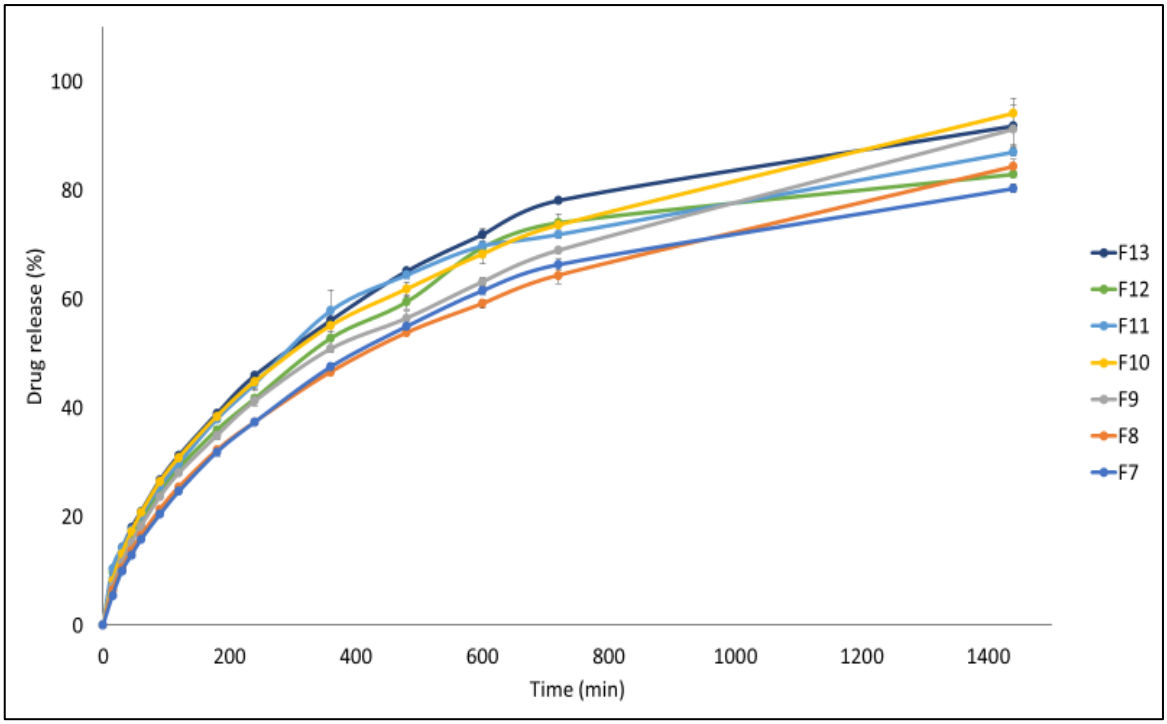


*Figure 6. 10: Dissolution of formulations 7 – 13 in pH 7.4 over 24 hours (using the drug release method detailed in chapter 2, section 2.17.4.1).*

Due to the large amount of degradation product still present in the formulations when 5 % w/w PEG 3350 was used as plasticiser, it was thought that a further increase in the PEG 3350 concentration might result in further lowering of the torque and pressure observed during the HME process, and result in less degradation. Formulations 14 and 15 detailed in table 6.6 correspond to formulations 8 and 9 in table 6.4, but have 10 % w/w PEG 3350 instead of 5 % w/w.

*Table 6. 6: Composition of formulations 14 - 18 extruded as described in chapter 2 section 2.2.2.3*

| Formulation | Gliclazide (% w/w) | Eudragit ® RLPO (% w/w) | Kollidon ® VA 64 (% w/w) | Meglumine (% w/w) | PEG 3350 (% w/w) | PXRD amorphous |
|---|---|---|---|---|---|---|
| **14** | 10 | 65 | 10 | 0 | 10 | No |
| **15** | 10 | 55 | 25 | 0 | 10 | No |
| **16** | 10 | 45 | 30 | 10 | 5 | Yes |
| **17** | 10 | 55 | 20 | 10 | 5 | Yes |
| **18** | 10 | 75 | 0 | 10 | 5 | Yes |

While the increase in PEG 3350 resulted in a statistically significant reduction in maximum torque and maximum pressure (table 6.7), the degradation product content was not reduced. While 100 % of the API was released over 24 h as desired (figure 6.10), the presence of large amounts of degradation product made the formulation unsuitable.

*Table 6. 7: Extruder readings and degradation product detected for formulations 14 to 18*

| Formulation | Residence time (min) | Max Torque ($Nm^{-1}$) | Max Pressure (bar) | Degradation product detected (%) |
|---|---|---|---|---|
| **14** | 2.04 ± 0.12 | 0.94 ± 0.15 | 10.32 ± 0.53 | 6.47 ± 0.19 |
| **15** | 2.12 ± 0.42 | 1.12 ± 0.13 | 10.42 ± 0.32 | 5.81 ± 0.15 |
| **16** | 2.31 ± 0.29 | 1.72 ± 0.21 | 18.81 ± 2.35 | 1.80 ± 0.12 |
| **17** | 2.20 ± 0.07 | 1.52 ± 0.14 | 16.35 ± 1.14 | 1.61 ± 0.13 |
| **18** | 2.10 ± 0.24 | 1.43 ± 0.08 | 15.30 ± 1.26 | 1.49 ± 0.06 |

Even though there was a reduction in the maximum torque and maximum pressure with an increase in PEG 3350 concentration, there was no reduction in the degradation product detected. We can conclude from these results that below a certain point, maximum torque and maximum pressure play no part in the formation of the degradation product. As a result, another factor must be contributing to degradation formation. As previously discussed, GLZ is unstable in acidic conditions, even at low temperatures. Due to the presence of the methacrylic acid ester in Eudragit® RLPO, upon melting during the HME process, it is thought that acidic conditions may arise, resulting in the degradation of GLZ. To counteract the acidic degradation, meglumine, or D-(-)-N-methylglucamine, an amino sugar (derived from sorbitol) with a $pK_a$ value of 9.6 was added to the formulation. Meglumine has previously been used as an alkalizing agent to alter the micro pH of the environment to which an API may be subjected (Motola et al. 1989; Taniguchi et al. 2014). One of the most important points of pH-modification in formulations is to ensure sufficient quantities of the pH-modifier, with adequate solubility and pKa, are present to maintain the appropriate microenvironmental pH (Siepe et al. 2006). Addition of pH modifiers can affect the manufacturability and stability of formulations, but they can also have an effect on the dissolution profiles (Taniguchi et al. 2014). 10 % w/w of meglumine was added to formulations 16 and 17 with the desired results being achieved, in terms of a significant reduction in degradation product detected (table 6.7). However, the negative aspect associated with the addition of meglumine was the observed rapid initial release of GLZ (figure 6.11). In order to reduce

this initial release, the pore former was removed (as per formulation 18, table 6.6), and the desired release profile was achieved, as seen for formulation 18 in figure 6.11. Formulation 18's dissolution profile was compared to the dissolution profiles of the marketed MR formulations seen in figure 6.5 (described in chapter 2, section 2.19.3). The similarity factor, $f_2$, is one of the most common practices used to compare the dissolution profiles between a reference profile and a test profile (Wang, Snee, et al. 2016). As we can see from the results in table 6.8, formulation 18 has a similar release profile to both the Diamicron® and Diaclide® brands ($f_2 > 50$) and as a result it was decided that the release profile proved satisfactory. Although the release profiles of formulation 18 and the Vitrile® brand were not considered similar ($f_2 < 50$), it was noted that the Diaclide® and Vitrile® release profiles, when compared were not similar either. As a result, the comparison between formulation 18 and Vitrile® release profiles were discarded from consideration.

*Table 6. 8: Comparison of the marketed GLZ MR formulations with formulation 18 and with one another, showing the similarity factor, $f_2$ (an $f_2$ of > 50 denotes similarity).*

| | Similarity factor, $f_2$ | | | |
|---|---|---|---|---|
| | Formulation 18 | Diamicron® | Diaclide® | Vitrile® |
| Formulation 18 | N/A | 51.81 | 65.37 | 43.79 |
| Diamicron® | 51.81 | N/A | 65.78 | 57.84 |
| Diaclide® | 65.37 | 65.78 | N/A | 49.32 |
| Vitrile® | 43.79 | 57.84 | 49.32 | N/A |

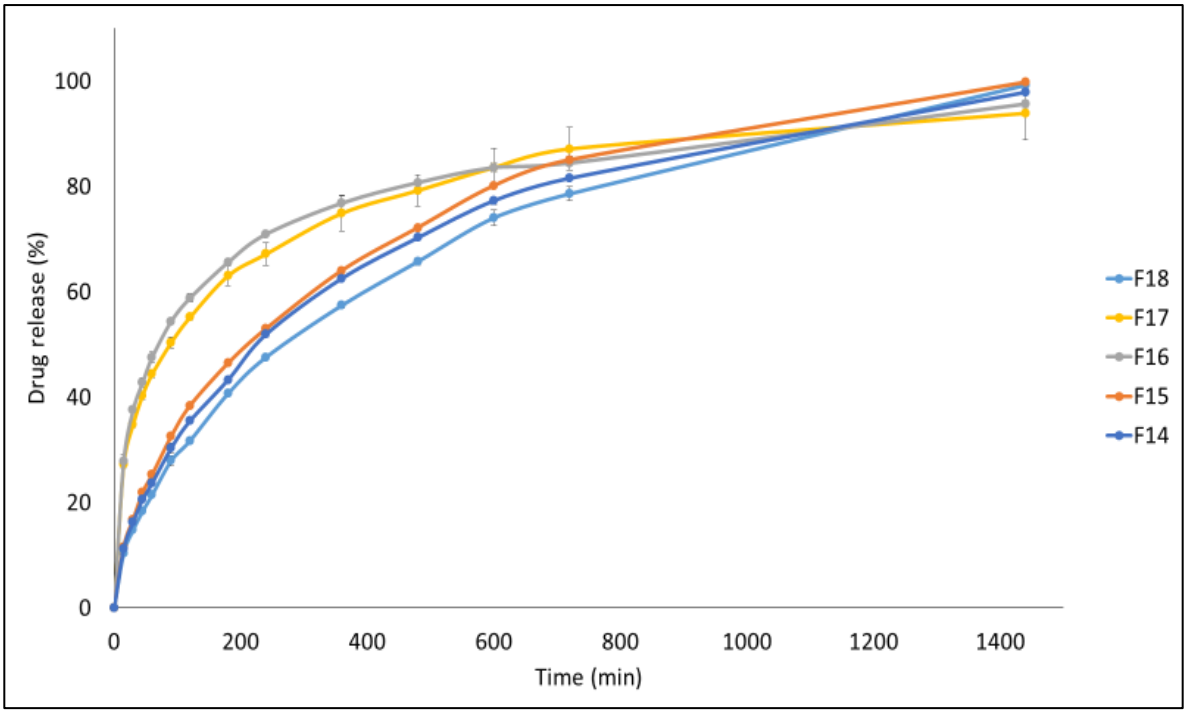


*Figure 6. 11: Dissolution of formulations 14 – 18 in pH 7.4 over 24 hours (using the drug release method detailed in chapter 2, section 2.17.4.1).*

Figure 6.12 shows the final product formulation 18 and details how it was manufactured.

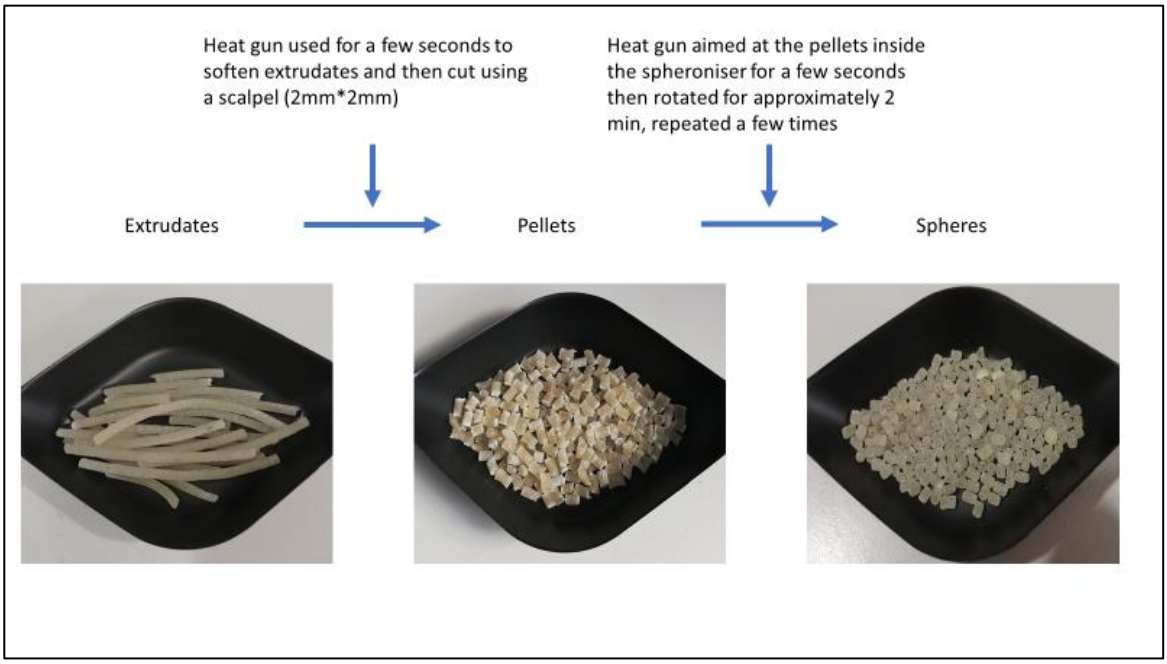


*Figure 6. 12: Photographs of the optimised formulation extrudates following extrusion. The extrudates are cut into 2 mm x 2 mm pellets before being spheronised while heat is applied from a heat gun. The spheres seen on the right are the final core materials to be transferred for coating.*

The addition of meglumine also had an effect on the solid state of the extrudates. While formulations without meglumine remained partially PXRD crystalline, the formulations with meglumine were PXRD amorphous. Figure 6.13 shows the PXRD patterns for GLZ, the physical mixture of the constituents of formulation 18 and the extruded formulation 18. GLZ showed characteristic Bragg peaks at 10.60 °(2θ), 15.05 °(2θ), 17.15 °(2θ), and 22.15 °(2θ), which are also consistent with the literature (Patil and Gaikwad 2011). We can clearly see the peaks in the physical mixture are the peaks associated with the crystalline GLZ, which make it a suitable method to assess the physical state of the API in the processed formulation. The peak seen at 9.00 °(2θ) in the physical mixture of the formulation is a PXRD peak associated with meglumine (figure 6.12 (b)). The lack of peaks in the extruded formulation indicates the formulation is fully PXRD amorphous.

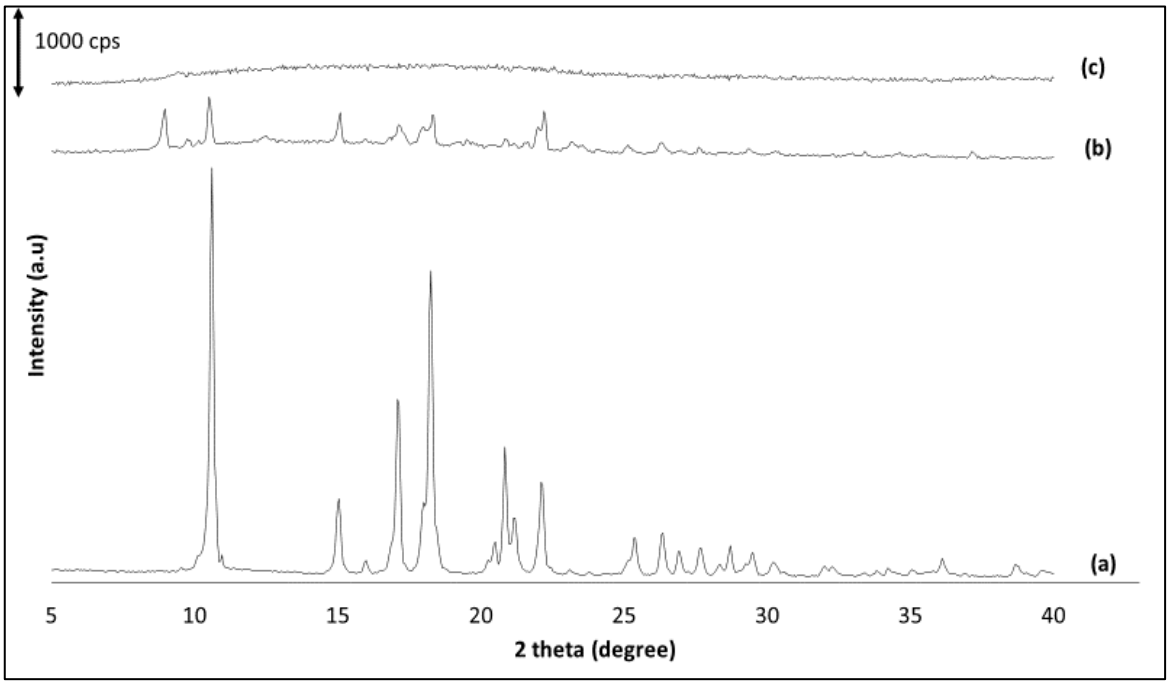


*Figure 6. 13: PXRD over the range of 5–40° 2θ of (a) gliclazide, (b) Physical mixture of formulation 18 and (c) extruded formulation 18.*

### 6.2.2 Sitagliptin coat formulation

Once GLZ core spherical pellets had been successfully manufactured with the desired sustained release profile, the next step in the process was to use a FBD to add an additional layer, comprising of SIT, to create the final novel FDC product. Pharmacoat 603® (HPMC) (Perfetti et al. 2012) was the polymer chosen for spray coating in conjunction with SIT. This polymer was chosen due to its immediate release profile characteristic, film forming ability and because it is one of the most commonly used polymers for spray coating (Bharadia and Pandya 2014). Due to the amount of time required to manufacture the core material for spray coating, initial coating studies were conducted using relatively small amounts of core materials (3 g of core material, equivalent to 10 dosage units). Larger amounts of core materials were used once initial studies were concluded (9 g, equivalent to 30 dosage units).

Both SIT and Pharmacoat® 603 are soluble in water, and water alone was trialled as the initial spray coating solvent, as described in chapter 2, section 2.2.4.2. For successful spray coating to occur, it is important that all components of the formulation are fully dissolved before beginning the process. The target dose of sitagliptin per dosage unit is 100 mg which is equivalent to 128.5 mg of SIT. Therefore, for 10 dosage units, 1285 mg of SIT and 1285 mg of Pharmacoat® 603 were dissolved in water. Table 6.9 describes the initial spray coating formulations trialled. Formulations 1 – 3 had the same GLZ and Pharmacoat® 603 content, with varying volumes of water used to dissolve the contents.

*Table 6. 9: Contents of initial formulation trialled for spray coating SIT.*

| Formulation | Pharmacoat® 603 (mg) | SIT (mg) | Volume of Water (ml) |
|---|---|---|---|
| **1** | 1285 | 1285 | 300 |
| **2** | 1285 | 1285 | 250 |
| **3** | 1285 | 1285 | 200 |

Formulation 1 proved unsuccessful. While the spherical pellets to be coated fluidized initially, due to the high boiling point of water (relative to the maximum temperature of 80 °C that the FBD can achieve), coated particles began to agglomerate to one another as well as to the walls of the FBD before the full amount of the formulation could be applied. For formulations 2 and 3, the volume of water was reduced in the hope that, by reducing the timeframe for coating application, this agglomeration problem might be overcome. However, all formulations with 100 % water used as solvent failed to deliver the targeted drug content due to agglomeration of the spherical pellets.

Formulation 4 consisted of the same quantities of core material to be coated (3 g) and the same quantities of coating polymer and API as was used for formulations 1-3, however, the solvent system used was changed to a 50:50 mixture of methanol and water (table 6.10) (chapter 2, section 2.2.4.2).

*Table 6. 10: Contents of formulation 4 used for spray coating.*

| Formulation | Pharmacoat® 603 (mg) | SIT (mg) | Volume of Water (ml) | Volume of Methanol (ml) |
|---|---|---|---|---|
| **4** | 1285 | 1285 | 100 | 100 |

By changing the solvent system to a mixture of water and methanol, it allowed the solvent to evaporate off at lower temperatures than the previous systems where water alone was used. By reducing the boiling point, it allowed the spherical pellets to fluidize throughout, avoiding the problem previously observed of pellets agglomerating. It was decided that this solvent system would be the solvent used going forward to optimize the spray coating.

In the process of spray coating using the Wurster method, a certain amount of the intended spray coating material is invariably lost to the filters during the process. With larger batch sizes to be spray coated, this is usually not a major issue, as the loss of product is minimal due to the efficiency of the coating process and the large batch size to be coated. However, as we are dealing with smaller batch sizes (relative to the maximum amount that can be coated in the FBD), larger amounts of material are lost (percentagewise). This is clearly evident in table 6.11, where the large difference in recovery rate (drug loading) between formulations 4 and 5 is indicated.

*Table 6. 11: Contents of formulations 4 – 7, the solvent used, and the SIT target dose achieved.*

| Formulation | Volume of Solvent used (50:50 water: methanol) (ml) | Pharmacoat® 603 (mg) | SIT (mg) | Core material to be coated (g) | SIT dosage target attained (%) |
|---|---|---|---|---|---|
| **4** | 200 | 1285 | 1285 | 3 | 5.03 ± 0.41 |
| **5** | 200 | 3855 | 3855 | 9 | 35.54 ± 2.25 |
| **6** | 400 | 7710 | 7710 | 9 | 81.45 ± 3.87 |
| **7** | 500 | 9638 | 9638 | 9 | 97.54 ± 3.14 |

Formulations 4 and 5 contain the maximum amount of SIT that would be spray coated on the core pellets if the spray coating process was 100 % effective. Due to the larger surface area available and the greater concentration of API and polymer in the solvent in formulation 5 compared to formulation 4, the process is far more effective at loading SIT onto the GLZ cores, however, the desired amount of API is still not achieved.

Formulation 6 represents a doubling up of the contents of formulation 5. Due to the solubility of SIT and Pharmacoat® 603 in the chosen solvent, 200 ml was not sufficient to fully dissolve both API and polymer and hence an increased volume of solvent was used. A negative outcome of this requirement was the increase in spray coating time required (the coating times went from 50 min with 200 ml of solvent to 1 hour 40 min with 400 ml and 2 hours with 500 ml). By increasing the time required to spray coat, costs invariably increase due to increased energy consumption.

Formulation 7 represents the contents of the formulation which provided the desired amount of SIT loaded onto the GLZ pellets. While large amounts of API are lost, we would expect a more efficient spray coating application to be achieved with larger batches of core material.

Figure 6.14 shows images of the final product produced post spray coating of formulation 7.

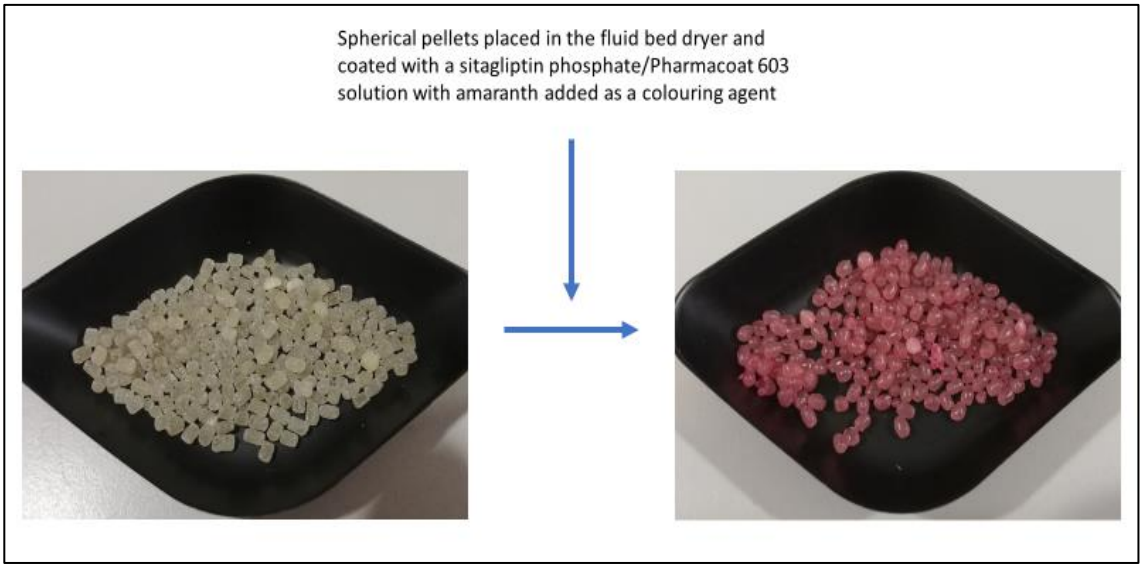


*Figure 6. 14: Images showing GLZ core material before and after spray coating with SIT and Pharmacoat® 603 (formulation 7).*

Figure 6.15 shows PXRD diffractograms for SIT raw material, the physical mixture of SIT and Pharmacoat® 603 and the spray coated material that coated the pellets. SIT shows characteristic Bragg peaks at 13.90 °(2θ), 16.1 °(2θ), 18.65 °(2θ), and 21.25 °(2θ), which are also consistent with the literature (Shantikumar et al. 2014). These characteristic Bragg peaks are also seen in the physical mixture of the formulation and therefore PXRD is suitable for testing the solid state of the formulation. Samples of the spray coating formulation were obtained from the FBD chamber post spray coating and analyzed to test for the final solid state of the spray coated material. Due to the difficult nature of removing the spray coated layer from the final FDC formulation, it was thought the spray coated material collected from the chamber would give an accurate representation of the coated layers' solid-state characteristics. As can be seen from figure 6.15 (c), the spray coating formulation is completely PXRD amorphous with no diffraction peaks evident for SIT.

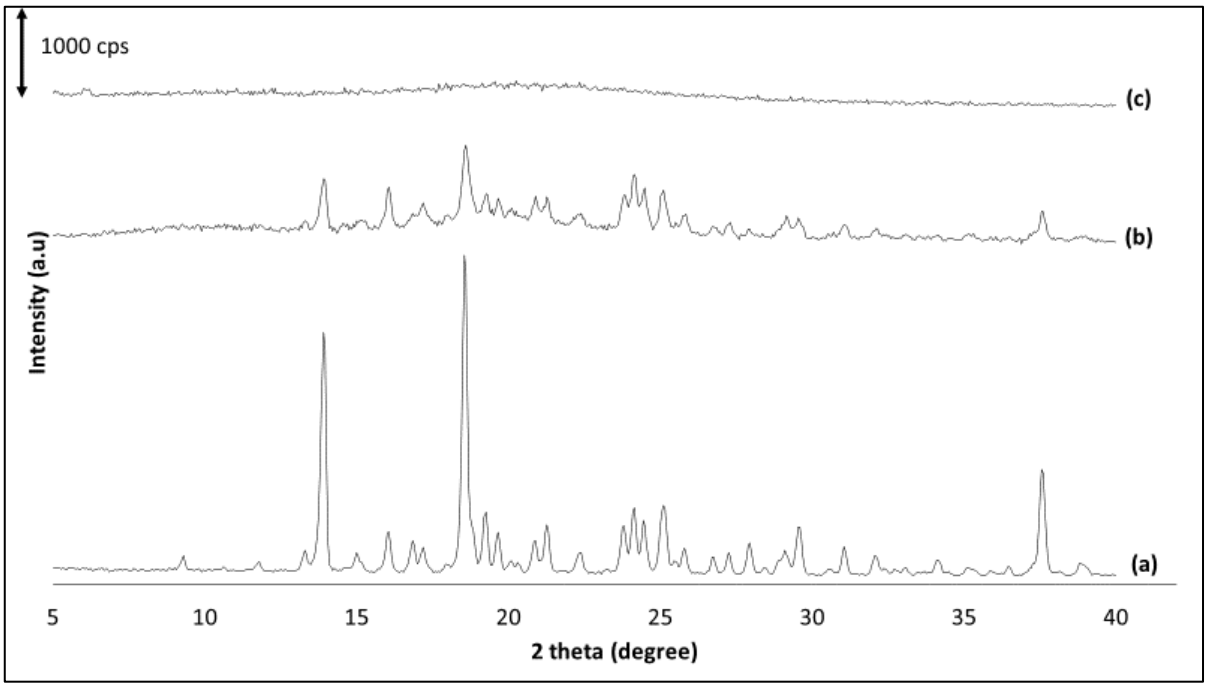


*Figure 6. 15: PXRD over the range of 5–40° 2θ of (a) sitagliptin phosphate, (b) Physical mixture of spray coating formulation and (c) spray coated formulation.*

### 6.2.3 Dissolution/ drug release of the final product

Dissolution/release testing of the final coated FDC product was conducted as described in chapter 2, section 2.17.4.1. which follows the dissolution criteria in the European Pharmacopoeia for testing GLZ solid oral dosage forms. Due to the lack of a monograph available for dissolution testing for this novel FDC product, it was decided to follow the dissolution conditions already applied during the development of the core material. As we

can see from figure 6.16, SIT is immediately released from the product with 100 % of it being released within 10 minutes. This meets our desired immediate release profile for SIT. The optimised GLZ formulation maintains the sustained release profile which is what we desire for our product. The addition of the spray coated layer does not affect the release profiles of either API.

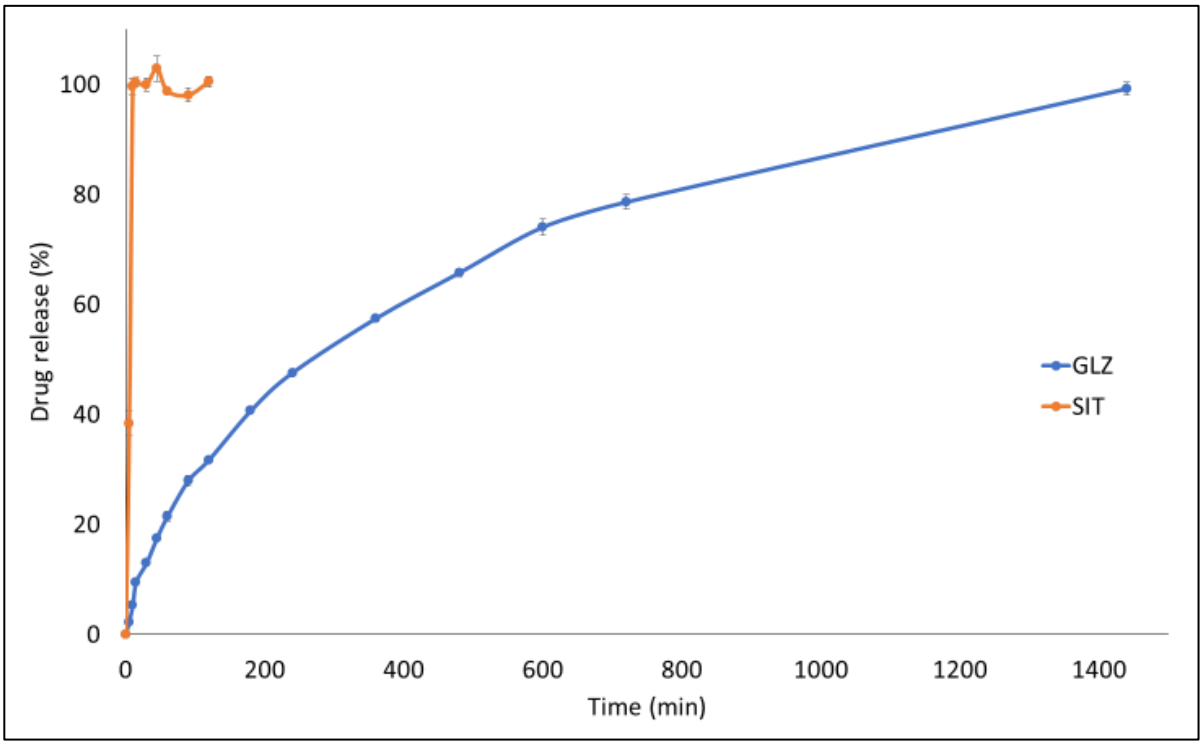


*Figure 6. 16: Dissolution behaviour of the final spray coated spheronised pellets combining an immediate release SIT formulation and a sustained release GLZ formulation (using the drug release method detailed in chapter 2, section 2.17.4.1).*

## 6.3 Conclusions

An optimized formulation for the production of a sustained release formulation of GLZ can be produced via HME while avoiding thermal degradation of the thermally labile API. Careful selection of plasticisers and pH modifiers may be used to prevent excessive GLZ degradation, while retaining desired release profile characteristics. In addition to the sustained release core material, an immediate release layer based on Pharmacoat® 603 was successfully developed to deliver SIT. Based on the results obtained, sustained release GLZ pellets may be coated with other immediate release diabetic treatment agents to prepare novel FDC products for patients.

# Chapter 7:

# General Discussion

The overall aim of the work conducted throughout the thesis was to manufacture fixed dose combination (FDC) products for the treatment of type II diabetes and cardiovascular diseases (CVDs) making use of continuous, or semi-continuous manufacturing techniques. In chapter 3, monolithic FDC products with a single-phase immediate release (IR) profile for the treatment of hypertension were manufactured via spray drying (SD) and hot melt extrusion (HME) with the influence the manufacturing technique had on the final product being assessed. Chapter 4 also involved work with monolithic FDC products with single-phase IR profiles, however, in this instance products were produced via SD and melt granulation (MG) and are for use in the treatment of type II diabetes. The work associated with chapter 5 involved manufacturing a novel FDC product for the treatment of hypercholesterolemia and hypertension. A delayed release core was manufactured via HME with an IR layer added to the core via spray coating (SC) to ensure a biphasic release profile. Chapter 6 involved manufacturing a novel FDC product for the treatment of type II diabetes. A sustained release core was manufactured via HME with an IR layer added to the core via SC to ensure a biphasic release profile.

## 7.1 Spray drying vs. hot melt extrusion

In chapter 3, both SD and HME were used to manufacture a monolithic FDC product of hydrochlorothiazide (HCTZ) and ramipril (RAM). The combination is currently available on the market in various strengths throughout the world and as a result is a suitable combination to study the effects of different manufacturing techniques on formulation characteristics. The combination also suits the overall aim of manufacturing FDC products for the treatment of CVDs; in this case, hypertension. SD and HME can be versatile manufacturing techniques and can potentially be used to manufacture combinations with varying release profiles if required; SD through the use of 3 or 4 fluid nozzles or by using solution/suspension combinations in a 2 fluid nozzle (Cal and Sollohub 2010); HME through using 2 or more extruders in a process known as hot melt co-extrusion (HMCE) (Dierickx et al. 2012). For this study, as there are no known physical or chemical incompatibilities between the two active pharmaceutical ingredients (APIs) and the desired release profiles of the two APIs are the same, a 2-fluid nozzle spray dryer and a single extruder were used to produce the FDCs for comparison.

SD is a very versatile manufacturing technique, largely due to the vast amounts of solvents available for dissolving formulations. While it may be good from a manufacturing point of view to have such versatility with solvents, from an environmental point of view, a lot of these solvents are potentially harmful and ideally would be avoided altogether. HME on the other hand is seen as more environmentally friendly due to no solvents

being required but is not as versatile as SD due to the necessity for glass transition temperatures ($T_g$s) or melting temperatures ($T_m$s) of the formulation constitutes being appropriate to enable product manufacture. As a result, one of the limiting factors in this work for comparing formulations is choosing formulations that are suitable for processing by both manufacturing techniques.

Several studies have previously been carried out comparing SD to HME formulations and determining the influence the manufacturing technique has on physicochemical properties of the products (Agrawal et al. 2013; Mahmah et al. 2014). The work in chapter 3 differs from the work published in these papers as the physicochemical state of the products being compared was found to be different, i.e. the SD formulations are fully amorphous with the HME formulations being partially crystalline. In work published previously comparing SD and HME, all products were amorphous solid dispersions (ASDs). The partially crystalline component of the HME formulations results from incomplete amorphisation of the HCTZ API, as seen via PXRD. As the conditions used in this study are conducted well below the $T_m$ of HCTZ, amorphisation is reliant upon HCTZ's solubility in the other components of the formulations. As the quantity of HCTZ is not fully soluble, it remains partially crystalline. Another difference between work conducted in chapter 3 with other work that has been published previously is that the formulations contain two APIs whereas all other comparative work has been conducted on formulations with a single API.

RAM is a thermolabile API which starts to degrade upon melting at 115.99 ± 1.23 °C. As with any thermolabile API, this provides a challenge for processing via HME due to the thermal nature of the process. The two immediate release polymers chosen for the study, Kollidon® VA 64 and Soluplus®, require processing temperature conditions to be higher than the melting point of RAM due to their respective $T_g$s. The work with RAM in chapter 3 highlights the difficulty using HME with thermolabile APIs as RAM degrades using the process when the respective polymers are used alone. It also highlights, however, that when appropriate plasticisers are added to the formulations, avoiding degradation is possible, as processing can be conducted at lower temperatures. These results correspond well to the published literature where results have shown addition of suitable plasticisers in the HME process allow for lower processing temperatures avoiding thermal degradation of thermolabile APIs (Huang, O'Donnell, et al. 2017; Repka et al. 1999). When looking at the SD formulations, no degradation is seen with RAM due to the low temperatures the formulations are exposed to, as well as the use of appropriate solvents which do not degrade the APIs. While it is possible to overcome thermal degradation in HME, SD may provide an alternative if API degradation

temperatures are so low that even the addition of appropriate excipients make processing unrealistic.

Based on publications in the literature, amorphous materials have an increased dissolution rate and higher solubility compared to their crystalline counterparts (Hancock and Parks 2000; Leuner and Dressman 2000). The dissolution testing for chapter 3 was undertaken using a Wood's apparatus to negate any effects the particle size of the formulations would have on the dissolution profiles (Wood et al. 1965). The findings from the dissolution studies provided two interesting results. Firstly, the release from the partially crystalline HME formulations resulted in statistically significantly greater release profiles compared to the equivalent SD formulations for both APIs. On further investigation, it was found that the reason for this unusual result was due to the surface roughness differences attained during compression of the formulations. An increase in surface roughness can lead to increased turbulence at the hydrodynamic layer, leading to significant effects on the rate of dissolution. The hydrodynamic effects experienced by the HME formulations are hypothesised to compensate for partial crystallinity, resulting in the hydrodynamics having a greater influence over the dissolution release profiles than the effects of the solid state, when comparing HME to SD formulations. The second interesting finding from the dissolution experiments relate to both HME and SD formulations containing the Soluplus® polymer. Soluplus® is marketed as an immediate release polymer that increases the solubility of poorly soluble drugs (BASF 2010). In chapter 3, the results of the dissolution for formulations containing Soluplus® saw no release of the APIs regardless of manufacturing technique used. Several possible reasons for this were discussed and presented. Soluplus® has previously been shown to be soluble at pH 1.2 in the literature (Sun and Lee 2015), however, one of the monomer components that make up the polymer, polyvinyl caprolactam, is described as being soluble in cold water, but, is no longer water soluble above 35 °C (Kroker et al. 1995) which may result in reduced solubility of the polymer at the experimental temperature (37 °C). Soluplus® is known to enter solution as single polymer chains which then organize into uni-chain polymer micelles (BASF 2010). As the concentration of Soluplus® increases, the uni-chain micelles come together to form multi-chain ones. The lower critical solution temperature has been reported to be between 37 °C (Ali et al. 2009) and 40 °C (Cavallari et al. 2016) for Soluplus® and at these temperatures the aspect of multi-chain polymer micelles forming is more relevant, as the chains lose the hydration crown and progressively associate, decreasing their solubility and forming a cloudy suspension that can precipitate. This behaviour is responsible for the gel-forming property of Soluplus®, which in turn is the most likely cause of the formulations inability to release

the APIs (Cavallari et al. 2016). In conclusion, for formulations containing high amounts of polymers that can gel and swell, e.g. Soluplus®, dissolution testing can prove difficult.

In terms of long-term stability, the work carried out in chapter 3 comparing the SD and HME formulations showed the SD amorphous material to be more physically stable over the course of a 60-day stability trial. Both SD and HME formulations remained chemically stable throughout the study with no additional degradation products seen post initial processing. Experimental data was collected via PXRD, DSC and HPLC. Due to the HME formulations being partially crystalline after processing, the crystal components of the formulations may encourage further crystallisation of the amorphous content due to the crystalline form being more thermodynamically favorable. This results in the HME formulations being less physically stable. In comparison, only one of the SD formulations can be seen to start to crystallise in the study (formulation containing the plasticiser stored at the high humidity conditions). The ASDs prepared via SD can be classed as physically stable. As already stated, many examples exist of studies conducted comparing HME and SD formulations, with stability studies included. Overall, due to the large variations that can exist in processing, formulation composition, excipients and APIs used, there is no standard formula available to predict whether SD formulations or HME formulations will provide the greater long term physical and chemical stability of ASDs.

## 7.2 Spray drying vs. melt granulation

In chapter 4, work was conducted with the high dose API, metformin (MET), and sitagliptin phosphate (SIT), which are used for the treatment of type II diabetes. As with the HCTZ and RAM combination, the MET and SIT combination product is also currently available on the market as an immediate release formulation. The main difficulty in working with high dose APIs is the narrow scope for addition of excipients in order for the product to remain small enough for the patient to consume without difficulty, while also being able to be manufactured successfully via the chosen technique. SD and MG were the two techniques chosen to produce the monolithic FDC products due to the suitability for the addition of minimum amounts of excipients for processing. In the work carried out, the influence of the polymer composition on the final compressed caplet product was studied, as well as the influence each manufacturing technique played.

SD and MG have been successfully employed in the literature previously to improve the compressibility of high drug load tablets of MET (Al-Zoubi et al. 2017; Barot et al. 2010; Lakshman et al. 2011; Vaingankar and Amin 2017). Different grades of HPC polymers were chosen to test the influence of polymer composition, as these polymers have been

previously reported in the literature as being successfully used with MET (Vaingankar and Amin 2017; Vasanthavada et al. 2011). Again, as is the case in the literature with SD and HME, the majority of work conducted to date with MG focuses on one API rather than a combination of two or more. No known physical or chemical incompatibilities exist between MET and SIT, and they are suitable for processing together. While MG can be conducted in several different ways, the work carried out in chapter 4 focuses on the use of an extruder to produce granules. The use of an extruder offers many advantages for the MG process, including the capacity to generate high temperatures and high shear stress, as well as being able to seamlessly incorporate the machine into a continuous manufacturing process due to the ability of having a continued input and output of material.

Ultimately, the goal of the work was to formulate a final product that could be consumed by a patient. This means that the final product has to pass all the common compendial tests for immediate release oral tablets. When looking at the results, only one of the manufactured formulations, manufactured via MG, was deemed to be successful. As regards the composition make-up of the HPC polymers used, the method of manufacture had direct implications on how the polymers implemented their effects.

In the MG process, the viscosity of the different grades of HPC plays a significant role in the outcome of the final granule characteristics. HPC – S has a lower $T_g$ and lower molecular weight than the HPC – A polymer, resulting in a lower viscosity when in the liquid state. The formulations for both HPC polymers were subjected to the same conditions in the extruder and displayed similar residence times. During the process, the two APIs are subjected to the molten polymer allowing both physical mixing and chemical interactions to occur. The lower viscosity HPC – S, even though it has fewer potential hydrogen bonding sites, interacts more intimately than the higher molecular weight HPC – A due to the differences in viscosity, allowing better mixing over the timeframe in the extruder. In contrast, in the SD process, regarding hydrogen bonding between the APIs and polymers, the timeframe issue of exposure to hydrogen binding sites is not relevant. All contents are fully dissolved prior to SD, which allows for homogeneous distribution of the polymers and time to interact and form hydrogen bonds with the APIs upon processing. The higher molecular weight HPC – A, as stated, has more potential hydrogen binding sites compared to the HPC – S and as a result interacts more intimately.

## 7.3 Hot melt extrusion, spheronisation and spray coating

The work carried out in chapters 5 and 6, focused on developing novel FDC products through a HME - spheronisation - SC process. HME – spheronisation has been previously used in the literature to manufacture spherical pellets that have successfully produced products with varying release profiles (Bhaskaran and Lakshmi 2010; Young et al. 2002). The big advantage of using spherical pellets is that they freely disperse in the gastrointestinal tract, avoiding potential "dose dumping", while also offering flexibility for further modification. While spheronisation was attempted directly after cutting the extrudate into cylindrical pellets, it proved unsuccessful without the addition of heat into the spheronisation process. Once heat was applied, successful spheronisation was achieved, as shown in chapters 5 and 6. Depending on the polymer composition and desired release profiles of APIs, the HME – spheronisation process offers great flexibility. The process can also be adjusted to perform as a continuous manufacturing process, with the HME product being fed directly into a pelletiser followed by feeding into a spheroniser and applying heat. Once spherical, it is then possible to directly transfer the pellets into a FBD for coating. The HME – pelletisation - spheronisation – SC process may be considered an alternative method to produce biphasic release systems instead of hot melt coextrusion (HMCE). HMCE is the co-extrusion of two or more materials through the same die simultaneously, creating a multi-layered extrudate (Vynckier, Dierickx, Voorspoels, et al. 2014). It has several advantages associated with it, including fewer processing steps (than, for example, the extrusion – pelletisation – spheronisation - SC process explored here) and being a solvent free method. However, the process is also associated with many challenges, including requirements for similarity in extrusion temperature and appropriate adhesion between the extrusion layers. If there are major differences in the viscosity of the two layers of the co-extrudate, then it can become exceedingly difficult to form an acceptable extrudate product (Dierickx et al. 2012).

SC of an additional layer of API onto the spherical pellets proved successful to formulate final FDC products. With spherical pellets, the SC process is conducted to a higher standard due to even distribution of the SC layer when compared to cylindrical pellets which may be coated unevenly given their geometry. The SC step adds another layer of flexibility to the FDC product manufacture. The dose of API in the core spherical pellets can be determined by the quantity put forward for SC, i.e. the dosage is variable, while the quantity of SC layer applied to the core material can also be varied, depending on the desired dose.

In chapter 5 the core material was developed to produce a delayed release formulation of simvastatin (SIM). The polymers chosen were pH dependent polymers which prevented SIM from releasing in the more acidic environment of the stomach but allowed drug release in the higher pH of the small intestine. It is hoped that by protecting the drug from the hostile environment of the upper gastrointestinal tract, where cytochrome P450 enzymes that degrade SIM are numerous, that SIM therapeutic activity can be enhanced while also reducing adverse events associated with SIM, such as muscular myopathy or rhabdomyolysis (Tubic-Grozdanis et al. 2008). The work highlights the possibility of using HME to manufacture products with delayed release dissolution profiles that are also suitable to be spheronised with the addition of heat. As people being treated for hypercholesterolemia often also suffer from hypertension, the idea of adding HCTZ and RAM was to suitably target the two conditions with one formulation. HCTZ and RAM were added through SC using the Wurster method, which is a bottom spray feed mechanism. Several different polymers were trialled along with different solvents before a successful formulation was developed.

The first part of the work carried out in chapter 6 deals with the manufacture of gliclazide (GLZ), a thermolabile API, via the HME – spheronisation process previously described. The main issues focused on in this work relate to finding a suitable formulation for HME that results in no degradation of the API as well as the desired extended release profile, similar to the single API formulations available on the market. Unlike the work carried out in chapter 5, where the formulations focused on polymers with pH dependent solubility, the GLZ formulation relies on polymers that have pH independent release characteristics due to the varying pH of the gastrointestinal tract. Several issues were highlighted throughout the course of developing a suitable formulation. While the polymers chosen, Eudragit® RLPO and Eudragit® RSPO, have $T_g$s sufficiently low enough to process below the melting point of GLZ, the interactions between the polymers and the API caused a melting point depression of the API, meaning the addition of a suitable plasticiser was required to process at lower temperatures, while also avoiding excess torque and pressure in the extruder. This highlighted two important factors to take into consideration when working with thermolabile APIs in the HME process. One, interactions between APIs and polymers can cause depression of the melting point leading to thermal degradation at lower temperatures than initially suspected and, two, suitable plasticisers can reduce the processing temperatures required as well as reducing residency times. By reducing residency times and processing temperatures, chances of thermal degradation are greatly reduced. The work also highlights the role pH modifiers have in the HME process. As the processing temperature was satisfactorily reduced, the

presence of GLZ degradation resulted in the conclusion that the local pH of the molten polymers was also having an influence. By adding in meglumine, an alkalizing agent, the acidic degradation of GLZ, even at the low processing temperatures it was exposed to was prevented. pH modifiers are used throughout the literature (Pudlas et al. 2015; Taniguchi et al. 2014) in the HME process, with the work in chapter 6 corresponding well to these previously published findings.

As with chapter 5, the core formulation was successfully pelletized and spheronised with the addition of heat into the process. This allowed the addition of the immediate release layer of SIT to be coated onto the pellets, manufacturing our novel FDC product.

## Main Findings

- The method of manufacturing chosen to develop monolithic FDC products has a critical role to play in the final product outcome. Desired physicochemical characteristics are reliant upon the APIs, excipients and the conditions chosen to process the formulations.

- Both HME and MG can be viewed as more suitable environmentally friendly alternatives to SD for the production of monolithic FDC products.

- HME can be used successfully to manufacture thermolabile APIs through the appropriate use of low $T_g$ polymers, plasticisers, pH modifiers and appropriate processing conditions.

- A wide variety of FDC products can be manufactured via the continuous processing techniques discussed throughout the thesis with varying desired release profiles.

## Proposed future work

- Carry out Design of Experiment (DoE) studies on the developed optimised formulations to identify the critical parameters of the processes involved in HME, SD, MG and SC and how they affect the product outcome.

- Development of relevant Process Analytical Techniques (PAT) and Quality by Design (QbD) to optimise and implement the continuous process technologies for the manufacture of FDC products, e.g. Raman spectroscopy, Near-infrared spectroscopy, etc.

- Transfer of successful lab scaled formulations to bigger industrial scale manufacturing in conjunction with industry partners on the project.

- Conduct further stability studies of the optimised formulations with varying degrees of stresses.

- Identification and development of further unique FDC products for the treatment of type II diabetes and CVDs with varying release profiles and compatibilities.

## References

Abdul, Shajahan, Anil V. Chandewar, and Sunil B. Jaiswal. 2010. “A Flexible Technology for Modified-Release Drugs: Multiple-Unit Pellet System (MUPS).” *Journal of Controlled Release* 147(1):2–16.

Abebe, Admassu, Ilgaz Akseli, Omar Sprockel, et al. 2014. “Review of Bilayer Tablet Technology.” *International Journal of Pharmaceutics* 461(1–2):549–58.

Abernethy, Darrell R. and Janice B. Schwartz. 1999. “Calcium-Antagonist Drugs” edited by A. J. J. Wood. *New England Journal of Medicine* 341(19):1447–57.

Abiad, M. G., M. T. Carvajal, and O. H. Campanella. 2009. “A Review on Methods and Theories to Describe the Glass Transition Phenomenon: Applications in Food and Pharmaceutical Products.” *Food Engineering Reviews* 1(2):105–32.

Agrawal, Anjali M., Mayur S. Dudhedia, Ashwinkumar D. Patel, et al. 2013. “Characterization and Performance Assessment of Solid Dispersions Prepared by Hot Melt Extrusion and Spray Drying Process.” *International Journal of Pharmaceutics* 457(1):71–81.

Agrawal, Anjali M., Mayur S. Dudhedia, and Ewa Zimny. 2016. “Hot Melt Extrusion: Development of an Amorphous Solid Dispersion for an Insoluble Drug from Mini-Scale to Clinical Scale.” *AAPS PharmSciTech* 17(1):133–47.

Al-Zoubi, Nizar, Faten Odeh, and Ioannis Nikolakakis. 2017. “Co-Spray Drying of Metformin Hydrochloride with Polymers to Improve Compaction Behavior.” *Powder Technology* 307:163–74.

Ali, Shaukat, Nigel Langley, Dejan Djuric, et al. 2009. “Eye on Excipients.” *Basf* 4. Retrieved (https://industries.basf.com/bin/bws/documentDownload.en.8805804190165).

Ambike, Anshuman A., K. R. Mahadik, and Anant Paradkar. 2005. “Spray-Dried Amorphous Solid Dispersions of Simvastatin, a Low Tg Drug: In Vitro and in Vivo Evaluations.” *Pharmaceutical Research* 22(6):990–98.

Ambrosioni, E., C. Borghi, and FV Costa. 1987. “Captopril and Hydrochlorothiazide: Rationale for Their Combination.” *British Journal of Clinical Pharmacology* 23(1 S):43S–50S.

Ambühl, Philipp, Dominik Felix, and Mahesh C. Khosla. 1994. “[7-D-ALA]-Angiotensin-(1–7): Selective Antagonism of Angiotensin-(1–7) in the Rat Paraventricular Nucleus.” *Brain Research Bulletin* 35(4):289–91.

American Diabetes Association, American Diabetes. 2011. “Diagnosis and Classification of Diabetes Mellitus.” *Diabetes Care* 34 Suppl 1(Supplement 1):S62-9.

Amidon, G. L., H. Lennernäs, V. P. Shah, et al. 1995. “A Theoretical Basis for a

Biopharmaceutic Drug Classification: The Correlation of in Vitro Drug Product Dissolution and in Vivo Bioavailability." *Pharmaceutical Research* 12(3):413–20.

Andrews, Gavin, Shu Li, Ammar Almajaan, et al. 2019. "Fixed Dose Combination Formulations: Multi-Layered Platforms Designed for the Management of Cardiovascular Disease." *Molecular Pharmaceutics* acs.molpharmaceut.8b01068.

Andrienko, Denis. 2018. "Introduction to Liquid Crystals." *Journal of Molecular Liquids* 267:520–41.

Arai, Keiko and George P. Chrousos. 2000. *Aldosterone Deficiency and Resistance*.

Arndt, Oscar Rupert and Peter Kleinebudde. 2018. "Influence of Binder Properties on Dry Granules and Tablets." *Powder Technology* 337:68–77.

Aronoff, Stephen L. and Kathy Berkowitz. 2004. "Glucose Metabolism and Regulation: Beyond Insulin and Glucagon." *Diabetes Spectrum* 17(3).

Ashland. 2017. *Klucel Hydroxypropylcellulose, Physical and Chemical Properties.*

Aulton, Michael E. and Kevin Taylor. 2013. *Aulton's Pharmaceutics: The Design and Manufacture of Medicines*. Fourth edi. Elsevier Health Sciences,.

Babu, N. Jagadeesh, Suryanarayan Cherukuvada, Ranjit Thakuria, et al. 2010. "Conformational and Synthon Polymorphism in Furosemide (Lasix)." *Crystal Growth & Design* 10(4):1979–89.

Badens, Elisabeth, Viktor Majerik, G. Horvth, et al. 2009. "Comparison of Solid Dispersions Produced by Supercritical Antisolvent and Spray-Freezing Technologies." *International Journal of Pharmaceutics* 377(1–2):25–34.

Baghel, Shrawan, Helen Cathcart, and Niall J. O'Reilly. 2016. "Polymeric Amorphous Solid Dispersions: A Review of Amorphization, Crystallization, Stabilization, Solid-State Characterization, and Aqueous Solubilization of Biopharmaceutical Classification System Class II Drugs." *Journal of Pharmaceutical Sciences* 105(9):2527–44.

Baird, Jared A., Roberto Olayo-Valles, Carlos Rinaldi, et al. 2010. "Effect of Molecular Weight, Temperature, and Additives on the Moisture Sorption Properties of Polyethylene Glycol." *Journal of Pharmaceutical Sciences* 99(1):154–68.

Balimane, Praveen V., Yong-Hae Han, and Saeho Chong. 2006. "Current Industrial Practices of Assessing Permeability and P-Glycoprotein Interaction." *The AAPS Journal* 8(1):E1–13.

Bangalore, Sripal, Gayathri Kamalakkannan, Sanobar Parkar, et al. 2007. "Fixed-Dose Combinations Improve Medication Compliance: A Meta-Analysis." *American Journal of Medicine* 120(8):713–19.

Barnett, Richard. 2019. "Type 2 Diabetes." *The Lancet* 394(10198):557. Retrieved March 22, 2018 (https://www.diabetes.co.uk/type2-diabetes.html).

Barot, Bhavesh, Punit Parejiya, Tushar Patel, et al. 2010. “Development of Directly Compressible Metformin Hydrochloride by the Spray-Drying Technique.” *Acta Pharmaceutica* 60(2):165–75.

BASF. 2008. “Technical Information Kollidon®VA64.” *BASF SE Care Chemicals Division Pharma Ingredients & Services* (September 2007):1–12. Retrieved (https://industries.basf.com/bin/bws/documentDownload.en.8805243988437).

BASF. 2010. “Technical Information Soluplus.” *BASF, Pharma Ingredients & Services* (July):1–8. Retrieved (https://pharmaceutical.basf.com/en/Drug-Formulation/Soluplus.html).

Batra, Amol, Dipen Desai, and Abu T. M. Serajuddin. 2017. “Investigating the Use of Polymeric Binders in Twin Screw Melt Granulation Process for Improving Compactibility of Drugs.” *Journal of Pharmaceutical Sciences* 106(1):140–50.

Bauer, John, Stephen Spanton, Rodger Henry, et al. 2001. “Ritonavir: An Extraordinary Example of Conformational Polymorphism.” *Pharmaceutical Research* 18(6):859–66.

Bell, David S. H. 2006. “The Case for Combination Therapy as First-Line Treatment for the Type 2 Diabetic Patient.” *Treatments in Endocrinology* 5(3):131–37.

Benkerrour, Loutfy, Olivier Galley, Francoise Quinet, et al. 2004. “MULTILAYERED TABLET CONTAINING PRAVASTATIN AND ASPIRIN AND METHOD FIELD OF THE INVENTION.”

Bevernage, Jan, Joachim Brouwers, Pieter Annaert, et al. 2012. “Drug Precipitation–permeation Interplay: Supersaturation in an Absorptive Environment.” *European Journal of Pharmaceutics and Biopharmaceutics* 82(2):424–28.

Bharadia, P. D. and Vikram M. Pandya. 2014. *A Review on Aqueous Film Coating Technology*.

Bhaskaran, Shyamala and P. K. Lakshmi. 2010. *Extrusion Spheronization-A Review*. Vol. 2.

Bhatt, Prashant M. and Gautam R. Desiraju. 2007. “Tautomeric Polymorphism in Omeprazole.” *Chemical Communications (Cambridge, England)* (20):2057–59.

Binder, C. and I. Bendtson. 1992. “Endocrine Emergencies. Hypoglycaemia.” *Bailliere’s Clinical Endocrinology and Metabolism* 6(1):23–39.

Blatnik, Sandra Urek, Rok Dreu, and Stanko Srčič. 2015. “Influence of PH Modifiers on the Dissolution and Stability of Hydrochlorothiazide in the Bi- and Three-Layer Tablets.” *Acta Pharmaceutica* 65(4):383–97.

Blessy, M., Ruchi D. Patel, Prajesh N. Prajapati, et al. 2014. “Development of Forced Degradation and Stability Indicating Studies of Drugs—A Review.” *Journal of Pharmaceutical Analysis* 4(3):159–65.

Boussageon, Rémy, Irène Supper, Theodora Bejan-Angoulvant, et al. 2012. "Reappraisal of Metformin Efficacy in the Treatment of Type 2 Diabetes: A Meta-Analysis of Randomised Controlled Trials" edited by L. Groop. *PLoS Medicine* 9(4):e1001204.

Boza, A., I. Caraballo, JF Alvarez, et al. 1999. "Evaluation of Eudragit RS-PO and Ethocel 100 Matrices for the Controlled Release of Lobenzarit Disodium." *Drug Dev Ind Pharm.* 25:229–33.

Brayfield, Alison, ed. 2014. *Martindale - The Complete Drug Reference*. Thirty-eig. Pharmaceutical Press.

Bretnall, A. E. and S. G. Clarke. 1998. *Metformin Hydrochloride - Analytical Profiles of Drug Substances and Excipients. Volume 25*. edited by H. G. Brittain. Academic Press.

Brough, Chris and R. O. Williams. 2013. "Amorphous Solid Dispersions and Nano-Crystal Technologies for Poorly Water-Soluble Drug Delivery." *International Journal of Pharmaceutics* 453(1):157–66.

Brown, C. L., C. I. Backhouse, J. C. Grippat, et al. 1990. "The Effect of Perindopril and Hydrochlorothiazide Alone and in Combination on Blood Pressure and on the Renin-Angiotensin System in Hypertensive Subjects." *European Journal of Clinical Pharmacology* 39(4):327–32.

Brown, G. K. 2000. "Glucose Transporters: Structure, Function and Consequences of Deficiency." *Journal of Inherited Metabolic Disease* 23(3):237–46.

Brown, Morris J. 2006. "Direct Renin Inhibition - a New Way of Targeting the Renin System." *Journal of the Renin-Angiotensin-Aldosterone System* 7(2):S7–11.

BRUNNER, HANS R., HARALAMBOS GAVRAS, BERNARD WAEBER, et al. 1979. "Oral Angiotensin-Converting Enzyme Inhibitor in Long-Term Treatment of Hypertensive Patients." *Annals of Internal Medicine* 90(1):19.

Bryan, J. and L. Aguilar-Bryan. 1999. "Sulfonylurea Receptors: ABC Transporters That Regulate ATP-Sensitive K(+) Channels." *Biochimica et Biophysica Acta* 1461(2):285–303.

Byrn, S. R., R. R. Pfeiffer, G. Stephenson, et al. 1994. *Solid-State Pharmaceutical Chemistry Solid-State Pharmaceutical Chemistry Encompasses a Wide Range of Studies on Pharmaceutical Solids Including (1) Determination of the Physical Properties of Polymorphs and Solvates, (2) Physical Transformations*. Vol. 6.

Byrn, Stephen, Ralph Pfeiffer, Michael Ganey, et al. 1995. "Pharmaceutical Solids: A Strategic Approach to Regulatory Considerations." *Pharmaceutical Research* 12(7):945–54.

Cagno, Massimiliano di, Paul C. Stein, Jakub Styskala, et al. 2012. "Overcoming

Instability and Low Solubility of New Cytostatic Compounds: A Comparison of Two Approaches." *European Journal of Pharmaceutics and Biopharmaceutics* 80(3):657–62.

Cal, Krzysztof and Krzysztof Sollohub. 2010. "Spray Drying Technique. I: Hardware and Process Parameters." *Journal of Pharmaceutical Sciences* 99(2):575–86.

Caramella, Carla, Paolo Colombo, Ubaldo Conte, et al. 1988. "A Physical Analysis of the Phenomenon of Tablet Disintegration." *International Journal of Pharmaceutics* 44(1–3):177–86.

Carlson, L. A. 2005. "Nicotinic Acid: The Broad-Spectrum Lipid Drug. A 50th Anniversary Review." *Journal of Internal Medicine* 258(2):94–114.

Casale, Antonio. and Roger S. (Roger Stephen) Porter. 1979. *Polymer Stress Reactions, Volume 2*. Academic Press.

Catapano, A. 2001. "Ezetimibe: A Selective Inhibitor of Cholesterol Absorption." *European Heart Journal Supplements* 3(suppl_E):E6–10.

Cavallari, Cristina, Selenia Ternullo, Fabrizio Tarterini, et al. 2016. "Release Problems for Nifedipine in the Presence of Soluplus." 3(2):1–13.

Chemburkar, Sanjay, John Bauer, Kris Deming, et al. 2000. "Dealing with the Impact of Ritonavir Polymorphs on the Late Stages of Bulk Drug Process Development."

Cheong, Chelim, Jamie C. Barner, Kenneth A. Lawson, et al. 2008. "Patient Adherence and Reimbursement Amount for Antidiabetic Fixed-Dose Combination Products Compared with Dual Therapy among Texas Medicaid Recipients." *Clinical Therapeutics* 30(10):1893–1907.

Cheung, Hong-Son, Feng-Lai Wang, Miguel A. Ondetti, et al. 1980. "Binding of Peptide Substrates and Inhibitors of Angiotensin-Converting Enzyme IMPORTANCE OF T H E COOH-TERMINAL DIPEPTIDE SEQUENCE*." *JOURNAL OF BIOLOGICAL CHEMISTRY* 255(2):401–5.

Childs, Scott L., Leonard J. Chyall, A. E. Bretnall, et al. 2004. "A Metastable Polymorph of Metformin Hydrochloride: Isolation and Characterization Using Capillary Crystallization and Thermal Microscopy Techniques." *Crystal Growth & Design* 4(3):441–49.

Childs, Scott L. and Kenneth I. Hardcastle. 2007. "Cocrystals of Piroxicam with Carboxylic Acids." *Crystal Growth & Design* 7(7):1291–1304.

Chowhan, Z. T. 1979. "Moisture, Hardness, Disintegration and Dissolution Interrelationships in Compressed Tablets Prepared by the Wet Granulation Process." *Drug Development and Industrial Pharmacy* 5(1):41–62.

Chrysant, S. G. 1994. "Antihypertensive Effectiveness of Low-Dose Lisinopril-Hydrochlorothiazide Combination. A Large Multicenter Study. Lisinopril-

Hydrochlorothiazide Group." *Archives of Internal Medicine* 154(7):737–43.

Conway, J. and P. Lauwers. 1960. "Hemodynamic and Hypotensive Effects of Long-Term Therapy with Chlorothiazide." *Circulation* 21:21–27.

Costantino, Henry R., Laleh Firouzabadian, Chichih Wu, et al. 2002. "Protein Spray Freeze Drying. 2. Effect of Formulation Variables on Particle Size and Stability." *Journal of Pharmaceutical Sciences* 91(2):388–95.

Couchman, P. R. 1978. "Compositional Variation of Glass-Transition Temperatures. 2. Application of the Thermodynamic Theory to Compatible Polymer Blends." *Macromolecules* 11(6):1156–61.

Couchman, P. R. and F. E. Karasz. 1978. "A Classical Thermodynamic Discussion of the Effect of Composition on Glass-Transition Temperatures." *Macromolecules* 11(1):117–19.

Craig, Duncan Q. M. 1995. "A Review of Thermal Methods Used for the Analysis of the Crystal Form, Solution Thermodynamics and Glass Transition Behaviour of Polyethylene Glycols." *Thermochimica Acta* 248(C):189–203.

Crowley, Michael M., Zhang Feng. 2007. "Pharmaceutical Applications of Hot-Melt Extrusion: Part I Review Article." *Drug Development and Industrial Pharmacy* 33(August 2016):909–26.

Crowley, Michael M., Feng Zhang, Michael A. Repka, et al. 2007. "Pharmaceutical Applications of Hot-Melt Extrusion: Part I." *Drug Development and Industrial Pharmacy* 33(9):909–26.

Dangel, C., G. Schepky, H. B. Reich, et al. 2000. "Comparative Studies with Kollicoat MAE 30 D and Kollicoat MAE 30 DP in Aqueous Spray Dispersions and Enteric Coatings on Highly Swellable Caffeine Cores." *Drug Development and Industrial Pharmacy* 26(4):415–21.

Dashevsky, A., K. Kolter, and R. Bodmeier. 2004. "Compression of Pellets Coated with Various Aqueous Polymer Dispersions." *International Journal of Pharmaceutics* 279(1–2):19–26.

Davit, Barbara M., Isadore Kanfer, Yu Chung Tsang, et al. 2016. "BCS Biowaivers: Similarities and Differences Among EMA, FDA, and WHO Requirements." *The AAPS Journal* 18(3):612–18.

Deacon, C. F., M. A. Nauck, M. Toft-Nielsen, et al. 1995. "Both Subcutaneously and Intravenously Administered Glucagon-Like Peptide I Are Rapidly Degraded From the NH2-Terminus in Type II Diabetic Patients and in Healthy Subjects." *Diabetes* 44(9):1126–31.

Desai, Divyakant, Jennifer Wang, Hong Wen, et al. 2013. "Formulation Design, Challenges, and Development Considerations for Fixed Dose Combination (FDC) of

Oral Solid Dosage Forms." *Pharmaceutical Development and Technology* 18(6):1265–76.

Descamps, M., J. F. Willart, E. Dudognon, et al. 2007. "Transformation of Pharmaceutical Compounds upon Milling and Comilling: The Role of Tg." *Journal of Pharmaceutical Sciences* 96(5):1398–1407.

Diabetes.co.uk. 2018. "Type 1 Diabetes." Retrieved March 21, 2018 (https://www.diabetes.co.uk/type1-diabetes.html).

Diabetes Prevention Program Research Group. 2002. "Reduction in the Incidence of Type 2 Diabetes with Lifestyle Intervention or Metformin." *N Engl J Med* 346(6):393–403.

Dierickx, L., L. Saerens, A. Almeida, et al. 2012. "Co-Extrusion as Manufacturing Technique for Fixed-Dose Combination Mini-Matrices." *European Journal of Pharmaceutics and Biopharmaceutics* 81(3):683–89.

DiNunzio, James C., Chris Brough, Justin R. Hughey, et al. 2010. "Fusion Production of Solid Dispersions Containing a Heat-Sensitive Active Ingredient by Hot Melt Extrusion and Kinetisol® Dispersing." *European Journal of Pharmaceutics and Biopharmaceutics* 74(2):340–51.

Djuris, Jelena, Ioannis Nikolakakis, Svetlana Ibric, et al. 2013. "Preparation of Carbamazepine-Soluplus Solid Dispersions by Hot-Melt Extrusion, and Prediction of Drug-Polymer Miscibility by Thermodynamic Model Fitting." *European Journal of Pharmaceutics and Biopharmaceutics* 84(1):228–37.

Donnelly, Conor, Yiwei Tian, Catherine Potter, et al. 2015. "Probing the Effects of Experimental Conditions on the Character of Drug-Polymer Phase Diagrams Constructed Using Flory-Huggins Theory." *Pharmaceutical Research* 32(1):167–79.

Dressman, J. B. (Jennifer B. .. and Johannes Krämer. 2005. *Pharmaceutical Dissolution Testing*. Taylor & Francis.

Dressman, Jennifer B. 1986. "Comparison of Canine and Human Gastrointestinal Physiology." *Pharmaceutical Research* 03(3):123–31.

Drucker, Daniel J. and Michael A. Nauck. 2006. "The Incretin System: Glucagon-like Peptide-1 Receptor Agonists and Dipeptidyl Peptidase-4 Inhibitors in Type 2 Diabetes." *The Lancet* 368(9548):1696–1705.

Duarte, Julio D. and Rhonda M. Cooper-DeHoff. 2010. "Mechanisms for Blood Pressure Lowering and Metabolic Effects of Thiazide and Thiazide-like Diuretics." *Expert Review of Cardiovascular Therapy* 8(6):793–802.

Dunn, Peter J., Andrew S. Wells, and Michael T. Williams. 2010. "Future Trends for Green Chemistry in the Pharmaceutical Industry." in *Green Chemistry in the Pharmaceutical Industry*. Weinheim, Germany: Wiley-VCH Verlag GmbH & Co.

KGaA.

Van Eerdenbrugh, Bernard and Lynne S. Taylor. 2011. “Application of Mid-IR Spectroscopy for the Characterization of Pharmaceutical Systems.” *International Journal of Pharmaceutics* 417(1–2):3–16.

Eisai Global. 2018. “World’s First Bile Acid Transporter Inhibitor ‘GOOFICE® 5mg Tablet’ Launched in Japan | News Release：2018 | Eisai Co., Ltd.” Retrieved February 7, 2019 (https://www.eisai.com/news/2018/news201833.html).

Elliott, William J. and C. Venkata S. Ram. 2011. “Calcium Channel Blockers.” *The Journal of Clinical Hypertension* 13(9):687–89.

Ellison, D. H., H. Velazquez, and F. S. Wright. 1987. “Thiazide-Sensitive Sodium Chloride Cotransport in Early Distal Tubule.” *American Journal of Physiology-Renal Physiology* 253(3):F546–54.

EMA. 2017. *Committee for Human Medicinal Products (CHMP) Guideline on Clinical Development of Fixed Combination Medicinal Products*.

Erdös, E. G. 1977. “The Angiotensin I Converting Enzyme.” *Federation Proceedings* 36(5):1760–65.

European Medicines Agency. 2019. *M9 Step 2b on Biopharmaceutics Classification System Based Biowaivers*.

European Pharmacopoeia. 2020a. “2.9.1. Disintegration of Table... - European Pharmacopoeia 10.0.” Retrieved January 18, 2020 (https://pheur.edqm.eu/app/10-0/content/10-0/20901E.htm?highlight=on&terms=disintegration).

European Pharmacopoeia. 2020b. “2.9.7. Friability of Uncoated ... - European Pharmacopoeia 10.0.” Retrieved January 18, 2020 (https://pheur.edqm.eu/app/10-0/content/10-0/20907E.htm?highlight=on&terms=friability).

European Pharmacopoeia. 2020c. “Hydrochlorothiazide Tablets - European Pharmacopoeia.” Retrieved January 18, 2020 (https://www.pharmacopoeia.com/bp-2020/formulated-specific/hydrochlorothiazide-tablets.html?date=2020-01-01&text=Hydrochlorothiazide).

European Pharmacopoeia. 2020d. “Metformin Tablets - European Pharmacopoeia.” Retrieved January 18, 2020 (https://www.pharmacopoeia.com/bp-2020/formulated-specific/metformin-tablets.html?date=2020-01-01&text=Metformin).

European Pharmacopoeia. 2020e. “Ramipril Tablets - European Pharmacopoeia.” Retrieved January 18, 2020 (https://www.pharmacopoeia.com/bp-2020/formulated-specific/ramipril-tablets.html?date=2020-01-01&text=ramipril).

European Pharmacopoeia. 2020f. “Sitagliptin Tablets - European Pharmacopoeia .” Retrieved January 18, 2020 (https://pheur.edqm.eu/app/10-0/content/10-

0/2927E.htm?highlight=on&terms=2927).

Evans, D. F., G. Pye, R. Bramley, et al. 1988. “Measurement of Gastrointestinal PH Profiles in Normal Ambulant Human Subjects.” *Gut* 29(8):1035–41.

Evans, Marc, Aled Roberts, and Alan Rees. 2003. “Pharmacological Management of Hyperlipidaemia.” *The British Journal of Diabetes & Vascular Disease* 3(3):204–10.

Fagerholm, Urban. 2008. “The Role of Permeability in Drug ADME/PK, Interactions and Toxicity—Presentation of a Permeability-Based Classification System (PCS) for Prediction of ADME/PK in Humans.” *Pharmaceutical Research* 25(3):625–38.

Fasano, Alessio. 1998. “Novel Approaches for Oral Delivery of Macromolecules.” *Journal of Pharmaceutical Sciences* 87(11):1351–56.

FDA. 2018. “CFR - Code of Federal Regulations Title 21.” Retrieved January 22, 2019 (https://www.accessdata.fda.gov/scripts/cdrh/cfdocs/cfcfr/CFRSearch.cfm?fr=210.3)

FDA, CDER, Purdie, et al. 2017. *Waiver of In Vivo Bioavailability and Bioequivalence Studies for Immediate-Release Solid Oral Dosage Forms Based on a Biopharmaceutics Classification System Guidance for Industry*.

FDA, U.S. Department of Health and Human Services, and Center for Drug Evaluation and Research. 2006. *Guidance for Industry Fixed Dose Combinations, Co-Packaged Drug Products, and Single-EntityVersions of Previously Approved Antiretrovirals for the Treatment of HIV Guidance for Industry Fixed Dose Combinations, Co-Packaged Drug Products, and Single-Entity*.

FDA, U.S. Department of Health and Human Services, and Center for Drug Evaluation and Research. 2007. *Guidance for Industry User Fee Waivers for FDC and Co-Packaged HIV Drugs for PEPFAR*.

Felder, Richard M., Ronald W. Rousseau, and Lisa G. Bullard. 2015. *Elementary Principles of Chemical Processes*.

Fell, J. T. and J. M. Newton. 1970. “Determination of Tablet Strength by the Diametral-Compression Test.” *Journal of Pharmaceutical Sciences* 59(5):688–91.

Ferrario, C. M. 1998. “Angiotension-(1-7) and Antihypertensive Mechanisms.” *Journal of Nephrology* 11(6):278–83.

Fischer, Mary A. 2008. “Implanon: A New Contraceptive Implant.” *Journal of Obstetric, Gynecologic & Neonatal Nursing* 37(3):361–68.

Fitzpatrick, J. .., T. Iqbal, C. Delaney, et al. 2004. “Effect of Powder Properties and Storage Conditions on the Flowability of Milk Powders with Different Fat Contents.” *Journal of Food Engineering* 64(4):435–44.

Folkow, Björn, Börje Johansson, and Stefan Mellander. 1961. “The Comparative Effects of Angiotensin and Noradrenaline on Consecutive Vascular Sections.” *Acta Physiologica Scandinavica* 53(2):99–104.

Fox, Alyson J., Umesh G. Lalloo, Maria G. Belvisi, et al. 1996. “Bradykinin–evoked Sensitization of Airway Sensory Nerves: A Mechanism for ACE–inhibitor Cough.” *Nature Medicine* 2(7):814–17.

Fox, T. G. 1956. “Influence of Diluent and of Copolymer Composition on the Glass Temperature of a Polymer System.” *The Bulletin of the American Physical Society* 1:123–32.

Freeman, R. E., J. R. Cooke, and L. C. R. Schneider. 2009. “Measuring Shear Properties and Normal Stresses Generated within a Rotational Shear Cell for Consolidated and Non-Consolidated Powders.” *Powder Technology* 190(1–2):65–69.

Freeman, Reg. 2007. “Measuring the Flow Properties of Consolidated, Conditioned and Aerated Powders — A Comparative Study Using a Powder Rheometer and a Rotational Shear Cell.” *Powder Technology* 174(1–2):25–33.

Friesen, Dwayne T., Ravi Shanker, Marshall Crew, et al. 2008. “Hydroxypropyl Methylcellulose Acetate Succinate-Based Spray-Dried Dispersions: An Overview.” *Molecular Pharmaceutics* 5(6):1003–19.

Fule, Ritesh, Vivek Paithankar, and Purnima Amin. 2016. “Hot Melt Extrusion Based Solid Solution Approach: Exploring Polymer Comparison, Physicochemical Characterization and in-Vivo Evaluation.” *International Journal of Pharmaceutics* 499(1–2):280–94.

Gandhi, Lal Kaul C, and Panchagnula. 1999. “Extrusion and Spheronization in the Development of Oral Controlled-Release Dosage Forms.” *Pharmaceutical Science & Technology Today* 4(2):160–70.

Gao, Yan, Zhonggang Li, Min Sun, et al. 2010. “Preparation, Characterization, Pharmacokinetics, and Tissue Distribution of Curcumin Nanosuspension with TPGS as Stabilizer.” *Drug Development and Industrial Pharmacy* 36(10):1225–34.

Garekani, H. A., J. L. Ford, M. H. Rubinstein, et al. 1999. “Formation and Compression Characteristics of Prismatic Polyhedral and Thin Plate-like Crystals of Paracetamol.” *International Journal of Pharmaceutics* 187(1):77–89.

Gautam, Chandler S. and Lekha Saha. 2008. “Fixed Dose Drug Combinations (FDCs): Rational or Irrational: A View Point.” *British Journal of Clinical Pharmacology* 65(5):795–96.

Gerbino, Philip P. and Omar Shoheiber. 2007. “Adherence Patterns among Patients Treated with Fixed-Dose Combination versus Separate Antihypertensive Agents.” *American Journal of Health-System Pharmacy : AJHP : Official Journal of the American Society of Health-System Pharmacists* 64(12):1279–83.

Gerich, John E., M. Arthur Charles, and Gerold M. Grodsky. 1974. “Characterization of the Effects of Arginine and Glucose on Glucagon and Insulin Release from the

Perfused Rat Pancreas." *The Journal of Clinical Endocrinology & Metabolism.* 77–82.

Ghadi, Rohan and Neha Dand. 2017. "BCS Class IV Drugs: Highly Notorious Candidates for Formulation Development." *Journal of Controlled Release* 248:71–95.

Ghebre-Sellassie, I., R. H. Gordon, R. U. Nesbitt, et al. 1987. "Evaluation of Acrylic-Based Modified-Release Film Coatings." *International Journal of Pharmaceutics* 37(3):211–18.

Gibaldi, Milo and Stuart Feldman. 1967. "Establishment of Sink Conditions in Dissolution Rate Determinations. Theoretical Considerations and Application to Nondisintegrating Dosage Forms." *Journal of Pharmaceutical Sciences* 56(10):1238–42.

Gille, Andreas, Erik T. Bodor, Kashan Ahmed, et al. 2008. "Nicotinic Acid: Pharmacological Effects and Mechanisms of Action." *Annual Review of Pharmacology and Toxicology* 48(1):79–106.

Giron, D., M. Mutz, and S. Garnier. 2004. "Solid-State of Pharmaceutical Compounds." *Journal of Thermal Analysis and Calorimetry* 77(2):709–47.

Goldbeck, Gerhard, Elna Pidcock, and Colin R. Groom. 2011. "Solid Form Informatics for Pharmaceuticals and Agrochemicals: Knowledge-Based Substance Development and Risk Assessment." *Cambridge Crystallographic Data Centre* 1–8.

Gordon, Manfred and James S. Taylor. 1952. "Ideal Copolymers and the Second-Order Transitions of Synthetic Rubbers. i. Non-Crystalline Copolymers." *Journal of Applied Chemistry* 2(9):493–500.

Gorre, Frauke and Hans Vandekerckhove. 2010. "Beta-Blockers: Focus on Mechanism of Action. Which Beta-Blocker, When and Why?" *Acta Cardiologica* 65(5):565–70.

Graffner, H., P. G. Gillberg, L. Rikner, et al. 2016. "The Ileal Bile Acid Transporter Inhibitor A4250 Decreases Serum Bile Acids by Interrupting the Enterohepatic Circulation." *Alimentary Pharmacology & Therapeutics* 43(2):303–10.

Grant, David J. W. 1999. *Polymorphism in Pharmaceutical Solids*. New York: M. Dekker.

Grassi, Guido, Raffaella Dell'Oro, Gino Seravalle, et al. 2002. "Short- and Long-Term Neuroadrenergic Effects of Moderate Dietary Sodium Restriction in Essential Hypertension." *Circulation* 106(15):1957–61.

Grbic, Sandra, Jelena Parojcic, Svetlana Ibric, et al. 2011. "In Vitro-in Vivo Correlation for Gliclazide Immediate-Release Tablets Based on Mechanistic Absorption Simulation." *AAPS PharmSciTech* 12(1):165–71.

Grymonpré, W., G. Verstraete, V. Vanhoorne, et al. 2018. "Downstream Processing from Melt Granulation towards Tablets: In-Depth Analysis of a Continuous Twin-Screw Melt Granulation Process Using Polymeric Binders." *European Journal of*

*Pharmaceutics and Biopharmaceutics* 124:43–54.

Guns, Sandra, Aswin Dereymaker, Pieterjan Kayaert, et al. 2011. “Comparison between Hot-Melt Extrusion and Spray-Drying for Manufacturing Solid Dispersions of the Graft Copolymer of Ethylene Glycol and Vinylalcohol.” *Pharmaceutical Research* 28(3):673–82.

Günther, Daniel, Bastian Heymel, Johannes Franz Günther, et al. 2014. “Continuous 3D-Printing for Additive Manufacturing.” *Rapid Prototyping Journal* 20(4):320–27.

Guo, Yuanyuan, Jun Luo, Songwei Tan, et al. 2013. “The Applications of Vitamin E TPGS in Drug Delivery.” *European Journal of Pharmaceutical Sciences* 49(2):175–86.

Guo, Zhiguo, Xueli Chen, Yang Xu, et al. 2015. “Effect of Granular Shape on Angle of Internal Friction of Binary Granular System.” *Fuel* 150:298–304.

Gupta, Simerdeep Singh, Tapan Parikh, Anuprabha K. Meena, et al. 2015. “Effect of Carbamazepine on Viscoelastic Properties and Hot Melt Extrudability of Soluplus (R).” *International Journal of Pharmaceutics* 478(1):232–39.

Gupta, Simerdeep Singh, Nayan Solanki, and Abu T. M. Serajuddin. 2016. “Investigation of Thermal and Viscoelastic Properties of Polymers Relevant to Hot Melt Extrusion, IV: Affinisol™ HPMC HME Polymers.” *AAPS PharmSciTech* 17(1):148–57.

Gylling, Helena and Piia Simonen. 2015. “Phytosterols, Phytostanols, and Lipoprotein Metabolism.” *Nutrients* 7(9):7965–77.

Hancock, Bruno C. 2002. “Disordered Drug Delivery : Destiny, Dynamics and the Deborah Number.” *Pharmacy and Pharmacology* (54):737–46.

Hancock, Bruno C. and Michael Parks. 2000. “What Is the True Solubility Advantage for Amorphous Pharmaceuticals?” *Pharmaceutical Research* 17(4):397–404.

Hancock, Bruno C., Sheri L. Shamblin, and George Zografi. 1995. “Molecular Mobility of Amorphous Pharmaceutical Solids Below Their Glass Transition Temperatures.” *Pharmaceutical Research* 12(6):799–806.

Hanyšová, L., M. Václavková, J. Dohnal, et al. 2005. “Stability of Ramipril in the Solvents of Different PH.” *Journal of Pharmaceutical and Biomedical Analysis* 37(5):1179–83.

Hao, Jing, Rosa Rodriguez-Monguio, and Enrique Seoane-Vazquez. 2015. “Fixed-Dose Combination Drug Approvals, Patents and Market Exclusivities Compared to Single Active Ingredient Pharmaceuticals.” *PLoS ONE* 10(10):1–13.

Hauner, Hans. 2002. “The Mode of Action of Thiazolidinediones.” *Diabetes/Metabolism Research and Reviews* 18 Suppl 2:S10-5.

Healy, Anne-Marie, Owen Corrigan, and J. E. M. Allen. 1995. “The Effect of Dissolution on the Surface Texture of Model Solid-Dosage Forms as Assessed by Non-Contact Laser Profilometry.” *Pharmaceutical Technology Europe* 9:14–22.

Healy, Anne Marie and O. I. Corrigan. 1996. “The Influence of Excipient Particle Size, Solubility and Acid Strength on the Dissolution of an Acidic Drug from Two-Component Compacts.” *International Journal of Pharmaceutics* 143(2):211–21.

Healy, Anne Marie, L. G. McCarthy, K. M. Gallagher, et al. 2002. “Sensitivity of Dissolution Rate to Location in the Paddle Dissolution Apparatus.” *The Journal of Pharmacy and Pharmacology* 54(3):441–44.

Healy, Anne Marie, Zelalem Ayenew Worku, Dinesh Kumar, et al. 2017. “Pharmaceutical Solvates, Hydrates and Amorphous Forms: A Special Emphasis on Cocrystals.” *Advanced Drug Delivery Reviews* 117:25–46.

Heart UK. 2019. “What Are Triglycerides & Lowering Triglycerides Levels | HEART UK | Expert Advice from HEART UK.” Retrieved February 6, 2019 (https://heartuk.org.uk/health-and-high-cholesterol/triglycerides).

Hendriksen, B. A. 1991. “Characterization of Calcium Fenoprofen: 3. Mechanism of Dissolution from Rotating Discs.” *International Journal of Pharmaceutics* 75(1):63–72.

Holtzman, Carol W., Barbara S. Wiggins, and Sarah A. Spinler. 2006. “Role of P-Glycoprotein in Statin Drug Interactions.” *Pharmacotherapy* 26(11):1601–7.

Holz, G. G., W. M. Kühtreiber, J. F. Habener, et al. 1993. “Pancreatic Beta-Cells Are Rendered Glucose-Competent by the Insulinotropic Hormone Glucagon-like Peptide-1(7-37).” *Nature* 361(6410):362–65.

Homayouni, Alireza, Fatemeh Sadeghi, Ali Nokhodchi, et al. 2015. “Preparation and Characterization of Celecoxib Dispersions in Soluplus((R)): Comparison of Spray Drying and Conventional Methods.” *Iranian Journal of Pharmaceutical Research : IJPR* 14(1):35–50.

Home, P. D., N. P. Jones, S. J. Pocock, et al. 2007. “Rosiglitazone RECORD Study: Glucose Control Outcomes at 18 Months.” *Diabetic Medicine : A Journal of the British Diabetic Association* 24(6):626–34.

Hu, Jun, Wai Kiong Ng, Yuancai Dong, et al. 2011. “Continuous and Scalable Process for Water-Redispersible Nanoformulation of Poorly Aqueous Soluble APIs by Antisolvent Precipitation and Spray-Drying.” *International Journal of Pharmaceutics* 404(1–2):198–204.

Huang, Siyuan, Kevin P. O. Donnell, Sophie M. Delpon, et al. 2017. “European Journal of Pharmaceutics and Biopharmaceutics Processing Thermally Labile Drugs by Hot-Melt Extrusion : The Lesson With.” *European Journal of Pharmaceutics and Biopharmaceutics* 119:56–67.

Huang, Siyuan, Kevin P. O’Donnell, Sophie M. Delpon de Vaux, et al. 2017. “Processing Thermally Labile Drugs by Hot-Melt Extrusion: The Lesson with Gliclazide.”

*European Journal of Pharmaceutics and Biopharmaceutics* 119:56–67.

Huang, Siyuan, Kevin P. O'Donnell, Justin M. Keen, et al. 2016. "A New Extrudable Form of Hypromellose: AFFINISOL™ HPMC HME." *AAPS PharmSciTech* 17(1):106–19.

Hughey, Justin R., Justin M. Keen, Dave A. Miller, et al. 2013. "The Use of Inorganic Salts to Improve the Dissolution Characteristics of Tablets Containing Soluplus(R)-Based Solid Dispersions." *European Journal of Pharmaceutical Sciences : Official Journal of the European Federation for Pharmaceutical Sciences* 48(4–5):758–66.

Ige, Pradum Pundlikrao and Surendra Ganeshlal Gattani. 2012. "Design and in Vitro and in Vivo Characterization of Mucoadhesive Matrix Pellets of Metformin Hydrochloride for Oral Controlled Release: A Technical Note." *Archives of Pharmacal Research* 35(3):487–98.

Inzucchi, Silvio E., Richard M. Bergenstal, John B. Buse, et al. 2012. "Management of Hyperglycemia in Type 2 Diabetes: A Patient-Centered Approach." *Diabetes Care* 35(6):1364–79.

Irish Heart Foundation. 2019a. "Irish Heart Cholesterol - Irish Heart." Retrieved February 6, 2019 (https://irishheart.ie/your-health/ways-to-live-better/cholesterol/).

Irish Heart Foundation. 2019b. "Irish Heart Heart Attack - Irish Heart." Retrieved February 6, 2019 (https://irishheart.ie/heart-and-stroke-conditions-a-z/heart-attack/).

De Jaeghere, W., T. De Beer, J. Van Bocxlaer, et al. 2015. "Hot-Melt Extrusion of Polyvinyl Alcohol for Oral Immediate Release Applications." *International Journal of Pharmaceutics* 492(1–2):1–9.

Jagdale, Swati C., Yashwant T. Dangat, and Bhanudas S. Kuchekar. 2013. "Solubility Enhancement and Formulation of Buccal Patches of Ramipril Cyclodextrin Complex." *Asian Journal of Pharmaceutical and Clinical Research* 6(2):83–90.

Javeer, Sharadchandra Dagadu, Rahul Patole, and Purnima Amin. 2013. "Enhanced Solubility and Dissolution of Simvastatin by HPMC-Based Solid Dispersions Prepared by Hot Melt Extrusion and Spray-Drying Method." *Journal of Pharmaceutical Investigation* 43(6):471–80.

Jenike, A. W. 1964. "Storage and Flow of Solids." *Bulletin 123, Engineering Experiment Station, University of Utah, USA*.

Joslin, Elliott P. and C. Ronald. Kahn. 2005. *Joslin's Diabetes Mellitus.* Lippincott Williams & Willkins.

Jun, Seoung Wook, Min-Soo Kim, Jeong-Soo Kim, et al. 2007. "Preparation and Characterization of Simvastatin/Hydroxypropyl-β-Cyclodextrin Inclusion Complex Using Supercritical Antisolvent (SAS) Process." *European Journal of Pharmaceutics and Biopharmaceutics* 66(3):413–21.

Kahn, S. E., R. L. Prigeon, D. K. McCulloch, et al. 1993. "Quantification of the

Relationship between Insulin Sensitivity and Beta-Cell Function in Human Subjects. Evidence for a Hyperbolic Function." *Diabetes* 42(11):1663–72.

Kahn, Steven E., Mark E. Cooper, and Stefano Del Prato. 2014. "Pathophysiology and Treatment of Type 2 Diabetes: Perspectives on the Past, Present, and Future." *The Lancet* 383(9922):1068–83.

Kahn, Steven E., Steven M. Haffner, Mark A. Heise, et al. 2006. "Glycemic Durability of Rosiglitazone, Metformin, or Glyburide Monotherapy." *New England Journal of Medicine* 355(23):2427–43.

Kang, Bok Ki, Jin Soo Lee, Se Kang Chon, et al. 2004. "Development of Self-Microemulsifying Drug Delivery Systems (SMEDDS) for Oral Bioavailability Enhancement of Simvastatin in Beagle Dogs." *International Journal of Pharmaceutics* 274(1–2):65–73.

Kawabata, Yohei, Koichi Wada, Manabu Nakatani, et al. 2011. "Formulation Design for Poorly Water-Soluble Drugs Based on Biopharmaceutics Classification System: Basic Approaches and Practical Applications." *International Journal of Pharmaceutics* 420(1):1–10.

Kell, Douglas B., Paul D. Dobson, Elizabeth Bilsland, et al. 2013. "The Promiscuous Binding of Pharmaceutical Drugs and Their Transporter-Mediated Uptake into Cells: What We (Need to) Know and How We Can Do So." *Drug Discovery Today* 18(5–6):218–39.

Kell, Douglas B., Paul D. Dobson, and Stephen G. Oliver. 2011. "Pharmaceutical Drug Transport: The Issues and the Implications That It Is Essentially Carrier-Mediated Only." *Drug Discovery Today* 16(15–16):704–14.

Kestur, Umesh S. and Lynne S. Taylor. 2010. "Role of Polymer Chemistry in Influencing Crystal Growth Rates from Amorphous Felodipine." *CrystEngComm* 12(8):2390.

Kieffer, T. J., C. H. McIntosh, and R. A. Pederson. 1995. "Degradation of Glucose-Dependent Insulinotropic Polypeptide and Truncated Glucagon-like Peptide 1 in Vitro and in Vivo by Dipeptidyl Peptidase IV." *Endocrinology* 136(8):3585–96.

Kim, Sang-Hyun, Sang-Ho Jo, Sang-Cheol Lee, et al. 2016. "Blood Pressure and Cholesterol-Lowering Efficacy of a Fixed-Dose Combination With Irbesartan and Atorvastatin in Patients With Hypertension and Hypercholesterolemia: A Randomized, Double-Blind, Factorial, Multicenter Phase III Study." *Clinical Therapeutics* 38(10):2171–84.

Kim, Wook and Josephine M. Egan. 2008. "The Role of Incretins in Glucose Homeostasis and Diabetes Treatment." *Pharmacological Reviews* 60(4):470–512.

Kirchhoff, Anne C., Melinda L. Drum, James X. Zhang, et al. 2008. "Hypertension and Hyperlipidemia Management in Patients Treated at Community Health Centers."

*Journal of Clinical Outcomes Management : JCOM* 15(3):125–31.

Kitabchi, Abbas E., Guillermo E. Umpierrez, John M. Miles, et al. 2009. “Hyperglycemic Crises in Adult Patients With Diabetes.” *Diabetes Care* 32(7):1335–43.

Klein, A. and V. P. Shah. 2008. “A Standardized Mini Paddle Apparatus as an Alternative to the Standard Paddle.” *AAPS PharmSciTech* 9(4):1179–84.

Kolter, K., A. Dashevsky, Muhamad Irfan, et al. 2013. “Polyvinyl Acetate-Based Film Coatings.” *International Journal of Pharmaceutics* 457(2):470–79.

Kolter, K. and D. Flick. 2000. “Structure and Dry Binding Activity of Different Polymers, Including Kollidon® VA 64.” *Drug Development and Industrial Pharmacy* 26(11):1159–65.

Kolter, K., Matthias Karl, and Andreas Gryczke. 2012. “Hot-Melt Extrusion with BASF Pharma Polymers.” *Hot-Melt Extrusion with BASF Pharma Polymers* 1–201. Retrieved (https://industries.basf.com/images/global/corp/Pharmaceuticals1/03_120803_hot_melt_extrusion_with_basf_pharma_polymers.pdf).

Kolter, Karl, Michael Schonerr, and Hermann Ascherl. 2001. “Solid Oral Dosage Forms with Delayed Release of Active Ingredient and High Mechanical Stability.”

Konno, Hajime and Lynne S. Taylor. 2008. “Ability of Different Polymers to Inhibit the Crystallization of Amorphous Felodipine in the Presence of Moisture.” *Pharmaceutical Research* 25(4):969–78.

Kroker, Jorg, Reinhard Schneider, Eberhard Schupp, et al. 1995. “Process for Preparing Aqueous Solutions of Poly(N-Vinyl-ε-Caprolactam) and Their Use.” Retrieved February 19, 2018 (https://patents.google.com/patent/US5739195).

Ku, M. Sherry and Wendy Dulin. 2012. “A Biopharmaceutical Classification-Based Right-First-Time Formulation Approach to Reduce Human Pharmacokinetic Variability and Project Cycle Time from First-In-Human to Clinical Proof-Of-Concept.” *Pharmaceutical Development and Technology* 17(3):285–302.

Kulkarni, C., A. L. Kelly, T. Gough, et al. 2018. “Application of Hot Melt Extrusion for Improving Bioavailability of Artemisinin a Thermolabile Drug.” *Drug Development and Industrial Pharmacy* 44(2):206–14.

Kwan, Henry K. and Stephen M. Liebowitz. 1992. “Stable Extended Release Oral Dosage Composition Comprising Loratadine and Pseudoephedrine.”

Kwei, T. K., Eli M. Pearce, John R. Pennacchia, et al. 1987. “Correlation between the Glass Transition Temperatures of Polymer Mixtures and Intermolecular Force Parameters.” *Macromolecules* 20(5):1174–76.

Lakshman, Jay P., James Kowalski, Madhav Vasanthavada, et al. 2011. “Application of Melt Granulation Technology to Enhance Tabletting Properties of Poorly

Compactible High-Dose Drugs." *Journal of Pharmaceutical Sciences* 100(4):1553–65.

Lang, Bo, James W. McGinity, and Robert O. Williams. 2014. "Hot-Melt Extrusion – Basic Principles and Pharmaceutical Applications." *Drug Development and Industrial Pharmacy* 40(9):1133–55.

Lee, Alfred Y., Deniz Erdemir, and Allan S. Myerson. 2011. "Crystal Polymorphism in Chemical Process Development." *Annual Review of Chemical and Biomolecular Engineering* 2(1):259–80.

Lee, S. .. 2015. "Modernizing Pharmaceutical Manufacturing: From Batch to Continuous Production." *Journal of Pharmaceutical Innovation* 10(3):191–99.

Lee, Sau(Larry). 2017. "Modernizing the Way Drugs Are Made: A Transition to Continuous Manufacturing." Retrieved February 19, 2018 (https://www.fda.gov/Drugs/NewsEvents/ucm557448.htm).

Lee, Y. J., Y. J. Lee, and H. J. Han. 2007. "Regulatory Mechanisms of Na + /Glucose Cotransporters in Renal Proximal Tubule Cells." *Kidney International* 72(SUPPL. 106):S27–35.

Lennernaäs, Hans. 1998. "Human Intestinal Permeability." *Journal of Pharmaceutical Sciences* 87(4):403–10.

Leppert, Wojciech. 2014. "Oxycodone/Naloxone in the Management of Patients with Pain and Opioid–Induced Bowel Dysfunction." *Current Drug Targets* 15(1):124–35.

Leuner, Christian and Jennifer Dressman. 2000. "Improving Drug Solubility for Oral Delivery Using Solid Dispersions." *European Journal of Pharmaceutics and Biopharmaceutics* 50(1):47–60.

Leung, Lap Yin, Chen Mao, Ishan Srivastava, et al. 2017. "Flow Function of Pharmaceutical Powders Is Predominantly Governed by Cohesion, Not by Friction Coefficients." *Journal of Pharmaceutical Sciences* 106(7):1865–73.

Lewis, James D., Laurel A. Habel, Charles P. Quesenberry, et al. 2015. "Pioglitazone Use and Risk of Bladder Cancer and Other Common Cancers in Persons With Diabetes." *JAMA* 314(3):265.

Lin, Dexi and Yanbin Huang. 2010. "A Thermal Analysis Method to Predict the Complete Phase Diagram of Drug–polymer Solid Dispersions." *International Journal of Pharmaceutics* 399(1):109–15.

Lin, Yi and Zhongjie Sun. 2010. "Current Views on Type 2 Diabetes." *Journal of Endocrinology* 204:1–11.

Lindberg, Nils-Olof, Magnus Pålsson, Ann-Christin Pihl, et al. 2004. "Flowability Measurements of Pharmaceutical Powder Mixtures with Poor Flow Using Five Different Techniques." *Drug Development and Industrial Pharmacy* 30(7):785–91.

Linn, Michael, Eva Maria Collnot, Dejan Djuric, et al. 2012. “Soluplus® as an Effective Absorption Enhancer of Poorly Soluble Drugs in Vitro and in Vivo.” *European Journal of Pharmaceutical Sciences* 45(3):336–43.

Lopez, Felipe L., Terry B. Ernest, Catherine Tuleu, et al. 2015. “Formulation Approaches to Pediatric Oral Drug Delivery: Benefits and Limitations of Current Platforms.” *Expert Opinion on Drug Delivery* 12(11):1727–40.

Madhavi, K., A. Shikha, and B. Suresh. 2016. “Formulation and in Vitro Characterization Solid Self Emulsifying Drug Delivery System of Ramipril Prepared by Adsorption Technique.” *International Journal of Current Pharmaceutical Research* 8(1):40–45.

Mahmah, Osama, Rami Tabbakh, Adrian Kelly, et al. 2014. “A Comparative Study of the Effect of Spray Drying and Hot-Melt Extrusion on the Properties of Amorphous Solid Dispersions Containing Felodipine.” *Journal of Pharmacy and Pharmacology* 66(2):275–84.

Makower, Benjamin and W. B. Dye. 1956. “Equilibrium Moisture Content and Crystallization of Amorphous Sucrose and Glucose.” *Journal of Agricultural and Food Chemistry* 4(1):72–77.

Malaisse, Willy J. 2003. “Pharmacology of the Meglitinide Analogs: New Treatment Options for Type 2 Diabetes Mellitus.” *Treatments in Endocrinology* 2(6):401–14.

Mamenko, Mykola, Oleg Zaika, and Oleh Pochynyuk. 2014. “Direct Regulation of ENaC by Bradykinin in the Distal Nephron. Implications for Renal Sodium Handling.” *Current Opinion in Nephrology and Hypertension* 23(2):122–29.

Mancia, G. and G. Grassi. 2010. “Management of Essential Hypertension.” *British Medical Bulletin* 94(1):189–99.

Mandal, Uttam and Tapan Kumar Pal. 2008. “Formulation and In Vitro Studies of a Fixed-Dose Combination of a Bilayer Matrix Tablet Containing Metformin HCl as Sustained Release and Glipizide as Immediate Release.” *Drug Development and Industrial Pharmacy* 34(3):305–13.

Maniruzzaman, Mohammed and Ali Nokhodchi. 2016. “Title: Continuous Manufacturing via Hot-Melt Extrusion and Scale up: Regulatory Matters.” *Drug Discovery Today*.

Maniruzzaman, Mohammed and Ali Nokhodchi. 2017. “Continuous Manufacturing via Hot-Melt Extrusion and Scale up: Regulatory Matters.” *Drug Discovery Today* 22(2):340–51.

Marek, Tamás, Károly Süvegh, István Kéry, et al. 2007. “The Effect of Plasticizer on the Ageing of Metolose Films.” *Radiation Physics and Chemistry* 76(2):165–68.

Markl, Daniel and J. Axel Zeitler. 2017. “A Review of Disintegration Mechanisms and Measurement Techniques.” *Pharmaceutical Research* 34(5):890–917.

Marks, V. and J. D. Teale. 1999. “Drug-Induced Hypoglycemia.” *Endocrinology and*

*Metabolism Clinics of North America* 28(3):555–77.

Mascia, Salvatore, Patrick L. Heider, Haitao Zhang, et al. 2013. “End-to-End Continuous Manufacturing of Pharmaceuticals: Integrated Synthesis, Purification, and Final Dosage Formation.” *Angewandte Chemie International Edition* 52(47):12359–63.

Masters, K. (Keith). 2002. *Spray Drying in Practice*. Charlottenlund: SprayDryConsult.

Mayo Clinic. 2018a. “Diabetes - Symptoms and Causes - Mayo Clinic.” Retrieved March 21, 2018 (https://www.mayoclinic.org/diseases-conditions/diabetes/symptoms-causes/syc-20371444).

Mayo Clinic. 2018b. “Type 1 Diabetes - Symptoms and Causes - Mayo Clinic.” Retrieved March 21, 2018 (https://www.mayoclinic.org/diseases-conditions/type-1-diabetes/symptoms-causes/syc-20353011).

Mayo Clinic. 2019a. “Alpha Blockers - Mayo Clinic.” Retrieved February 2, 2019 (https://www.mayoclinic.org/diseases-conditions/high-blood-pressure/in-depth/alpha-blockers/art-20044214?pg=1).

Mayo Clinic. 2019b. “High Cholesterol - Symptoms and Causes - Mayo Clinic.” Retrieved February 5, 2019 (https://www.mayoclinic.org/diseases-conditions/high-blood-cholesterol/symptoms-causes/syc-20350800).

Mayo Clinic. 2019c. “Stroke - Symptoms and Causes - Mayo Clinic.” Retrieved February 2, 2019 (https://www.mayoclinic.org/diseases-conditions/stroke/symptoms-causes/syc-20350113).

medicines.ie. 2018. “Januvia 25mg, 50mg, 100mg Film-Coated Tablets - Summary of Product Characteristics (SPC).” Retrieved February 4, 2019 (http://www.medicines.ie/medicine/15284/SPC/Januvia+25mg%2C+50mg%2C+100mg+film-coated+tablets/).

medicines.ie. 2019a. “Actos Tablets - Summary of Product Characteristics (SPC).” Retrieved February 5, 2019 (http://www.medicines.ie/medicine/11442/SPC/Actos+tablets/#CONTRAINDICATIONS).

medicines.ie. 2019b. “Cozaar 12.5mg, 50mg & 100mg Film-Coated Tablets - Summary of Product Characteristics (SPC).” Retrieved February 5, 2019 (http://www.medicines.ie/medicine/14518/SPC/Cozaar+12.5mg%2C+50mg+%26+100mg+Film-coated+Tablets/#PHARMACODYNAMIC_PROPS).

medicines.ie. 2019c. “Diamicron 80mg Tablets - Summary of Product Characteristics (SmPC) - (EMC).” Retrieved July 16, 2019 (https://www.medicines.org.uk/emc/product/1150/smpc#PHARMACOKINETIC_PROPS).

medicines.ie. 2019d. “Diamicron MR 30 Mg - Summary of Product Characteristics

(SPC).” Retrieved February 5, 2019 (http://www.medicines.ie/medicine/1789/SPC/Diamicron#PHARMACODYNAMIC_PROPS).

medicines.ie. 2019e. “NovoNorm 0.5 Mg, 1 Mg and 2 Mg Tablets - Summary of Product Characteristics (SPC).” Retrieved February 1, 2019 (http://www.medicines.ie/medicine/5976/SPC).

medicines.ie. 2019f. “Victoza 6 Mg/Ml Solution for Injection in Pre-Filled Pen - Summary of Product Characteristics (SPC).” Retrieved February 2, 2019 (http://www.medicines.ie/medicine/14374/SPC/Victoza+6+mg+ml+solution+for+injection+in+pre-filled+pen/).

medicines.org.uk. 2019. “Starlix 60mg Film Coated Tablets - Summary of Product Characteristics (SmPC) - (EMC).” Retrieved February 4, 2019 (https://www.medicines.org.uk/emc/medicine/4622).

Medicines and Healthcare products Regulatory Agency. 2019a. “Ezetrol 10mg Tablets - Summary of Product Characteristics (SmPC) - (EMC).” Retrieved January 21, 2019 (https://www.medicines.org.uk/emc/product/6792/smpc).

Medicines and Healthcare products Regulatory Agency. 2019b. “Simvastatin 20mg - Summary of Product Characteristics (SmPC) - (EMC).” Retrieved January 21, 2019 (https://www.medicines.org.uk/emc/product/5686/smpc).

Van Melkebeke, Barbara, Brenda Vermeulen, Chris Vervaet, et al. 2006. “Melt Granulation Using a Twin-Screw Extruder: A Case Study.” *International Journal of Pharmaceutics* 326(1–2):89–93.

Mentlein, Rolf. 1999. “Dipeptidyl-Peptidase IV (CD26)-Role in the Inactivation of Regulatory Peptides.” *Regulatory Peptides* 85(1):9–24.

Merck. 2016. “Glucophage Film-Coated Tablets - Summary of Product Characteristics (SPC).” Retrieved March 26, 2018 (http://www.medicines.ie/medicine/3578/SPC/Glucophage+Film-Coated+Tablets/#PHARMACODYNAMIC_PROPS).

Miller, Jonathan M., Benjamin M. Collman, Landon R. Greene, et al. 2005. “Identifying the Stable Polymorph Early in the Drug Discovery–Development Process.” *Pharmaceutical Development and Technology* 10(2):291–97.

Moneghini, Mariarosa, Nicola De Zordi, Dario Solinas, et al. 2010. “Characterization of Solid Dispersions of Itraconazole and Vitamin E TPGS Prepared by Microwave Technology.” *Future Medicinal Chemistry* 2(2):237–46.

Motola, Soloman, Alan Branfman, Gary Agisim, et al. 1989. “Acid Addition Salt of Ibuprofen and Meglumine.”

Muscari, Antonio, Giovanni M. Puddu, and Paolo Puddu. 2002. “Lipid-Lowering Drugs:

Are Adverse Effects Predictable and Reversible?" *Cardiology* 97(3):115–21.

Nagai, T., S. Obara, H. Kokubo, et al. 1997. *Application of HPMC and HPMCA Aqueous Film Coating of Pharmaceutical Dosage Forms. In Aqueous Polymeric Coatings for Pharmaceutical Dosage Forms*. 2nd ed. edited by J. W. McGinity. New York: Marcel Dekker INc.

Nangia, Ashwini. 2008. "Conformational Polymorphism in Organic Crystals." *Accounts of Chemical Research* 41(5):595–604.

Nathan, D. M., J. B. Buse, M. B. Davidson, et al. 2006. "Management of Hyperglycemia in Type 2 Diabetes: A Consensus Algorithm for the Initiation and Adjustment of Therapy: A Consensus Statement from the American Diabetes Association and the European Association for the Study of Diabetes." *Diabetes Care* 29(8):1963–72.

National Institute for Clinical Excellence. 2016. "Recommendations | Cardiovascular Disease: Risk Assessment and Reduction, Including Lipid Modification | Guidance | NICE." Retrieved May 15, 2019 (https://www.nice.org.uk/guidance/cg181/chapter/1-Recommendations#identifying-and-assessing-cardiovascular-disease-cvd-risk-2).

National Institute for Clinical Excellence. 2018. "Algorithm for Blood Glucose Lowering Therapy in Adults with Type 2 Diabetes." Retrieved February 1, 2019 (https://www.nice.org.uk/guidance/ng28/resources/algorithm-for-blood-glucose-lowering-therapy-in-adults-with-type-2-diabetes-pdf-2185604173).

National Institute for Health & Clinical Excellence. 2019. "Hypertension in Adults: Diagnosis and Management | Guidance and Guidelines | NICE." Retrieved February 2, 2019 (https://www.nice.org.uk/guidance/cg127/chapter/Key-priorities-for-implementation).

Nauck, M. A., G. Meininger, D. Sheng, et al. 2007. "Efficacy and Safety of the Dipeptidyl Peptidase-4 Inhibitor, Sitagliptin, Compared with the Sulfonylurea, Glipizide, in Patients with Type 2 Diabetes Inadequately Controlled on Metformin Alone: A Randomized, Double-Blind, Non-Inferiority Trial." *Diabetes, Obesity and Metabolism* 9(2):194–205.

Nissen, Steven E. and Kathy Wolski. 2007. "Effect of Rosiglitazone on the Risk of Myocardial Infarction and Death from Cardiovascular Causes." *New England Journal of Medicine* 356(24):2457–71.

Noyes, Arthur A. and Willis R. Whitney. 1897. "The Rate of Solution of Solid Substances in Their Own Solutions." *Journal of the American Chemical Society* 19(12):930–34.

O'Neill, Maryadele J., ed. 2013. *The Merck Index : An Encyclopedia of Chemicals, Drugs, and Biologicals*. Fifteenth. Royal Society of Chemistry.

Obermuller, N., P. Bernstein, H. Velazquez, et al. 1995. "Expression of the Thiazide-Sensitive Na-Cl Cotransporter in Rat and Human Kidney." *American Journal of*

*Physiology-Renal Physiology* 269(6):F900–910.

Oneda, F. and M. I. Ré. 2003. “The Effect of Formulation Variables on the Dissolution and Physical Properties of Spray-Dried Microspheres Containing Organic Salts.” *Powder Technology* 130(1):377–84.

Oswald, Patrick, Pawel Pieranski, and Pawel Pieranski. 2005. *Smectic and Columnar Liquid Crystals*. Vol. 20056744. CRC Press.

Pan, Feng, Michael E. Chernew, and A. Mark Fendrick. 2008. “Impact of Fixed-Dose Combination Drugs on Adherence to Prescription Medications.” *Journal of General Internal Medicine* 23(5):611–14.

Panneerselvam, M., R. Natrajan, S. Selvaraj, et al. 2010. “A Novel Drug-Drug Solid Dispersion of Hydrochlorothiazide - Losartan Potassium.” *International Jounal of Pharma and Biosciences* 1(4):68–80.

Papich, Mark G. and Marilyn N. Martinez. 2015. “Applying Biopharmaceutical Classification System (BCS) Criteria to Predict Oral Absorption of Drugs in Dogs: Challenges and Pitfalls.” *The AAPS Journal* 17(4):948–64.

Paradkar, Anant, Anshuman A. Ambike, Bhimrao K. Jadhav, et al. 2004. “Characterization of Curcumin-PVP Solid Dispersion Obtained by Spray Drying.” *International Journal of Pharmaceutics* 271(1–2):281–86.

Paradkar, Anant, Adrian Kelly, Phil Coates, et al. 2009. “Shear and Extensional Rheology of Hydroxypropyl Cellulose Melt Using Capillary Rheometry.” *Journal of Pharmaceutical and Biomedical Analysis* 49(2):304–10.

Parikh, Dilip M. 2010. *Handbook of Pharmaceutical Granulation Technology*. Informa Healthcare USA.

Passerini, Nadia, Beatrice Albertini, Marisa L. González-Rodríguez, et al. 2002. “Preparation and Characterisation of Ibuprofen-Poloxamer 188 Granules Obtained by Melt Granulation.” *European Journal of Pharmaceutical Sciences : Official Journal of the European Federation for Pharmaceutical Sciences* 15(1):71–78.

Patil, Moreshwar Pandharinath and Naresh Janardan Gaikwad. 2011. “Characterization of Gliclazide-Polyethylene Glycol Solid Dispersion and Its Effect on Dissolution.” *Brazilian Journal of Pharmaceutical Sciences* 47(1):161–66.

Patra, Ch. Niranjan, Richa Priya, Suryakanta Swain, et al. 2017. “Pharmaceutical Significance of Eudragit: A Review.” *Future Journal of Pharmaceutical Sciences* 3(1):33–45.

Paudel, Amrit, Jan Van Humbeeck, and Guy Van den Mooter. 2010. “Theoretical and Experimental Investigation on the Solid Solubility and Miscibility of Naproxen in Poly(Vinylpyrrolidone).” *Molecular Pharmaceutics* 7(4):1133–48.

Paudel, Amrit, Zelalem Ayenew Worku, Joke Meeus, et al. 2013. “Manufacturing of Solid

Dispersions of Poorly Water Soluble Drugs by Spray Drying: Formulation and Process Considerations." *International Journal of Pharmaceutics* 453(1):253–84.

Pearnchob, Nantharat and Roland Bodmeier. 2003. "Dry Polymer Powder Coating and Comparison with Conventional Liquid-Based Coatings for Eudragit® RS, Ethylcellulose and Shellac." *European Journal of Pharmaceutics and Biopharmaceutics* 56(3):363–69.

Percy, Samuel R. 1872. "Improvement in Drying and Concentrating Liquid Substances by Atomizing."

Perfetti, Giacomo, Thibault Alphazan, W. J. Wildeboer, et al. 2012. "Thermo-Physical Characterization of Pharmacoat® 603, Pharmacoat® 615 and Mowiol® 4-98." *Journal of Thermal Analysis and Calorimetry* 109(1):203–15.

Picker-Freyer, Katharina M. and Thomas Dürig. 2007. "Physical Mechanical and Tablet Formation Properties of Hydroxypropylcellulose: In Pure Form and in Mixtures." *AAPS PharmSciTech* 8(4):82.

Piñero-Piloña, Antonio and Philip Raskin. 2001. "Idiopathic Type 1 Diabetes." *Journal of Diabetes and Its Complications* 15(6):328–35.

Pitt, Kendal G. and Matthew G. Heasley. 2013. "Determination of the Tensile Strength of Elongated Tablets." *Powder Technology* 238:169–75.

Plakogiannis, Roda, Henry Cohen, and David Taft. 2005. "Effects of Morning versus Evening Administration of Atorvastatin in Patients with Hyperlipidemia." *American Journal of Health-System Pharmacy* 62(23):2491–94.

Podczeck, Fridrun and Yasmin Mia. 1996. "The Influence of Particle Size and Shape on the Angle of Internal Friction and the Flow Factor of Unlubricated and Lubricated Powders." *International Journal of Pharmaceutics* 144(2):187–94.

Poudel, ReshamRaj. 2013. "Renal Glucose Handling in Diabetes and Sodium Glucose Cotransporter 2 Inhibition." *Indian Journal of Endocrinology and Metabolism* 17(4):588.

Preis, Maren. 2015. "Orally Disintegrating Films and Mini-Tablets—Innovative Dosage Forms of Choice for Pediatric Use." *AAPS PharmSciTech* 16(2):234–41.

Priyadarshini, Rosy, Gouranga Nandi, Abhijit Changder, et al. 2016. "Gastroretentive Extended Release of Metformin from Methacrylamide-g-Gellan and Tamarind Seed Gum Composite Matrix." *Carbohydrate Polymers* 137:100–110.

Process Worldwide. 2019. "Coating Goes Conti." Retrieved August 20, 2019 (https://www.process-worldwide.com/coating-goes-conti-a-856570/).

Proud, D. and A. P. Kaplan. 1988. "Kinin Formation: Mechanisms and Role in Inflammatory Disorders." *Annual Review of Immunology* 6(1):49–83.

Pudlas, Marieke, Samuel O. Kyerematen, Leonardo A. M. Williams, et al. 2015.

"Analyzing the Impact of Different Excipients on Drug Release Behavior in Hot-Melt Extrusion Formulations Using FTIR Spectroscopic Imaging." *European Journal of Pharmaceutical Sciences* 67:21–31.

Qiao, Mingxi, Liqiang Zhang, Yingliang Ma, et al. 2013. "A Novel Electrostatic Dry Coating Process for Enteric Coating of Tablets with Eudragit® L100-55." *European Journal of Pharmaceutics and Biopharmaceutics* 83(2):293–300.

Quodbach, Julian and Peter Kleinebudde. 2015. "A Critical Review on Tablet Disintegration." *Pharmaceutical Development and Technology* 1–12.

Radwan, A., M. Wagner, GL Amidon, et al. 2014. "Bio-Predictive Tablet Disintegration: Effect of Water Diffusivity, Fluid Flow, Food Composition and Test Conditions." *European Journal of Pharmaceutical Sciences : Official Journal of the European Federation for Pharmaceutical Sciences* 57:273–79.

Rajabi-Siahboomi, Ali R. 2017. "Overview of Multiparticulate Systems for Oral Drug Delivery." Pp. 1–4 in. Springer, New York, NY.

Ramirez, Elena, Olga Laosa, Pedro Guerra, et al. 2010. "Acceptability and Characteristics of 124 Human Bioequivalence Studies with Active Substances Classified According to the Biopharmaceutic Classification System." *British Journal of Clinical Pharmacology* 70(5):694–702.

Rang, H. P., J. M. Ritter, R. J. Flower, et al. 2015. *Rang & Dale's Pharmacology*. 8th ed. Churchill Livingstone.

Rao, Monica, Yogesh Mandage, Kaushik Thanki, et al. 2010. "Dissolution Improvement of Simvastatin by Surface Solid Dispersion Technology." *Dissolution Technologies*.

Ratanatriwong, Puntarika and Sheryl Barringer. 2007. "Particle Size, Cohesiveness and Charging Effects on Electrostatic and Nonelectrostatic Powder Coating." *Journal of Electrostatics* 65(10–11):704–8.

Raza, Kaisar. 2014. "Polymorphism: The Phenomenon Affecting the Performance of Drugs." *SOJ Pharmacy & Pharmaceutical Sciences*.

Reading, M., A. Luget, and R. Wilson. 1994. "Modulated Differential Scanning Calorimetry." *Thermochimica Acta* 238:295–307.

Rebitski, Ediana P., Pilar Aranda, Margarita Darder, et al. 2018. "Intercalation of Metformin into Montmorillonite." *Dalton Transactions* 47(9):3185–92.

Regier, Loren and Sharon Downey. 1997. "Calcium Channel Blockers."

Repka, M. a, T. G. Gerding, S. L. Repka, et al. 1999. "Influence of Plasticizers and Drugs on the Physical-Mechanical Properties of Hydroxypropylcellulose Films Prepared by Hot Melt Extrusion." *Drug Development and Industrial Pharmacy* 25(5):625–33.

Repka, Michael a, Sunil Kumar Battu, Sampada B. Upadhye, et al. 2007. "Pharmaceutical Applications of Hot-Melt Extrusion: Part II." *Drug Development and*

*Industrial Pharmacy* 33(10):1043–57.

Reynolds, Jonathan Kent, Joshua J. Neumiller, and R. Keith Campbell. 2008. “Janumet ™ : A Combination Product Suitable for Use in Patients with Type 2 Diabetes.” *Expert Opinion on Investigational Drugs* 17(10):1559–65.

Ridker, P. M., C. L. Gaboury, P. R. Conlin, et al. 1993. “Stimulation of Plasminogen Activator Inhibitor in Vivo by Infusion of Angiotensin II. Evidence of a Potential Interaction between the Renin-Angiotensin System and Fibrinolytic Function.” *Circulation* 87(6):1969–73.

Riekes, Manoela Kl??ppel, Gislaine Kuminek, Gabriela Schneider Rauber, et al. 2014. “HPMC as a Potential Enhancer of Nimodipine Biopharmaceutical Properties via Ball-Milled Solid Dispersions.” *Carbohydrate Polymers* 99:474–82.

Risch, Sara J. 1995. “Encapsulation: Overview of Uses and Techniques.” Pp. 2–7 in.

Russell-Jones, D., A. Vaag, O. Schmitz, et al. 2009. “Liraglutide vs Insulin Glargine and Placebo in Combination with Metformin and Sulfonylurea Therapy in Type 2 Diabetes Mellitus (LEAD-5 Met+SU): A Randomised Controlled Trial.” *Diabetologia* 52(10):2046–55.

Sachan, Nikhil K., A. Bhattacharya, Seema Pushkar, et al. 2014. “Biopharmaceutical Classification System: A Strategic Tool for Oral Drug Delivery Technology.” *Asian Journal of Pharmaceutics (AJP): Free Full Text Articles from Asian J Pharm* 3(2).

Sahoo, J., P. N. Murthy, S. Biswal, et al. 2009. “Formulation of Sustained-Release Dosage Form of Verapamil Hydrochloride by Solid Dispersion Technique Using Eudragit RLPO or Kollidon®SR.” *AAPS PharmSciTech* 10(1):27–33.

Sahoo, SK, S. Dhal, P. Mohapatro, et al. 2007. “Effect of Processing Temperature on Eudragit RSPO Microsphere Characteristics in the Solvent Evaporation Process.” *Pharmazie* 62:638–39.

Saleem, I., K. Petkar, and S. Somavarapu. 2017. “Rationale for Pulmonary Vaccine Delivery: Formulation and Device Considerations.” *Micro and Nanotechnology in Vaccine Development* 357–71.

Sanphui, Palash, V. Kusum Devi, Deepa Clara, et al. 2015. “Cocrystals of Hydrochlorothiazide: Solubility and Diffusion/ Permeability Enhancements through Drug−Coformer Interactions.” *Molecular Pharmaceutics* 12(5):1615–1622.

Sarkar, Debjani, Gouranga Nandi, Abhijit Changder, et al. 2017. “Sustained Release Gastroretentive Tablet of Metformin Hydrochloride Based on Poly (Acrylic Acid)-Grafted-Gellan.” *International Journal of Biological Macromolecules* 96:137–48.

Sarode, Ashish, Peng Wang, Catherine Cote, et al. 2013. “Low-Viscosity Hydroxypropylcellulose (HPC) Grades SL and SSL: Versatile Pharmaceutical Polymers for Dissolution Enhancement, Controlled Release, and Pharmaceutical

Processing." *AAPS PharmSciTech* 14(1):151.

Sastry, Srikonda V., Michael D. Degennaro, Lndra K. Reddy, et al. 1997. "Atenolol Gastrointestinal Therapeutic System. I. Screening of Formulation Variables." *Drug Development and Industrial Pharmacy* 23(2):157–65.

Sastry, Srikonda Venkateswara, Janaki Ram Nyshadham, and Joseph A. Fix. 2000. "Recent Technological Advances in Oral Drug Delivery – a Review." *Pharmaceutical Science & Technology Today* 3(4):138–45.

Schaber, Spencer D., Dimitrios I. Gerogiorgis, Rohit Ramachandran, et al. 2011. "Economic Analysis of Integrated Continuous and Batch Pharmaceutical Manufacturing: A Case Study." *Industrial & Engineering Chemistry Research* 50(17):10083–92.

Schaefer, T. 1992. "Melt Pelletization in a High Shear Mixer I. Effects of Process Variables and Binder." *Acta Pharm. Nord.* 4:133–40.

Schæfer, Torben and Christina Mathiesen. 1996. "Melt Pelletization in a High Shear Mixer. VIII. Effects of Binder Viscosity." *International Journal of Pharmaceutics* 139(1–2):125–38.

Schilling, Sandra U., Hélène L. Lirola, Navnit H. Shah, et al. 2010. "Influence of Plasticizer Type and Level on the Properties of Eudragit S100 Matrix Pellets Prepared by Hot-Melt Extrusion." *Journal of Microencapsulation* 27(6):521–32.

Schilling, Sandra U., Navnit H. Shah, a Waseem Malick, et al. 2007. "Citric Acid as a Solid-State Plasticizer for Eudragit RS PO." *The Journal of Pharmacy and Pharmacology* 59(11):1493–1500.

Schneider, Hans Adam. 1989. "Glass Transition Behaviour of Compatible Polymer Blends." *Polymer* 30(5):771–79.

Scholze, J., A. Breitstadt, V. Cairns, et al. 1993. "Short Report: Ramipril and Hydrochlorothiazide Combination Therapy in Hypertension: A Clinical Trial of Factorial Design. The East Germany Collaborative Trial Group." *Journal of Hypertension* 11(2):217–21.

Scicli, A. G. and O. A. Carretero. 1986. "Renal Kallikrein-Kinin System." *Kidney International* 29(1):120–30.

Seitz, James A. and Gerald M. Flessland. 1965. "Evaluation of the Physical Properties of Compressed Tablets I: Tablet Hardness and Friability." *Journal of Pharmaceutical Sciences* 54(9):1353–57.

Sethia, S. and E. Squillante. 2004. "Solid Dispersion of Carbamazepine in PVP K30 by Conventional Solvent Evaporation and Supercritical Methods." *International Journal of Pharmaceutics* 272(1–2):1–10.

Shakya, Sunita. 2015. *Formulation and Optimization of Immediate Release Tablet of*

*Sitagliptin Phosphate Using Response Surface Methodology Anti-Diabetic View Project Formulation and Optimization of Immediate Release Tablet of Sitagliptin Phosphate Using Response Surface Method*. Vol. 4.

Shamma, Rehab N. and Mona Basha. 2013. "Soluplus ® : A Novel Polymeric Solubilizer for Optimization of Carvedilol Solid Dispersions : Formulation Design and Effect of Method of Preparation." *Powder Technology* 237:406–14.

Shanmugam, Srinivasan. 2015. "Granulation Techniques and Technologies: Recent Progresses." *BioImpacts : BI* 5(1):55–63.

Shantikumar, S., G. Sreekanth, K. V. SurendraNath, et al. 2014. "Compatibility Study between Sitagliptin and Pharmaceutical Excipients Used in Solid Dosage Forms." *Journal of Thermal Analysis and Calorimetry* 115(3):2423–28.

Shimpi, Shyam, Bhaskar Chauhan, K. R. Mahadik, et al. 2004. "Preparation and Evaluation of Diltiazem Hydrochloride-Gelucire 43/01 Floating Granules Prepared by Melt Granulation." *AAPS PharmSciTech* 5(3):e43.

SICA, D. 2006. "Aliskiren, a Novel Renin Inhibitor, Is Well Tolerated and Has Sustained BP-Lowering Effects Alone or in Combination with HCTZ during Long-Term (52 Weeks) Treatment of Hypertension [Abstract]." *Eur Heart J* 27:797.

Siepe, Stefanie, Barbara Lueckel, Andrea Kramer, et al. 2006. "Strategies for the Design of Hydrophilic Matrix Tablets with Controlled Microenvironmental PH." *International Journal of Pharmaceutics* 316(1–2):14–20.

Siepmann, Florence, Juergen Siepmann, Mathias Walther, et al. 2006. "Aqueous HPMCAS Coatings: Effects of Formulation and Processing Parameters on Drug Release and Mass Transport Mechanisms." *European Journal of Pharmaceutics and Biopharmaceutics* 63(3):262–69.

Siew, Adeline. 2014. "Tackling Challenges in the Development of Fixed-Dose Combinations." *Pharmaceutical Technology* 38(4).

Sigma Aldrich. 2019. *Hydroxypropyl Cellulose*.

Simon, Levente L., Hajnalka Pataki, György Marosi, et al. 2015. "Assessment of Recent Process Analytical Technology (PAT) Trends: A Multiauthor Review." *Organic Process Research & Development* 19(1):3–62.

Singh, Abhishek and Guy Van den Mooter. 2016. "Spray Drying Formulation of Amorphous Solid Dispersions." *Advanced Drug Delivery Reviews* 100:27–50.

Six, Karel, Geert Verreck, Jef Peeters, et al. 2004. "Increased Physical Stability and Improved Dissolution Properties of Itraconazole, a Class II Drug, by Solid Dispersions That Combine Fast- and Slow-Dissolving Polymers." *Journal of Pharmaceutical Sciences* 93(1):124–31.

Song, Yuejun, Lianyan Wang, Ping Yang, et al. 2013. "Physicochemical Characterization

of Felodipine-Kollidon VA64 Amorphous Solid Dispersions Prepared by Hot-Melt Extrusion." *Journal of Pharmaceutical Sciences* 102(6):1915–23.

Soon Ahn, Jae, Kang Min Kim, Chan Young Ko, et al. 2011. "Increased Bioavailability of Eprosartan by Vitamin E TPGS and PVP K29 Bull Absorption Enhancer and Polymer (Vitamin E TPGS and PVP K29) by Solid Dispersion Improve Dissolution and Bioavailability of Eprosartan Mesylate." *Korean Chem. Soc* 32(5):1587.

Stahl, Harald. 2014. "Preventing Tablet Capping." Retrieved March 21, 2019 (https://www.gea.com/en/stories/preventing-tablet-capping.jsp).

Stanton, T. and J. L. Reid. 2002. "Fixed Dose Combination Therapy in the Treatment of Hypertension." *Journal of Human Hypertension* 16(2):75–78.

Stillinger, Frank H. 1988. "Supercooled Liquids, Glass Transitions, and the Kauzmann Paradox." *J Chem*.

Stumvoll, Michael, Barry J. Goldstein, and Timon W. van Haeften. 2005. "Type 2 Diabetes: Principles of Pathogenesis and Therapy." *The Lancet* 365(9467):1333–46.

Sugano, Kiyohiko, Manfred Kansy, Per Artursson, et al. 2010. "Coexistence of Passive and Carrier-Mediated Processes in Drug Transport." *Nature Reviews Drug Discovery* 9(8):597–614.

Sun, Dajun D. and Ping I. Lee. 2015. "Probing the Mechanisms of Drug Release from Amorphous Solid Dispersions in Medium-Soluble and Medium-Insoluble Carriers." *Journal of Controlled Release* 211:85–93.

Suryanarayana, C. 2001. "Mechanical Alloying and Milling." *Progress in Materials Science* 46(1):1–184.

Szakonyi, Gergely and Romána Zelkó. 2012. "The Effect of Water on the Solid State Characteristics of Pharmaceutical Excipients: Molecular Mechanisms, Measurement Techniques, and Quality Aspects of Final Dosage Form." *International Journal of Pharmaceutical Investigation* 2(1):18–25.

Tajber, Lidia, Owen I. Corrigan, and Anne Marie Healy. 2005. "Physicochemical Evaluation of PVP-Thiazide Diuretic Interactions in Co-Spray-Dried Composites - Analysis of Glass Transition Composition Relationships." *European Journal of Pharmaceutical Sciences* 24(5):553–63.

Takano, Ryusuke, Noriyuki Takata, Ryoichi Saito, et al. 2010. "Quantitative Analysis of the Effect of Supersaturation on in Vivo Drug Absorption." *Molecular Pharmaceutics* 7(5):1431–40.

Taniguchi, Chika, Yohei Kawabata, Koichi Wada, et al. 2014. "Microenvironmental PH-Modification to Improve Dissolution Behavior and Oral Absorption for Drugs with PH-Dependent Solubility." *Expert Opinion on Drug Delivery* 11(4):505–16.

Taupitz, Thomas, Jennifer B. Dressman, Charles M. Buchanan, et al. 2013. "Cyclodextrin-Water Soluble Polymer Ternary Complexes Enhance the Solubility and Dissolution Behaviour of Poorly Soluble Drugs. Case Example: Itraconazole." *European Journal of Pharmaceutics and Biopharmaceutics* 83(3):378–87.

Taylor, L. S. and G. Zografi. 1997. "Spectroscopic Characterization of Interactions between PVP and Indomethacin in Amorphous Molecular Dispersions." *Pharmaceutical Research* 14(12):1691–98.

Taylor, Lynne S., Frans W. Langkilde, and George Zografi. 2001. "Fourier Transform Raman Spectroscopic Study of the Interaction of Water Vapor with Amorphous Polymers." *Journal of Pharmaceutical Sciences* 90(7):888–901.

Terra, Steven G. 2003. "Cardiology Patient Page. Angiotensin Receptor Blockers." *Circulation* 107(24):e215-6.

Thakral, Seema, Naveen K. Thakral, and Dipak K. Majumdar. 2013. "Eudragit®: A Technology Evaluation." *Expert Opinion on Drug Delivery* 10(1):131–49.

Thibert, Roch and Bruno C. Hancock. 1996. "Direct Visualization of Superdisintegrant Hydration Using Environmental Scanning Electron Microscopy." *Journal of Pharmaceutical Sciences* 85(11):1255–58.

Tian, Yiwei, Jonathan Booth, Elizabeth Meehan, et al. 2013. "Construction of Drug-Polymer Thermodynamic Phase Diagrams Using Flory-Huggins Interaction Theory: Identifying the Relevance of Temperature and Drug Weight Fraction to Phase Separation within Solid Dispersions." *Molecular Pharmaceutics* 10(1):236–48.

Tian, Yiwei, David S. Jones, and Gavin P. Andrews. 2015. "An Investigation into the Role of Polymeric Carriers on Crystal Growth within Amorphous Solid Dispersion Systems." *Molecular Pharmaceutics* 12(4):1180–92.

Tobert, Jonathan A. 2003. "Lovastatin and beyond: The History of the HMG-CoA Reductase Inhibitors." *Nature Reviews Drug Discovery* 2(7):517–26.

Tokyo Chemical Industries. 2015. "Liquid Crystals (LC) Materials." Retrieved March 21, 2019 (https://www.tcichemicals.com/eshop/pt/br/category_index/12775/).

Tubic-Grozdanis, Marija, John M. Hilfinger, Gordon L. Amidon, et al. 2008. "Pharmacokinetics of the CYP 3A Substrate Simvastatin Following Administration of Delayed Versus Immediate Release Oral Dosage Forms." *Pharmaceutical Research* 25(7):1591–1600.

Turner, Robert C., Carole A. Cull, Valeria Frighi, et al. 1999. "Glycemic Control With Diet, Sulfonylurea, Metformin, or Insulin in Patients With Type 2 Diabetes Mellitus<SUBTITLE>Progressive Requirement for Multiple Therapies (UKPDS 49)</SUBTITLE>" *JAMA* 281(21):2005.

UK Prospective Diabetes Study (UKPDS) Group. 1998. "Effect of Intensive Blood-

Glucose Control with Metformin on Complications in Overweight Patients with Type 2 Diabetes (UKPDS 34). UK Prospective Diabetes Study (UKPDS) Group." *Lancet (London, England)* 352(9131):854–65.

UK Prospective Diabetes Study Group (UKPDS). 1998. "Intensive Blood-Glucose Control with Sulphonylureas or Insulin Compared with Conventional Treatment and Risk of Complications in Patients with Type 2 Diabetes (UKPDS 33)." *Lancet (London, England)* 352(9131):837–53.

Vaingankar, Pradnya and Purnima Amin. 2017. "Continuous Melt Granulation to Develop High Drug Loaded Sustained Release Tablet of Metformin HCl." *Asian Journal of Pharmaceutical Sciences* 12(1):37–50.

Valladao, D. M. S., L. C. S. De Oliveira, J. Zuanon Netto, et al. 1996. "Thermal Decomposition of Some Diuretic Agents." *Journal of Thermal Analysis* 46(5):1291–99.

Vander, A. J. and G. W. Geelhoed. 1965. "Inhibition of Renin Secretion by Angiotensin .II." *Experimental Biology and Medicine* 120(2):399–403.

Vanhoutte, P. M. 1989. "Endothelium and Control of Vascular Function. State of the Art Lecture." *Hypertension (Dallas, Tex. : 1979)* 13(6 Pt 2):658–67.

Vasanthavada, Madhav, Yanfeng Wang, Thomas Haefele, et al. 2011. "Application of Melt Granulation Technology Using Twin-Screw Extruder in Development of High-Dose Modified-Release Tablet Formulation." *Journal of Pharmaceutical Sciences* 100(5):1923–34.

Vasconcelos, Teófilo, Sara Marques, José das Neves, et al. 2016. "Amorphous Solid Dispersions: Rational Selection of a Manufacturing Process." *Advanced Drug Delivery Reviews* 100:85–101.

Vasilakou, Despoina, Thomas Karagiannis, Eleni Athanasiadou, et al. 2013. "Sodium-Glucose Cotransporter 2 Inhibitors for Type 2 Diabetes: A Systematic Review and Meta-Analysis." *Annals of Internal Medicine* 159(4):262–74.

Vippagunta, Sudha R., Harry G. Brittain, and David J. W. Grant. 2001. "Crystalline Solids." *Advanced Drug Delivery Reviews* 48(1):3–26.

Vynckier, Dierickx, Saerens, et al. 2014. "Hot-Melt Co-Extrusion for the Production of Fixed-Dose Combination Products with a Controlled Release Ethylcellulose Matrix Core." *International Journal of Pharmaceutics* 464(1–2):65–74.

Vynckier, Dierickx, Voorspoels, et al. 2014. "Hot-Melt Co-Extrusion: Requirements, Challenges and Opportunities for Pharmaceutical Applications." *Journal of Pharmacy and Pharmacology* 66(2):167–79.

Wang, Yifan, Sara Koynov, Benjamin J. Glasser, et al. 2016. "A Method to Analyze Shear Cell Data of Powders Measured under Different Initial Consolidation

Stresses.” *Powder Technology* 294(294):105–12.

Wang, Yifan, Ronald D. Snee, Golshid Keyvan, et al. 2016. “Statistical Comparison of Dissolution Profiles.” *Drug Development and Industrial Pharmacy* 42(5):796–807.

Wawer, I. 2008. “QNMR in Solid State.” *NMR Spectroscopy in Pharmaceutical Analysis* 63–82.

Weir, Matthew R. and Victor J. Dzau. 1999. “The Renin-Angiotensin-Aldosterone System: A Specific Target for Hypertension Management.” *American Journal of Hypertension* 12(3):205–12.

Wesdyk, R., Y. M. Joshi, J. De Vincentis, et al. 1993. “Factors Affecting Differences in Film Thickness of Beads Coated in Fluidized Bed Units.” *International Journal of Pharmaceutics* 93(1–3):101–9.

Williams, A. J., M. V Merrick, and M. A. Eastwood. 1991. “Idiopathic Bile Acid Malabsorption--a Review of Clinical Presentation, Diagnosis, and Response to Treatment.” *Gut* 32(9):1004–6.

Williams, Marcia, Yiwei Tian, David Jones, et al. 2010. “Hot-Melt Extrusion Technology: Optimizing Drug Delivery.” *European Journal of Parenteral and Pharmaceutical Sciences* (7):7–10.

Wood, John H., John E. Syarto, and Herbert Letterman. 1965. “Improved Holder for Intrinsic Dissolution Rate Studies.” *Journal of Pharmaceutical Sciences* 54(7):1068.

World Health Organisation. 2017. “WHO | Cardiovascular Diseases (CVDs).” *WHO*. Retrieved March 29, 2018 (http://www.who.int/cardiovascular_diseases/en/).

World Health Organization. 2016. “Cardiovascular Diseases (CVDs).” Retrieved (http://www.who.int/cardiovascular_diseases/en/).

World Health Organization. 2017a. “Cardiovascular Diseases (CVDs) Factsheet.” Retrieved February 20, 2018 (http://www.who.int/mediacentre/factsheets/fs317/en/).

World Health Organization. 2017b. “WHO | Hypertension.” *WHO*. Retrieved April 3, 2018 (http://www.who.int/topics/hypertension/en/).

World Health Organization. 2017c. “WHO Model List of Essential Medicines 20th Edition.” *Essential Medicines and Health Products* (August). Retrieved February 1, 2018 (http://www.who.int/entity/medicines/publications/essentialmedicines/20th_EML2017_FINAL_amendedAug2017.pdf?ua=1).

Wu, C. and J. W. McGinity. 2001. “Influence of Ibuprofen as a Solid-State Plasticizer in Eudragit RS 30 D on the Physicochemical Properties of Coated Beads.” *AAPS PharmSciTech* 2(4):1–9.

Wu, Chi-Yuan and Leslie Z. Benet. 2005. “Predicting Drug Disposition via Application of BCS: Transport/Absorption/ Elimination Interplay and Development of a

Biopharmaceutics Drug Disposition Classification System." *Pharmaceutical Research* 22(1):11–23.

Wunderlich, Bernhard. 2005. *Thermal Analysis of Polymeric Materials*. 1st ed. Knoxville: Springer Science & Business Media,.

Yap, Angela Frances, Thiru Thirumoorthy, and Yu Heng Kwan. 2016. "Medication Adherence in the Elderly." *Journal of Clinical Gerontology and Geriatrics* 7(2):64–67.

Yki-Järvinen, Hannele. 2004. "Thiazolidinediones." *New England Journal of Medicine* 351(11):1106–18.

Yoshioka, Minoru, Bruno C. Hancock, and George Zografi. 1994. "Crystallization of Indomethacin from the Amorphous State below and above Its Glass Transition Temperature." *Journal of Pharmaceutical Sciences* 83(12):1700–1705.

Yoshioka, Sumie and Yukio Aso. 2007. "Correlations between Molecular Mobility and Chemical Stability During Storage of Amorphous Pharmaceuticals." *Journal of Pharmaceutical Sciences* 96(5):960–81.

Young, Christopher R., John J. Koleng, and James W. McGinity. 2002. "Production of Spherical Pellets by a Hot-Melt Extrusion and Spheronization Process." *International Journal of Pharmaceutics* 242(1–2):87–92.

Yu, Lian. 2001. "Amorphous Pharmaceutical Solids: Preparation, Characterization and Stabilization." *Advanced Drug Delivery Reviews* 48(1):27–42.

Zaid, A. N., M. Ghanem, L. Maqboul, et al. 2016. "Biowaiver Eligibility of a Lower Strength Ramipril/Hydrochlorothiazide Immediate Release Tablets Using a New Validated HPLC Analytical Method." *Drug Research* 66(10):539–46.

Zander, Mette, Sten Madsbad, Jan Lysgaard Madsen, et al. 2002. "Effect of 6-Week Course of Glucagon-like Peptide 1 on Glycaemic Control, Insulin Sensitivity, and β-Cell Function in Type 2 Diabetes: A Parallel-Group Study." *The Lancet* 359(9309):824–30.

Zhang, Geoff G. Z. and Deliang Zhou. 2009. "Crystalline and Amorphous Solids." *Developing Solid Oral Dosage Forms* 25–60.

Zhang, Yong, Meirong Huo, Jianping Zhou, et al. 2010. "DDSolver: An Add-In Program for Modeling and Comparison of Drug Dissolution Profiles." *The AAPS Journal* 12(3):263–71.

Zhang, Yuanyuan, Yuxin Liu, Yanfei Luo, et al. 2014. "Extruded Soluplus/SIM as an Oral Delivery System: Characterization, Interactions, *in Vitro* and *in Vivo* Evaluations." *Drug Delivery* 7544(August 2017).

Zhong, Yue, Guanghui Jing, Bin Tian, et al. 2016. "Supersaturation Induced by Itraconazole/Soluplus® Micelles Provided High GI Absorption in Vivo." *Asian*

*Journal of Pharmaceutical Sciences* 11(2):255–64.

Zhu, Yucun, Navnit H. Shah, A. Wasee. Malick, et al. 2002. “Solid-State Plasticization of an Acrylic Polymer with Chlorpheniramine Maleate and Triethyl Citrate.” *International Journal of Pharmaceutics* 241(2):301–10.

Zimmet, Paul, K. G. M. M. Alberti, and Jonathan Shaw. 2001. “Global and Societal Implications of the Diabetes Epidemic.” *Nature* 414:782–87.

Zisaki, Aikaterini, Ljubisa Miskovic, and Vassily Hatzimanikatis. 2015. “Antihypertensive Drugs Metabolism: An Update to Pharmacokinetic Profiles and Computational Approaches.” *Current Pharmaceutical Design* 21(6):806–22.

# Appendices

## Appendix 1

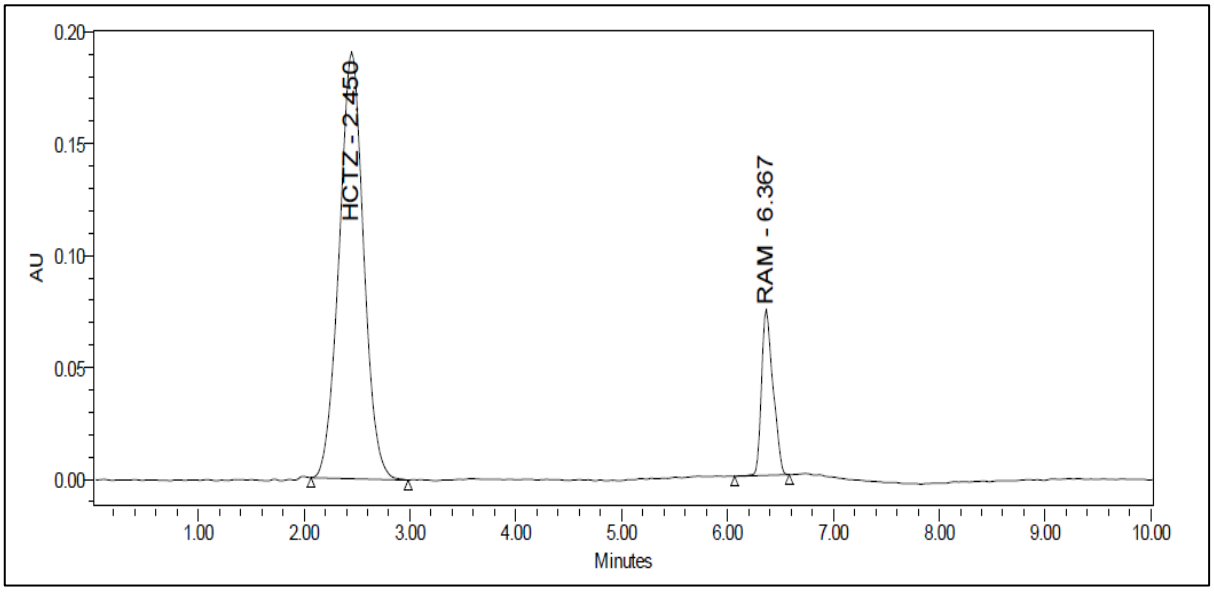


*Figure A1. 1: HPLC chromatogram of hydrochlorothiazide (2.45 min) and ramipril (6.37 min) using HPLC (method described in chapter 2, section 2.12.1).*

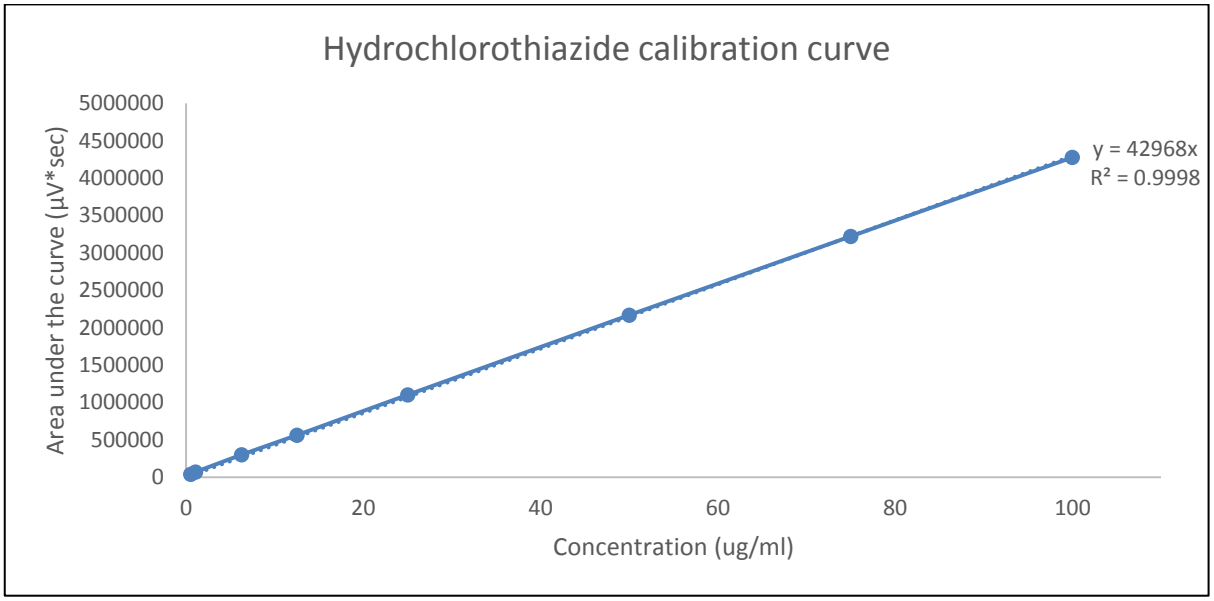


*Figure A1. 2: Calibration curve of hydrochlorothiazide in 0.1M HCl pH 1.2*

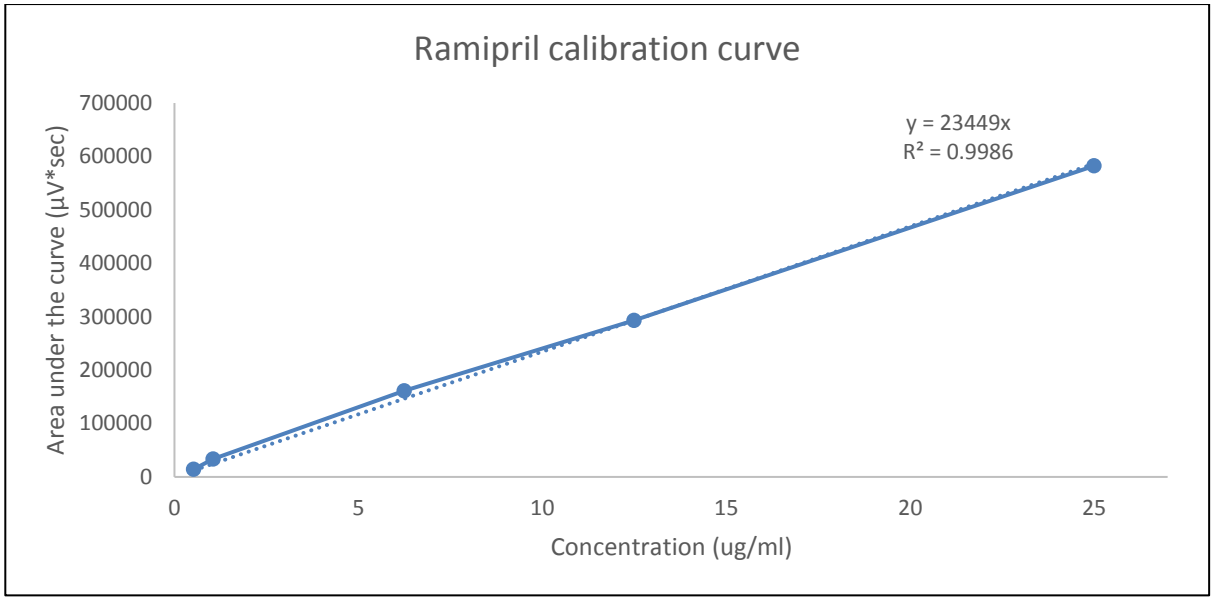


*Figure A1. 3: Calibration curve of ramipril in 0.1M HCl pH 1.2*

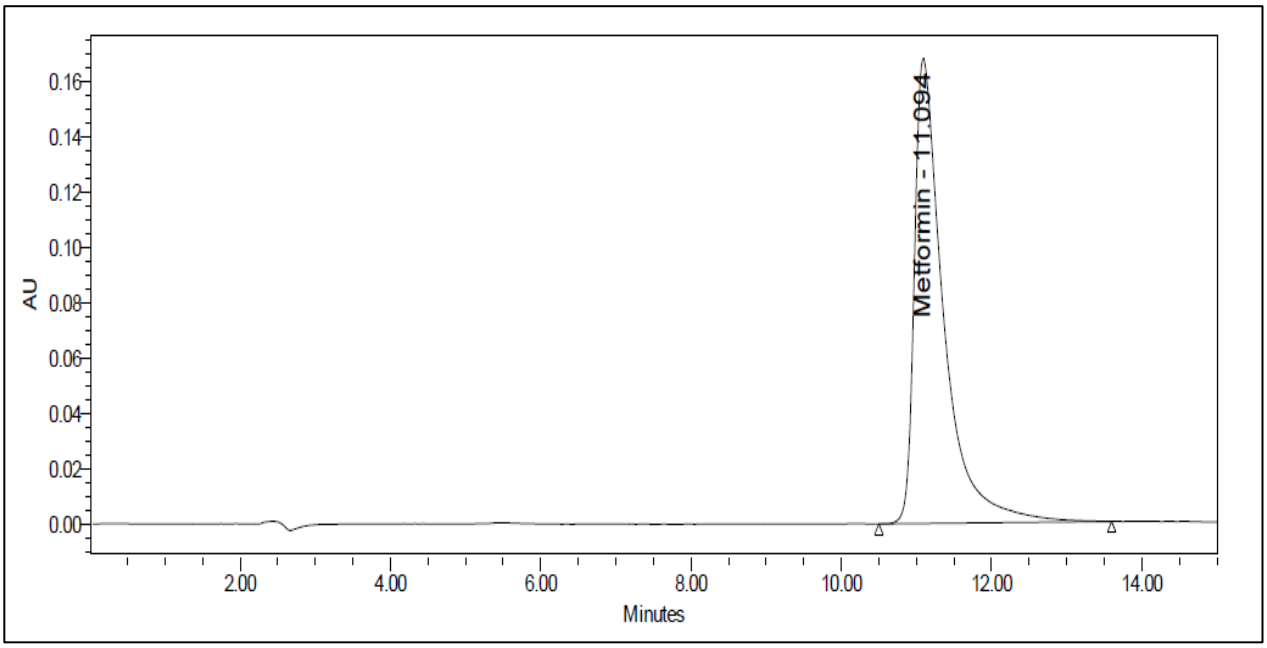


*Figure A1. 4: HPLC chromatogram of metformin hydrochloride (11.1 min) using HPLC (method described in chapter 2, section 2.12.2).*

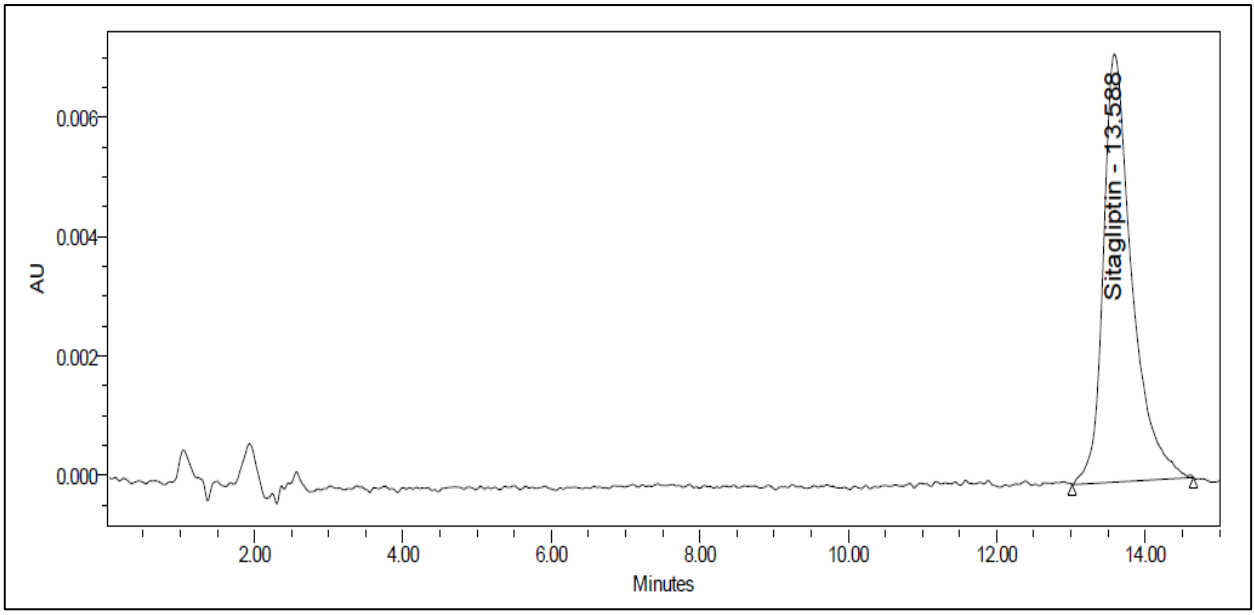


*Figure A1. 5: HPLC chromatogram of sitagliptin phosphate (13.6 min) using HPLC (method described in chapter 2, section 2.12.2).*

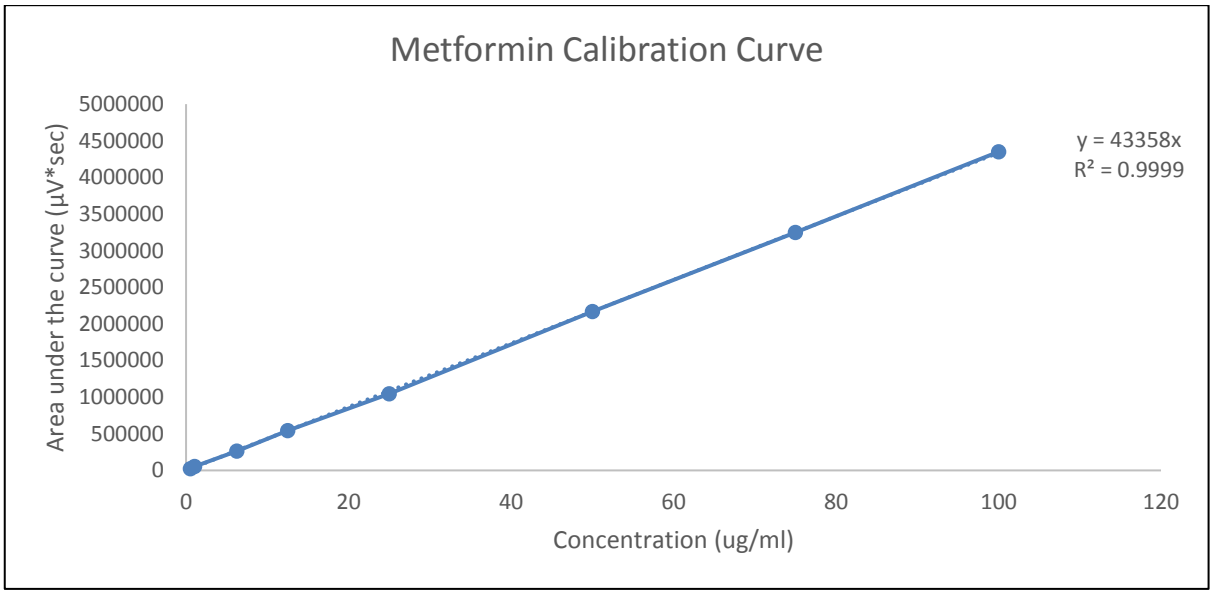


*Figure A1. 6: Calibration curve of metformin hydrochloride in 0.1M HCl pH 1.2.*

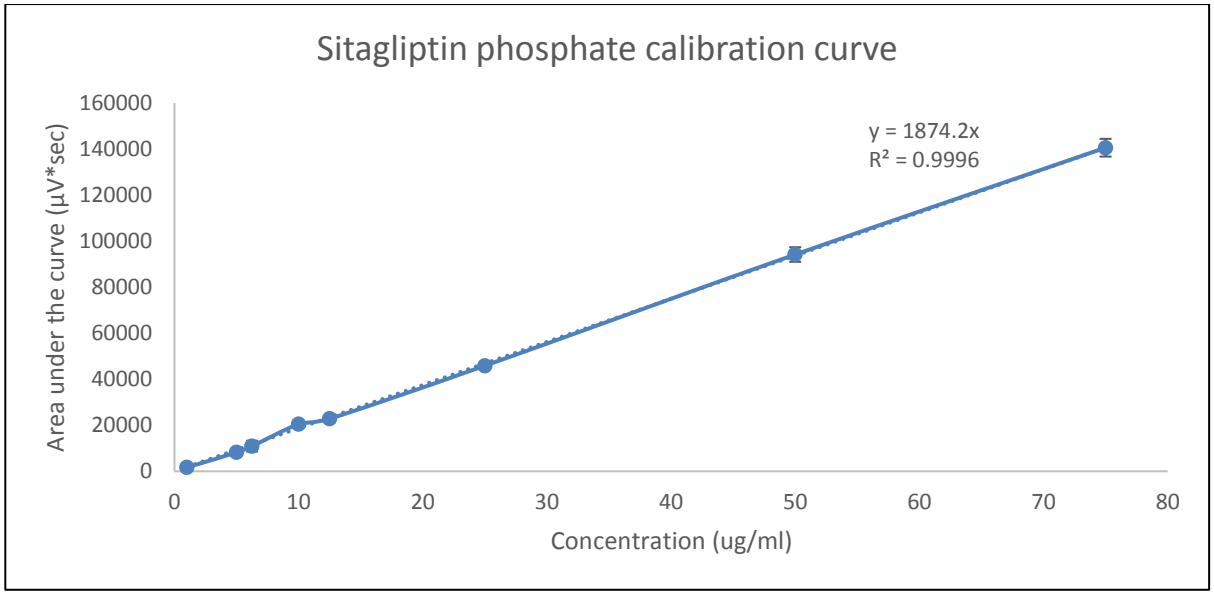


*Figure A1. 7: Calibration curve of sitagliptin phosphate in 0.1M HCl pH 1.2*

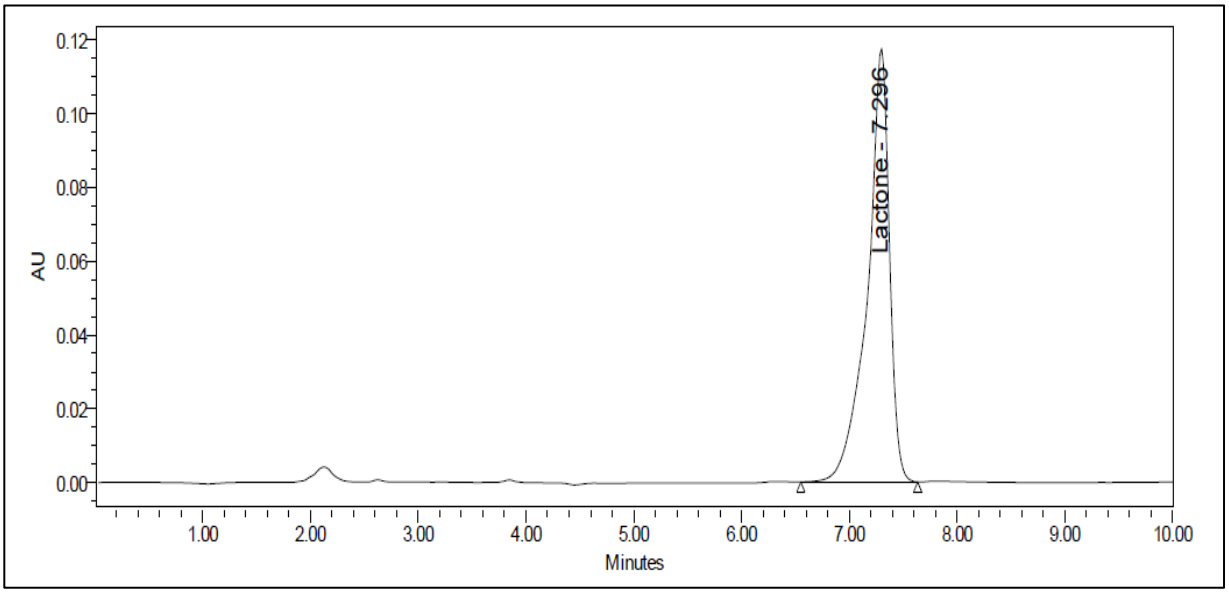


*Figure A1. 8: HPLC chromatogram of simvastatin lactone (7.3 min) using HPLC (method described in chapter 2, section 2.12.3).*

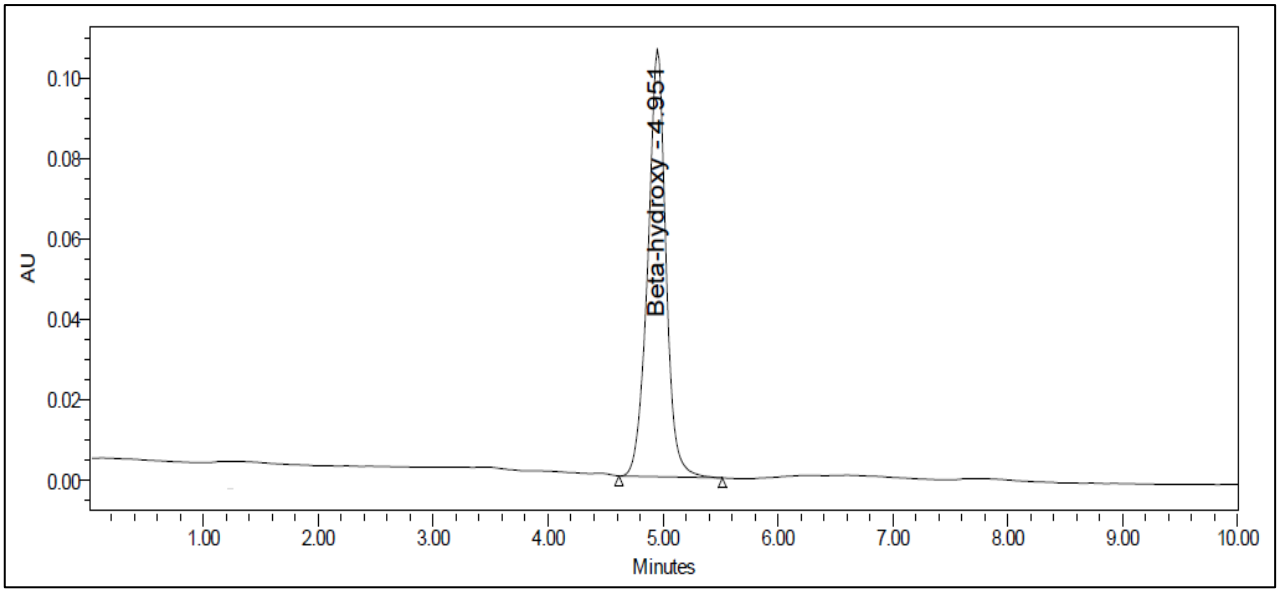


*Figure A1. 9: HPLC chromatogram of simvastatin beta-hydroxy acid (4.95 min) using HPLC (method described in chapter 2, section 2.12.3).*

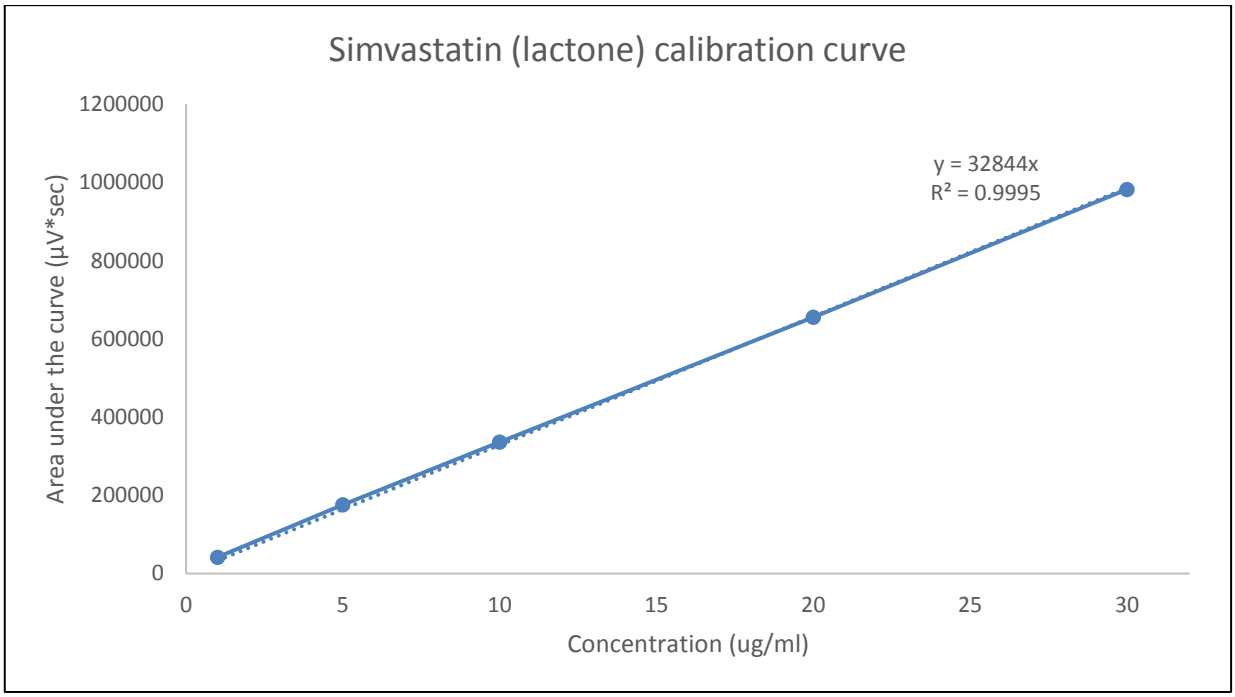


*Figure A1. 10: Calibration curve of simvastatin (lactone) in acetonitrile*

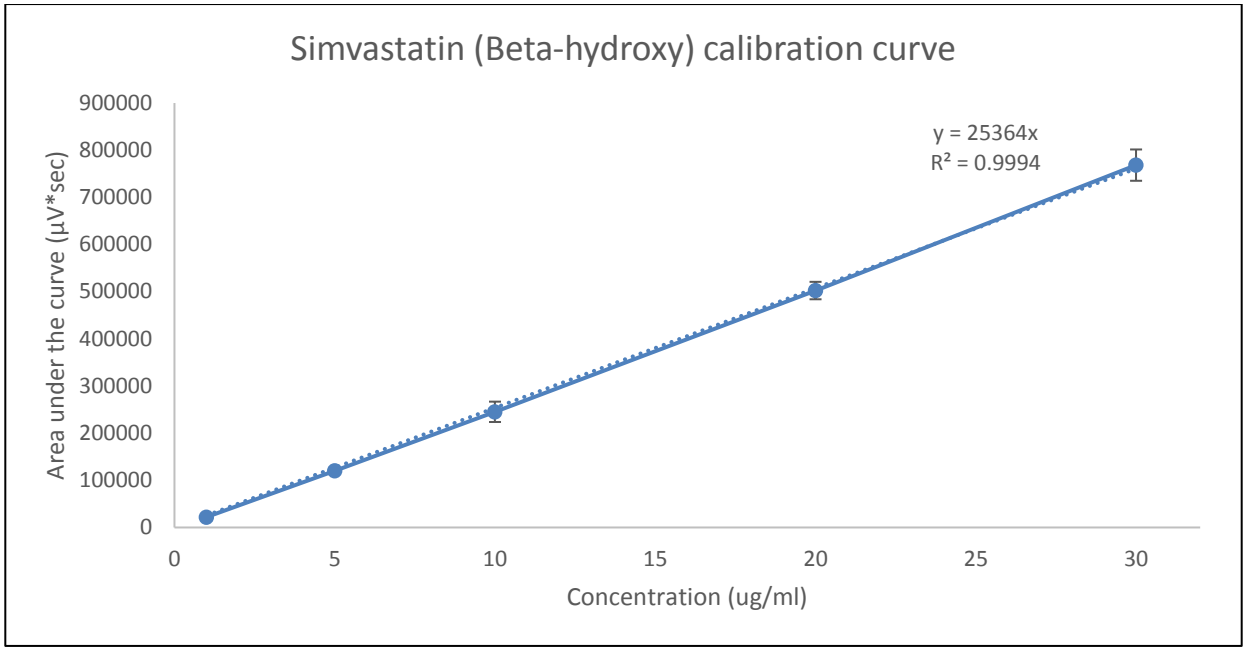


*Figure A1. 11: Calibration curve of simvastatin (beta-hydroxy) calibration curve*

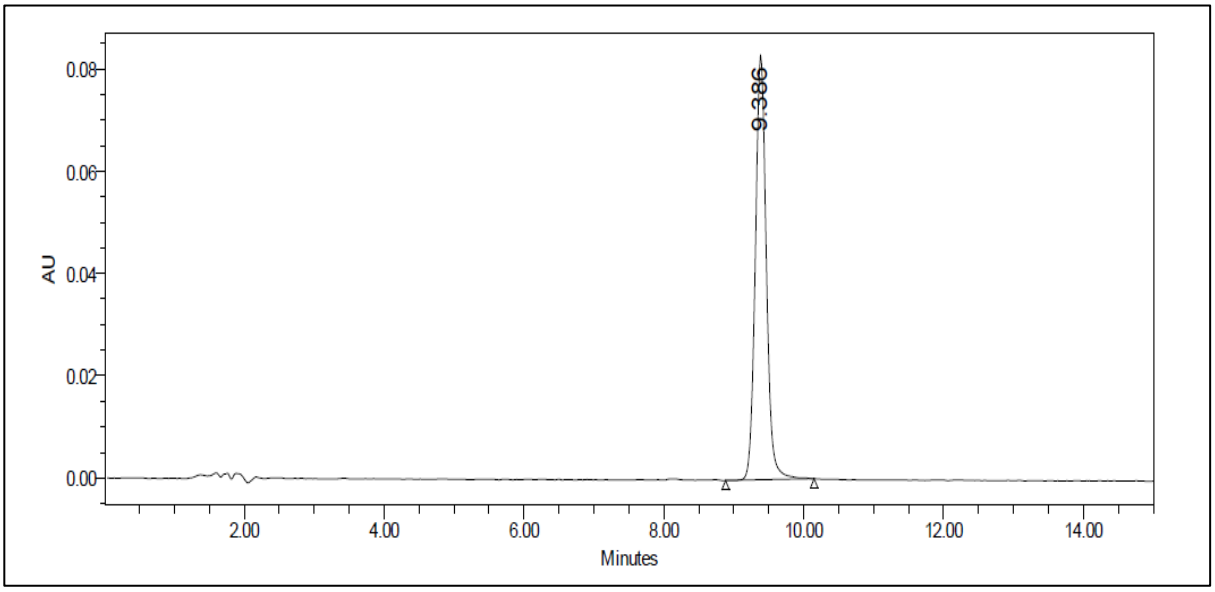


*Figure A1. 12: HPLC chromatogram of gliclazide (9.38 min) using HPLC (method described in chapter 2, section 2.12.4).*

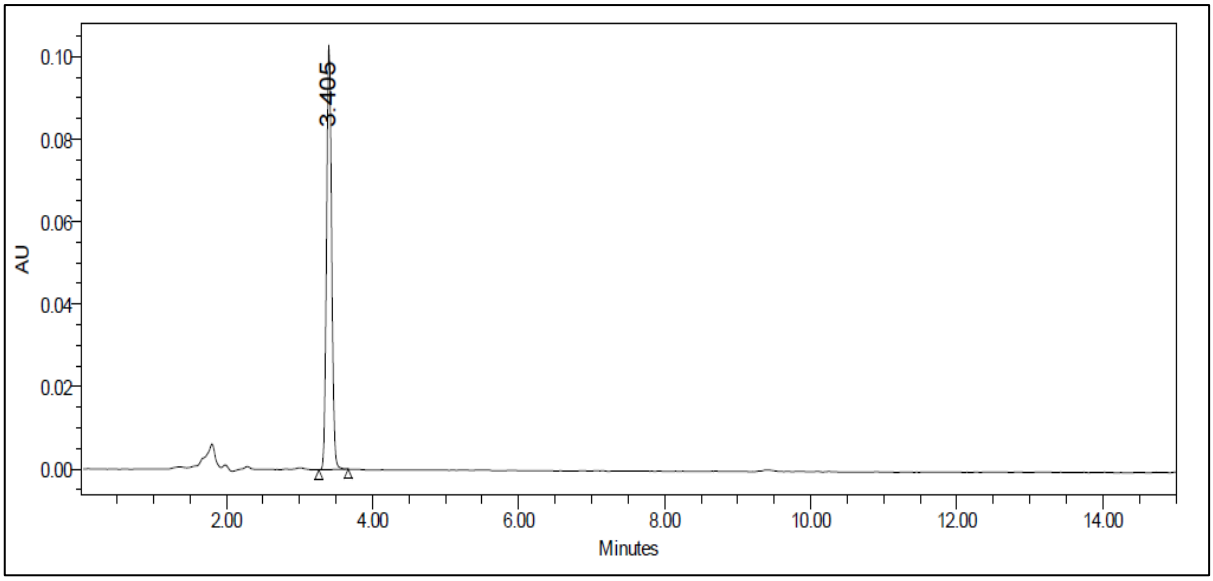


*Figure A1. 13: HPLC chromatogram of gliclazide degradation product A (3.40 min) using HPLC (method described in chapter 2, section 2.12.4).*

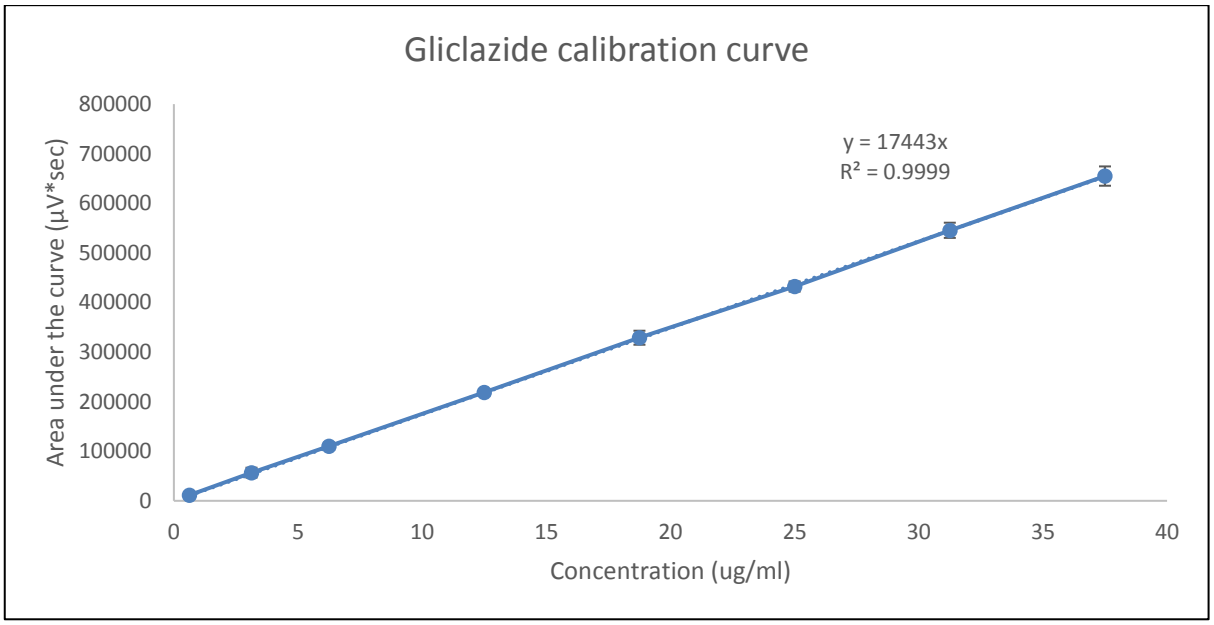


*Figure A1. 14: Calibration curve of gliclazide in phosphate buffer pH 7.4*

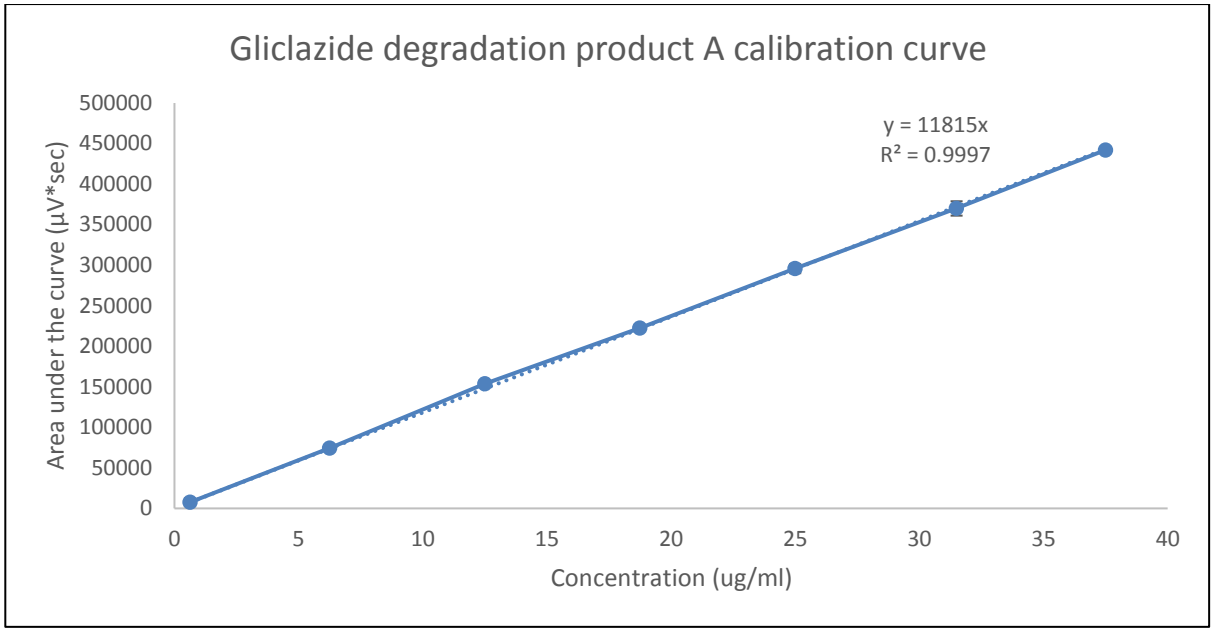


*Figure A1. 15: Calibration curve of gliclazide degradation product A in 0.1M HCl pH 1.2*

## Appendix 2

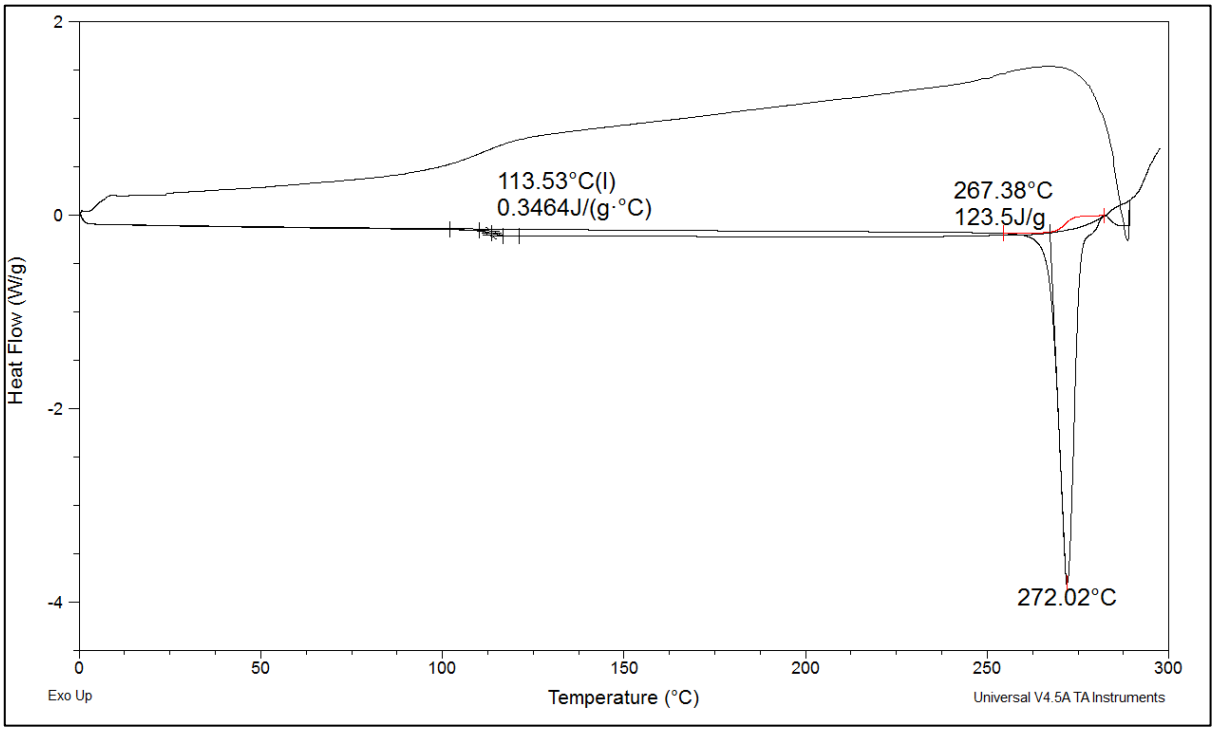


*Figure A2. 1: Heat cool heat cycles at 10 ℃ /min heating and cooling rate cycles of hydrochlorothiazide showing a melting point endotherm at 272.02 ± 2.47 °C of the crystalline raw material and a glass transition temperature at 113.53 ± 1.25 ℃ for the amorphous form of the drug.*

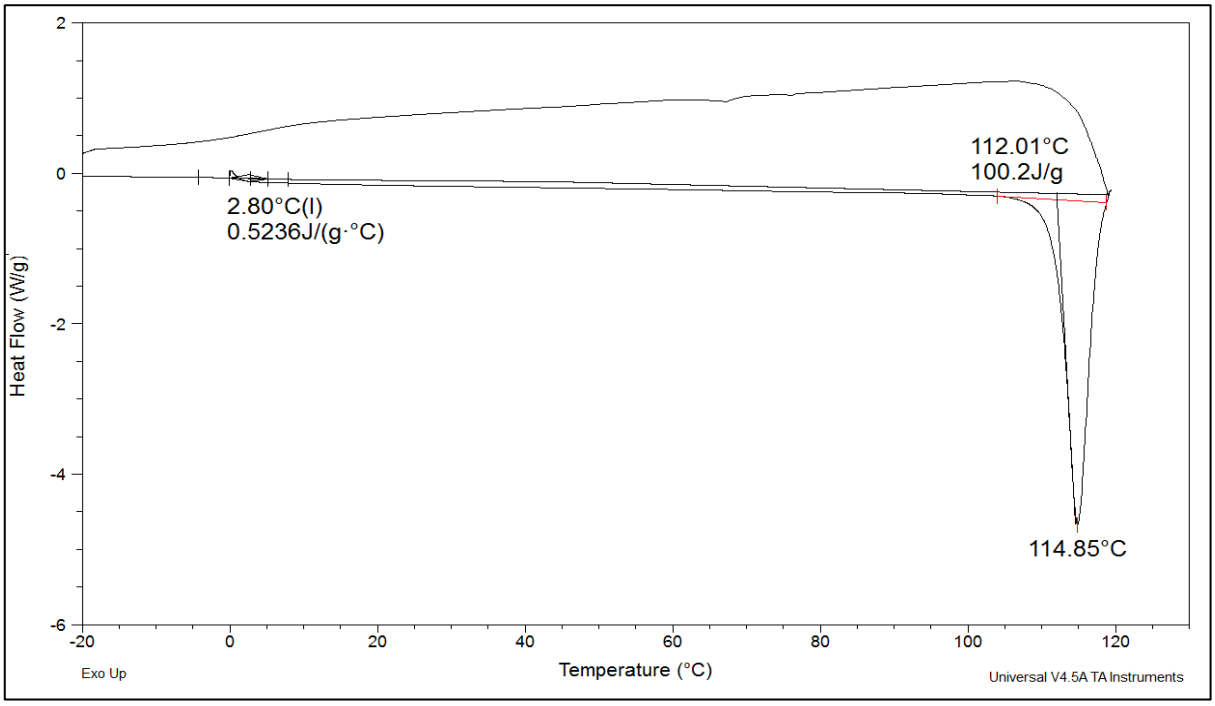


*Figure A2. 2: Heat cool heat cycles at 10 °C /min heating and cooling rate cycles of ramipril showing a melting point endotherm at 114.85 ± 1.27 °C of the crystalline raw material and a glass transition temperature at 2.80 ± 0.45 °C for the amorphous form of the drug.*

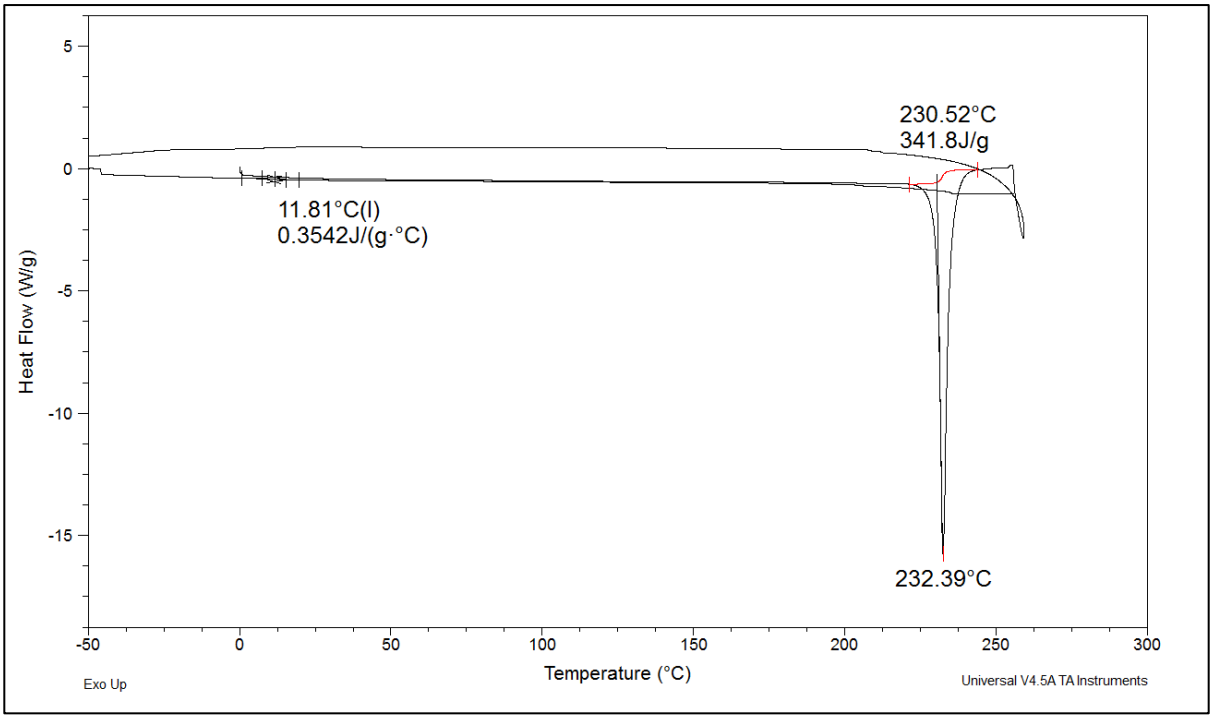


*Figure A2. 3: Heat cool heat cycles at 10 °C /min heating and cooling rate cycles of metformin hydrochloride showing a melting point endotherm at 232.39 ± 2.26 °C of the crystalline raw material and a glass transition temperature at 11.81 ± 1.31 °C for the amorphous form of the drug.*

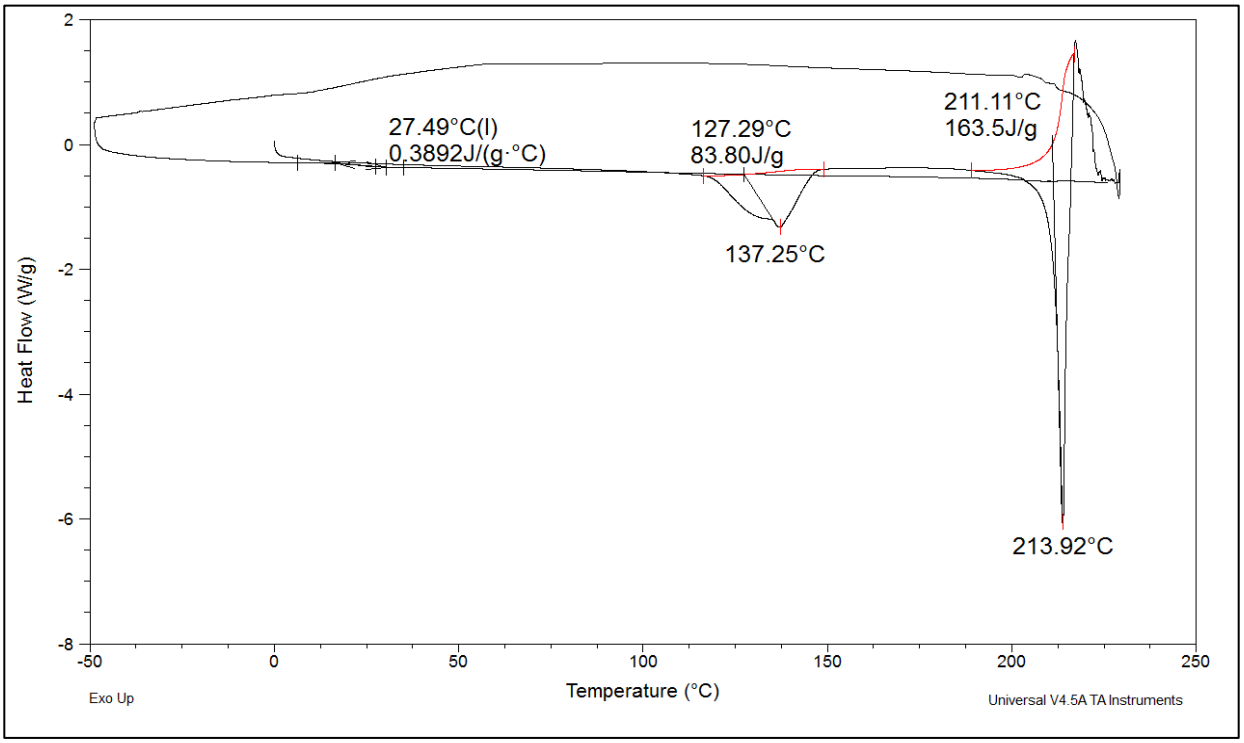


*Figure A2. 4: Heat cool heat cycles at 10 °C /min heating and cooling rate cycles of sitagliptin phosphate monohydrate showing a melting endotherm at 137.25 °C associated with the loss of a water molecule, a melting point endotherm at 213.92 ± 0.98 °C of the crystalline raw material and a glass transition temperature at 27.49 ± 1.01 °C for the amorphous form of the drug.*

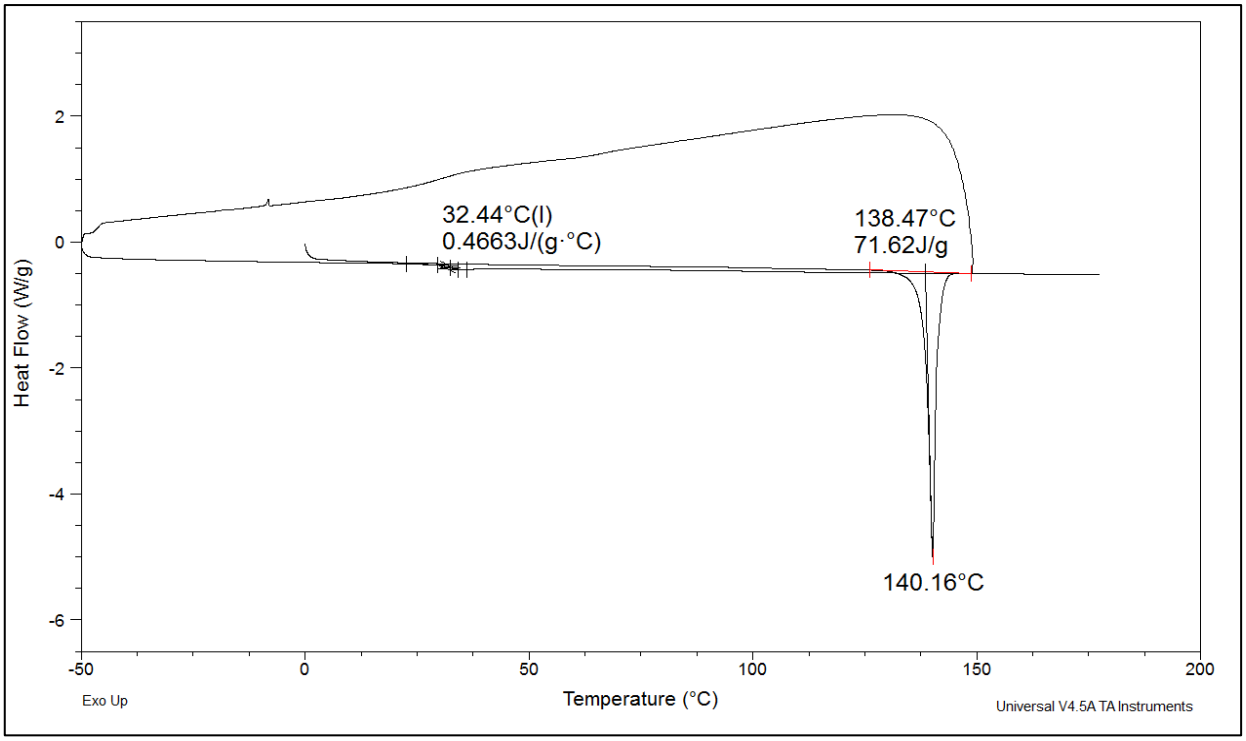


*Figure A2. 5: Heat cool heat cycles at 10 °C /min heating and cooling rate cycles of simvastatin showing a melting point endotherm at 140.16 ± 1.21 °C of the crystalline raw material and a glass transition temperature at 32.44 ± 0.68 °C for the amorphous form of the drug.*

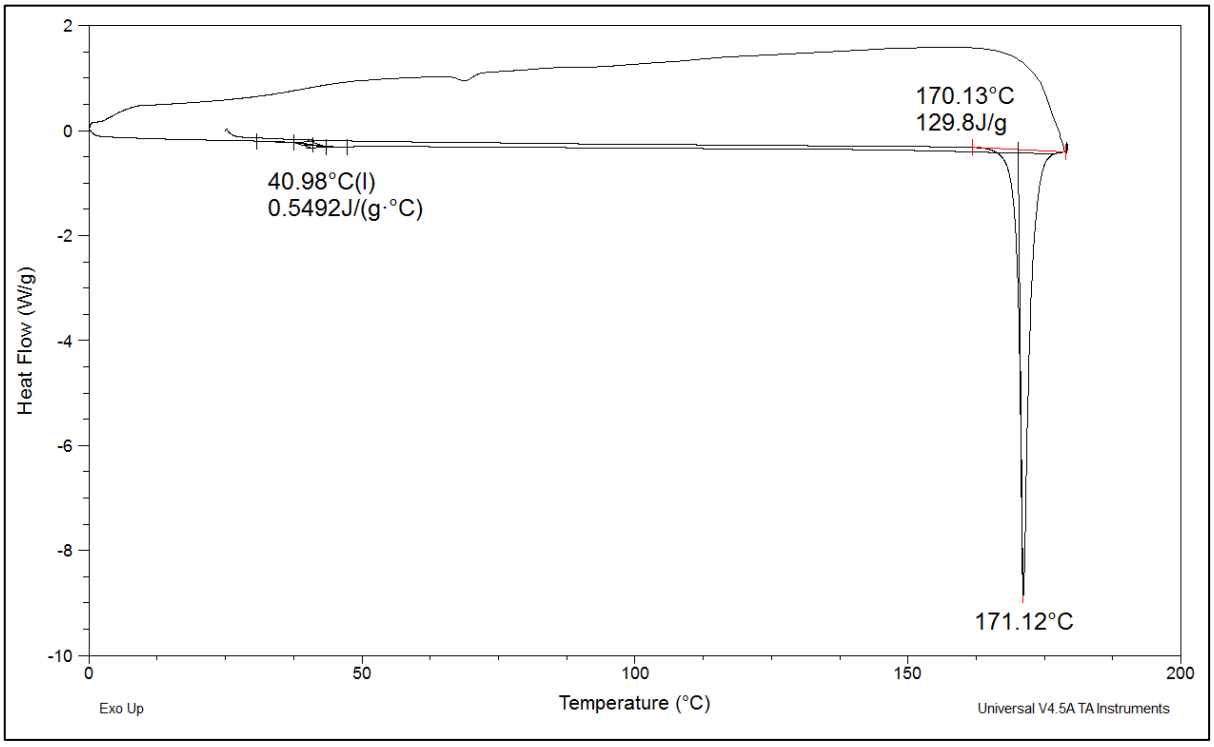


*Figure A2. 6: Heat cool heat cycles at 10 °C /min heating and cooling rate cycles of gliclazide showing a melting point endotherm at 171.12 ± 1.09 °C of the crystalline raw material and a glass transition temperature at 40.98 ± 2.34 °C for the amorphous form of the drug.*